The Role of Sphingosine-1-Phosphate in Bone Regeneration: A Synergy of Vessel-Dependent and Independent Mechanisms

Inaugural dissertation

for the attainment of the title of doctor
in the Faculty of Mathematics and Natural Sciences
at the Heinrich Heine University Düsseldorf

presented by

Annalena Wille
from Bielefeld

Düsseldorf, June 2024

from the Institute of Molecular Medicine III
at the Heinrich Heine University Düsseldorf

Published by permission of the
Faculty of Mathematics and Natural Sciences at
Heinrich Heine University Düsseldorf

Examiners:
1. Prof. Dr. Bodo Levkau
2. Prof. Dr. Jürgen Scheller

Date of the oral examination: 1 October 2024

Parts of this thesis have been published in the follwing:

Paper 1:

Annalena Wille, Sarah Weske, Karin von Wnuck Lipinski, Philipp Wollnitzke, Nathalie H. Schröder, Nadine Thomas, Melissa K. Nowak, Jennifer Deister-Jonas, Björn Behr, Petra Keul and Bodo Levkau (2024). "Sphingosine-1-phosphate promotes osteogenesis by stimulating osteoblast growth and neovascularization in a vascular endothelial growth factor–dependent manner." Journal of Bone and Mineral Research 39 (3): 357-372.[1]

Contributions: Annalena Wille (Conceptualization, Data curation, Formal analysis, Investigation, Methodology, Project administration, Visualization, Writing - original draft, Writing - review and editing); Sarah Weske (Methodology, Validation); Karin von Wnuck Lipinski (Methodology, Validation); Philipp Wollnitzke (Data curation, Methodology, Validation); Nathalie H. Schröder (Investigation, Validation); Nadine Thomas (Investigation, Validation); Melissa K. Nowak (Investigation, Validation); Jennifer Deister-Jonas (Investigation, Validation); Björn Behr (Methodology, Validation); Petra Keul (Methodology, Validation); Bodo Levkau (Conceptualization, Data curation, Funding acquisition, Project administration, Supervision, Writing - original draft, Writing - review and editing)

Paper 2:

Johannes Maximilian Wagner*, **Annalena Wille***, Maria Fueth, Sarah Weske, Sebastian Lotzien, Felix Reinkemeier, Christoph Wallner, Alexander Sogorski, Stephanie Dittfeld, Mustafa Becerikli, Thomas Schildhauer, Marcus Lehnhardt, Bodo Levkau and Björn Behr (2023). "Pharmacological elevation of sphingosine-1-phosphate by S1P lyase inhibition accelerates bone regeneration after post-traumatic osteomyelitis." J Cell Mol Med 27(23): 3786-3795.[2]

* Authors contributed equally

Contributions: Johannes Maximilian Wagner (Conceptualization, Funding acquisition, Project administration, Writing - original draft, Writing - review and editing); Annalena Wille (Data curation, Formal analysis, Methodology, Writing - review and editing); Maria Fueth (Data curation, Formal analysis, Investigation); Sarah Weske (Formal analysis, Investigation); Sebastian Lotzien (Conceptualization, Data curation, resources); Felix Reinkemeier (Conceptualization, Project administration, Software, Supervision); Christoph Wallner (Validation, Visualization, Writing – review and editing); Alexander Sogorski (Investigation, Methodology); Stephanie Dittfeld (Data curation, Formal analysis, resources); Mustafa Becerikli (Project administration, Supervision); Thomas Schildhauer (Project administration, Supervision); Marcus Lehnhardt (Conceptualization, Funding acquisition, Project administration, Resources); Bodo Levkau (Project administration, Supervision, Validation, Writing - original draft, Writing - review and editing); Björn Behr (Conceptualization, Data curation, Funding acquisition, Project administration)

Table of Contents

Summary

Sphingosine-1-phosphate (S1P) is a bioactive sphingolipid. It plays a crucial role in bone development and homeostasis. Despite its recognized impact on these processes, the understanding of its therapeutic potential for bone strengthening remains incomplete. This study explored the role of S1P in bone anabolic therapy. To assess the effect of S1P signaling on bone regeneration, S1P levels were elevated *in vivo* through pharmacological inhibition or genetic deletion of the enzyme responsible for S1P degradation, the S1P lyase. Specific receptor knockout animals were used to understand distinct mechanisms influenced by S1P. In addition, several *in vitro* experiments were performed to reveal the involvement of osteoblasts and bone marrow endothelial cells.

This study demonstrated that S1P increased trabecular bone formation and cortical strengthening. Trabecular bone formation was shown to be dependent on S1P receptor 3 (S1PR3). S1P/S1PR3 signaling was identified to act in two distinct ways: Firstly, S1P stimulated the production of Vascular Endothelial Growth Factor A (VEGFa) in osteoblasts through S1PR3 activation, intrinsically enhancing the mineralization of these cells. Secondly, S1P/S1PR3 signaling triggered the formation of a pro-osteogenic vessel phenotype within the bone, the H-type vessels. Subsequently, an increase in trabecular bone volume was observed. Additionally, S1PR2 contributed to the formation of cortical bone, as proven by cortical thickening and increased bone strength after S1P lyase inhibition. The deletion of S1PR2 prevented these changes. This mechanism was found to be VEGFa and vessel-independent. Pharmacological S1P lyase inhibition was evaluated in a mouse model of post-traumatic osteomyelitis to validate these effects in a bone defect model. This treatment enhanced the bone healing capacity and increased vascular invasion at the defect site linked to S1PR3 signaling. Human bone samples displaying an increase in bone volume after cultivation with the S1P lyase inhibitor further confirmed the translational relevance of these findings.

In summary, this study identified two distinct mechanisms of S1P signaling that influence the bone formation capacity in bone regeneration and healing. These mechanisms of S1P signaling have been identified as potent inducers of both cortical and trabecular bone regeneration. The findings provide a new basis for potential treatment options for bone anabolic therapy, particularly in conditions such as osteoporosis and bone healing.

Zusammenfassung

Sphingosine-1-Phosphat (S1P), ein bioaktives Sphingolipid, spielt eine wichtige Rolle in der Knochenentwicklung und -homöostase. Obwohl die Wirkung von S1P in diesen Prozessen bereits vielfältig untersucht wurde, ist die Auswirkung von S1P auf die Knochenregeneration noch nicht in Gänze erforscht. Ziel dieser Studie war es, die Wirkung von S1P als mögliche anabole Therapie in der Knochenregeneration zu untersuchen. Um den S1P-Spiegel *in vivo* zu erhöhen, wurde die S1P Lyase, das Enzym, welches den Abbau von S1P katalysiert, pharmakologisch gehemmt oder genetisch deletiert. Dadurch stiegen die globalen und lokalen S1P-Spiegel an. Die genauen Auswirkungen dieser S1P Erhöhung wurden mithilfe von S1P-Rezeptor deletierten Mäusen untersucht. Darüber hinaus wurde die Beteiligung bestimmter im Knochen vorkommender Zelltypen an diesen Prozessen durch Kultivierungsexperimente mit Osteoblasten und Endothelzellen des Knochenmarks näher untersucht.

Durch die globale Erhöhung des S1P-Spiegels *in vivo* wurde das Knochenvolumen sowohl in den Trabekeln als auch in der Kortikalis erhöht. Der Sphingosine-1-Phosphat-Rezeptor 3 (S1PR3) spielte eine wichtige Rolle bei der Erhöhung des Volumens der Trabekelknochen. Er ist auf zwei Arten an der Knochenbildung beteiligt: Einerseits wurde durch die Aktivierung des S1PR3 in Osteoblasten die Produktion des vaskulären endothelialen Wachstumsfaktors A (VEGFa) angeregt. VEGFa aktivierte intrinsisch die Mineralisierung der Osteoblasten. Andererseits regeten S1P/S1PR3-Signale die Bildung von spezifischen, pro-osteogenen H-Type Blutgefäßen im Knochen an. Dieses steigerte die trabekuläre Knochenbildung. Zusätzlich wurde eine Beteiligung des S1PR2 an der Bildung von kortikalem Knochen identifiziert. Die Aktivierung von S1P/S1PR2 führte zu einer Verdickung des kortikalen Knochens und zu einer Erhöhung der Stabilität. Dieser Mechanismus war unabhängig von VEGFa-Signalen und von den im Knochen enthaltenen Blutgefäßen. Um die neuen Erkenntnisse über die Regulation von S1P im Knochen in einem weiteren Modell zu überprüfen, wurde der S1P-Spiegel in einem Modell der post-traumatischen Osteomyelitis durch Hemmung der S1P Lyase erhöht. Dieses Modell zeichnet sich durch nach einem Knochenbruch entstehende Entzündungsreaktionen aus. Es konnte ein Effekt auf die Knochenregeneration und -heilung bestätigt werden, der von S1PR3 abhängig war. Außerdem wurde eine S1PR3 anhängige erhöhte Invasion

von Endothelzellen in den Knochendefekt gezeigt. Die Ergebnisse wurden durch die Kultivierung von menschlichen Knochenproben bestätigt, bei denen ebenfalls ein Anstieg des Knochenvolumens durch die Hemmung der S1P Lyase festgestellt wurde.
Zusammenfassend lässt sich sagen, dass in dieser Studie zwei unabhängige Mechanismen identifiziert wurden, in denen S1P die Knochenbildung und -regeneration anregt. Diese Mechanismen wirten sowohl auf das Wachstum der Trabekel, als auch auf die Kortikalis. Diese Erkenntnisse eröffnen neue Perspektiven und können für die Entwicklung potenzieller therapeutischer Interventionen zur anabolen Knochenbehandlung von Bedeutung sein, insbesondere bei Bedingungen wie Osteoporose und Knochenheilung.

Abbreviations

ABC	ATP-binding cassette
ACER	Alkaline ceramidases
ALK	Activin receptor-like kinase
ALP	Alkaline phosphatase
aPKC	Atypical protein kinase
ApoM	Apolipoprotein M
ASAH	Acid ceramidase
BACE1	Beta-site amyloid precursor protein cleaving enzyme
BMD	Bone mineral density
BMEC	Bone marrow endothelial cell
BMP	Bone morphogenic protein
BSA	Bovine Serum Albumin Fraction V
BV/TV	Trabecular bone volume per total tissue volume
CAD	Coronary artery disease
CAMP	Cathelicidin antimicrobial peptide
cDNA	Complementary DNA
CERT	Ceramide transfer protein
CRMP	Collapsin response rediator protein
Ct.Ar./Tt.Ar.	Cortical area per total tissue area
CT-1	Cardiotrophin 1
Cxcl9	CXC ligand 9
DAG	Diacylglycerol
Dll	Delta-like ligands
DMSO	Dimethylsulfoxid
DOP	4-deoxypyridoxin
EC	Endothelial cells
ECM	Extracellular matrix
Edg	Endothelial differentiation genes
EDTA	Ethylenediaminetetraacetic acid

ELISA	Enzyme-linked Immunosorbent Assays
eNOS	endothelial Nitric oxide synthase
ERK	Extracellular signal-regulated protein kinases
EtOH	Ethanol
FALDH	Fatty aldehyde dehydrogenase
FBS	Fetal bovine serum
FGF	Fibroblast growth factor
FTY720	Fingolimod
GDP	Guanosine diphosphate
GPCR	G-protein coupled receptors
GTP	Guanosine triphosphate
HDAC	Histone deacetylases
HDL	High-density lipoproteins
HEK293	Human embryonic kidney cells
HUVEC	Human umbilical vein endothelial cells
IL	interleukin
IP3	Inositol 1,4,5-trisphosphate
LDL	Low-density lipoproteins
LPP	Phosphate phosphatases
MAKP	Mitogen-activated protein kinase
M-CSF	Macrophage colony-stimulating factor
MEF	Mouse embryonic fibroblasts
MeOH	Methanol
MFI	Mean fluorescence intensity
MFSD2B	Major facilitator superfamily transporter 2b
µCT	micro-Computed tomography
MS	Multiple sclerosis
mTORC1	mammalian Target of rapamycin complex 1
n.d.	not detected
NF-κB	kappa-light-chain-enhancer of activated B-cells
NK-cell	Natural killer cell
NO	Nitric oxide

NRP1	Neuropilin-1
OB	Osteoblast
OC	Osteoclast
OPG	Osteoprotegerin
OSX	Osterix
PDGF	Platelet-derived growth factor
PDGFR	PDGF receptor
PDK1	Phosphoinositide-dependent kinase-1
PE	Phosphatidylethanolamine
PFA	Paraformaldehyde
PHB2	Prohibitin 2
PI3K	Phosphoinositide 3-kinase
PIP2	Phosphatidylinositol 4,5-bisphosphate
PKC	Protein kinase C
PLC	Phospholipase C
PMA	Phorbol 12-myristate 13-acetate
pOB	primary Osteoblast
PPARγ	Peroxisome proliferator-activated receptor gamma
PTH	Parathyroid hormone
qRT-PCR	Quantitative reverse transcriptase polymerase chain reaction
RANKL	Receptor activator of NF-κB Ligand
RIP1	Receptor-interacting Protein 1
ROCK	Rho-associated protein kinase
RUNX2	Runt-related transcription factor 2
S. aureus	*Staphylococcus aureus*
s.d.	Standard deviation
S1P	Sphingosine-1-phosphate
S1PR	S1P receptor
SCEM	Super Cryo Embadding Medium
SGPL1	S1P lyase
siRNA	small interfering RNA
Slit3	Slit guidance ligand 3

SOST	Sclerostin
SPHK	Sphingosine kinases
SPLIS	Sphingosine phosphate lyase insufficiency syndrome
SPNS2	Spinster homolog 2
SPP	S1P phosphatase
Tb.N.	Trabecular number
Tb.Sp.	Trabecular spacing
Tb.Th.	Trabecular thickness
TERT	Telomerase reverse transcriptase
TGFβ	Transforming growth factor β
TNFα	Tumor necrosis factor α
TRAF2	TNFα receptor-associated factor 2
TRPC	Transient receptor potential canonical
VEGFa	Endothelial Growth Factor A
VEGFR	VEGF receptor
ZO1	Zonula occludens 1

SI Units

%	Percent
$^{\circ}\mathrm{C}$	Degrees Celsius
min	Minutes
g	Gram
mg	Milligram
µg	Microgram
mL	Milliliter
μ**L**	Microliter
M	Molar
μ**M**	Micromolar
mm	Millimeter
μ**m**	Micrometer
cm^2	Cubic centimeter
xg	Relative centrifugal force/Times gravity

List of Figures

List of Tables

1 Introduction

1.1 Sphingolipids

Sphingolipids are one of the primary classes of eukaryotic lipids and were initially described by J.W.L. Thudichum in the late 19th century.[3] Thudichum successfully identified this lipid class in the human brain and differentiated its characteristic structure from other known lipids.[4] A common building block of all sphingolipids is a long chain base, mostly sphingosine or sphinganine. An amide bond to the C2 atom allows the binding of a fatty acid differing from C14 to C32 in length and saturation. A head group, such as phosphate or glucose, can be bound to the C1 atom.[5] This broad range of combinations allows for a vast array of sphingolipids, with approximately 5000 lipids documented to date.[6]
In the 1980s, the bioactive functions and involvement in cell structure and metabolism were studied in detail.[3] These examinations led to the identification of three main functions of sphingolipids. One is their significant role in the composition of the plasma membrane, accounting for up to 30% of the total membrane lipids in the cell. Ceramide, sphingosine, sphingosine-1-phosphate (S1P) and ceramide-1-phosphate have been demonstrated to have bioactive functions and play a significant role in signal transduction and gene regulation. In particular, S1P, which consists of a sphingosine chain and a phosphate head group, has been extensively studied and is known to have bioactive functions in the vasculature, immune system and nervous system.[7] Furthermore, sphingolipids are involved in constructing lipid rafts, which cluster with sterols to form hubs for efficient signal transduction.[8,9]

1.1.1 The Sphingolipid Metabolism

De novo synthesis of sphingolipids occurs at the cytoplasmic domain of the endoplasmic reticulum membrane (Figure 1).[10] Serine and palmitoyl-CoA are condensed at this site by the serin-palmitoyl-transferase to produce 3-keto-dihydrosphingosine.[11] This product is subsequently reduced to dihydrosphingosine by the 3-keto-dihydrosphingosine-reductase and transformed into dihydroceramide.[10] Ceramide, a key intermediate in sphingolipid metabolism, is then formed by the desaturation of dihydroceramide by the dihydroceramide reductase.[12]

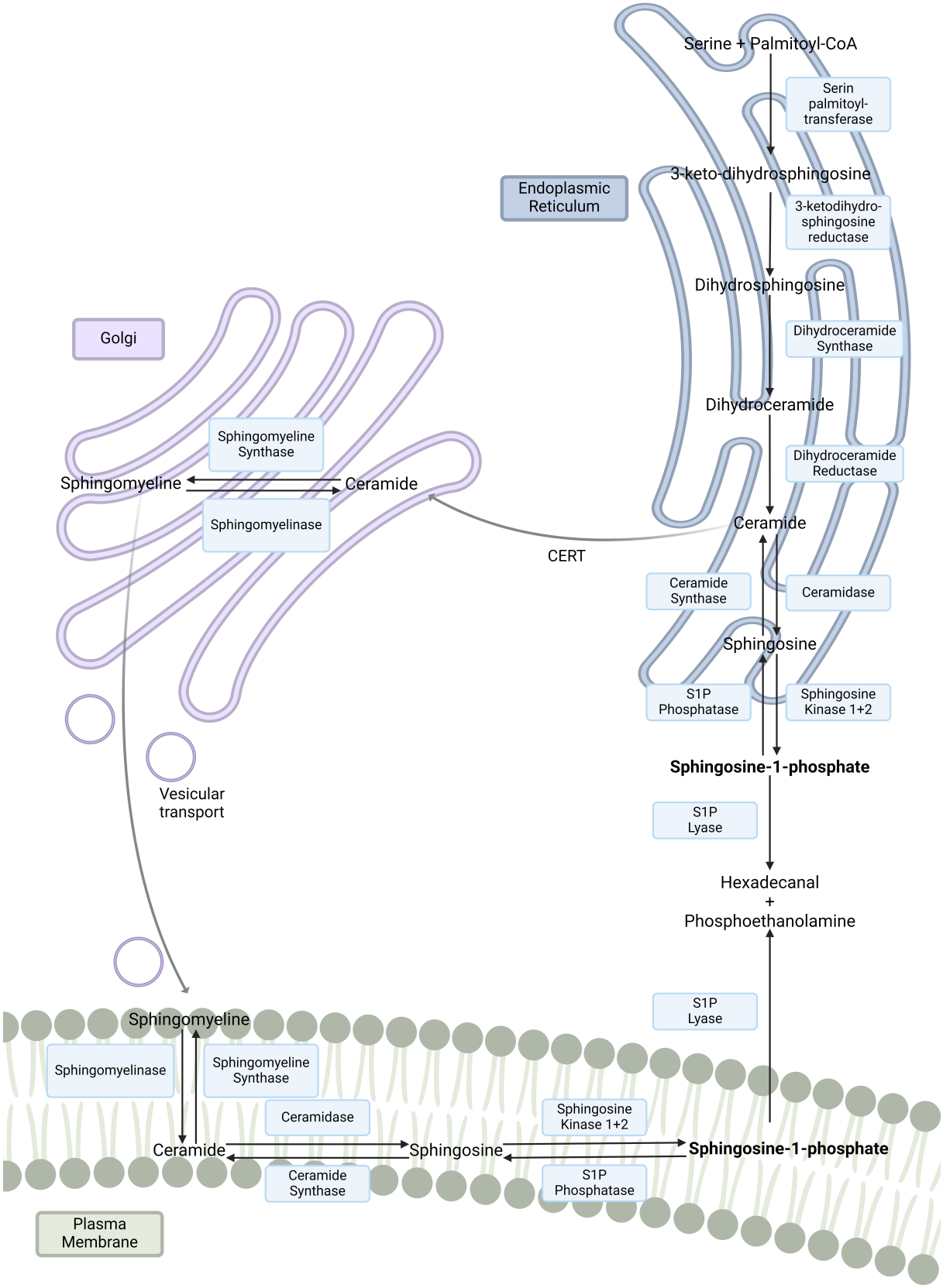

Figure 1: Schematic overview of the sphingolipid pathway. *De novo* formation of ceramide, a key intermediate, occurs in the endoplasmic reticulum. Ceramide is converted to sphingosine-1-phosphate (S1P) or transported to the Golgi apparatus by ceramide transporter proteins (CERT). Here, it is converted to sphingomyelin, which can be transported to the plasma membrane by vesicles and converted to S1P. The S1P lyase ultimately degrades S1P into hexadecenal and phosphoethanolamine. Created with BioRender.com

From this point, ceramide can follow either the salvage pathway, where it remains within the endoplasmic reticulum, or be transferred to the Golgi lumen by the ceramide transfer protein (CERT) before entering into the hydrolytic pathway.[13] Within the hydrolytic pathway, a phosphatidylcholine headgroup is transferred to the ceramide backbone. This results in sphingomyelin formation in the Golgi lumen's proximal region.[14,15] The sphingomyelinase can reverse the aforementioned reaction whereby sphingomyelin is cleaved into phosphatidylcholine and ceramide.[16] Alternatively, sphingomyelin can be transformed to sphingosine and S1P within the membrane.[17,18]

Ceramidases catalyze the removal of the N-acyl-linked fatty acid from ceramide, forming sphingosine and releasing free fatty acids that are essential for the salvage pathway.[19] Five membrane-bound ceramidases have been identified, each with unique subcellular localization and optimal reaction conditions. Acid ceramidase (ASAH1) is primarily present in lysosomes and requires an acidic environment. Neutral ceramidase (ASAH2) is located in mitochondrial membranes. In addition, there are three alkaline ceramidases (ACER) that operate in high pH environments: ACER1 is localized in the endoplasmic reticulum, ACER2 in the Golgi apparatus and ACER3 in both the endoplasmic reticulum and Golgi.[20]

Subsequently, one of two sphingosine kinases (SPHK1 and SPHK2) phosphorylated sphingosine to produce S1P.[21] Both sphingosine kinases exhibit redundant functions, as genetic deletion of only one kinase does not result in a drastic reduction of S1P levels or significant defects in different mouse models. However, simultaneous deletion of both kinases results in a dramatic decrease in plasma S1P levels, coupled with a severe phenotype and high lethality due to severe developmental hemorrhage.[22] A closer examination of these enzymes' cellular and global distribution revealed differences in their location and expression levels. SPHK1 is a cytosolic enzyme that translocates to the plasma membrane in response to phorbol 12-myristate 13-acetate (PMA).[23,24] In contrast, SPHK2 is mainly found in the nucleus and is exported to the cytoplasm upon phosphorylation.[25] During development, differences in expression patterns are evident, with SPHK1 predominantly expressed until embryonic day E7, followed by a switch to increased SPHK2 expression until embryonic day E17.[26] In adult tissues, both kinases are detectable with SPHK1 showing high expression in lung, liver and spleen and SPHK2 showing the highest expression in liver, heart, brain, testis and kidney.[27,28]

S1P is recycled into the sphingolipid pathway through the action of two distinct enzyme classes: S1P phosphatases (SPPs) and lipid phosphate phosphatases (LPPs). SPPs

dephosphorylate S1P back to sphingosine, with SPP1 being ubiquitously expressed throughout the body, with the highest expression in the kidney and placenta and the lowest in peripheral blood and small intestine. SPP2 expression is more organ-specific and is found in brain, heart, colon, kidney, small intestine and lung.[29] SPPs are membrane proteins located predominantly in the endoplasmic reticulum.[30] In addition, LPPs (LPP1-3) catalyze the dephosphorylation of S1P and other phospholipids, such as diacylglycerol and lysophosphatidate, further emphasizing the complexity of the sphingolipid pathway.[31] Subsequently, sphingosine is transformed back into ceramide via CoA-dependent ceramide synthases.[32] These enzymes are primarily located in the endoplasmic reticulum with lesser accumulation in mitochondrial membranes, microsomes and the Golgi apparatus.[33] Six ceramide synthases catalyze this reaction, each influencing the length of the N-acyl chain attached to the backbone and thus the biological function of ceramide.[34]

Alternatively, S1P is irreversibly degraded by the S1P lyase (SGPL1). The enzyme is mainly associated with the endoplasmic reticulum membrane but is also found to some extent in mitochondrial membranes.[35] SGPL1 is the only enzyme responsible for this irreversible degradation of S1P making it a key regulator of S1P levels. The enzyme is expressed and active in various tissues with the highest expression in the kidney, lungs, heart and brain.[36] It catalyzes the cleavage of S1P between the C2 and C3 bond releasing phosphoethanolamine and 2-trans-hexadecenal.[37] 2-trans-hexadecenal has been shown to induce cellular responses including cytoskeletal rearrangements, cell detachment and apoptosis.[38] In addition, fatty aldehyde dehydrogenase (FALDH) can convert 2-trans-hexadecenal to palmitic acid by reducing its double bond and oxidizing the carbonyl group, allowing it to re-enter the sphingolipid pathway via palmitoyl-CoA.[39] Phosphoethanolamine activated by cytidine 5'-diphosphate forms phosphatidylethanolamine (PE) by binding to diacylglycerol.[40] PE is a phospholipid that is abundant in plasma membranes and functions as a membrane anchor for several enzymes involved in lipid metabolism and as a neurotransmitter.[41]

1.1.2 Sphingosine-1-Phosphate Homeostasis: Gradients, Cellular Efflux and Carrier Proteins

S1P plays a central role in regulating numerous physiological and developmental processes. In particular, the natural gradient of S1P is critical. While S1P levels in plasma and lymph are relatively high in the micromolar (μM) range, S1P levels in tissues and other body fluids are only in the nanomolar (nM) range.[42,43] These gradients are essential for normal physiological functions. Hematopoietic stem and progenitor cells migrate from low S1P concentrations in extramedullary hematopoietic tissues to high S1P lymph.[44] In addition, lymphocyte trafficking relies on this S1P gradient. Lymphocytes migrate from relatively low-S1P concentrated lymphoid organs into the high-S1P bloodstream and lymph.[45,46]

Building and maintaining this gradient is critical since many critical processes are regulated by this S1P gradient. Three major cell types are responsible for the release of S1P. Erythrocytes maintain and regulate plasma S1P levels. They can take up circulating S1P, store it due to a lack of S1P-degrading enzymes and release it to maintain balanced plasma S1P levels.[45,47] When S1P export from these cells is blocked, plasma S1P levels are drastically reduced by up to 50%.[48] In addition, platelets store large amounts of S1P and release it upon activation.[49,50] Endothelial cells of various origins also contribute to S1P levels.[51–53]

To establish the concentration gradient and enable its extracellular signaling functions, S1P must be transported from the intracellular milieu of the cells where it is synthesized to the extracellular space. Several transport mechanisms have been identified for this S1P efflux. ATP-binding cassette (ABC) transporters are prominent facilitators of S1P efflux in various cell types. Among these, ABCC1 has been extensively studied and found to be present in numerous cell types. For example, Mitra *et al.* demonstrated ABCC1-mediated S1P efflux in mast cells, as evidenced by reduced extracellular S1P levels following transporter inhibition or downregulation using small interfering RNAs.[54] Similar findings have been reported in Langerhans cells,[55] brain and spinal cord endothelial cells[56] and fibroblasts.[57] Other ABC transporters involved in S1P transport include ABCG2[58] and ABCA1.[59,60] ABCA1 has been implicated in S1P efflux from erythrocytes, with reduced efflux observed upon inhibition by the transporter inhibitor glyburide.[59] Furthermore, ABCA1 has been identified to play a role in S1P efflux from astrocytes, as evidenced by reduced efflux in

ABCA1-deficient mice.[60]

The transporter spinster homolog 2 (SPNS2) also has critical functions in S1P efflux. Initially identified as an S1P transporter in zebrafish,[61] its knockout results in a mutant phenotype characterized by impaired heart development due to reduced extracellular S1PR signaling.[62] In mouse models, SPNS2 is primarily expressed in vascular endothelial cells.[63] Its knockout significantly reduces plasma S1P levels, ultimately leading to hearing loss and abnormal retinal capillary formation.[63,64] Detailed studies have revealed a proton- and sodium-independent transport mechanism for SPNS2 that relies on a central gating mechanism with an opening and closing mechanism,[65] ultimately facilitating S1P efflux by diffusion.[66]

In contrast, the orphan major facilitator superfamily transporter 2b (MFSD2B) regulates S1P efflux in erythrocytes and platelets through a proton gradient.[48,67] The deficiency of this transporter results in a decreased plasma S1P level of up to 54%, accompanied by massive S1P accumulation within the cells.[48] In addition, MFSD2B has been identified in MEDEP-E14 erythroid cells.[68] Due to their complementary functions, the knockout of both SPNS2 and MFSD2B transporters is embryonic lethal, highlighting the necessity of proper S1P efflux for vascular maturation, integrity and homeostasis.[69] MFSD2B knockout mice exhibit increased susceptibility to anaphylaxis, hemolysis, stress-induced erythropoiesis[48] and impaired platelet function and morphology due to reduced S1P efflux from platelets and erythrocytes.[70]

Once secreted, S1P has a relatively short half-life of approximately 15 minutes.[52] During this time, free extracellular S1P in plasma is dephosphorylated to sphingosine and reabsorbed by cells.[71] To ensure the stability of S1P in the bloodstream, it is transported bound to specific carrier proteins. These so-called lipoproteins carry various lipid components, such as cholesterol and triglycerides, ensuring their solubility and proper transport. These proteins are classified into different types based on their composition and size.[72] Approximately 30% of S1P in the bloodstream is bound to albumin[73,74] and 70% of S1P is associated with high-density lipoproteins (HDL) and low-density lipoproteins (LDL) with the majority bound to HDL. 5% of HDL is bound to apolipoprotein M (ApoM), which is essential for S1P binding, further highlighting the importance of HDL in S1P transport.[75,76] Isolation of plasma HDL showed S1P content only in ApoM-containing plasma and not in the ApoM-deficient HDL fraction. In addition, ApoM$^{-/-}$ mice showed no HDL-bound S1P, whereas ApoM overexpression led to an increase in HDL-bound S1P in mice.[75] ApoM is

expressed in liver hepatocytes and tubular epithelial cells of the kidney and is secreted into circulation. During the development phase expression in these cell types increases until strong expression and secretion are reached in adulthood.[77]

Different biological functions are observed depending on the chaperoning lipoprotein bound to S1P. HDL-ApoM-bound S1P is associated with several biological functions, including maintenance of endothelial cell barrier function,[78] protection against ischemia,[79] inflammation and development of type 2 diabetes.[80] In contrast, albumin-bound S1P is associated with increased activation of Gi-coupled receptors and receptor endocytosis.[81]

1.1.3 Sphingosine-1-Phosphate Receptor Signaling and Intracellular Pathways

S1P-Receptor Signaling

S1P signals extracellularly through five receptors that belong to the family of G protein-coupled receptors (GPCRs).[82] GPCRs demonstrate a definite structure comprising seven transmembrane domains fused by three interhelical loops on each side of the membrane, an extracellular amino-terminus and an intracellular N-terminus.[83] Binding of the ligand to the extracellular domain of the receptor results in conformational changes on the intracellular side and binding of three subunits of G-proteins, α, β and γ, of which the α-subunit is decisive for the triggered signaling pathway. Depending on the specific receptor conformation, the coupling to one of the four G_α-subunits is triggered: G_s, G_i, G_q, or $G_{12/13}$.[84] Upon binding of the heterotrimeric G-protein, the intracellularly bound guanosine diphosphate (GDP) on the α-subunit is replaced by guanosine triphosphate (GTP), resulting in receptor activation.[85] Each of the five S1P receptors (S1PR) displays unique signaling activity by binding to various subtypes of Gα proteins (Figure 2a). S1PR1 exclusively associates with G_i,[86,87] while S1PR2 and S1PR3 can signal through G_i, G_q, or $G_{12/13}$.[87] S1PR4 signaling is mediated through the binding of G_i[88] and $G_{12/13}$,[89] similar to S1PR5 signaling. Depending on the bound G_α-Subunits, different signaling pathways are activated (Figure 2b). The G_i-subunits activate a wide range of signaling pathways. They can trigger the activation of Mitogen-activated protein kinase (MAKP) through subsequent activation of Ras and Raf. This activation, in turn, activates the Extracellular signal-regulated protein kinases 1 and 2 (ERK1/2), ultimately controlling cell cycle and proliferation.[86,90] Moreover, either Rac1 or Akt signaling facilitated via Phosphoinositide-dependent kinase-1 (PDK1),

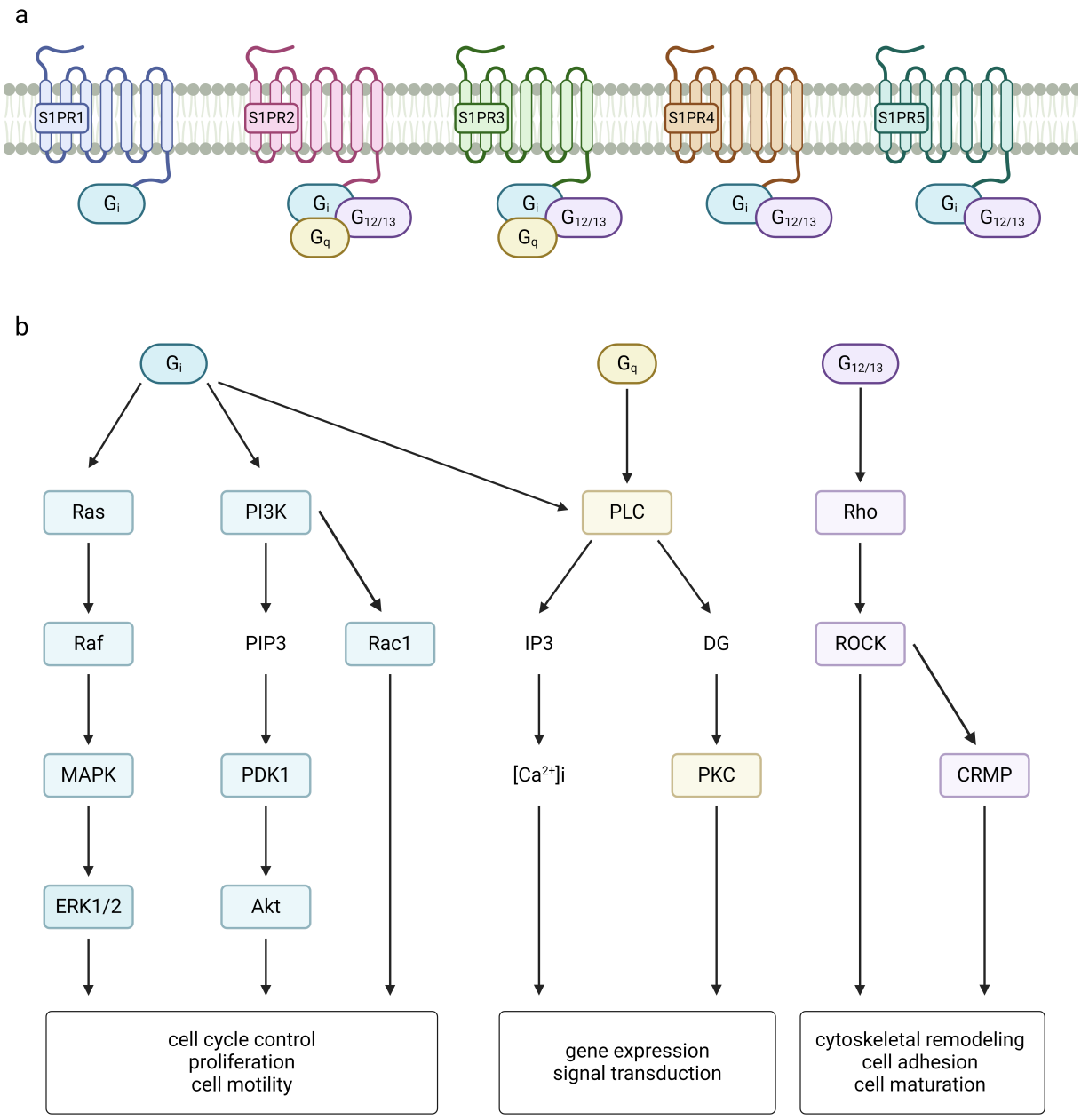

Figure 2: Schematic overview of S1P receptors and the corresponding signaling cascades.(a) S1P signaling is transduced through five G-protein coupled receptors, each associated with distinct G-protein α-subunits. (b) Different signaling pathways are activated depending on the associated Gα-protein, resulting in numerous effects on the cell. Created with BioRender.com

is activated by Phosphoinositide 3-kinase (PI3K) phosphorylation, which additionally affects the cell cycle and motility.[90–92] Both G_i and G_q can activate Phospholipase C (PLC). This causes phosphatidylinositol 4,5-bisphosphate (PIP2) to be cleave into inositol 1,4,5-trisphosphate (IP3) and diacylglycerol (DAG). Subsequently, cellular responses in Ca^{2+} are enhanced, activating Protein kinase C (PKC). This pathway can influence gene expression and subsequent signaling pathways.[90,92,93] $G_{12/13}$ activates the GTPase Rho, which impacts the Rho-associated protein kinase (ROCK). The latter acts on cytoskeletal remodeling, cell adhesion and cell maturation directly or through the Collapsin response mediator protein (CRMP).[92,94,95]

Intracellular S1P Signaling

While S1P is known for its receptor-mediated signaling through GPCRs, it also triggers receptor-independent signaling mechanisms as a second messenger. In the cytoplasm, S1P binds to tumor necrosis factor-alpha (TNFα) receptor-associated factor 2 (TRAF2), leading to ubiquitination of Receptor-interacting Protein 1 (RIP1) and subsequent activation of nuclear factor kappa-light-chain-enhancer of activated B-cells (NF-κB) gene expression.[96] This pathway is involved in the production of cathelicidin antimicrobial peptide (CAMP), which suggests a role in innate immune responses. In addition, S1P interacts with the heat shock proteins HSP90α and GRP94, highlighting its involvement in stress responses.[97] Cell survival is regulated by S1P-mediated activation of cytoplasmic atypical protein kinase (aPKC), which suppresses apoptosis and promotes cell survival in HeLa cells.[98] In endothelial cells, S1P binding to PGC1β activates peroxisome proliferator-activated receptor gamma (PPARγ) signaling, which promotes tube formation and vascular development.[99]

Intracellular S1P also affects calcium signaling. In endothelial cells, the S1P-dependent activation of PLC and IP3 leads to increased calcium influx and release from intracellular stores.[100] This mechanism triggered by photolysis of caged S1P has been observed in several cell types including HEK293, HepG2 and SKNMC cells.[101] In addition, S1P activates calcium transporters such as Transient receptor potential canonical 6 (TRPC6) in neuronal cells and TRPC5 in vascular smooth muscle cells, thereby increasing calcium influx and cell motility.[102,103]

S1P is additionally present in the nucleus, binding to histone deacetylases (HDAC1, HDAC2 and HDAC3).[104,105] This binding inhibits HDAC activity, increasing histone acetylation and

gene regulation at the epigenetic level.[105] S1P impacts the cell cycle control via p21 cyclin-dependent kinase expression, oxidative stress responses via NLRP3 expression and cardiac regeneration in neonatal mice via increased cardiomyocyte proliferation.[106,107] Furthermore, reduced intracellular S1P levels achieved by deletion of SPHK2 impair spatial memory and fear discrimination in mice.[108] S1P also stabilizes telomerase reverse transcriptase (TERT) through phosphorylation, thereby promoting telomere stability and cell proliferation, particularly in tumor cells. Decreasing cellular S1P levels by depleting SPHK2 reduces TERT stability and leads to cell senescence. Thus, targeting S1P-TERT binding may be a promising strategy for tumor therapy.[109] Within mitochondria S1P binds to prohibitin 2 (PHB2) to regulate mitochondrial assembly and function. Downregulation of intracellular S1P by SPHK deletion impairs complex IV assembly leading to impaired mitochondrial respiration.[110] In ischemia-reperfusion models, S1P protects mitochondrial function through PHB2 binding, demonstrating a cardioprotective role.[111]

S1P signaling involves both intracellular and extracellular pathways and affects a wide range of cellular mechanisms. Understanding these complex signaling networks is essential for unraveling S1P's diverse physiological and pathological roles.

1.1.4 Biological Functions of S1P in Physiology and Pathophysiology

S1P is a crucial bioactive lipid involved in immunity and inflammatory processes. The S1P gradient between the thymus, secondary lymphoid organs, blood and lymphatic fluid facilitates lymphocyte egress via S1PR1 with high circulating S1P levels driving this migration.[46,112] S1PR5 is particularly important for natural killer (NK) cell recruitment from lymph nodes and bone marrow. Stimulation of S1PR5 induces T-bet gene expression, which promotes cell egress.[113] Maintaining a proper S1P gradient is essential for immune function, as disrupting the S1P gradient can lead to immunosuppression.[46] Building on S1P's role in immune cell migration, its influence extends to cytokine expression and leukocyte recruitment, further highlighting its importance in immune responses. S1P influences the production of the pro-inflammatory cytokine interleukin-8 (IL-8), which enhances the chemotaxis of neutrophils.[114] The recruitment of leukocytes to organs is mediated by the S1P/S1PR3 signaling pathway in a P-selectin-dependent manner.[109]

This involvement in immunity and inflammation makes S1P a target for multiple sclerosis

(MS), a disease characterized by lymphocyte infiltration into the central nervous system. Four S1P receptor-modulating treatments are currently approved for MS therapy.[115] Fingolimod (FTY720), a modulator of S1PR1, S1PR3, S1PR4 and S1PR5 has been shown to prevent lymphocyte egress through S1PR1 internalization, which correlates to reduced lesion formation and relapse rates in MS.[116–118] Other approved treatments with similar efficacies in reducing MS relapses include the S1PR1 and S1PR5 modulating agents siponimod[119] and ozanimod[120,121] and the S1PR1 modulating agent ponsimod.[122] While the therapeutic potential of S1P receptor modulation in MS is well established, its involvement in neurodegenerative diseases like Alzheimer's disease further demonstrates the broad physiological effects of S1P. In neuronal cells, elevated levels of S1P are associated with Alzheimer's disease. S1P interacts with the beta-site amyloid precursor protein cleaving enzyme (BACE1) leading to the accumulation of amyloid-beta plaques. High levels of S1P interfere with the breakdown of precursor proteins and contribute to disease progression.[123,124]

Beyond its neurodegenerative implications, S1P's role in cardiovascular health, particularly atherosclerotic lesion development, reveals its multiple pathological relevance. S1PR3 influences atherosclerotic lesion formation, as demonstrated in an ApoE$^{-/-}$ atherosclerosis mouse model where receptor deletion increased lesion formation.[125] FTY720 has been proposed as an effective treatment that significantly reduces atherosclerotic lesion volume and macrophage recruitment.[126] Modulating macrophage and lymphocyte function by S1P and S1PR modulation may attenuate pro-inflammatory processes.[127] In a related cardiovascular context research on coronary artery disease (CAD) demonstrates the importance of S1P, particularly when bound to HDL. Higher levels of HDL-bound S1P correlated with milder forms of the disease compared to severe phenotypes with low S1P-HDL levels.[128]

HDL-S1P concentrations also play a central role in ischemic heart disease. Inverse correlations between S1P-HDL concentrations and the incidence of ischemic heart disease suggest a protective role for HDL-bound S1P.[129] Higher S1P levels are associated with better left ventricular ejection fraction and reduced dyspnea suggesting protection against adverse pathophysiological phenotypes.[130] Elevated S1P levels also have a protective effect against ischemia-reperfusion injury. However, decreased S1P levels are observed for up to two years after infarction.[131,132]

The impact of S1P is not limited to acquired conditions: genetic disorders related to

S1P levels, such as sphingosine phosphate lyase insufficiency syndrome (SPLIS), are characterized by mutations that affect S1P lyase function. This leads to accumulation of S1P.[133] Symptoms range from impaired motor function and muscle weakness[133] to adrenal calcification[134] and congenital nephrotic syndrome.[135,136] A similar phenotype has been observed in *Sgpl1*$^{-/-}$ mice making this a promising model to study processes during SPLIS and other conditions related to S1P dysregulation.[135] Anti-S1P monoclonal antibodies counteract these high levels of S1P, reducing lymphocyte trafficking and angiogenesis, suggesting potential treatments for S1P-related diseases.[137] In addition, *Sgpl1* gene replacement via gene therapy is showing promising effects. Incorporation of human Sgpl1 into the *Sgpl1*$^{-/-}$ mouse model using adeno-associated virus 9 successfully reduced S1P levels and symptoms. This highlights gene therapy as a possible successful future treatment.[138] The following sections will discuss the involvement of S1P in vascular and bone processes in more detail.

1.2 Blood Vessels

Highly organized and branched blood vessels constitute a system in the body that ensures the transportation of oxygen and nutrients throughout the body, supporting normal organ function and maintaining homeostasis. Consequently, waste products are cleared from the tissues.[139] Blood vessels consist of a thin layer of closely connected endothelial cells (ECs) forming the lumen. A basement membrane supports the vascular system and larger vessels are further reinforced with mural cells, including pericytes or smooth muscle cells.[140,141]

Depending on the microenvironment and specific organ, ECs exhibit unique traits that affect their molecular pattern and function. This heterogeneity enables them to influence neighboring cells and thus organ-specific processes.[139,142] In particular, the secretion of angiocrine growth factors plays an essential role in actively regulating organ-specific processes.[141] Therefore, the dysregulation of the vasculature can lead to various pathologies, such as cancer, inflammation or osteoporosis.[140]

1.2.1 Vascular Development: Vasculogenesis and Angiogenesis

De novo formation of the vasculature, also known as vasculogenesis, begins as early as embryonic day E7. A blood island, composed of endothelial and hematopoietic cells derived from mesodermal cells, develops in close proximity to the endoderm of the yolk sac (Figure 3a). A primary capillary network arises from this structure.[143–145] The maturation process of pre-existing vessels begins with the formation of an endothelial monolayer. Subsequently, a basement membrane and mural cell coverage are arranged until the vasculature reaches its quiescent state.[146,147]

Remodeling of the pre-existing vasculature occurs through sprouting angiogenesis (Figure 3b).[148] After matrix degradation and loss of mural cell coverage, a tip cell forms, projecting filopodia that facilitate migration into surrounding tissue and influence EC behavior. Through migration, a new sprouting vessel is formed. This newly formed vessel is constructed by stalk cells[149] with blood flow resulting in lumen introduction to the new sprout.[150] Once the sprout is established, it is secured by forming the basement membrane and mural cell coverage. Subsequently, ECs achieve quiescence again.[151]

Several signaling pathways and factors are involved in vasculogenesis, angiogenesis and vascular quiescence, including vascular endothelial growth factor (VEGF), platelet-derived growth factor (PDGF) and Notch signaling.[145,146] The roles of S1P and VEGF signaling are further discussed in detail below.

1.2.2 S1P Signaling: Implications in Vascular Development and Function

S1P plays a significant role in the process of angiogenesis and vascular development. Identified initially as endothelial differentiation genes (Edg), S1P receptors are associated with the ability to stimulate the formation of vessel-like structures in ECs.[152] During the developmental phase S1PR1 plays a key role, as evidenced by embryonic lethality and severe vascular malformations in mice lacking this receptor . EC S1PR1 signaling directly affects vascular coverage with vascular smooth muscle cells and impaired signaling leads to increased vascular leakage.[153] Furthermore, S1PR2 and S1PR3 counteract each other during vascular development. Although single-knockout animals for each receptor do not display a severe phenotype during development, it was demonstrated that the combined deletion of both receptors results in embryonic lethality accompanied by vascular

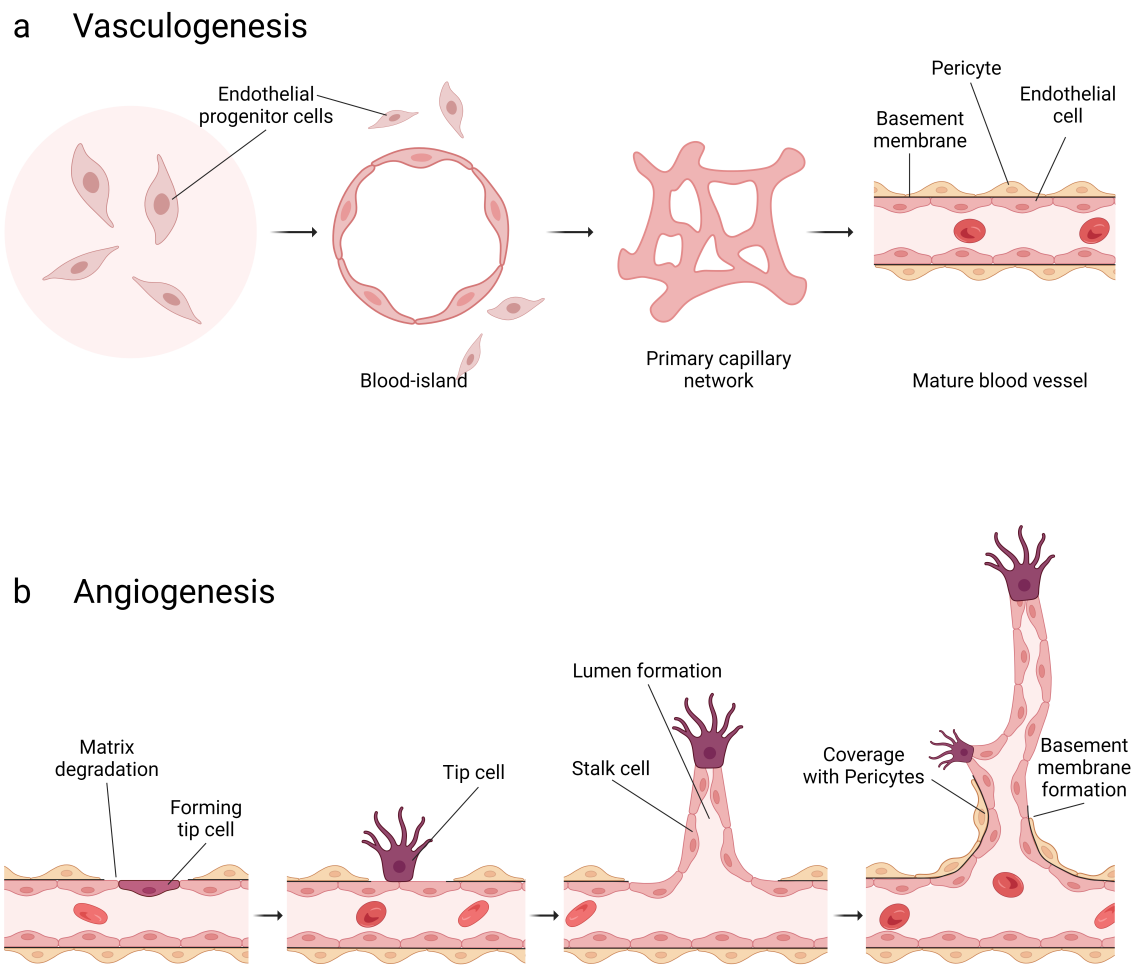

Figure 3: Schematic overview of *de novo* vessel formation and sprouting angiogenesis.(a) *De novo* formation of the vasculature (vasculogenesis) starts with the formation of endothelial progenitor cells during early embryonal development. Within the yolk sac, these cells form a blood island, which develops into a primary capillary network. Endothelial cells are covered with mural cells and a basement membrane develops until the mature vasculature is formed. (b) New blood vessels are formed from these pre-existing blood vessels by means of sprouting angiogenesis. The basement membrane is degraded and coverage with mural cells is interrupted once a tip cell starts to form. This tip cell then develops filopodia and grows out of the existing vessel, leading to lumen formation and forming a new vascular sprout through so-called stark cells. Newly formed vessels build a basement membrane and are covered with mural cells to reach their mature state. Created with BioRender.com

abnormalities and hemorrhages.[154]

Postnatally, S1P remains critical for maintaining vascular integrity and promoting blood vessel growth. S1PR1, S1PR2 and S1PR3 work together to achieve a balance in regulating sprouting angiogenesis. Specifically, S1PR2 and S1PR3 signaling, which activates Rho, promotes sprouting angiogenesis. This results in the formation of tip cells and cytoskeletal rearrangements that promote the stabilization of newly formed vessels.[155,156] In contrast, S1PR1 has been demonstrated to have a negative impact on vasculature sprouting and branching.[157,158] This can occur via direct S1P signaling or by activating S1PR1 through sheer stress, which shows a negative feedback loop to stop active angiogenesis once a suitable vascular network has formed.[159]

After establishing a proper vascular network S1P plays a crucial role in regulating endothelial barrier formation. Disruption of S1PR1 in mice leads to increased hemorrhage formation and early embryonic lethality due to defective endothelial barrier formation and insufficient coverage of the vasculature by smooth muscle cells and pericytes.[160] The formation of adherence and tight junctions regulates the endothelial barrier. In response to blood follow and circulating S1P, adherence junctions are established. A gradient is formed from high S1P in the maturing vasculature to low S1P in the growing vascular. This ensures the foundation of proper vascular junctions and stabilization once proper blood flow is established.[158] In S1PR1 knockout mice, this process is disrupted, which causes destabilized adherens junctions and impaired vascular barrier function.[158] Adherens junction proteins such as VE-cadherin and beta-catenin are critical mediators of S1P-induced vascular barrier function. Stimulation of human lung ECs with the S1P analog FTY-720S phosphate increased the distribution of these junction proteins within the intracellular space.[161] This VE-cadherin stabilization at the junction is mediated by S1PR1.[157] Disruption of S1PR1 signaling in human endothelial cells leads to decreased VE-cadherin stability.[162] While S1PR1 and S1PR3 promote adhesion junction assembly,[91] S1PR2 signaling disrupts adhesion junctions and increases vascular leakage.[163] S1P also influences the formation of tight junctions by activating zonula occludens 1 (ZO1) in an S1PR1-dependent manner.[164,165] Additionally, S1P regulated cell-cell interaction between endothelial cells and mural cells through modulation of N-cadherin activation and translocation in response to S1PR1 signaling.[166]

The integrity of the vascular barrier is crucial for normal physiological functions and plays a significant role in various pathological conditions such as ischemia, inflammation and

cancer.[167] Paul *et al.* identified a downregulation of the S1P transporter SPNS2 under inflammatory conditions, leading to dysregulated S1P levels and disrupted endothelial barrier functions.[168] Furthermore, S1P-mediated barrier function is linked to anaphylactic shock. Selective downregulation of S1P plasma levels correlates with worsened outcomes and impaired survival following anaphylactic shock, suggesting that S1PR1 agonist treatment could be beneficial.[169] In ischemic stroke, reduced S1P levels are associated with more severe brain injury. S1PR1 supports blood-brain barrier function, which is protective in ischemic stroke.[170]

In addition to its roles in vascular development and barrier integrity, S1P is also a critical contributor to tumor angiogenesis. In a mouse model of breast cancer, S1P has been shown to mediate angiogenesis. Lowering S1P levels using SPHK1 inhibition resulted in reduced tumor size due to inhibited angiogenesis.[171] S1PR1 signaling is associated with increased tumor angiogenesis and sprouting. A substantial increase in S1PR1 expression was observed in ECs within the tumor vasculature. Both the injection of S1PR1 silencing small interfering RNA (siRNA) and endothelial-specific knockdown of S1PR1 led to suppression of angiogenesis within the tumor, subsequently reducing tumor burden.[172,173] Additionally, treatment with S1PR1 antagonists or anti-S1P antibodies reduced tumor angiogenesis and tumor burden in a model of diffuse large B-cell lymphoma.[174] In contrast, S1PR2 is associated with the downregulation of tumor angiogenesis and growth. S1PR2 knockout mice exhibited increased tumor growth due to enhanced cell migration and angiogenesis after lung carcinoma or melanoma cell implantation.[175]

Beyond its role in angiogenesis and tumor growth, S1P is essential in regulating blood pressure and vascular tone. Specifically, the activation of endothelial nitric oxide synthase (eNOS) by S1P and the subsequent production of nitric oxide (NO) are potent regulators of blood pressure.[176,177] S1PR1 has been identified as a critical factor in regulating eNOS activity. In S1PR1 knockout mice a decrease in NO activity was observed accompanied by dysregulated and elevated blood pressure.[176] Additionally, S1PR2 and S1PR3 have been implicated in vasoconstriction and vasodilation. Nofer *et al.* reported increased NO release in ECs following S1P stimulation, ultimately leading to vasoconstriction. Evaluation of S1P's effect in S1PR3 knockout mice showed a 60% decrease in vasodilation capacity indicating the involvement of S1PR3 in this process.[178] Similarly, S1P-mediated constriction was observed in the basilar arteries of rats and mice, whereas this effect was absent in S1PR3 knockout mice further underscoring the role of this receptor.[179] S1PR2's

involvement was identified during vasoconstriction in hamster arteries. The vasorestrictive effect of phenylephrine was significantly decreased in the aortae of S1PR2 knockout mice highlighting the receptor's role in this process.[180] S1P regulates blood pressure, vasoconstriction and vasodilation through S1PR1, S1PR2 and S1PR3. This demonstrates the multifaceted involvement of these receptors in vascular function.

1.2.3 VEGFa Signaling in Blood Vessel Formation and Regulation

Vascular endothelial growth factor A (VEGFa) along with VEGF-B, VEGF-C and VEGF-D is part of a gene family crucial for lymphatic angiogenesis and vascularization.[181] VEGFa exists in four isoforms due to alternative splicing, each with different lengths of amino acid chains. The shortest isoform, $VEGFa_{121}$, is soluble, while the longest isoforms, $VEGFa_{189}$ and $VEGFa_{206}$, are bound to proteoglycans in the extracellular matrix (ECM). $VEGFa_{165}$, the most abundant isoform, can be found within the Golgi apparatus bound to ECM or diffusing inside the cell.[182,183] VEGF binds to the receptors VEGFR1/*Flt1*, VEGFR2/*Flk1* and neuropilin-1 (NRP1), significantly influencing vasculogenesis, angiogenesis and pathological conditions.[184]

VEGFR signaling is essential for developing the vasculature during embryogenesis and early postnatal stages. Even heterozygous deletion of the *Vegfa* gene disrupts blood vessel development and the formation of blood islands in the yolk sac, while homozygous deletion is embryonically lethal.[185,186] The highest expression of VEGFR2/*Flk1* occurs in early embryonic development in mice at embryonic day E7 indicating its crucial role in early vascular development. VEGFR2 is responsible for the organization of hemangioblasts and the formation of blood islands within the yolk sac.[187–189] During endothelial sprouting VEGFR2 activation drives the formation of EC filopodia and their migration to the growth front. Disruption of receptor signaling impairs sprouting, whereas increased receptor activation in a mouse model leads to enhanced filopodia formation.[190,191] VEGFR1 impacts vascular organization by governing the number of endothelial cell progenitors to ensure proper vessel formation.[187,192] Deletion of VEGFR1 results in embryonic lethality due to disorganized endothelial cells and abnormal vessel formation.[193] As this deletion is associated with an increase in EC proliferation, VEGFR1 signaling is mainly associated with negative regulation of angiogenesis.[194] Additionally, VEGFR1 signaling is related to

the regulation of sprout formation during angiogenesis. VEGFR1 loss leads to decreased formation of sprouts and therefore, reduced branching of the vasculature.[195] Furthermore, regulating VEGFR1 and VEGFR2 expression is a competent regulator of endothelial cell fate decisions towards tip or stark cells during angiogenesis.[196] Notably, NRP1 is a VEGF receptor that directly affects angiogenesis by binding to VEGFa. NRP1 also enhances VEGFa binding to VEGFR2, although VEGFa binding to NRP1 can inhibit EC growth by also preventing VEGFR2 binding, demonstrating its multiple roles.[197,198]

Beyond its role during development, VEGFa continues to influence vascular integrity and function in postnatal life and pathological conditions. Postnatally, inhibition of VEGFa has been shown to impair regular growth and organ development, increasing mortality due to reduced proliferation and survival of ECs. However, the dependency on VEGFa diminishes as ECs become quiescent and mural cell coverage is achieved.[199,200] Inhibition of VEGFR1 signaling results in endothelial alterations and impaired EC proliferation and survival during early postnatal days. However, blocking VEGFR1 four weeks postnatally shows no effects, indicating its predominant involvement in embryonic and early postnatal stages.[200]

In pathological conditions, VEGFa significantly influences inflammation, wound healing and tumor vasculature by regulating vascular permeability. VEGFR2 activation increases the expression and secretion of cell adhesion molecules ICAM1, VCAM1 and E-Selectin enhancing leukocyte adhesion and migration through the endothelial barrier.[201,202] VEGF signaling through VEGFR2 leads to phosphorylation of VE-cadherin and disruption of the VE-cadherin/beta-catenin complex in endothelial junctions, enhancing vascular leakage.[203,204] VEGFR1 signaling enhances monocyte recruitment and migration in inflammatory processes.[205,206] During regenerative processes such as wound healing, increased VEGFa levels lead to the formation of microvascular structures due to enhanced angiogenesis.[207,208] Similarly, VEGFa treatment after occlusion of the left circumflex coronary artery increases collateral blood flow and the formation of intramyocardial vessels during recovery.[209]

Furthermore, VEGFa signaling promotes tumor vascularization and growth.[210] Comparing VEGFR1 and VEGFR2 expression levels in the vasculature in colorectal cancer metastases in the liver compared to the healthy surrounding vasculature revealed increased expression in these ECs.[211] Additionally, enhanced expression of these factors was observed to be connected to metastasis occurrence and cancer progression.[212] Targeting VEGFa signaling has shown to be promising in cancer treatment. VEGFR2 inhibition reduces cell viability

and increases apoptosis in tumor endothelial cells, thereby reducing tumor growth.[213] VEGFa blockade using anti-VEGFa antibodies similarly reduces tumor angiogenesis and growth.[214–216] Deleting VEGFa in cervical cancer cells also demonstrates antiangiogenic effects.[217]

The involvement of VEGFa signaling in both vascular development and the regulation of postnatal vascular regeneration in pathologies and regeneration underlines its importance in numerous biological processes.

1.3 Bone

Bones form the basic framework of the body, providing essential structural support and protecting internal organs. They also support muscle movement and help maintain physical mobility. Bones are the primary source and storage site for crucial minerals such as calcium and phosphates, thereby significantly maintaining mineral balance within the body. Furthermore, bones also store and release numerous growth factors.[218,219]

There are two primary bone structural types: cortical and trabecular.[220] Cortical bone is densely packed, making up 80% of all skeletal mass with high resistance. It forms the outer part of all bones and primarily contributes to the stability of the bone. Trabecular bone constitutes the remaining 20% of bone mass. Trabecular bone is found inside long bones and larger flat bones. It has a less dense and, therefore, more elastic structure. It features a thinner, more branched shape, making 80% of the bone surface trabecular. As it performs the primary metabolic functions of the bone, a high turnover rate is observed, characterized by continuous bone remodeling.[219,221]

Structurally, bone is composed of type I collagen fibers with a lamellar organization. In cortical bone, concentric lamellar formations are evident, whereas in trabecular bone these structures are parallel, defining the compactness of each bone.[219] Additionally, intercalated non-collagenous proteins like proteoglycans, Gly-proteins and Gla-proteins can be found, further enhancing the distinct properties of bones. The calcified, inorganic matrix that contributes to the hardening of bone is made up of hydroxyapatite, which is present in both collagen and matrix structures.[222]

1.3.1 Osteogenesis during Development: From Mesenchymal Stem Cells to Bone Formation

During development, bone forms in two different ways. Intramembranous ossification occurs primarily in flat bones such as the skull and is characterized by the direct condensation of mesenchymal cells into mineralizing osteoblasts (OBs).[223] Endochondral bone formation, as shown in Figure 4, is the more common and the more complex process of bone development. During long bone formation, mesenchymal cells aggregate and then differentiate into chondrocytes. These cells produce collagen and aggrecan and establish a scaffold of hyaline cartilage (Figure 4a). Chondrocytes enter their hypertrophic, non-proliferative phase in the center of this scaffold. This mechanism is linked to the recruitment of blood vessels and the regulation of OB differentiation, initiating the apoptosis of hypertrophic chondrocytes. Subsequently, OBs secrete bone matrix, creating a periosteal bone collar (Figure 4b). This ultimately leads to the formation of a primary ossification center as cells and blood vessels invade the center of the hyaline cartilage. This is coupled with ongoing matrix formation (Figure 4c).[224] Hematopoietic stem cells infiltrate the bone matrix and begin to develop into bone marrow, which expands during bone formation. At the same time, chondrocytes either continue to proliferate at the ends of the scaffold, promoting greater bone growth or form a columnar structure. Chondrocytes undergo hypertrophy at the outer border of these columns and resorb the calcified cartilage matrix. This process attracts blood vessels toward the site and promotes OB formation, resulting in the development of secondary ossification centers in the later epiphyseal regions of the bone (Figure 4d).[225] Once the bone matrix is established in these areas, including the central diaphyseal region of the bone, longitudinal growth occurs solely through chondrocyte proliferation within the epiphyseal growth plate (Figure 4e). The growth plate disappears at maturity, leaving an epiphyseal line between the epiphysis and the trabecular metaphysis.[226] The fully developed bone is framed by compact bone in its diaphyseal region, known as the corticalis. It gives the bone stability and is lined by the periosteum. The bone marrow and bone marrow vasculature are found in the medullary cavity of the diaphysis, ensuring adequate oxygen and nutrient supply (Figure 4f).[223,225]

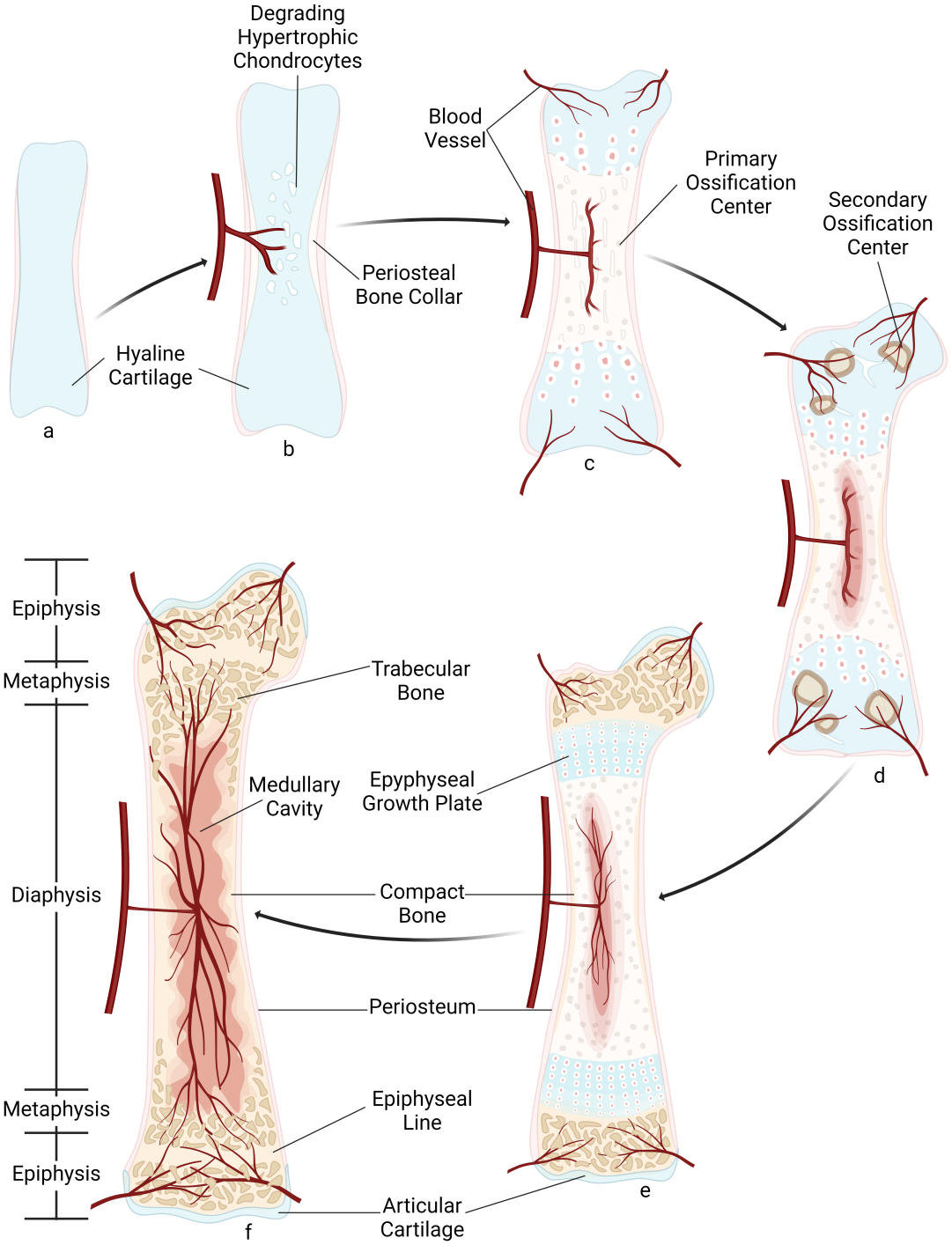

Figure 4: Schematic overview of endochondral bone formation.(a) During early development, a hyaline cartilage mold serves as a scaffold for bone development. (b) A periosteal bone collar is built and blood vessels migrate into the bone ensuring nutrient supply. (c) The primary ossification center is built within the center of the scaffold and (d) secondary ossification centers are built within the epiphyseal regions. (e) As endochondral ossification progresses, trabecular bone fomes within the epiphyseal and metaphyseal regions of the bone, (f) compact bone stabilizes the diaphysis. Blood vessels expand and the medullary cavity gives space for the bone marrow. Created with BioRender.com

1.3.2 The Bone Marrow Niche: Regulation and Maintenance of Bone Homeostasis

Osteoclasts (OC) and osteoblasts (OB) are the primary cell types responsible for maintaining bone homeostasis. OBs, as bone-forming cells, originate from mesenchymal stem cells (Figure 5). Runt-related transcription factor 2 (RUNX2) is recognized as a crucial factor that stimulates OB differentiation from these stem cells. If RUNX2 is absent, it can hinder OB maturation and prevent ossification.[227,228] Furthermore, the absence of Osterix (OSX), which operates downstream of RUNX2, diminishes OB differentiation and hinders matrix mineralization, highlighting its role in osteoblastogenesis and OB function.[229] Moreover, Wnt signaling has a central function in embryonic bone development. Beta-catenin, a principal controller of canonical Wnt signaling, is indispensable for OB differentiation from mesenchymal stem cells. Disruption of Wnt signaling results in impaired bone formation by preventing OB differentiation.[230,231] Once maturation is completed, OBs secrete a collagen matrix and initiate the mineralization of the bone. As soon as this mineralization is terminated, OBs become apoptotic or differentiate into bone-lining cells or osteocytes. Matrix-enclosing of mature OB thereby leads to the initiation of osteocyte differentiation.[232,233] Consequently, the resulting oxygen tension further pushes osteocyte maturation.[234] Matrix metalloproteinase MT1 (MT1-MMP) and Transforming growth factor β (TGFβ) signaling initiate the reprogramming and development of mature osteocytes. After their differentiation, these cells reside in the bone matrix and regulate bone homeostasis.[235] Unlike other bone cells, OCs are derived from hematopoietic stem cells that primarily enter the monocyte/macrophage lineage driven by macrophage colony-stimulating factor (M-CSF) (Figure 5).[236,237] Their lineage commitment is determined by c-Fos, a crucial regulator of OC and dendritic cell differentiation.[238] The transcription factor PU.1 drives the development of mononucleated pre-osteoclasts during ongoing osteoclastogenesis.[239] This process is enhanced by M-CSF and Receptor activator of NF-κB Ligand (RANKL) binding.[240] Pre-osteoclast fusion, governed by RANKL and NF-κB, ultimately creates multinucleated, bone-resorbing OCs.[241–243]

Bone is a highly dynamic tissue that relies on constant remodeling and renewal. This process is a tightly controlled interaction between bone formation and resorption. During bone formation, bone synthesis occurs in two main steps: First, an organic bone matrix is deposited at the site of bone formation. This so-called osteoid matrix consists of collagen proteins, mainly type I collagen and non-collagenous proteins such as osteonectin and

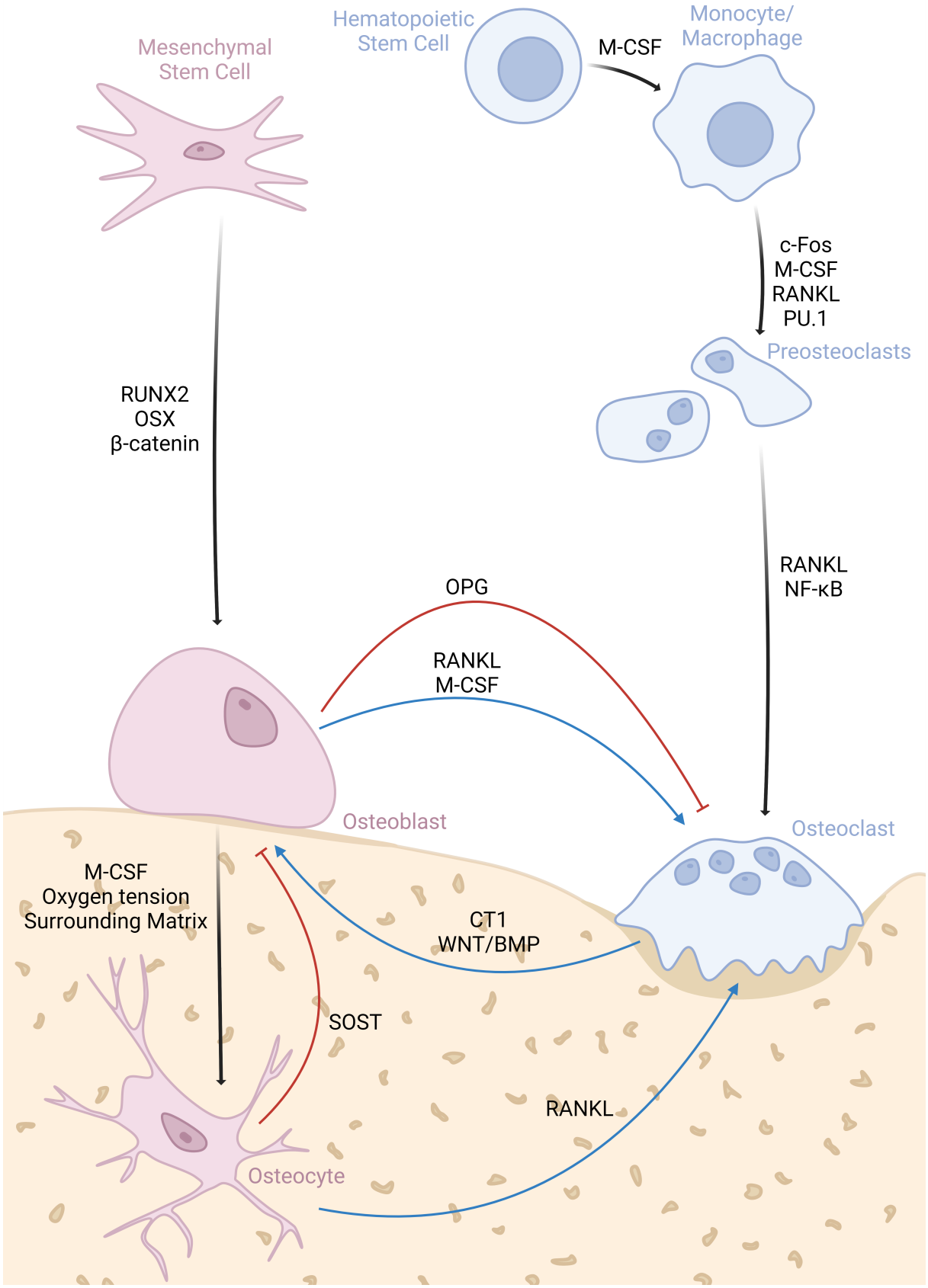

Figure 5: Schematic overview of cell differentiation and bone homeostasis. Mesenchymal stem cells differentiate into osteoblasts and subsequently osteocytes. Hematopoietic stem cells differentiate into monocytes and macrophages and specific transcription factors drive their differentiation into pre-osteoclasts. These pre-osteoclasts fuse to form mature osteoclasts. To ensure bone homeostasis, cells within the bone rely on intense crosstalk. Created with BioRender.com

osteopontin.[244] Second, the osteoid is mineralized. OBs, chondrocytes and odontoblasts produce matrix vesicles, which release hydroxyapatite crystals into the extracellular space. These crystals ultimately form the inorganic mineralization components within the collagenous matrix.[244,245] Bone resorption is driven by OCs. The release of protons between these cells and the bone surface forms an acidic resorption compartment. These protons allow the inorganic matrix compounds, the hydroxyapatite crystals, to be solubilized and release calcium and phosphate compounds.[246,247] In addition, pH-sensitive acid proteases are released by OCs into the acidified resorption compartment, resulting in the digestion of the organic bone matrix.[248]

During normal bone homeostasis, cells within the bone influence each other to maintain a balance between bone resorption and formation, enabling proper bone function, stability and repair (Figure 5). OBs can enhance osteoclastogenesis and bone resorption by secreting M-CSF, which in turn stimulates the formation of pre-osteoblasts and the subsequent maturation of OCs.[249] Moreover, M-CSF enhances OC mobility, proliferation and survival, improving bone resorption.[250,251] Additionally, OBs are a significant source of RANKL, accelerating their ability to promote pre-osteoclast formation and fusion to mature OCs.[252] However, OBs stimulate osteoclastic bone resorption and can potentially hinder RANKL-mediated osteoclastogenesis via secreting osteoprotegerin (OPG).[243] OPG directly interferes with differentiation towards pre-osteoclasts and the further ability of fusion to form mature OCs by disrupting cell-cell contacts.[253,254] In addition, it should be noted that OPG affects the ability of OCs to resorb bone. This is achieved by OPG binding directly to RANKL, ultimately blocking the necessary cytoskeletal rearrangements required for resorption.[255] As osteoblastic cells are the primary source of OPG, the importance of regulation is further strengthened through OPG knockout in OBs. In the absence of OPG inhibition, mice with this mutation showed increased bone resorption, resulting in reduced bone mass.[256,257] Osteocytes, the cells of osteoblastic origin, have gene expression patterns similar to those of OBs. Osteocytes, like OBs, secrete RANKL, which promotes the formation of OCs and bone resorption. Moreover, animal models with a selective RANKL deficiency solely in their osteocytic cells have a reduced number of OCs and a consequent increase in bone density.[258,259]

The bone resorption capacity is influenced not only by the surrounding cells but also by bone formation capacity. As osteocytes develop once adequate bone mineralization is achieved, increased sclerostin (SOST) expression can be observed within these cells.

SOST has been shown to regulate bone mineralization by inhibiting OB differentiation and further matrix formation.[260,261] In contrast to osteocytes, OCs have a positive effect on bone-forming cells. Particularly during bone repair, proper recruitment of OBs to the site of bone resorption is essential. OCs attract these cells by secreting S1P and bone morphogenic protein 6 (BMP6), further stimulating bone formation and matrix secretion via Wnt/BMP signaling.[262] In addition, cardiotrophin 1 (CT-1), an upstream activator of RUNX2, is secreted by OCs, leading to enhanced OB differentiation and maturation. The beneficial effect of CT-1 was further demonstrated by a reduction in bone mass in mice lacking this protein.[263]

1.3.3 Osteoporosis and Treatment Options

Once bone homeostasis is disrupted, dysregulation can lead to osteoporosis. Osteoporosis is a severe skeletal disease and is characterized by reduced bone mineral density (BMD) and elevated fracture risk.[264] It is associated with frequent hospitalizations and slow or often failed recovery.[265] Although osteoporosis is also diagnosed in men, it is more common in women and more prevalent in older people. In Germany, in 2015, about 24% of women and 5.6% of men over the age of 65 years were found to be affected by osteoporosis.[266] A similar occurrence was observed in the United States of America in 2017, where overall 19.6% of women and 4.4% of men were diagnosed with osteoporosis, reaching up to 27.1% in women over the age of 65. In recent years, these incidences are steadily increasing.[267]

The most commonly used osteoporosis treatments are bisphosphonates, of which zoledronate, alendronate, risedronate or ibandronate are the most frequently used. All of these have been shown to significantly reduce the risk of osteoporotic fractures by increasing BMD. Long-term use was associated with a low incidence of side effects. These treatments are usually given for several years, followed by a treatment break.[268–271]

Another commonly used antiresorptive agent is denosumab, a monoclonal antibody against RANKL. Blocking RANKL blocks osteoclast-mediated bone resorption and dramatically reduces the number of OCs.[272] Long-term treatment has been shown to significantly increase BMD and reduce the number of osteoporotic fractures.[273] After a treatment break of 48 months, BMD values return to pre-treatment baseline levels.[274]

As osteoporosis is most common in postmenopausal women after estrogen levels have declined, hormone replacement therapies are employed as well. Raloxifene is an estrogen receptor modulator that, like the other known treatments, reduces fracture prevalence and increases BMD.[275] Similar effects are seen with tibolone treatments, which have estrogenic and proestrogenic effects.[276]

In addition to the commonly used antiresorptive agents, anabolic agents are becoming increasingly important. Teriparatide, as a parathyroid hormone (PTH) analog, stimulates OBs and thus leads to increased bone formation, ultimately resulting in increased BMD and reduced fracture prevalence. In addition, an increase in serum calcium levels has been observed.[277,278] After one year of treatment, there are no further effects and a combination with other therapies is needed to further strengthen the bone.[279] Like teriparatide, abaloparatide activates the parathyroid hormone type 1 receptor, thereby inducing bone formation. This results in increased BMD, fewer fractures and reversal of hypercalcemia.[280] Romosozumab has a different mechanism of action. It binds the osteoblast inhibitor SOST, thereby activating osteoblastic bone formation. An increase in bone formation markers is observed,[281] leading to increased trabecular thickness and connectivity.[282] However, the increase in bone formation markers is accompanied by an increase in bone resorption markers. This leads to an overall reduction in bone remodeling.[281]

Despite the availability of several treatment options, the challenge of managing osteoporosis is becoming more challenging as the number and incidence of osteoporotic fractures increase each year. Frequently, not all treatment options are available to all patients and not all patients respond to available treatments.[283] The most commonly used bisphosphonates only result in a slight increase in BMD and a decrease in fracture incidence. In addition, they only act as antiresorptive agents. More anabolic treatment options are needed to properly treat osteoporosis in the future.[284] Therefore, it is essential to better understand the processes involved in bone remodeling and identify potential targets for new treatments.

1.3.4 Post-Traumatic Osteomyelitis

While osteoporosis is primarily characterized by the weakening of bones due to reduced bone density, other critical aspects of bone regeneration include injuries and infections,

such as post-traumatic osteomyelitis. Post-traumatic osteomyelitis is a severe infection of the bone that occurs following bone trauma resulting from injury or surgery. This condition is often associated with bacterial infections affecting the bone and bone cells, with *Staphylococcus aureus* (*S. aureus*) being the predominant causative organism.[285,286] In particular, infections with methicillin-resistant *S. aureus* strains present significant challenges to antibiotic treatments.[287] The infection can be characterized by various aspects, involving direct invasion of bacterial cells in the surrounding tissues, including ECs and cells within the bone niche such as OBs, OCs and osteocytes.[288,289] The internalization of bacterial cells within OBs and osteocytes presents a demanding challenge as these cells undergo a phenotypic switch, serving as reservoirs for persistent infections.[290–292] Additionally, these colonies are resistant to various therapeutic interventions and immune responses. After the death of the host cell, reinfections frequently occur as bacterial cells are released into the surrounding tissue.[291] Moreover, *S. aureus* internalization within OCs leads to intracellular proliferation and propagation of bacterial cells.[293] Biofilm formation within the infected region further complicates the situation, as these biofilms exhibit reduced susceptibility to antibiotic penetration and immune responses, leading to further difficulties in treatment.[286] Additionally, bacterial colonies invade the long bone and position themselves in close proximity to osteocytic lacunae within the cortical bone, providing mechanical protection for the colonies.[294,295]

Diagnosing osteomyelitis is challenging and influenced by factors such as the site of infection, time since the onset of infection and previous surgeries.[296] Additionally, various risk factors, including age and pre-existing conditions like diabetes, can impact disease diagnosis, progression and treatment outcomes.[297,298] The treatment typically involves a combination of antibiotic therapy and debridement of the infected site.[298,299] However, the success rate varies, reaching around 53%, with studies emphasizing the effectiveness of the combined approach.[298,300] Nonetheless, after debridement, a reduction in bone regeneration accompanied by increased osteoclastogenesis has been observed, complicating the overall treatment strategy.[301] These challenges emphasize the complexity of treating bacterial infections in osteomyelitis sites and achieving proper bone regeneration. This underlines the need for improved treatment options.

1.3.5 S1P Signaling in Bone: Implications for Physiology and Therapeutics

S1P has been described to play several roles in bone development and metabolism. OCs, the primary cells responsible for bone resorption, were shown to express S1PR1-3. Conditional S1PR1 knockout in OCs and monocytes led to the development of an osteoporotic phenotype. It has been demonstrated that S1P regulates OC migration and motility by signaling through this receptor. This leads to an increased number of OCs on the bone surface and therefore increased bone resorption.[302] In contrast, S1PR2 knockout in OCs leads to osteopetrosis due to reduced bone resorption. This effect was mimicked by treatment with the S1PR2 antagonist JTE013 and caused by a reduced number of OCs on the bone surface.[303]

In OBs, S1P has been shown to enhance mineralization through upregulation of alkaline phosphatase (ALP) and OPG expression, mediated by the PI3K/Akt pathway.[304] S1PR1 signaling enhances OB proliferation and S1PR2 plays an essential role in the recruitment and differentiation of OB progenitors.[305,306] Global S1PR2 knockout mice develop an osteoporotic phenotype. Osterix and PParγ expression are regulated by S1PR2 signaling, thereby regulating osteoblastogenesis.[307] In contrast to S1PR2 knockouts, S1PR3 knockout mice develop an osteoporotic phenotype only with increasing age. Keller textitet al. showed reduced bone volume in these mice at eight months of age. In addition, S1P has been shown to induce calcification and matrix secretion in OBs via S1PR3.[308,309]

Previous studies have shown a close relationship between OBs and OCs.[310] OCs have been shown to regulate SPHK1 expression through intracellular cathepsin K levels, a protein highly involved in bone remodeling and resorption. The elevated S1P levels in OC supernatants have been shown to subsequently lead to OB mineralization.[311] Furthermore, S1P has been shown to induce OPG expression in OBs, inhibiting osteoclastogenesis.[307]

S1P affects bone formation and homeostasis at the cellular level and has also been implicated in the development and progression of osteoporosis. Most studies in patients with osteoporotic fractures show a negative correlation between plasma S1P levels and fracture prevalence. Furthermore, high plasma S1P levels correlate with poor response to bisphosphonate treatment.[312] BMD measurements and trabecular bone score negatively correlate with plasma S1P.[313–315] This may be explained by the positive correlation between plasma S1P and bone resorption markers in osteoporotic patients.[313] In contrast, the population-based SHIP-Trend study showed a positive correlation between plasma S1P,

bone formation markers and plasma calcium levels. PTH was shown to be negatively correlated with S1P levels.[307] As there are conflicting results on the association of plasma S1P levels with the development of osteoporosis, an influence of bone marrow S1P levels has been proposed as an essential factor. The level of S1P in the bone marrow has been shown to be significantly reduced in patients with osteoporotic fractures . Therefore, Kim *et al.* proposed the plasma-to-bone marrow S1P ratio as a critical factor in bone metabolism rather than plasma S1P alone. As bone marrow S1P levels have been shown to be reduced in patients with osteoporosis, the result is an increase in plasma/bone marrow S1P levels.[316]

These studies show that the mechanism of S1P in human bone metabolism is not yet fully understood. More detailed investigations are needed to fully understand S1P's potential as a biomarker for osteoporosis.

1.3.6 The Role of the Bone Microvasculature in Bone Physiology

Not only have bone-forming cells been shown to play an important role in bone homeostasis, but the surrounding tissues also appear to influence the strength and mass of bone. As early as in the 1960s, a specific vascular phenotype within the bone marrow was described as being associated with osteogenesis.[317] In recent years, this unique vasculature has received renewed attention. Ramasamy *et al.* described these vessels in detail and were able to associate unique pro-osteogenic properties with them. Within the bone marrow, two subsets of endothelium have been described. Due to their low marker expression, the diaphyseal capillaries with intermediate Endomucin and low CD31 expression are referred to as L-type vessels. They make up the majority of the bone vasculature. The so-called H-type vessels show a high expression of both endothelial markers. They are associating with osteoprogenitor cells and therefore stimulate an increase in bone mass, suggesting a coupling role of ECs and OB proliferation.[318,319]

Several factors influence the formation of the H-type vasculature. The phenotype of ECs is intrinsically influenced by EC integrinβ1 and lamininα5. Loss of these factors in ECs has been shown to reduce the abundance of H-type ECs and consequently reduce bone volume.[320] In addition, the endothelial phenotype is influenced by osteogenic cells. OCs have been shown to significantly impact the formation of H-type vessels through PDGF-BB

secretion.[321] OBs have also been shown to influence angiogenesis. Secretion of PDGF and VEGFa positively affect angiogenesis of the bone marrow endothelium, whereas CXC ligand 9 (Cxcl9) and mammalian target of rapamycin complex 1 (mTORC1) lead to normalization of the vasculature.[322,323] In addition, osteoblastic slit guidance ligand 3 (Slit3) is required for H-type vessel formation.[324]

Furthermore, it has been shown that several pro-osteogenic factors are secreted by bone marrow endothelial cells (BMECs), mainly in the H-type vasculature. When these factors are reduced, severe bone malformations can be observed during development.[325,326] Kusumbe *et al.* demonstrated differential expression of several growth factors within the H-type vasculature compared to the L-type vasculature, namely *Pdgfa*, *Pdgfb*, *Fgf1* and *Tgfb1*, which are associated with bone morphology and development. It was also observed that the proportion of H-type vessels is reduced and the distinct expression pattern is lost with age. Thus, the association of osteoprogenitor cells with the vasculature decreases.[318] These observations suggest an interplay between BMECs and surrounding osteogenic cells, regulating bone development and homeostasis.

1.3.7 VEGFa Signaling in Bone: Regulation and Implications for Bone Health and Regeneration

One of the factors known to couple angiogenesis and osteogenesis is VEGFa. In particular, $VEGFa_{165}$ has been shown to play an important role in blood vessel recruitment to the primary ossification center and perichondrium during bone formation. Additionally, it directly affects the recruitment of OBs to the site of active bone formation.[327] Blockade of VEGFa signaling during development results in the impaired vascular invasion reduced chondrocyte recruitment and differentiation and cartilage zone elongation. These defects ultimately result in decreased trabecular bone formation.[328] Conditional knockout of VEGFa in chondrocytes showed that blood vessel attraction to the primary ossification center is chondrocyte dependent and that changes in the hypertrophic chondrocyte zone are the result of reduced chondrocyte survival.[329] Furthermore, ongoing VEGFa expression could be positively correlated with ongoing bone formation, with peak expression occurring shortly before maximum bone formation is reached.[330] Bone matrix formation has also been shown to be dependent on VEGFa. At the site of bone formation, VEGFa acts

as a chemoattractive cue for mesenchymal progenitor cells, which then proliferate and differentiate into OBs.[327,331,332] Continued VEGFa stimulation increases matrix secretion and nodule formation in these cells. VEGFR1- and VEGFR2 signaling enhances ALP activity and calcium secretion.[333,334] Conditional knockout of VEGFa in OBs decreased bone mass due to reduced osteoprogenitor numbers and mineralization. Similarly, the blockade of VEGFR1 and VEGFR2 has been shown to result in reduced bone density.[335,336] Osteoblastic VEGFa plays a central role not only in endochondral bone formation but also in intramembranous bone formation. This was demonstrated by reduced mandibular and calvarial bone mass after VEGFa knockout in osteoblastic cells.[337]

The influence of VEGFa on OCs has been studied only to a limited degree. Nakagawa *et al.* showed a positive impact on OC survival and increased bone resorption, probably mediated by VEGFR1 and VEGFR2 signaling.[338] Furthermore, upregulation of RANK expression in OCs directly and secretion by ECs was observed upon VEGFa treatment. This further leads to an increase in OPG expression and stimulation of bone remodeling.[339,340]

Because of its influence on multiple cells involved in bone formation and repair, the potential of VEGFa-mediated bone healing has been extensively studied. Several animal studies have already demonstrated a positive effect of VEGFa on bone formation, mainly in bone defect models. Administration via VEGFa-expressing fibroblasts or a matrix containing a VEGFa-expressing plasmid to the site of a bone defect resulted in enhanced bone healing. Not only ossification but also vascular invasion at the defect site was increased, demonstrating a close relationship between VEGFa, vascular invasion and bone healing.[341,342] Blocking VEGFa during bone healing with a VEGFa-blocking antibody also confirmed the positive effect. Once VEGFa signaling is blocked, bone healing is impaired.[343]

In mice with genetically increased Hif1a levels due to blocked degradation, an increase in VEGFa was observed. Furthermore, these mice are resistant to ovariectomy-induced bone loss, suggesting a close link between the development of osteoporosis and VEGFa expression.[344] To support this, Yao *et al.* described exercise-induced changes in bone mass in rats. They identified a VEGFa-dependent increase in bone vascular density, followed by an increase in BMD.[345]

The relationship between VEGFa levels and osteoporosis remains controversial in humans. Cebi *et al.* compared VEGFa plasma levels in osteoporosis patients and healthy controls and found no differences between the groups.[346] In addition, a study correlating VEGFa plasma levels in 152 postmenopausal women with BMD found no correlation.[347] In

contrast, Senel *et al.* found a correlation between BMD and VEGFa plasma levels and a reduction in VEGFa plasma levels in osteoporosis patients compared to age-matched healthy subjects.[348] Similar correlations were found in a study comparing pre-, peri- and postmenopausal women. Histomorphometric analysis showed a positive correlation between VEGFa expression, osteoanabolic markers and bone density in these women. Resorption markers were negatively correlated with VEGFa expression.[349]

As there is a close link between VEGFa and bone formation, targeting VEGFa for osteoporosis and bone regeneration treatment seems promising. However, as there are still controversial findings regarding the influence of VEGFa in osteoporosis, further studies are needed.

2 Research Aim

Given that bones are essential for mobility and structural support, the proper functioning of bone remodeling and homeostasis is essential. As seen in osteoporosis, disruption of these processes contributes to reduced bone stability and increased fracture susceptibility. Despite the availability of several treatment options, the increasing incidence of osteoporotic fractures and variability in patient response highlight the need for new innovative and targeted therapies. In addition, deregulation of bone homeostasis due to defects such as post-traumatic osteomyelitis may result in impaired bone healing capacity. Frequently used treatment regimens include surgical removal of the infected bone tissue and antibiotic treatment. However, impaired healing of the defect area is often observed. These issues need to be addressed to improve patient care and treatment options.

Recent research identified an association between a specific type of bone vasculature, the H-type vessels and bone density. This suggests an important interplay between bone marrow endothelial cells and osteogenic cells in regulating bone development and homeostasis. While this relationship has primarily been investigated during developmental stages, this study aims to extend the understanding of this crosstalk by assessing the functional role of the pro-osteogenic vasculature in relation to bone remodeling.

The central aim of this study is to understand the role of S1P – a factor known to influence both osteogenesis and angiogenesis – in the crosstalk between the bone vasculature and osteoblasts. To investigate the influence of S1P signaling on vessel-bone-crosstalk *in vivo*, global S1P levels are increased in mice. Two approaches are used to increase S1P levels: pharmacological inhibition of S1P lyase, the enzyme responsible for the irreversible degradation of S1P, using 4-deoxypyridoxin (DOP) and genetic deletion of the same enzyme. Assessing bone vasculature, bone formation and bone strength aims to unravel the S1P-dependent links between these processes. At the cellular level, primary osteoblasts (pOBs) and bone marrow endothelial cells (BMECs) are used to study the underlying processes and to reveal the signaling pathways involved. Therefore, these cells are cultured under several conditions and receive various treatments, including S1P, S1PR antagonists and specific pathway-blocking antibodies. In addition, the study is investigating the role of S1P receptors by using S1PR2 and S1PR3 knockout mice, providing insights into the specific receptors involved in the observed effects.

To translate the observed S1P-mediated effects during bone homeostasis to a post-traumatic osteomyelitis bone defect model, mice harboring a bone defect are treated with DOP and the bone healing capacity is evaluated. Additionally, S1P effects are tested on human bone samples to ensure a translation of this research also to human mechanisms. This approach will not only improve our understanding of the impact of the S1P signaling pathway on bone health but will also set the stage for potential therapeutic interventions by identifying the key players in these interrelated processes.

3 Material and Methods

3.1 Material

3.1.1 Devices

Table 1: List of used devices

Device	Company
Axiovert 100 Microscope	Carl Zeiss Microscopy, Jena, Germany
BX51 Transmitted Light Microscope	Olympus, Shinjuku, Japan
Cell counter EVE TM Plus	NanoEntek, Seoul, South Korea
Centrifuge 1K15	Sigma-Aldrich, St. Louis, USA
Centrifuge 5810 R	Eppendorf, Hamburg, Germany
CKX54 Cell Culture Microscope	Olympus, Shinjuku, Japan
CO2 Incubator HERAcell vios 250i	Thermo Fisher Scientific, Waltham, USA
Column oven CTO-40C	Shimadzu, Kyoto, Japan
Degassing Unit DGU-405	Shimadzu, Kyoto, Japan
GalliosTM 10/3 flow Cytometer	Beckmann Coulter, Brea, USA
Handheld Drilling Device Ultimate 450	Nakanishi, Tochigi, Japan
Leica CM1850 Cryostat	Leica Biosystems, Wetzlar, Germany
LSM 880 Airyscan	Carl Zeiss Microscopy, Jena, Germany
Mass spectrometer LCMS-8050	Shimadzu, Kyoto, Japan
Material Testing System EZ Test - SX	Shimadzu, Kyoto, Japan
Microplate reader, CLARIOstar Plus	BMG Labtech, Ortenberg, Germany
Nanodrop One	Thermo Fisher Scientific, Waltham, USA
Nitrogen-generator NGM 22-LC	CMC Instruments, Eschborn, Germany
Objective U Plan FLN 4x	Olympus, Shinjuku, Japan
Objektiv Plan-Apochromat 10x/0,45 M27	Carl Zeiss Microscopy, Jena, Germany
Real-Time System CFX96™	BioRad, Hercules, USA
Rotary Pump E2M28	Shimadzu, Kyoto, Japan
SC180 camera	Olympus, Shinjuku, Japan
SkyScan x-ray Microtomograph 1072	SkyScan, Belgium

Solvent Delivery Unit LC-40D X3	Shimadzu, Kyoto, Japan
Stereomicroscope SMZ800	Nikon, Minato, Japan
System controller SCL-40	Shimadzu, Kyoto, Japan
Thermal Cycler C100™	BioRad, Hercules, USA
UHPLC Autoinjector SIL-40CX3	Shimadzu, Kyoto, Japan

3.1.2 Comsumables

Table 2: List of used comsumables

Comsumable	**Company**
0.5 mL Reaction Tubes	Sarstedt, Nümbrecht, Germany
1.5 mL Reaction Tubes	Sarstedt, Nümbrecht, Germany
24 well cell culture plate	Sarstedt, Nümbrecht, Germany
6 well cell culture plate	Sarstedt, Nümbrecht, Germany
70 µm cell strainer	Miltenyi Biotec, Berglisch-Gladbach, Germany
BD Microlance 3 18 G	Becton Dickinson, Franklin Lakes, USA
BD Microlance 3 25 G	Becton Dickinson, Franklin Lakes, USA
Cover Glass	Engelbrecht, Edermünde, Germany
Cryofilm type IIIC (16UF)	Section Lab, Yokohama, Japan
Epredia™SuperFrost Plus™Adhesion slides	Menzel, Braunschweig, Germany
High precision cover glasses	Paul Marienfeld, Lauda-Königshofen, Germany
Microscope slides Histo Bond	Paul Marienfeld, Lauda-Königshofen, Germany
Microtome Blade - N35	Feather, Osaka, Japan
60 x 2.0 mm MultoHigh 100 RP18 column	CS Chromatography Service, Langerwehe, Germany
0.9% NaCl solution	Fresenius Kabi, Bad Homburg vor der Höhe, Germany
Omnifix-F Luer Solo Syringe - 1ml	B. Braun, Melsungen, Germany
Super Cryo Embadding Medium (SCEM)	Section Lab, Yokohama, Japan

T-175 cell culture flask	Sarstedt, Nümbrecht, Germany
T-25 cell culture flask	Sarstedt, Nümbrecht, Germany
T-75 cell culture flask	Sarstedt, Nümbrecht, Germany
Tissue culture dish 30 x 15mm	Sarstedt, Nümbrecht, Germany

3.1.3 Chemicals and Reagents

Table 3: List of used chemicals and reagents

Chemical/Reagent	**Company**
10x PBS Buffer	AppliChem, Darmstadt, Germany
2-Phospho L-Ascorbic Acid	Sigma-Aldrich, St. Louis, USA
4-Deoxy-pyridoxin hydrochlorid (DOP)	Sigma-Aldrich, St. Louis, USA
Alizarin Red S	Sigma-Aldrich, St. Louis, USA
Ammonium chloride	Sigma-Aldrich, St. Louis, USA
Axitinib	LC Laboratories, Woburn, USA
Azur-A-eosinate	Sigma-Aldrich, St. Louis, USA
Bovine Serum Albumin Fraction V (BSA)	Serva, Heidelberg, Germany
Calcium chloride	AppliChem, Darmstadt, Germany
Cetylpyridinium chloride	Sigma-Aldrich, St. Louis, USA
Collagenase type 1	Merck, Darmstadt, Germany
Corn Oil	Sigma-Aldrich, St. Louis, USA
DAPI solution	Thermo Fisher Scientific, Waltham, USA
Dimethylsulfoxid (DMSO)	Sigma-Aldrich, St. Louis, USA
di-Sodium hydrogen phosphate	AppliChem, Darmstadt, Germany
Ethanol, 100% (EtOH)	Carl Roth, Karlsruhe, Germany
Ethylenediaminetetraacetic acid (EDTA)	Sigma-Aldrich, St. Louis, USA
Fluoromount G	Thermo Fisher Scientific, Waltham, USA
Formaldehyde 38%	AppliChem, Darmstadt, Germany
Gelatin from porcine skin	Sigma-Aldrich, St. Louis, USA
Glycerin	AppliChem, Darmstadt, Germany
Isoflurane	Pinama Critical care, Maharashtra, India
Methanol (MeOH)	Carl Roth, Karlsruhe, Germany

Methyl violet	Sigma-Aldrich, St. Louis, USA
Methylene blue chloride	Serva, Heidelberg, Germany
Paraformaldehyde	Sigma-Aldrich, St. Louis, USA
Polyethylene Glycol 400	Sigma-Aldrich, St. Louis, USA
Polyvinyl pyrrolidone	Sigma-Aldrich, St. Louis, USA
Potassium bicarbonate	Merck, Darmstadt, Germany
Potassium ferricyanide	Sigma-Aldrich, St. Louis, USA
Rimadyl (Carprofen)	Zoetis, Parsippany, USA
Roti-Histofix 4.5%	Carl Roth, Karlsruhe, Germany
Serum Host Animal (Normal Donkey Serum)	Biozol, Eiching, Germany
Silver nitrate	Merck, Darmstadt, Germany
Sodium azide	Sigma-Aldrich, St. Louis, USA
Sodium carbonate	Sigma-Aldrich, St. Louis, USA
Sodium chloride	Carl Roth, Karlsruhe, Germany
Sodium fluoride	AppliChem, Darmstadt, Germany
Sodium thiosulfate	Sigma-Aldrich, St. Louis, USA
Sphingosine 1-Phospahte (D17:1; C_{17} S1P)	Merck, Darmstadt, Germany
Sphingosine 1-Phosphate, D-erythro (S1P)	Enzo Life Sciences GmbH, Lörrach, Germany
Sucrose	Sigma-Aldrich, St. Louis, USA
Tamoxifen	Sigma-Aldrich, St. Louis, USA
Triton X 100	Sigma-Aldrich, St. Louis, USA
TY-52168	Cayman Chemical, Ann Abor, USA
Vitro-Clud®Embedding Medium	Langenbrink, Emmendingen, Germany
β-Glycerophosphate	Sigma-Aldrich, St. Louis, USA

3.1.4 Kits

Table 4: List of used kits

Kit	Company
Ancillary Kit 2	R&D Systems, Minneapolis, USA
Duo Set mouse Osteoprotegerin/TNFRSF 11b	R&D Systems, Minneapolis, USA
innuPrep RNA isolation Kit	Analytic Jena, Jena, Germany
iQ™ SYBERGreen	BioRad, Hercules, USA
Quantikine ELISA TANCE/RANKL	R&D Systems, Minneapolis, USA
Quantikine ELISA VEGFa	R&D Systems, Minneapolis, USA
RevertAidTM First Strand cDNA Synthesis Kit	Thermo Scientific, Waltham, USA

3.1.5 Antibodies

Table 5: List of used antibodies

Antibody	Company
AlexaFluor 647 Donkey anti-rabbit IgG	Biolegend, San Diego, USA
AlexaFluor 594 Rabbit anti-rat IgG	Thermo Scientific, Waltham, USA
CD31 AF-488	Biolegend, San Diego, USA
CD31 (MEC 13.3)	BD Biosciences, Franklin Lakes, USA
CD45.2 V500	BD Biosciences, Franklin Lakes, USA
Endomucin (V.7C7)	Santa Cruz Biotechnology, Dallas, USA
Endomucin (V.7C7) AF-647	Santa Cruz Biotechnology, Dallas, USA
FC Block	Invitrogen, Waltham, USA
OSX AF-547	Santa Cruz Biotechnology, Dallas, USA
Rat IgG2a, κ Isotye control	Biolegend, San Diego, USA
Ter 199 PE	Miltenyi Biotec, Bergisch Gladbach, Germany
Ultra-LEAF™Purified anti-mouse VEGF-A	Biolegend, San Diego, USA

3.1.6 Bacterial Strains and Cell Culture

Table 6: List of used bacterial and mammalian cells

Discription	Company
Staphylococcus aureus	ATCC, Manassas, USA
Bone Marrow Endothelial Cells	Cell Biologics, Chicago, USA

3.1.7 Media, Buffer and Solutions

Media

Table 7: List of used media components and buffers

Component	Company
0.05% Trypsin/EDTA	Gibco Life Technologies, Carlsbad, USA
Antibiotic-Antimycotic (100 x) Solution	Gibco Life Technologies, Carlsbad, USA
Ceftazidime	Sigma-Aldrich, St. Louis, USA
DMEM+GlutaMAX™1 g/L Glucose	Gibco Life Technologies, Carlsbad, USA
DPBS, without Calcium and Magnesium	Gibco Life Technologies, Carlsbad, USA
Endothelial Cell Basal Medium	Cell Biologics, Chicago, USA
Endothelial cell Medium Supplement Kit	Cell Biologics, Chicago, USA
Fetal bovine serum (FBS)	Gibco Life Technologies, Carlsbad, USA
Gelatin-Based Coating Solution	Cell Biologics, Chicago, USA
HBSS	Gibco Life Technologies, Carlsbad, USA
L-Glutamine	Gibco Life Technologies, Carlsbad, USA
RPMI 1640	Gibco Life Technologies, Carlsbad, USA
α-MEM Glutamax, nucleosides	Gibco Life Technologies, Carlsbad, USA

Osteblast Proliferation Medium	DMEM+GlutaMAX™1 g/L Glucose + 10% FBS + 1% Antibiotic-Antimycotic Solution + 100 μM 2 Phospho L Ascorbic acid + 25 μg/mL Ceftazidim
Osteoblast Differentiation Medium	α-MEM Glutamax, nucleosides + 10% FBS + 1% Antibiotic-Antimycotic Solution + 4mM L-Glutamine + 100 μM 2 Phospho L Ascorbic acid + 10 mM β4-Glycerophospahte
Bone marrow Endothelial Cell Medium	Endothelial Cell Basal Medium + 5% FBS + 1% Antibiotic-Antimycotic Solution + 4 mM L-Glutamine + 0.1% VEGF Supplement + 0.1% ECGS Supplement + 0.1% Heparin Supplement + 0.1% EGF Supplement + 0.1% Hydrocortisone Supplement
R10 Medium	RPMI 1640 + 10% FBS

Human Bone Sample Medium	α-MEM Glutamax, nucleosides
	+ 10% FBS
	+ 1% Antibiotic-Antimycotic Solution

Buffer

FACS-Sheath (pH 7,4)	0.9 g NaCl
	1.9 g Di-Natriumhydrogenphosphat
	0.4 g EDTA
	0.4 g KCl
	0.2 g Na-dihydrogenphosphat
	0.3 g Natriumfluorid
	10 g BSA
	Ad 1L PBS
FACS-Buffer	1% BSA
	0.1% Sodium-Azide
	in PBS
ACK-Buffer	150 mM Ammonium chloride
	10 mM Potassium bicarbonate
	0.1 mM EDTA
	Adjust pH 7.2-7.4

Solutions

Sucrose solution	20% Sucrose 1% Polyvinyl pyrrolidone in ddH_2O
Embedding medium	15% Sucrose 1.5% Polyvinyl pyrrolidone 8% Gelatin from porcine skin in ddH_2O
Blocking solution	1% BSA 0.1% Triton X 100 5% Serum of Host animal in PBS
Antibody solution	1% BSA 0.1% Triton X 100 in PBS
Antibody solution – Cell culture Staining	2% BSA 0.5% Triton X 100 0.1 mM CaCl2 in PBS
Alizarin Red Staining Solution	0.1% Alizarin Red S in PBS

Sodium carbonate stock solution	0.64 mM Sodium carbonat in H_2O
Sodiumcarbonat-Formaldehyde Solution	150 mL Sodium carbonate stock solution 50 mL 38% Formaldehyde solution
Farmers Reducer	200 mL 10% Natriumthiosilfate solution 10 mL 10% Potassium ferricyanide solution
Tatrachrome-Stock solution	0.1% Methylene blue chloride 0.16% Azur-A-eosinate 0.02% Methy violet 50% Methanol 50% Glycerin

3.1.8 Primer

Table 8: List of used qPCR Primer

Gene	Product/5‘-3‘Sequence	Company
Gapdh	Fw: AGGTCGGTGTGAACGGATTTG	Eurofins Genomics, Ebersberg,
	Rv: TGTAGACCATGTAGTTGAGGTCA	Germany
Pdgfa	Fw: GAGGAAGCCGAGATACCCC	Eurofins Genomics, Ebersberg,
	Rv: TGCTGTGGATCTGACTTCGAG	Germany
Pdgfb	Fw: CATCCGCTCCTTTGATGATCTT	Eurofins Genomics, Ebersberg,
	Rv: GTGCTCGGGTCATGTTCAAGT	Germany
Vegfa	Mm_Vegfa_1_SG QuantiTect Primer Assay	Quiagen, Hilden, Germany
Tgfb1	Mm_Tgfb1_1_SG QuantiTect Primer Assay	Quiagen, Hilden, Germany
Bglap	Fw: GCGCTCTGTCTCTCTGACCT	Eurofins Genomics, Ebersberg,
	Rv: ACCTTATTGCCCTCCTGCTT	Germany
Sparc	Fw: GTGGAAATGGGAGAATTTGAGGA	Eurofins Genomics, Ebersberg,
	Rv: CTCACACACCTTGCCATGTTT	Germany
Postn	Fw: CCTGCCCTTATATGCTCTGCT	Eurofins Genomics, Ebersberg,
	Rv: AAACATGGTCAATAGGCATCACT	Germany
Sp7	Fw: ATGGCGTCCTCTCTGCTTG	Eurofins Genomics, Ebersberg,
	Rv: TGAAAGGTCAGCGTATGGCTT	Germany
Spp1	Fw: AGCAAGAAACTCTTCCAAGCAA	Eurofins Genomics, Ebersberg,
	Rv: GTGAGATTCGTCAGATTCATCCG	Germany

3.1.9 Mouse Diets

Normal Chow	**Ssniff, Soest, Germany**
	67% (w/v) Carbohydrates
	24% (w/v) Protein
	9% (w/v) Fat
	21 mg/kg Vitamin B6
Normal Chow without vitamin B6	**Altromin, Lage, Germany**
	66% (w/v) Carbonhydrates
	24% (w/v) Protein
	10% (w/v) Fat
	0.033 mg/kg Vitamin B6

3.1.10 Software

Table 9: List of used Software

Software	Company
LabSolutions 5.114	Shimadzu, Kyoto, Japan
GraphPad Prism 9	GraphPad Software, Boston, USA
TrapeziumX	Shimadzu, Kyoto, Japan
OriginPro 2020b 9.7.5.184	OriginLab, Northampton, USA
Image J 1.52	Schindelin et al. 2012[350]
CTAnalyzer (version 1.18.9.0+)	SkyScan, Belgium
NRecon software (version 1.6.9.4	SkyScan, Belgium

3.2 Methods

3.2.1 Animals

All animal experiments were performed in accordance with the directive 2010/63/EU of the European Parliament and the Council on the protection of animals used for scientific purposes and approved by the LANUV (Landesamt für Natur, Umwelt und Verbraucherschutz North Rhine Westphalia, Recklinghausen, Germany) Az. 81-02.04.2020.A007 and AZ 81-02.04.2020.A075 . Animals were bred and housed in the animal facility of Heinrich-Heine University Düsseldorf, Germany (Zentrale Einrichtung für Tierforschung und wissenschaftliche Tierschutzaufgaben, ZETT).

Mouse Strains

Table 10: List of used Mouse Strains

Mouse Strain	Origin
C57BL/6J	Charles River Laboratories, Wilmington, USA
Sgpl1$^{flox/flox}$ abtb-CreERT2	Andreas Billich, Novatis, Basel, Switzerland[351]
S1PR3$^{+/+}$	Richard Proia, NIH, Bethesda, USA[154]
S1PR3$^{-/-}$	Richard Proia, NIH, Bethesda, USA[154]
S1PR2$^{+/+}$	Jerold Chun, Scripps Research Institute, San Diego USA[352]
S1PR2$^{-/-}$	Jerold Chun, Scripps Research Institute, San Diego, USA[352]

Tamoxifen Induction of Cre-Recombinase

The Cre recombinase system under the control of the actb-CreERT2 promotor in the *Spgl1*$^{flox/flox}$ Cre$^{+/-}$ (in the following Cre^{+}) animals was induced via Tamoxifen injection (dissolved in 90% corn oil and 10% ethanol) at 8-10 weeks of age. Tamoxifen was injected intraperitoneal in a concentration of 40 mg/kg/d for five consecutive days. *Sgpl1*$^{flox/flox}$ Cre$^{-/-}$ (in the following Cre^{-}) animals serve as controls and received tamoxifen injections accordingly. Experiments started eight weeks after tamoxifen injections.

DOP Treatment

4-deoxypyridinoline (DOP) was given to the mice by drinking water *ad libido* in a concentration of 3 mg/L or 180 mg/L. Low dose DOP-treated animals were fed with a vitamin 6 reduced diet (Altromin, Lage, Germany). The treatment was given for 2, 3 or 6 weeks. Specific DOP treatment durations and concentrations are stated in the figure legends.

Axitinib Treatment

Axitinib was given daily via intraperitoneal injection in a concentration of 25 mg/kg/d for 6 weeks. Control animals received vehicle injections (40% Polyethylenglycol 400, 60% acidified Water) at equal volumes.

Post-Traumatic Osteomyelitis Model

A model of post-traumatic osteomyelitis was created using twelve-week-old C57BL/6J animals or *S1PR3*$^{-/-}$ and the corresponding *S1PR3*$^{+/+}$ control animals. The animals were deeply anesthetized with isoflurane. The tibial plateau was exposed through a skin incision. A cortical defect was introduced by drilling a 1 mm hole using the handheld drilling device Ultimate 450 (Nakanishi, Tochigi, Japan). To replicate an infection similar to that observed during osteomyelitis, 1000 CFUs of *Staphylococcus aureus* were injected into the bone defect. The hole has been sealed with bone wax. The infection was allowed to incubate for two weeks to simulate the processes that occur during osteomyelitis. Subsequently, the bone was exposed again through a skin incision and the infected and necrotic bone tissue was removed. After thorough cleaning with sterile NaCl solution, the wound was closed once again. Immediately after the second surgery, treatment with 180 mg/mL DOP was started. Control animals underwent the same surgical procedure. Tibiae were collected for μCT analysis to assess bone healing capacity.

The procedure was carried out at the surgical unit of the animal facility located at Heinrich-Heine University Düsseldorf, Germany (Zentrale Einrichtung für Tierforschung und wissenschaftliche Tierschutzaufgaben, ZETT). The surgical procedures were performed in collaboration with Dr. med. Johannes M. Wagner, Department of Plastic Surgery, BG University Hospital Bergmannsheil Bochum, Germany.

Human Bone Specimen

All procedures were conducted according to regulations of the local ethical committee. Prior to participation, informed and written consent was obtained. Bone specimens from patients undergoing surgery for post-traumatic tibial osteomyelitis were provided by Prof. Björn Behr, Department of Plastic Surgery, BG University Hospital Bergmannsheil Bochum, Germany. Specimens were collected during segmental resection and bone transport.

After verification of the absence of acute infections and bacterial colonization, baseline bone volume data were collected using μCT analysis. Bone samples were then cultivated in human bone sample medium at 37°Cand 5% CO_2 for four weeks in the presence or absence of 0.2 mM DOP. In order to ensure comparability, both the treated and the untreated samples were taken from the same patient.

Samples were cultivated over a period of 28 days with a daily change of medium and addition of DOP treatment. After the incubation period, bone volume was once again obtained using µCT and compared to baseline values.

3.2.2 Cell Culture

Osteoblast Isolation

For the isolation of primary osteoblasts (pOBs) C57BL/6J, *S1PR3*$^{+/+}$ and *S1PR3*$^{-/-}$ mice were used. Primary osteoblasts isolation was adapted to Declercq *et al.*[353] Shortly, nine-day-old mice were sacrificed and hind limb tibiae and femurs isolated. The bones were cleaned thoroughly and all surrounding tissue was removed. Epiphyseal regions and joints were removed and the diaphysis of femurs and tibiae was flushed using pre-warmed HBSS to remove the bone marrow. The bones were cut into 1-2 mm long pieces and placed on a 3 cm petri dish. After drying the dish for 15 minutes at 37 $^{\circ}$C, bone pieces stuck to the dish and could carefully be covered with osteoblast proliferation medium, containing 2-phospho L-ascorbic acid to enhance osteoblast differentiation from mesenchymal cells in the bone. Cells were cultivated at 37 $^{\circ}$C, 90% humidity and 5% CO_2.

After 7-10 days, the cells reached confluence. Cells were washed twice with pre-warmed DPBS and detached using 0.05% Trypsin/EDTA. After detachment of the cells, new medium was added and cells were transferred to a T25 culture flask and expended further. Cells were used up to passage 4. For experiments, cells were seeded at 2x10^4 cells/cm^2

and cultivates in osteoblast differentiation medium.

Bone Marrow Endothelial Cells

Primary mouse Bone Marrow Endothelial Cells (BMEC) isolated from C57BL/6J mice were obtained from cell Biologics (Chicago, USA). For cultivation, cell culture flasks were pre-coated with gelatin base solution for 5 minutes. Cells were cultured in Bone Marrow Endothelial Cell Medium at 37 $^{\circ}\mathrm{C}$, 90% humidity and 5% CO_2. At confluence, cells were washed with DPBS and detached using 0.05% Trypsin/EDTA. The cells were splitted in a 1:2 ratios and used up to passage 5. For experiments, cells were seeded at 2.1x10^4 cells/cm^2.

Treatments

For RNA isolation and collection of supernatants, pOBs were seeded on a 6 well culture dish. After attachment, proliferation medium was substituted for osteoblast differentiation medium. S1P, dissolved in MeOH, was used in a concentration of 1 μM for treatment of pOBs for 6 or 24 hours. The S1P receptor 3 antagonist TY-52156 was dissolved in DMSO and 10 μM treatment was performed 30 minutes prior to the S1P stimulation. The corresponding solvent controls were added to control cells to exclude effects of the solvents.

For alizarin red staining, cells were seeded in a 24 well culture plate and incubated for 21 days is osteoblast differentiation medium. 1 μM S1P was spiked daily, the according solvent is spiked to control cells. For blockade of VEGFa, Ultra-LEAF™Purified anti-mouse VEGF-A Antibody (BioLegend, San Diego, USA) was used in a concentration of 1 μg/mL. Rat IgG2a, κ (BioLegend, San Diego, USA) was used as the corresponding isotype control. To assure sufficient nutrient supply, 50% of the medium was refreshed every other day.

For treatment with pre-conditioned medium, pOBs were cultured in T175 cell culture flasks and stimulated with 1 μM S1P or solvent control for 7 days in osteoblast differentiation medium. Media were collected and added to BMECs seeded in 6 well culture dishes for two hours. Purified anti-mouse VEGF-A Antibody or Rat IgG2a, κ isotype control (BioLegend, San Diego, USA) were used in a concentration of 1 μg/mL.

Co-culture and Staining

For direct co-culture experiments, BMEC were seeded on gelatin-coated cell culture dishes at a concentration of 1.25x10^4 cells/cm^2 in bone marrow endothelial cell medium 24 hours before the addition of pOBs. The cells were then washed thoroughly and pOBs were added at a concentration of 0.83x10^4 cells/cm^2 in pOB Differentiation Medium supplemented with Endothelial Cell Growth Supplements (Cell Biologics, Chicago, USA).

Cells were cultured for 72 hours with daily addition of 1 μM S1P or vehicle control. Images were captured at 24, 48 and 72 hours using a CKX54 microscope (Olympus, Shinjuku, Japan).

After 72 hours, cells were thoroughly washed in PBS and fixed with 4% PFA for 20 minutes. After three additional washes, cells were stained with fluorescently labeled antibodies against CD31 (AF-488, Biolegend, San Diego, USA, 1:100) and OSX (AF-548, Santa Cruz Biotechnology, Dellas, USA, 1:100) in a cell culture staining solution containing 0.5% Triton X, 0.1 mM CaCl2 and 2% BSA in PBS for 2 hours. After three additional PBS washes, DAPI solution (0.5 μg/mL; Thermo Fisher Scientific, Waltham, USA) was added for 5 minutes, followed by thorough washing with PBS and mounting with FlouromountG (Thermo Fisher Scientific, Waltman, USA). Fluorescence images were captured using a Zeiss 880 LSM confocal microscope (Carl Zeiss, Jena, Germany).

Alizarin Red

Alizarin Red staining was used to identify the calcification of pOBs. Cells were washed twice with PBS and fixed with 100% EtOH for 15 minutes. After two additional PBS washes, Alizarin Red staining solution was added to the cells for 20 minutes at room temperature. To remove the residual staining solution, the cells were washed with ddH2O until unspecific staining was washed out completely. After air-drying of the cells, images were acquired using the stereomicroscope SMZ800 (Nikon, Minota, Japan). For quantification of the staining, Alizarin Red was extracted using 100 μL 100 mM cetylpyridinium chloride for two hours under constant shakingAbsorbance was measured in a 96-well plate at 570 nm using a CLARIOStar Plus microplate reader (BMG Labtech, Ortenberg, Germany).

3.2.3 Enzyme-linked Immunosorbent Assay (ELISA)

Enzyme-linked Immunosorbent Assays (ELISA) were performed using mouse plasma samples or cell culture supernatants. Blood plasma was collected using whole blood with EDTA added as and centrifuged at 1500 xg for 10 min at 4°C. Blood plasma was collected. For in vitro analysis, primary osteoblast cell culture supernatants were collected after 24 h or 21 days of treatment. All used ELISA kits are listed in Table 4 and performed according to the manufacturer's protocol. Absorption was measured using a CLARIOStar Plus microplate reader (BMG Labtech, Ortenberg, Germany).

3.2.4 Quantitative Reverse Transcriptase Polymerase Chain Reaction (qRT-PCR)

RNA isolation

RNA was isolated using the innuPREP RNA Mini Kit 2.0 (Analytic Jena, Jena, Germany) according to the protocol for RNA extraction from eukaryotic cells. For isolation, experiments were performed using 6-well tissue culture plates. Cells were harvested using 400 μL Lysis solution and RNA was extracted immediately according to the protocol.
RNA concentrations were determined using the Nanodrop ONE (Thermo Fisher Scientific, Waltham, USA).

First Strand Complementary DNA (cDNA) Synthesis

cDNA synthesis was performed using the RevertAid First Strand cDNA Synthesis Kit (Thermo Fisher Scientific, Waltham, USA). Shortly, RNA concentration was adjusted to 200 ng per reaction and diluted using nuclease free water. Oligo(dT)18 primers were used for synthesis. PCR reactions were performed using the Thermo Cycler T100 (BioRad, Hercules, USA).

qRT-PCR Reaction

Quantitative reverse transcription polymerase chain reaction (qRT-PCR) was performed using the iQ SYBR Green Supermix (BioRad, Hercules, USA). Each reaction was prepared according to Table 11. Used primers are listet in Table 8.

Table 11: Reaction mixture used for quantitative reverse transcriptase polymerase chain reactions

Component	**μL**
cDNA	1 µL
Forward Primer	0.5 μL
Reverse Primer	0.5 μL
H2O	8 μL
iQ SYBR Green Supermix	10 μL
Total reaction volume	20 μL

The reaction was carried out using the C100TermalCycler/CFX96 RealTime System (BioRad, Hercules, USA) and reactions were run according to Table 12.

Table 12: Reaction protocol used for quantitative reverse transcriptase polymerase chain reactions

Step	**Temperature ($^{\circ}$C)**	**Time (min:sec)**	**No. of Cycles**
Initial Denaturation	95	10:00	1
Denaturation	95	00:10	
Hybridization	55	00:10	40
Elongation	72	00:30	
Fluorescence detection			
Denaturation	95	00:10	1

Gene expression was analyzed normalizing to Gapdh expression. Relative gene expression values were calculated according to the $2^{-\Delta CT}$ method, fold change expression values were calculated according to the $2^{-\Delta\Delta CT}$ method.[354,355]

3.2.5 Micro Computer Tomography (μCT)

Quantitative analysis of all bone samples was performed using a SkyScan X-ray Microtomograph 1072 (SkyScan, Belgium). The specimens were placed in a plastic tube and the images were acquired at 70 kV and 114 µA using a 180° circular acquisition with 0.45° steps between the projections. Bone was acquired with a pixel size of 11.32 μm for trabecular bone volume analysis and evaluation of osteomyelitis defects. For the analysis

of cortical bone thickness and human bone samples, a pixel size of 18.88 μm was used. NRecon software (version 1.6.9.4; SkyScan, Belgium) was used to reconstruct the images. Hydroxyapatite standards with densities of 250 mg/cm^3 and 750 mg/cm^3 were used for density calibration. Appropriate corrections were made to adjust the grayscale values according to these standards.

Trabecular bone volume was calculated in a region covering a region of 1.427 mm slides, starting 0.566mm from the growth plate. Cortical thickness was calculated in the mid-diaphysis. For the calculation of Ct.Ar./Tt.Ar., a region of 0.955 was analyzed in the mid-diaphysis. Cortical defects in the osteomyelitis model are analyzed in a region of 4.530 mm surrounding the defect area. Lamellar bone is measured with a threshold of 60, while newly formed bone callus is analyzed with a threshold of 50. To calculate the total bone volume of human bone samples, the total tissue area was calculated using a threshold of 37. All analyses were performed using CTAnalyzer (version 1.18.9.0+; SkyScan, Belgium). The analysis was performed in accordance with the guidelines for assessment of bone microstructure in rodents using micro-computed tomography.[356]

3.2.6 3pbt

Mechanical testing of bones was performed using the Material Testing System Shimadzu EZ Test EZ-SX device (Shimadzu, Kyoto, Japan). Femora were placed on two supportive points 5 mm from each other and a loading point was placed to the mid-diaphysis. A constant loading of 3 mm/min was applied using a 500-N load cell until failure occurs at the loading site. Load and displacement were measured every 5 ms using the TrapeziumX Software (Shimadzu, Kyoto, Japan). For analysis, the OriginPro 2020b 9.7.5.184 software was used. Ultimate force (strength) is calculated from the load-displacement curve as the point where the failure occurs, the stiffness is calculated using the slope of the curve.

3.2.7 Histology

Specimen Preparation

For histological staining, tibiae were embedded in Super Cryo Embedding Medium (SCEM, Section Lab, Yokohama, Japan) and snap frozen using liquid nitrogen immediately after preparation. Cryosections were prepared according to Kawamoto *et al.*[357] Shortly, specimens were sectioned in a cryostat CM1850 (Leica Biosystems, Wetzlar, Germany) using a N35 blade. To assure the accuracy of uniform 5 µm thick sections, cryofilm type IIIC (Section Lab, Yokohama, Japan) was used. The cryofilm was applied to the exposed bone in the cryoblock und quickly attached using light pressure before cutting. Sections were glued to a microscope slide and air-dried overnight before staining.

Von Kossa/NcNeil staining

Prior to staining, samples were dehydrated in 100% ethanol for five minutes and fixed in 4% PFA solution for additional five minutes. To remove residual fixative, slides were washed thoroughly in ddH_2O and then incubated in 5% silver nitrate solution for ten minutes in the dark. Slides were washed with ddH_2O followed by incubation in sodium carbonate/formaldehyde solution for two minutes. Staining was enhanced by incubation in former's reducer for one minute, followed by thorough washing with tap water for 20 minutes.

Samples are then counterstained with 5% tetrachrome solution in water for 20 minutes, followed by two washes with 70%, 95% and 100% ethanol, respectively. Specimens were embedded in Vitro-Clud®Embadding Medium (Langenbrink, Emmendingen, Germany) and images were captured using the transmitted light microscope BX51 (Olympus, Shinjuku, Japan) with a SC180 camera (Olympus, Shinjuku, Japan) and U Plan FLN 4x Objective (Olympus, Shinjuku, Japan).

The bone marrow region was selected for analysis of bone volume per total volume. Automated thresholding using ImageJ 1.52 was used to distinguish calcified bone from the bone marrow.

3.2.8 Endomucin Staining of Thick Femoral Sections

Specimen preparation

For thick sections of bone used for immunofluorescent staining, bones were fixed in 4.5% PFA overnight at 4°C after preparation. For decalcification, bones were transferred to 0.5 M EDTA and incubated at 4°C overnight, followed by overnight incubation in 20% Sucrose and 1% Polyvinylpyrrolidone solution. Bones were finally embedded in cryoembedding medium (8% Gelatine, 15% Sucrose, 1.5% Polyvenylpyrrolidone) using dry ice. For sectioning N35 blades were used and 40 µm thick sections were obtained using a cryostat CM1850 (Leica Biosystems, Wetzlar, Germany).

Staining

Sections were air dried and rehydrated in PBS for 15 minutes, followed by fixation in ice-cold methanol for 5 minutes. After removal of residual fixative with three 5-minute PBS washes, sections were blocked with blocking solution containing 5% host animal serum and 0.1% Triton X in PBS for 1 hour at room temperature. Primary endomucin antibody (1:100; Santa Cruz Biotechnology, Dallas, USA) was incubated overnight at 4°C in antibody solution containing 0.1% Triton X and 1% BSA in PBS. After three 5-minute washes, secondary AlexaFluor 647 donkey anti-rabbit IgG antibody (1:1000; Biolegend, San Diego, USA) was added to the antibody solution and incubated for 2 hours at room temperature. After three 5-minute washes in PBS, sections were mounted with FlouromountG (Thermo Fisher Scientific, Waltham, USA).

Image Acquisition

The Zeiss 880 LSM confocal microscope (Carl Zeiss, Jena, Germany) with a Plan-APOchromat 10x objective (Carl Zeiss, Jena, Germany) was used for acquisition of immunofluorescence images.

Image Analysis

To quantify the vessel area, length and branching points, automated analysis using ImageJ 1.52 was used. To unify the analysis, 3000 μm were measured starting from the diaphyseal growth plate and the whole bone marrow area within this region was analyzed. The measurement of the whole bone marrow area was conducted through

manual thresholding, while the measurement of the vessel area was carried out using a self-scripted macro. Additionally, automated threshold methods were utilized in the process. The percentage of vessel area within the bone marrow of the analyzed region was calculated.

Vessel length and branching points were quantified using conversion of the vasculature to tubes and skeletonizing. The number of branching points was counted automatically, as well as total vessel length using a self-scripted macro. Additionally, the average distance between branching points was calculated. For analysis of Endomucin expression, the mean fluorescence of the vascular area within 1000 μm of the growth plate was measured using automated thresholding. Detailed source codes are listed in the supplement.

3.2.9 CD31 Staining of Murine Post-Traumatic Osteomyelitis Samples and Human Samples

Tibial samples collected from the post-traumatic osteomyelitis model and human bone samples were fixed overnight in 4.5% PFA at 4°Cand decalcified overnight in 0.5 M EDTA at 4°Cand embedded in paraffin. Bone sections were prepared at 9 μm thickness. CD31 antibody (BD Biosciences, Franklin Lakes, USA) and anti-rabbit IgG conjugated to Alexa Flour 594 secondary antibody (Thermo Fisher Scientific, Waltham, USA) were used for immunohistology staining of the vasculature. Images were acquired using the Zeiss Axivert 100 (Carl Zeiss, Jena, Germany) microscope. Semi-automated pixel quantification was conducted for quantification using Adobe Photoshop.[358]

Preparation of samples, staining, image acquisition and analysis of the prost-traumatic osteomyelitis samples and human bone samples was carried out at the Department of Plastic Surgery, BG University Hospital Bergmannsheil Bochum, Germany.

3.2.10 Flow Cytometric Analysis

Isolation of BMEC

To isolate bone marrow cell, one femur and one tibia was collected and adjacent tissue was removed. The epiphyseal regions were removed to open the bone. For bone marrow harvesting, a 0.5 mL microcentrifuge tube was prepared by inserting an 18 G needle

through the bottom and placed in a 1.5 mL microcentrifuge tube. Afterwards the bones were placed in the 0.5 mL tube and centrifuged for 1 minute at 2500 xg to collect the bone marrow.

Collected bone marrow was resuspended in R10 medium and the suspension was digested in the addition of 0.5 mg/mL col Type I for 10 minutes at 37°Cto obtain a single cell solution. To remove residual cell clumps and bone tissue, the suspension was subsequently filtered through a 70 µm cell strainer and rinsed twice using R10 medium.

For lysis of red blood cells, the cells were collected by centrifugation for 5 minutes at 400 xg and resuspended in ACK buffer. After incubation of 2 minutes at room temperature the cells were washed in R10 medium.

Staining of BMECs

For flow cytometric analysis of the obtained bone marrow single cell solution, 1x10^6 cells per sample were stained in 100 μL FACS-Buffer. To avoid nonspecific antibody staining, cells were preincubated using FC-Block (1:100, Invitrogen, Waltham, USA) for 5 minutes at room temperature. The antibody solution was added and incubated for 45 minutes at 4°C. The concentrations of the antibodies used are listed in Table 13.

Table 13: Antibodies and the corresponding dilutions used for the staining of cells for flow cytometric analysis

Antobodyt	Dilution
Ter119 PE	1:50
CD45.2 V500	1:125
CD31 AF-488	1:40
Emcn AF-647	1:50

The cell suspension was washed twice with the FACS buffer and resuspended in 200 μL of the FACS buffer for the acquisition.

Flow Cytometric Analysis

Cells were acquired using the Gallios™10/3 flow Cytometer (Beckmann Coulter, Brea, USA). Bone marrow endothelial cells were identified as Ter119$^-$, CD45$^-$, CD31$^+$ and

$Emcn^+$.

3.2.11 S1P Measurements

Plasma Preparation

Blood plasma was collected using whole blood with EDTA added as anticoagulant. The blood was centrifuged at 1500 xg for 10 min at 4°C and blood plasma was collected. 50 µL plasma was resuspended in 250 mL MeOH and 10 pmol C_{17} S1P were added as internal standard for normalization. Samples were kept at -80°C overnight for precipitation. Afterward, samples were centrifuged at 21,000 xg for 10 minutes and supernatants were collected for S1P measurements.

BM Preparation

For the collection of bone marrow for S1P measurements, one femur was collected and adjacent tissue was removes. The epiphyseal regions were removed to open the bone and the bone was placed in a 0.5 mL centrifuge tube, prepared by inserting an 18 G needle through the bottom and placed in a 1.5 mL microcentrifuge tube. To collect the bone marrow, the tubes were centrifuged at 10,000 xg for 15 seconds.

For normalization, bone marrow was weighed and thoroughly resuspended in 200 µL MeOH. 10 pmol C_{17} S1P standard was added for normalization. After overnight precipitation at -80°C, the solution was centrifuged at 21,000 xg for 10 minutes and the supernatants were collected for S1P measurements.

LS/MS-MS Measurements

Plasma S1P was detected with an LCMS-8050 triple quadrupole mass spectrometer (Shimadzu, Kyoto, Japan) with the following settings: A nebulizer flow rate of 3 L/min, a interface temperature of 300°C, a desolvation temperature of 526°C, a heat block temperature of 400°C and a drying gas flow rate of 10 L/min. The gradient separation was carried out on a Nexera X3 UHPLC system (Shimadzu, Kyoto, Japan) using a 60 x 2.0 mm MultoHigh 100 RP18 column (CS Chromatography Service, Langerwehe, Germany) at a temperature of 40°C. The mobile phase gradients, as listed in Table 14 were used at a flow rate of 0.4 mL/min. The data were analyzed with LabSolutions 5.114 (Shimadzu,

Kyoto, Japan). The LC/MS-MS measurements and analysis were carried out by Dr. Philipp Wollnitzke.

Table 14: Mobile phase gradients used for LC/MS-MS measurements

Time [min]	MeOH dilution [%]	1% aq. Formic Acid dilutuin [%]	Curve
0	10	90	-2
3	100	0	0
12	100	0	0
12.01	10	0	0

3.2.12 Statistics

The results are presented as mean ± standard deviation (s.d.). Statistical analysis was performed using GraphPad Prism 9, with paired or unpaired t-test, one-way ANOVA or two-way ANOVA followed by Tukey test. All statistical tests performed are stated in the figure legends.

Groups were considered significant for P-values ≥ 0.05.

4 Results

4.1 DOP-Mediated S1P Lyase Inhibition Leads to the Accumulation of S1P Within the Body

The primary goal of this study was to unravel the S1P-mediated changes in bone vasculature and the connection to bone regeneration in adult mice. Therefore, 20-week-old male C57BL/6J mice were treated with 4-deoxydiridoxine (DOP) for three and six weeks, respectively. DOP is a well-known S1P lyase inhibitor and vitamin B6 antagonist[112] and therefore, prevents the irreversible degradation of S1P to 2-trans-hexadecenal and phosphoethanolamine.[37]

As expected, the administration of DOP led to a 1.5-fold elevation of plasma S1P in mice treated for three weeks compared to untreated control mice, which remains at a high level after six weeks of treatment (Figure 6a). Additionally, a massive increase in local S1P levels within the bone marrow could be detected (Figure 6b) upon DOP treatment. This ultimately leads to a 30-fold increase in the ratio of bone marrow S1P compared to plasma S1P (Figure 6c).

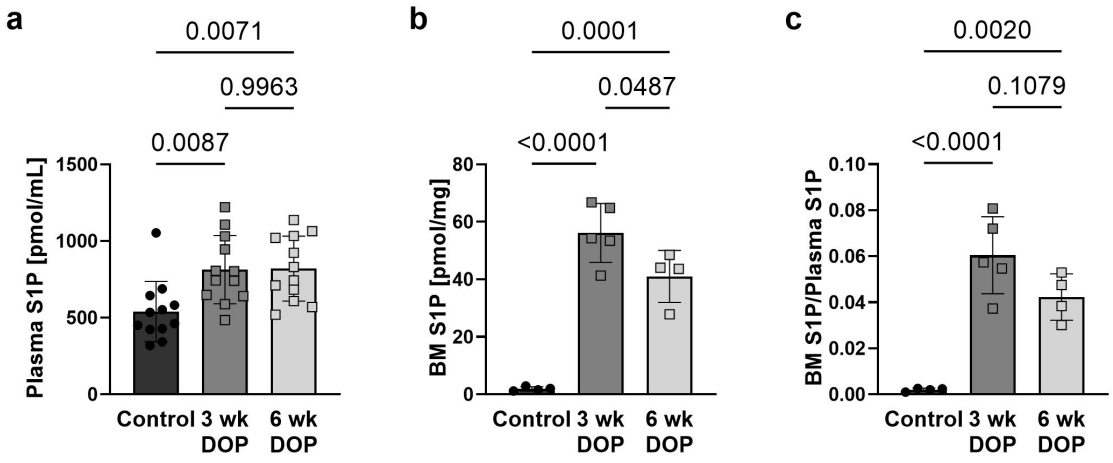

Figure 6: Global and local S1P levels rise upon pharmacological S1P lyase inhibition through DOP treatment. S1P levels in (a) plasma (n=12/12/12) and (b) whole bone marrow (n=4/5/4) from C57BL/6J animals after three and six weeks of 3 mg/L DOP administration and control animals measured using LC-MS/MS. (c) Bone marrow to plasma S1P ratio in these animals (n=4/5/4). Data are represented as mean ± s.d., One-way ANOVA was used for statistical analysis.

4.2 S1P Lyase Inhibition Leads to an Increase in Vessel Density and a Phenotypic Switch of Endothelial Cells Towards Pro-Osteogenic H-Type Vessels

To examine the effects of the elevation of S1P levels within the body on the bone vasculature, thick Endomucin-stained bone sections of C57BL/6J mice were analyzed after three and six weeks of DOP treatment. An increase in total vessel area was detected after three weeks of DOP treatment, further increasing up to 18% after six weeks (Figure 7a+b). This was accompanied by increased vessel density and branching after three and six weeks of DOP treatment (Figure 7c+e). Due to the increased branch number, the length between branches was reduced after DOP treatment (Figures 7d).

To confirm the DOP-mediated effects, *Sgpl1*$^{flox/flox}$ mice harboring a Cre inducible genetic deletion of the S1P lyase (*Sgpl1*) under the control of the β-actin promotor (actb-CreERT2) were used. These mice were previously described to have elevated S1P levels in several organs and blood.[351] The conditional deletion of the S1P lyase was archived through tamoxifen administration to Cre^{+} mice, Cre^{-} mice receiving the same treatment served as controls. Eight weeks after tamoxifen treatment, the bone marrow vasculature was analyzed and a 23% increase in total vessel area accompanied by increased vessel density and branching was observed (Figure 8a-e). These results confirm the effects observed after DOP treatment.

Previously, a specific vessel phenotype, the H-type vessel, was extensively described. These vessels were shown to associate with osteoprogenitor cells and secrete pro-osteogenic factors, promoting bone growth.[318] Characteristics of this vascular phenotype include the high expression of two endothelial markers, CD31 and Endomucin.[318,319] To further evaluate the influence of S1P on the bone marrow vasculature and the formation of H-type vessels, the mean fluorescence intensity (MFI) of Endomucin-stained vessels after DOP treatment was evaluated. Indeed, fluorescence intensities were increased by 25% after three and six weeks of treatment (Figure 9), indicating a phenotypic switch towards the specialized H-type vasculature.

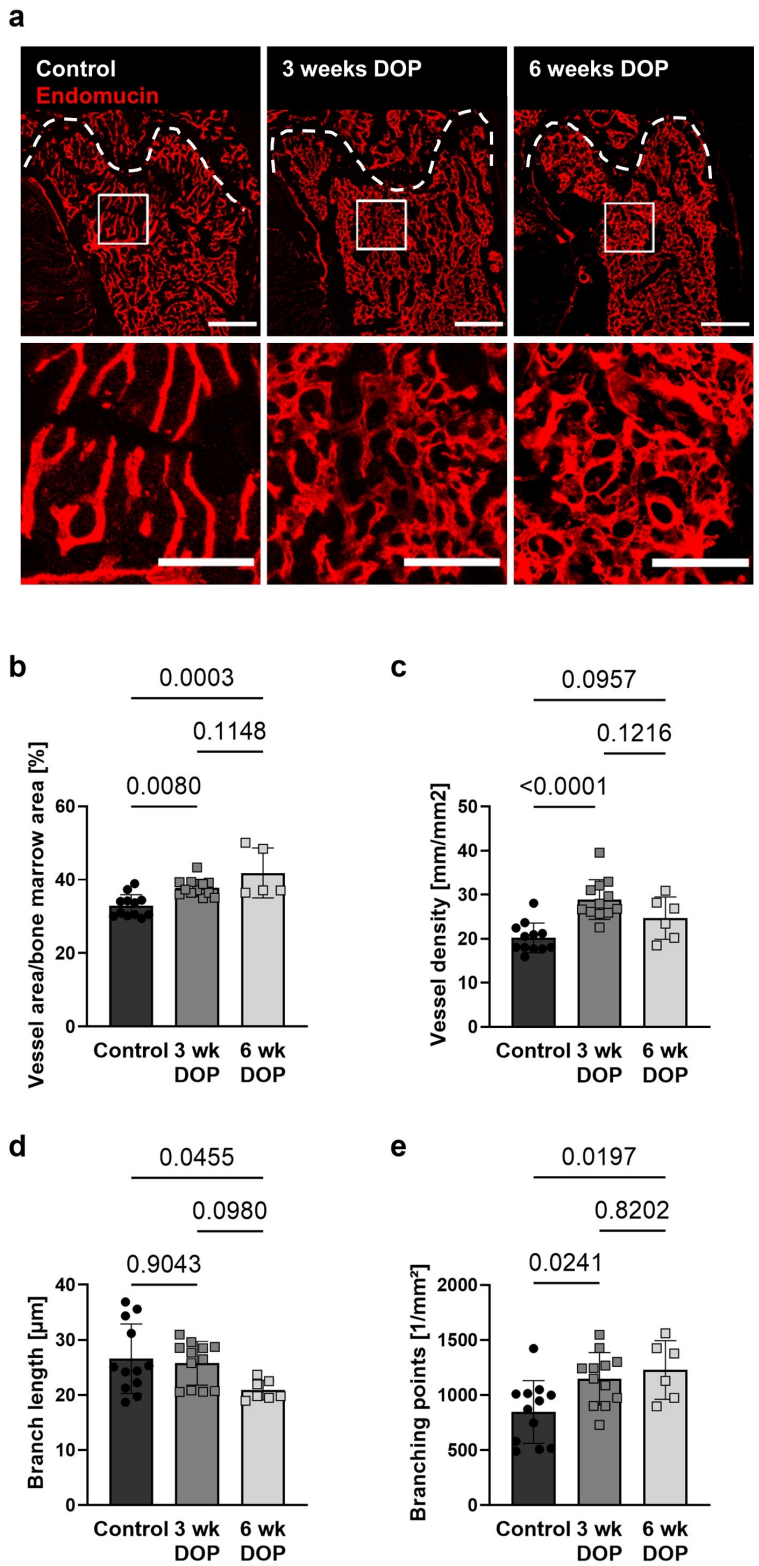

Figure 7: DOP treatment leads to an increase in vascular density and branching of the bone marrow vasculature. (a) Representative images of thick Endomucin stained femoral sections of C57BL/6J control animals and animals treated with 3 mg/L DOP for three and six weeks; scale bar = 500 μm (top) and 200 μm (bottom). (b) Quantification of vascular area/bone marrow area (n=12/12/5), (c) vascular density (n=12/12/6), (d) branch length (n=12/12/7) and (e) number of branching points (n=12/12/6). Data are represented as mean ± s.d., One-way ANOVA was used for statistical analysis.

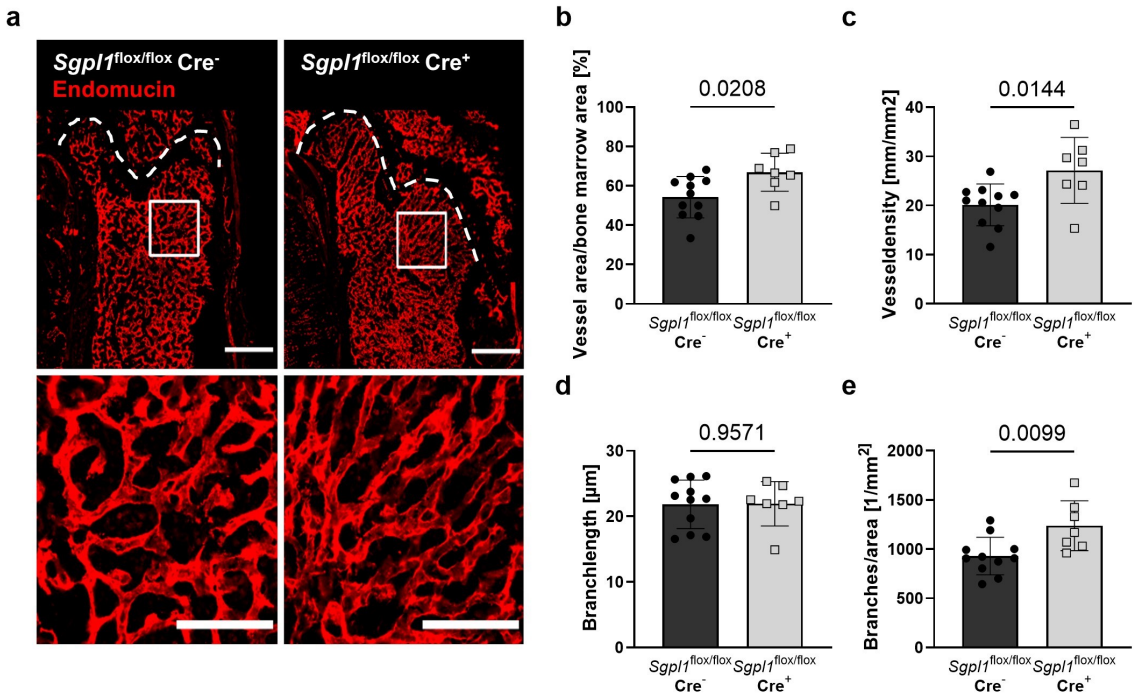

Figure 8: Genetic deletion of *Sgpl1* leads to increased vascular density and branching in the metaphyseal bone marrow vasculature. (a) Representative images of thick Endomucin stained femoral bone sections of *Sgpl1*$^{flox/flox}$ Cre^{-} and *Sgpl1*$^{flox/flox}$ Cre^{+} animals eight weeks after tamoxifen-induced deletion of the S1P lyase. Quantification of (b) vascular area within the bone marrow area (n=11/7), (c) vessel density (n=11/7), (d) branch length (n=11/7) and (e) number of branching points (n=11/7) within the bone marrow area of the sections. Data are represented as mean ± s.d., Two-tailed t-test was used for statistical analysis.

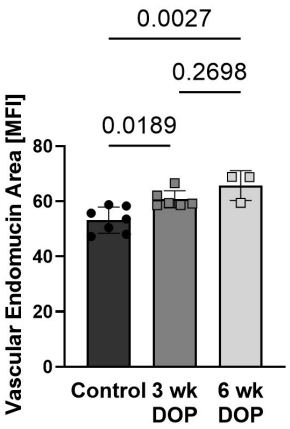

Figure 9: DOP treatment leads to an increase in Endomucin expression within the bone vasculature. Mean fluorescence intensity (MFI) of Endomucin staining in the vessel area of thick Endomucin-stained femoral sections (n=7/6/3) of C57BL/6J animals after three and six weeks of 3 mg/L DOP treatment. Data are represented as mean ± s.d., One-way ANOVA was used for statistical analysis.

As CD31 staining of the bone vasculature diminishes with age,[318] flow cytometry was used as a more sensitive method to further characterize isolated BMECs after three weeks of DOP treatment. To do so, CD45^{-} and Ter119^{-} bone marrow cells were analyzed for their expression of the endothelial markers CD31 and Endomucin (Figure 10a). The CD31 mean fluorescence intensity of ECs within the bone increased by 16% after DOP treatment (Figure 10b). The mean fluorescent intensity of Endomucin showed a tendency to rise after DOP treatment (Figure 10c). Together with the already detected increase in Endomucin staining in Figure 9, this indicated a shift of the endothelial phenotype within the bone marrow towards the H-type after DOP treatment. Additionally, an increase in total H-type ECs per bone was identified, resulting in a 1.68-fold increase in the percentage of H-type ECs of total BMECs (Figure 10d+e).

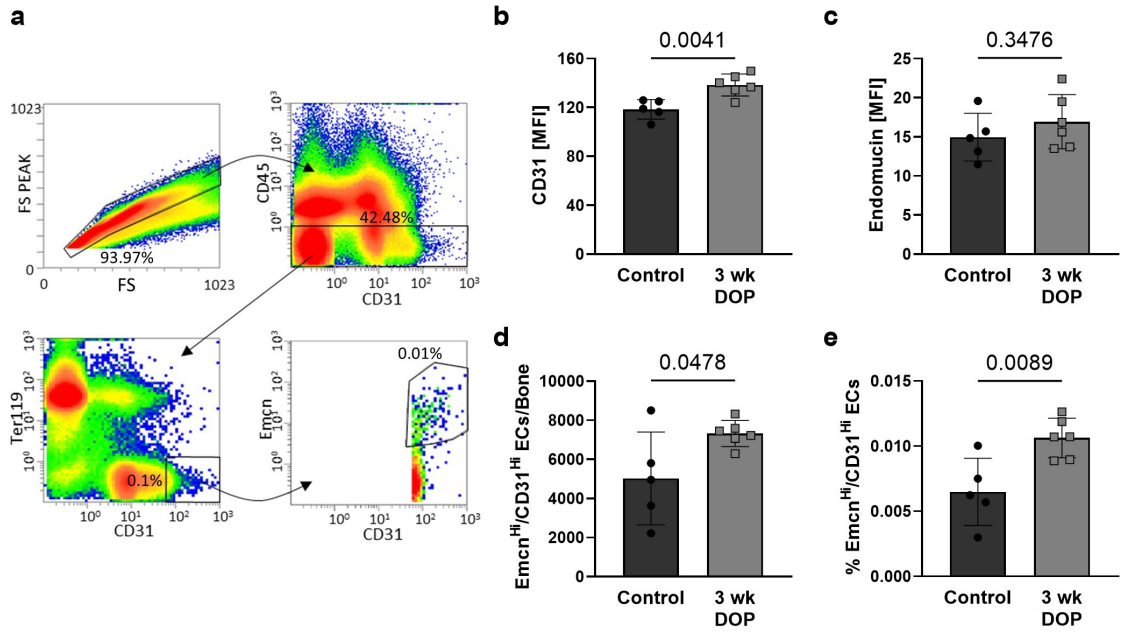

Figure 10: DOP treatment leads to a phenotypic switch of bone marrow endothelial cells toward the H-type. (a) Representative flow cytometry gating strategy of CD45^{-}, Ter119^{-}, CD31^{+} and Endomucin (Emcn)$^{+}$ endothelial cells. Quantification of (b) CD31 mean fluorescence intensities (n=5/6), (c) Endomucin mean fluorescence intensities (n=5/6), (d) number of CD31^{Hi}/Emcn^{Hi} endothelial cells per bone (n=5/6) and (e) percentage of CD31^{Hi}/Emcn^{Hi} endothelial cells per total bone marrow endothelial cells (n=5/6) in control C57BL/6J animals and after three weeks of 3 mg/L DOP treatment. Data are represented as mean ± s.d., Two-tailed t-test was used for statistical analysis.

In summary, these results show an S1P-mediated increase in the total bone vasculature density and a phenotypic switch of BMECs towards a pro-osteogenic phenotype.

4.3 The S1P-Mediated Formation of H-Type Vessels is Followed by an Increase in Bone Volume and Strength

As H-type vessels were previously described to have pro-osteogenic effects,[318] the bone volume and strength of DOP-treated mice were evaluated after three and six weeks of DOP treatment. Analysis of the distal region of femoral bones of these mice using micro-computed tomography (μCT) revealed a 1.9-fold increase in trabecular bone volume per total tissue volume (BV/TV) after six weeks of treatment (Figure 11a+b). This increase in bone volume is explained by an increase in trabecular thickness (Tb.Th.) (Figure 11c) and trabecular number (Tb.N.) (Figure 11d). Additionally, a decrease in trabecular spacing (Tb.Sp.) (Figure 11e) was observed. As the changes in the bone structure only occur after six weeks of treatment, a phenotypic switch of the bone marrow vasculature precedes changes in the bone structure. This possibly shows the induction of vessel-mediated bone strengthening after DOP treatment.

To further confirm the increase in trabecular bone volume after DOP treatment, tibiae of the same mice were analyzed using von Kossa/McNeal´s Tetrachrome staining. Quantifying trabecular bone volume per total tissue volume (BV/TV) again showed an increase after six weeks of DOP treatment. After three weeks of treatment, no changes could be detected (Figure 12a+b).

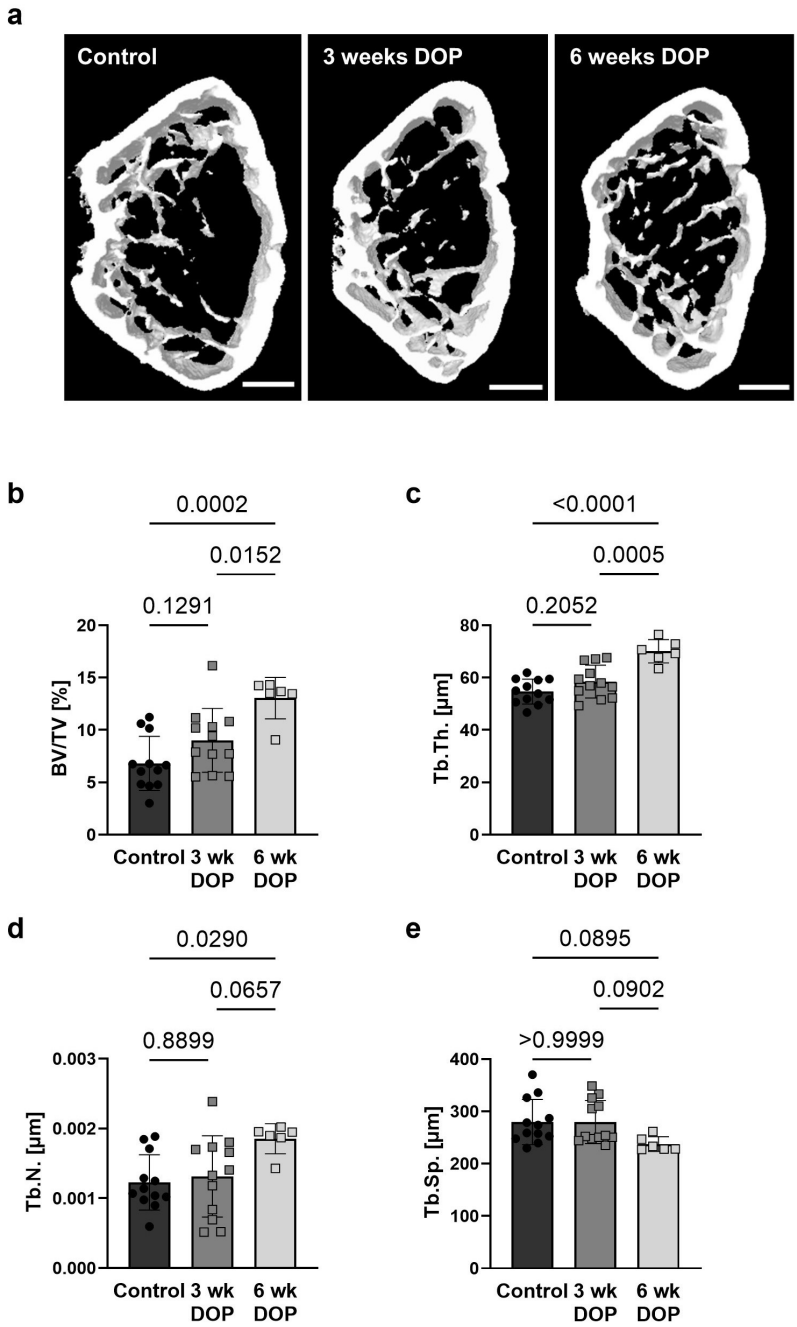

Figure 11: DOP-mediated changes in trabecular bone structures occur after six weeks of treatment. (a) Representative μCT images of C57BL/6J control mice and after three and six weeks of 3 mg/L DOP administration; scale bar=500 μm. Quantification of (b) bone volume/total volume (n=12/12/6), (c) trabecular thickness (n=12/12/6), (d) trabecular number (n=12/12/6) and (e) trabecular spacing (n=12/12/6). Data are represented as mean ± s.d., One-way ANOVA was used for statistical analysis.

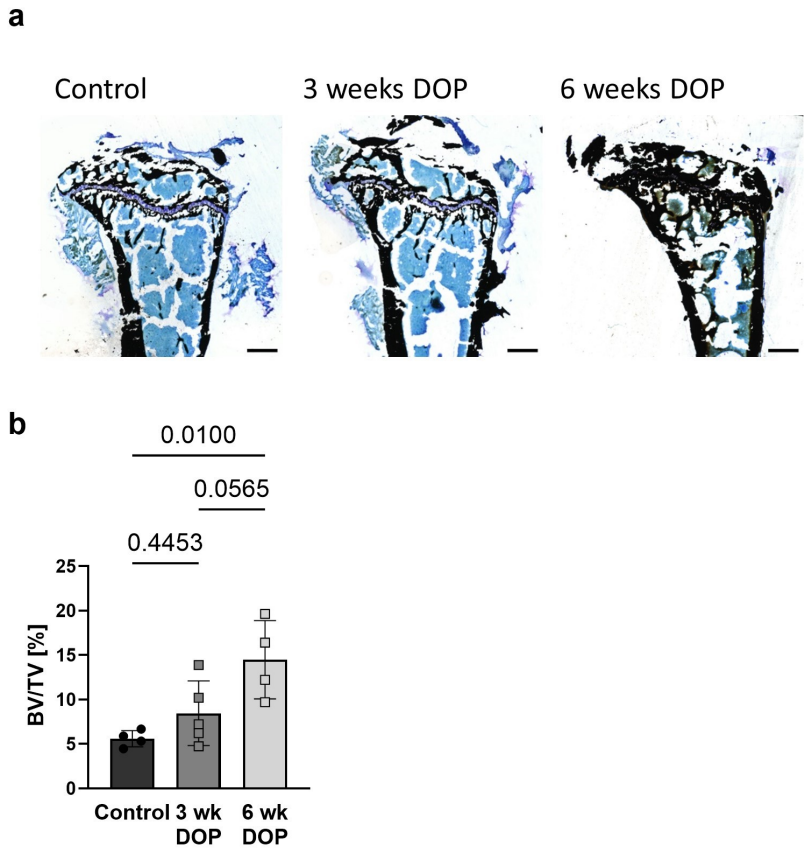

Figure 12: DOP treatment increases trabecular bone volume in tibiae. (a) Representative images of tibia sections of C57BL/6J control mice and after three and six weeks of 3 mg/L DOP treatment stained with Van Kossa/McNeil´s Tetrachrome staining; scale bar = 500 μm. (b) Quantification of trabecular bone volume per total tissue volume in these sections (n=4/4/5). Data are represented as mean ± s.d., One-way ANOVA was used for statistical analysis.

Femoral bones were further analyzed for changes in cortical thickening and strength. Therefore, cortical thickness was measured using μCT analysis at the mid-shaft of the bone. This revealed a thickening of the corticalis after three weeks, further increasing up to 13% after six weeks of DOP treatment (Figure 13a+b). Additionally, the cortical area per total tissue area (Ct.Ar./Tt.Ar.) was increased after three and six weeks of DOP treatment (Figure 13b).

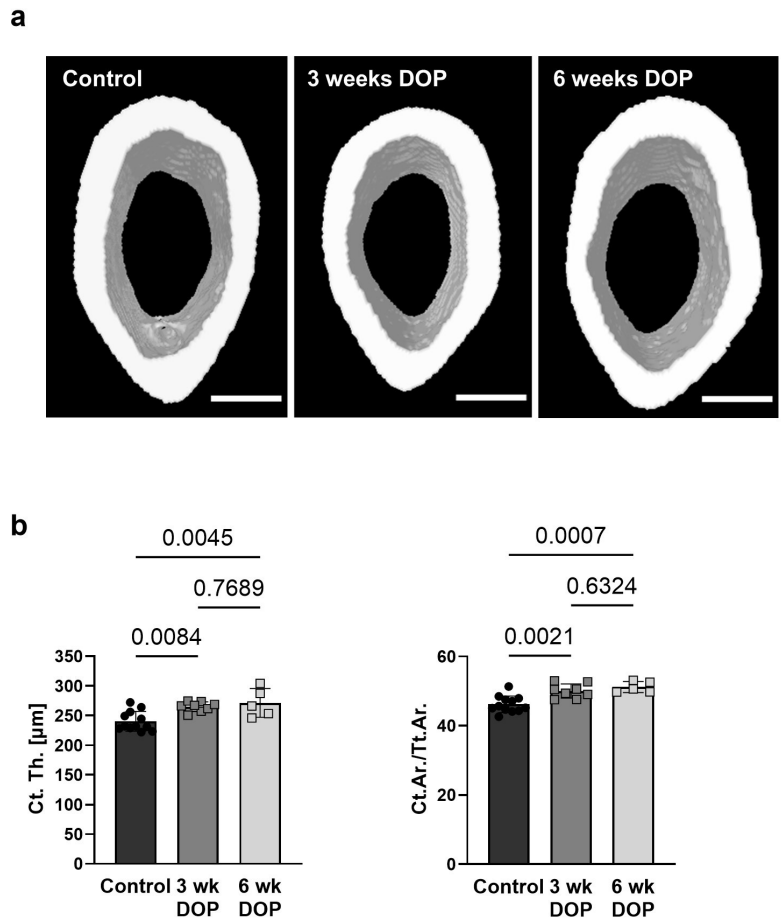

Figure 13: DOP leads to an increase in cortical thickness and area after three and six weeks of treatment. (a) Representative μCT images of cortical sections at the mid-shaft of femora of control C57BL/6J animals after three and six weeks of 3 mg/L DOP administration. (b) Quantification of cortical thickness (n=12/8/5) and cortical area per total tissue area (n=12/8/5). Data are represented as mean ± s.d., One-way ANOVA was used for statistical analysis.

As the corticalis provides the bone with strength and stability,[219] a rise in thickness indicates increased bone stability. To test this, a three-point bending test was used to apply mechanical stress to the bone. After three weeks, bone stiffness slightly increased, leading to significantly increased bone stiffness after six weeks of DOP treatment (Figure 14a+b). After six weeks of treatment, an increase of 16% of the ultimate force was needed to reach the point of bone failure, clearly indicating an increase in bone strength due to elevated S1P levels (Figure 14c).

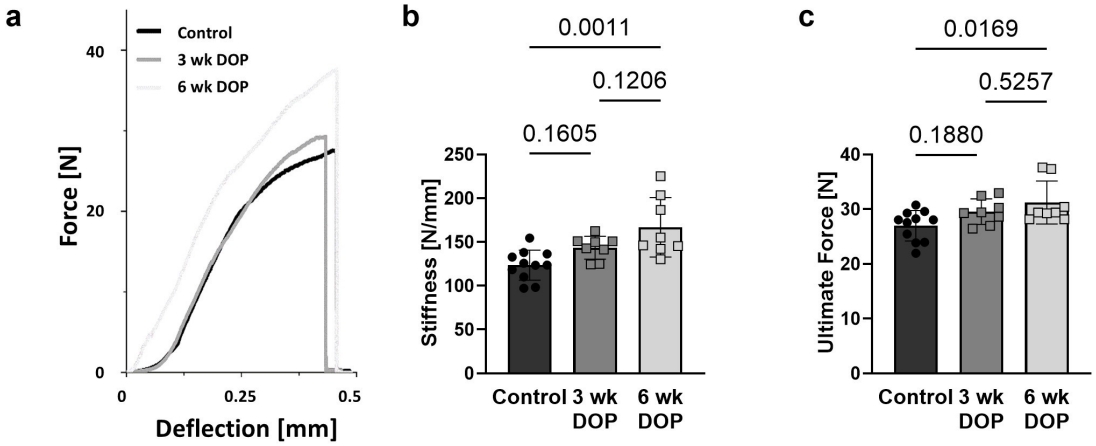

Figure 14: Bone strength increases after six weeks of DOP treatment. (a) Representative force/deflection graphs resulting from a three-point bending test of femora from C57BL/6J control animals and after three and six weeks of 3 mg/L DOP administration. Quantification of (b) stiffness (n=12/8/8) and (c) ultimate force (n=12/8/8). Data are represented as mean ± s.d., One-way ANOVA was used for statistical analysis.

The previous investigations only focused on male mice. Therefore, the sex-independent effects of DOP treatment were evaluated by treating female C57BL/6J animals with DOP for six weeks and the most critical parameters were assessed. After DOP treatment, an increase in BV/TV, Tb.Th. and Tb.N. and a decrease in Tb.Sp. were observed in the femoral bone (Figure 15a). In addition, an increase in vessel area and vessel area/bone marrow area was observed in these mice after DOP treatment (Figure 15b). These results emphasize the sex-independent effects of DOP treatment on bone and vascular parameters.

Due to the need for constant remodeling during bone formation, several cell types and factors are involved in this process.[219] Therefore, the influence of DOP treatment on bone formation and resorption markers was assessed. Evaluating these markers in blood plasma revealed DOP-mediated changes in RANKL as a bone resorption marker and OPG as a bone formation marker (Figure 16a+b). S1P led to increased bone formation and decreased bone resorption as demonstrated by a 59% reduced RANKL/OPG Ratio (Figure 16c) after DOP treatment.

In summary, these results show S1P-mediated changes in bone density and strength after a phenotypic switch of the vasculature occurred. This indicates that the changes in the bone are mediated through the bone vasculature. DOP led to both increased bone formation and decreased in bone resorption, ultimately leading to vessel-mediated strengthening of the bone after six weeks.

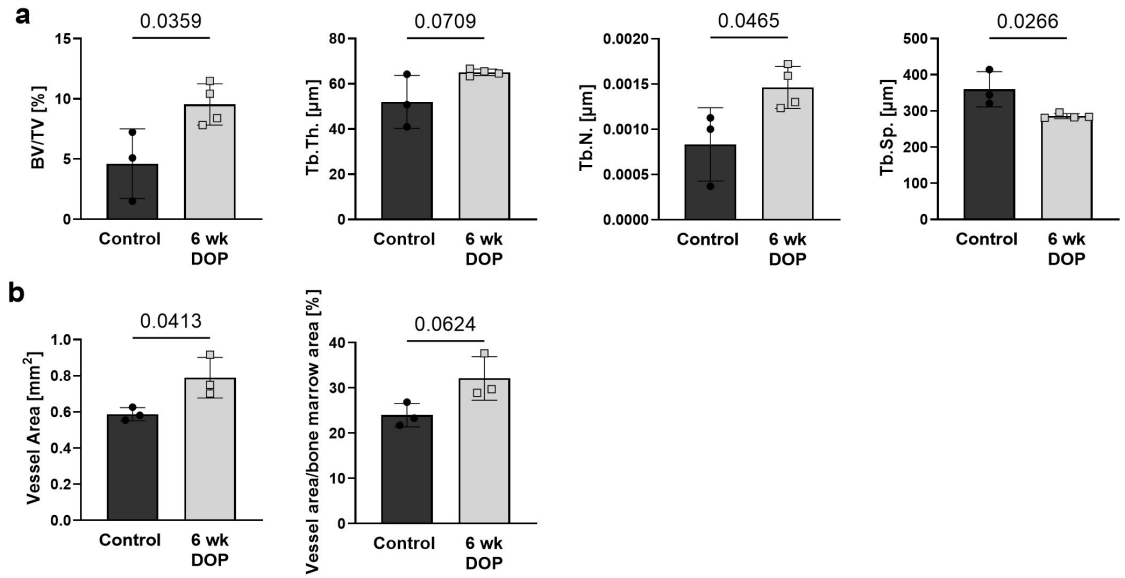

Figure 15: DOP mediates sex-independent changes in bone volume and vessel density. BV/TV, Tb.Th., Tb.N. and Tb.Sp. of female C57BL/6J mice after 3 mg/L DOP treatment for six weeks and control animals(n=3/4) and (b) vessel area and vessel area per bone marrow area assessed by Endomucin staining (n=3/3). Data are presented as mean ± s.d., and a two-tailed t-test was used for statistical analysis.

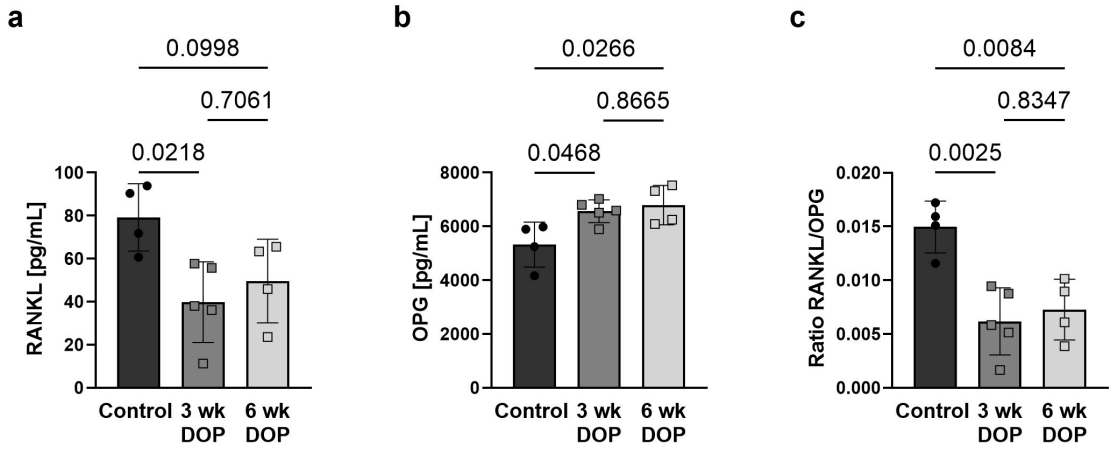

Figure 16: DOP leads to reduced bone resorption and increased bone formation marker levels. Quantification of plasma (a) RANKL (n=4/5/4) and (b) OPG (n=4/5/4) levels of C57BL/6J control mice and after three and six weeks of 3 mg/L DOP treatment as assessed by ELISA (c) and the resulting RANKL/OPG plasma ratio (n=4/5/4). Data are represented as mean ± s.d., One-way ANOVA was used for statistical analysis.

4.4 Elevation of S1P Levels Leads to Increased VEGFa Plasma Levels Due to Stimulated Production and Secretion by Osteoblasts

VEGFa is known as an important regulator of angiogenesis and bone healing.[185,328] Therefore, VEGFa plasma levels were measured in C57BL/6J mice after DOP treatment and in Sgpl1flox/flox mice after tamoxifen-induced knockout of the S1P lyase. After DOP treatment, a slight increase in VEGFa plasma levels was detected after three weeks, further increasing up to 20% after six weeks (Figure 17a). The S1P-mediated effect could further be validated using *Sgpl1*$^{flox/flox}$ Cre^{+} mice in comparison to their Cre^{-} littermate controls (Figure 17b).

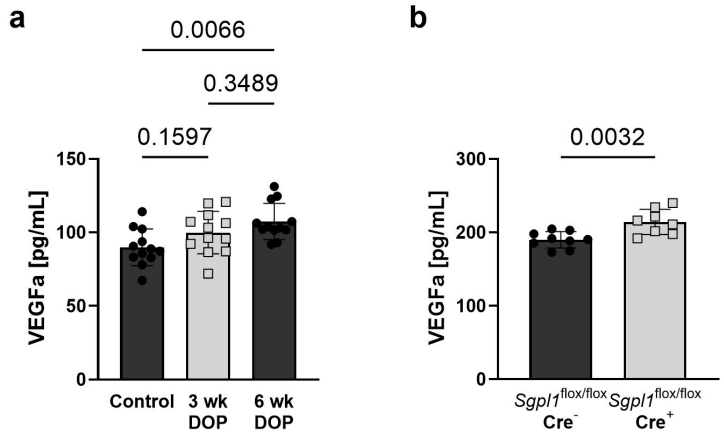

Figure 17: Pharmacological S1P lyase inhibition and genetic *Sgpl1*-knockout lead to an increase in plasma VEGFa levels.(a) Plasma VEGFa levels of C57BL/6J control mice and after three and six weeks of treatment (n=12/12/11) and (b) plasma VEGFa levels of *Sgpl1*$^{flox/flox}$ Cre^{+} mice and their littermate Cre^{-} controls eight weeks after tamoxifen-induced knockout (n=9/8) assessed by ELISA. Data are represented as mean ± s.d., One-way ANOVA (a) or two-tailed t-test (b) was used for statistical analysis.

To identify which cells are responsible for the elevation of VEGFa levels, gene expression and protein secretion in the supernatant of primary BMECs and primary OBs were assessed. Vegfa gene expression was weak in BMEC and considerable in pOBs (Figure 18a). This could be confirmed by measuring protein secretion. VEGFa was not detectable in the supernatant of BMEC, whereas VEGFa secretion after 24 hours of cultivation was detected in pOBs (Figure 18b).

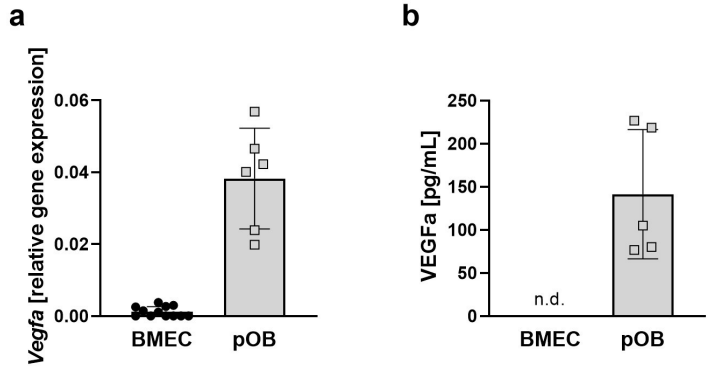

Figure 18: VEGFa is expressed and secreted by primary osteoblasts. (a) Relative gene expression of *Vegfa* in BMEC and pOBs normalized to *Gapdh* (n=12/6). (b) VEGFa levels in cell culture supernatants of BMECs and pOBs after 24 hours of cultivation (n=6/5) were measured using ELISA. Data are represented as mean ± s.d., n.d. = not detectable.

After identifying pOBs as a source of VEGFa within the bone, pOBs were treated with 1 μM S1P to mimic the DOP-mediated S1P elevation *in vitro*. After six hours of S1P treatment, an increase in *Vegfa* gene expression was detected (Figure 19a), resulting in a 1.81-fold elevation of VEGFa protein secretion as detected in the supernatant of these cells after 24 hours (Figure 19b). To evaluate the long-term effects, pOBs were treated with 1 μM S1P daily for 21 consecutive days. VEGFa levels in the supernatant remained high, with a 1.49-fold elevation after 21 days of treatment (Figure 19c), indicating continuous VEGFa production and enhancement of expression after S1P treatment.

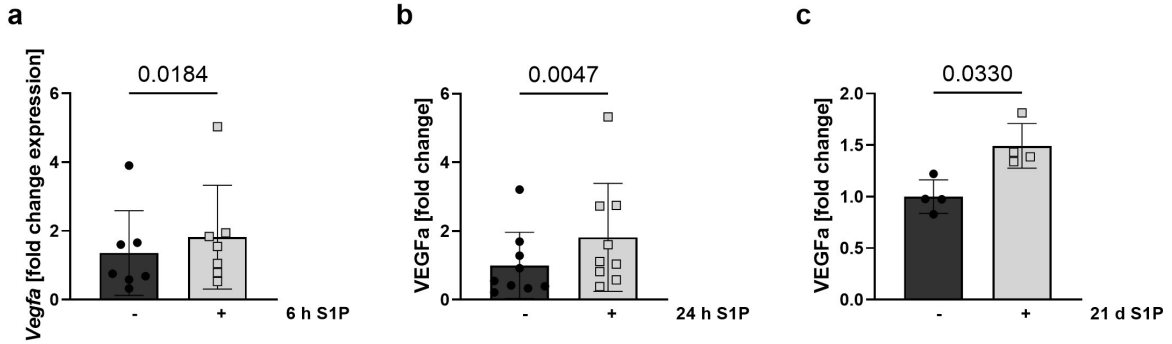

Figure 19: S1P treatment leads to increased *Vegfa* expression and VEGFa protein secretion in pOBs. (a) Fold change *Vegfa* expression in pOB after six hours of 1 μM S1P treatment compared to vehicle-treated controls (n=7/7). (b) Fold change VEGFa levels in the supernatant of 1 μM S1P treated pOBs after 24 hours (n=9/9) and after (c) long-term treatment of 21 days with daily addition of 1 μM S1P (n=4/4) measured with ELISA. Data are represented as mean ± s.d., Paired two-tailed t-test was used for statistical analysis.

4.5 S1P Leads to VEGFa-Mediated pOB Calcification and Expression of Pro-Osteogenic Factors in Endothelial Cells and Osteoblasts

S1P was previously described to enhance osteoblast calcification.[307] To test these effects on mouse pOBs, these cells were cultivated in a pro-osteogenic medium and treated daily with 1 μM S1P to stimulate the formation of calcified nodules. The previously S1P-mediated effects were confirmed using Alizarin Red staining as an indicator for calcification. After S1P treatment for 21 days, a 1.2-fold increase in staining was detected, displaying elevated calcification of pOBs (Figure 20a+b).

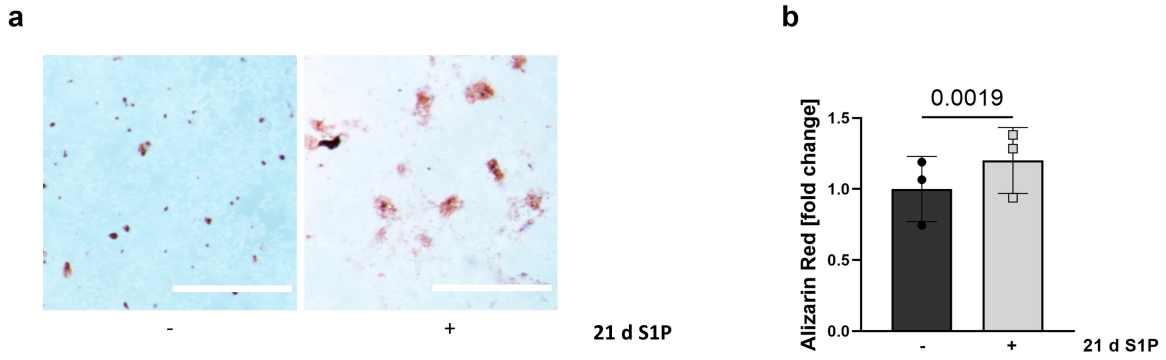

Figure 20: S1P treatment increases calcified nodule formation in pOBs. (a) Representative images of differentiated pOBs after 21 days of culture with daily addition of 1 μM S1P or vehicle control. Calcified nodules are stained using Alizarin Red, scale bar = 1mm. (b) Quantification of Alizarin Red staining of these pOB cultures after dissolving in cetylpyrridoumchloride (n=3/3). Data are represented as mean ± s.d., Paired two-tailed t-test was used for statistical analysis.

As previously described, the secretion of VEGFa is elevated in pOBs after S1P treatment. To test the involvement of VEGFa in osteoblastic calcification, a VEGFa-blocking antibody or its isotype control was added to pOBs during S1P treatment for 21 days. The expected increase in calcification, indicated by Alizarin Red staining, was observed after S1P treatment in the presence of the isotype control antibody. The addition of a VEGFa-blocking antibody prevented the S1P-mediated increase in calcification (Figure 21a+b).

These findings indicate a dependency on VEGFa in S1P-mediated calcification of pOBs. Additionally, the osteoblastic-secreted VEGFa seems to act intrinsically, enhancing pOB calcification.

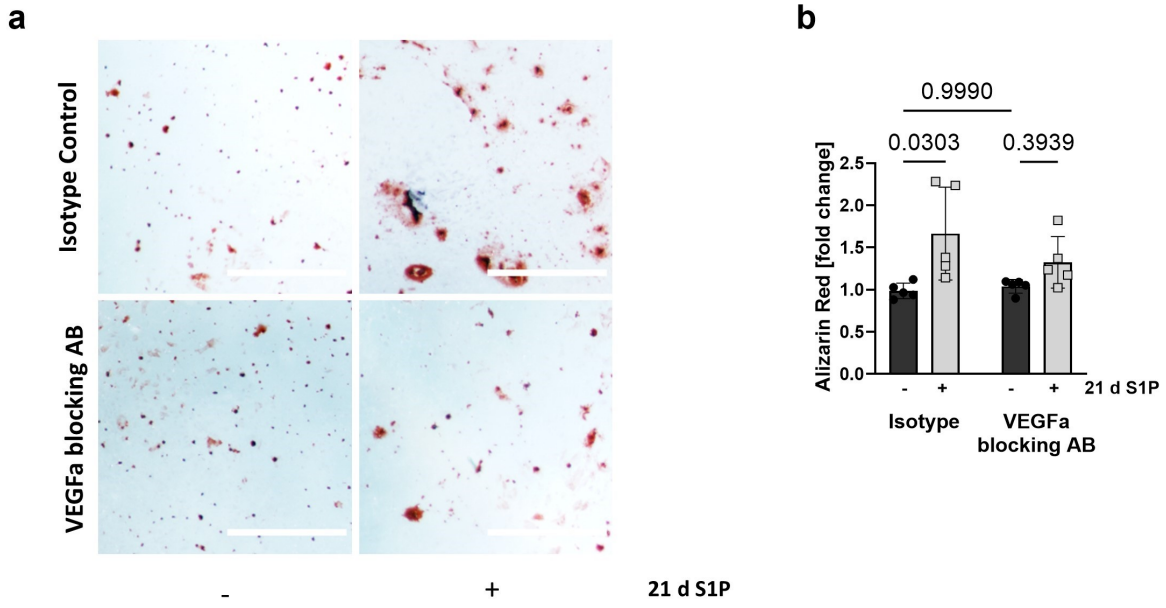

Figure 21: S1P-mediated pOB calcification is VEGFa dependent. (a) Representative images of differentiated pOBs after 21 days of culture with daily addition of 1 μM S1P or vehicle control in the presence of 1 μg/mL VEGFa blocking antibody or its Isotype control. Calcified nodules are stained with Alizarin Red; scale bar = 1mm. (b) Quantification of Alizarin Red staining after dissolving with cetylpyrridoumchloride in these cultures (n=5/5/5/5). Data are represented as mean ± s.d., Paired Two-way ANOVA was used for statistical analysis.

As VEGFa is a well-known stimulator of ECs,[185] the effect of the pOB-secreted VEGFa was evaluated in BMECs. To do so, pOBs were cultivated with and without daily S1P treatment for seven days and the pre-conditioned medium was added to BMECs. In the presence of an isotype control antibody, the expression of pro-osteogenic factors *Pdgfa*, *Pdgfb* and *Tgfb1* was elevated in cells treated with S1P-preconditioned medium. This elevation was blocked by a VEGFa-blocking antibody (Figure 22a-c), indicating a VEGFa-mediated switch of ECs towards a pro-osteogenic type.

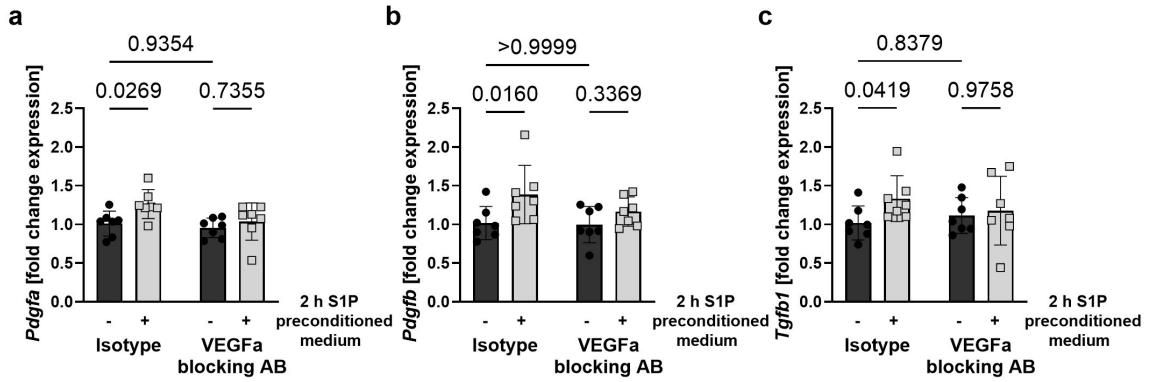

Figure 22: Pre-conditioned pOB medium leads to the VEGFa-dependent expression of pro-osteogenic factors in BMECs. Fold change gene expression of (a) *Pdgfa* (n=7/7/7/7), (b) *Pdgfb* (n=7/7/7/7) and (c) *Tgfb1* (n=7/7/7/7) in BMECs after the addition of seven days precondition medium from vehicle-treated pOBs or 1 μM S1P treated pOBs for two hours. Additionally, 1 μg/mL VEGFa blocking antibody or its Isotype control was added. Data are represented as mean ± s.d., Paired Two-way ANOVA was used for statistical analysis.

To further evaluate the crosstalk between BMECs and pOBs, experiments were performed where murine BMECs were co-cultured with murine pOBs. The formation of vascular-like structures was observed after 24 hours of culture and the network continued to expand for up to 72 hours of culture. The formation of these structures was not observed in monocultures of BMECs or OBs (data not shown). In addition, the formation of this vascular-like network was further enhanced by S1P treatment with an earlier onset of structure formation and a more dominant branching structure formed (Figure 23a+b).

The observed results indicate a VEGFa-mediated intrinsic effect of S1P treatment on pOBs, enhancing their calcification. Additionally, POB-secreted VEGFa after S1P treatment leads to the expression of pro-osteogenic factors in BMECs, possibly further enhancing the pro-osteogenic effects of S1P. The described results also demonstrate the formation of vascular-like structures, indicating a positive impact of OB/BMEC crosstalk on the bone vasculature.

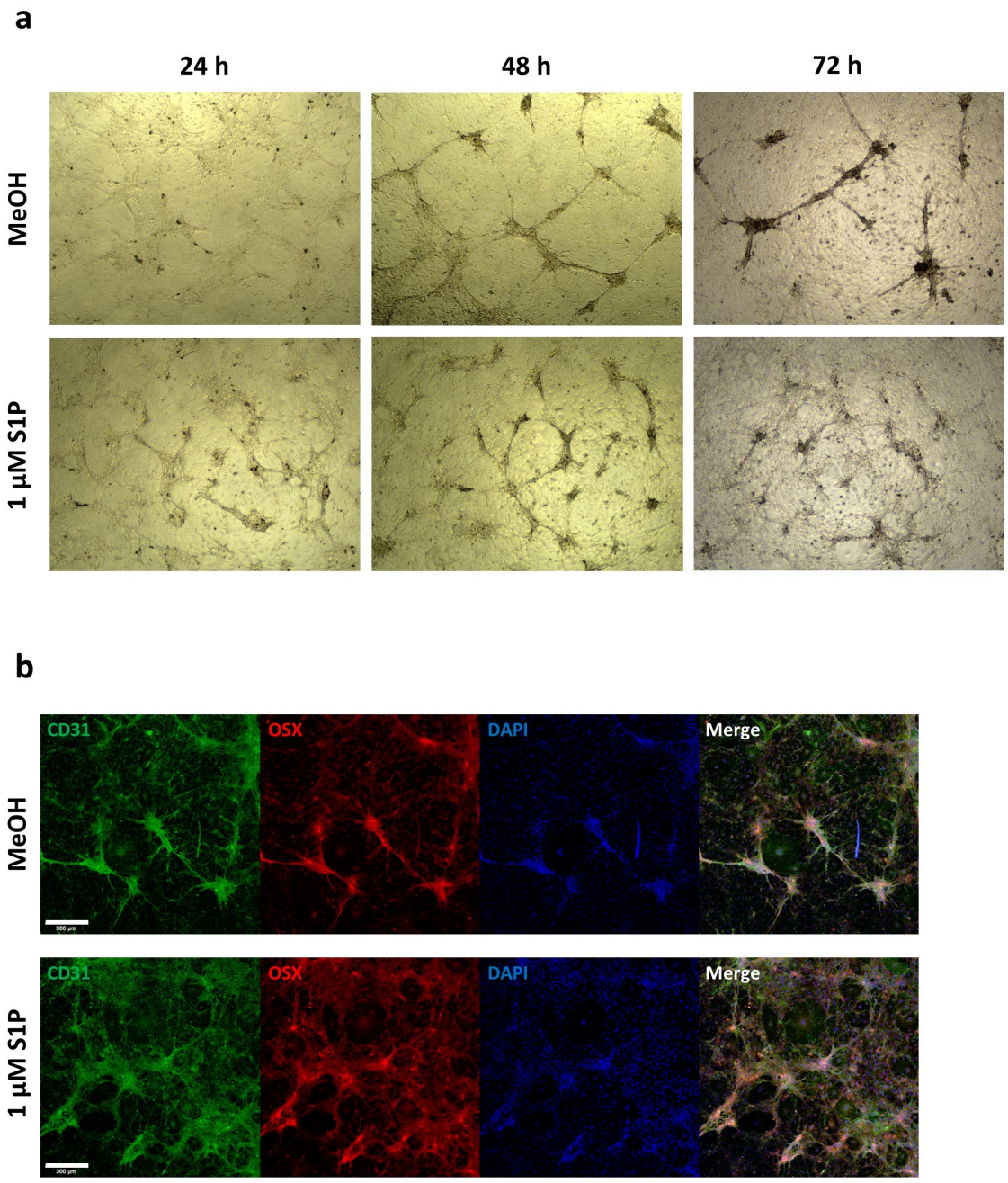

Figure 23: Co-culture of BMEC and pOBs enhances the formation of vessel-like structures. (a) Brightfield images of pOB and BMEC co-cultures after 24, 48 and 72 hours of cultivation and (b) fluorescence staining of CD31, OSX and DAPI after 72 hours of coculture with and without daily S1P treatment; scale bar = 300 μm.

4.6 S1P-Mediated Changes in Bone Vasculature and Structure are VEGF-Receptor Dependent

As a VEGFa-dependent effect on pOBs and BMEC after S1P treatment was demonstrated in vitro, the influence of VEGF-receptor blockade on DOP-mediated vascular and bone changes was additionally assessed in vivo. Therefore, Axitinib, a tyrosine kinase inhibitor with the highest inhibitor capacity toward VEGFR1-3[359] or vehicle control, was injected intraperitoneally for six weeks with and without additional treatment with DOP.

An evaluation of the DOP-mediated vascular changes in thick Endomucin-stained femoral sections showed a clear elevation of the vascular area and vessel density (Figure 24a-c). The previous increase in branching points and decreased vascular length between branches could not be detected (Figure 24d+e). The DOP-mediated changes in the vasculature were inhibited after additional administration of Axitinib (Figure 24a-c). This clearly shows the necessity of VEGF-receptor signaling for the increase in bone vessel density by S1P.

Evaluation of the trabecular bone of these animals using μCT analysis revealed an increase in BV/TV, Tb.N. and a decrease in Tb.Sp. after 6 weeks of DOP treatment (Figure 25a-e). However, these changes were prevented with additional Axitinib treatment, further showing the involvement of VEGF-receptor signaling in this process (Figure 25a-e).

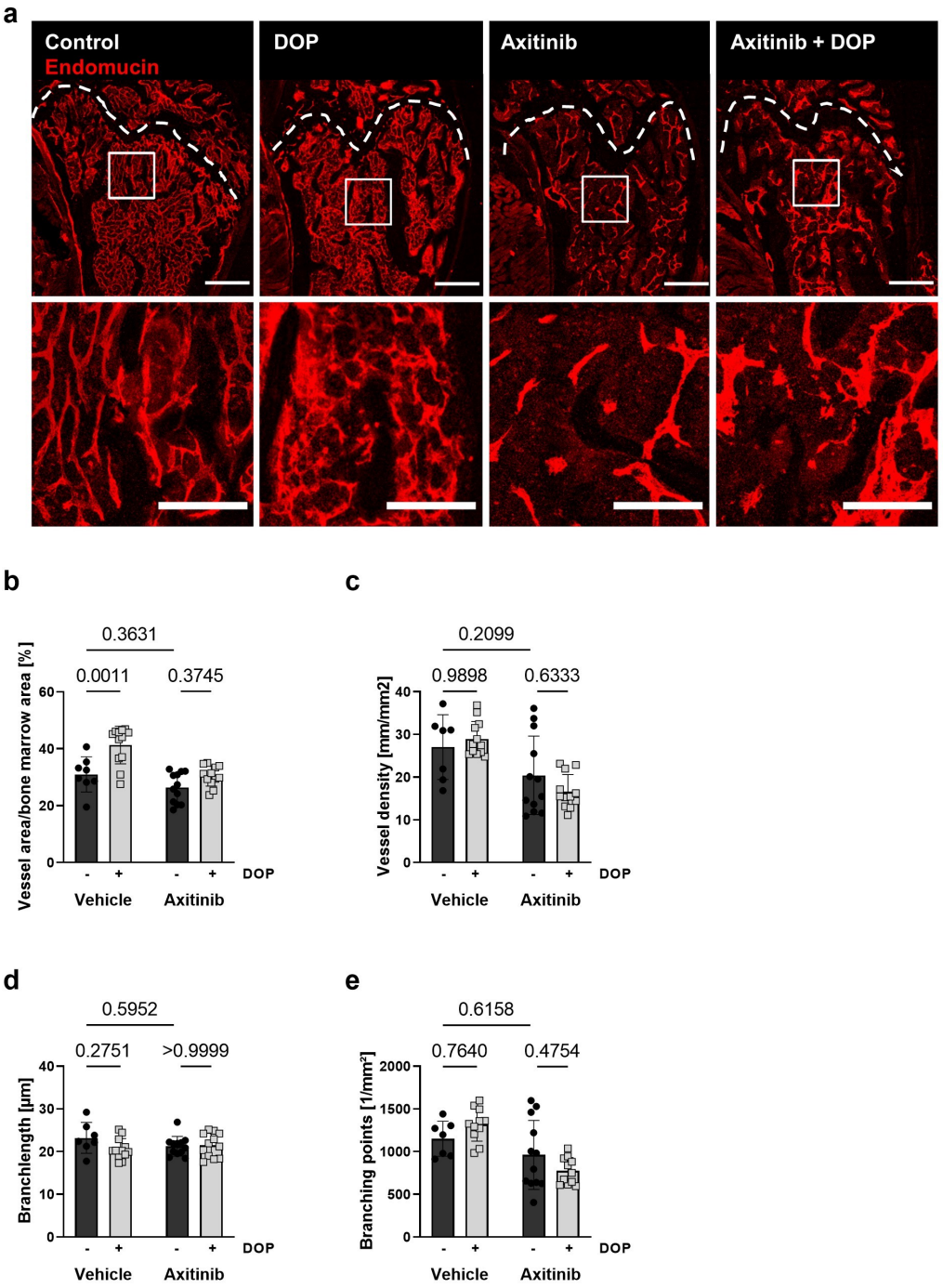

Figure 24: VEGF-receptor blockade prevents the DOP-mediated increase in vascular area and branching. (a) Representative images of thick Endomucin stained femoral sections of C57BL/6J control animals and animals treated for six weeks with 3 mg/L DOP in addition to 25 mg/kg/d of Axitinib or vehicle control administration; scale bar = 500 μm (top) and 200 μm (bottom). (b) Quantification of vascular area/bone marrow area (n=8/12/12/12), (c) vascular density (n=7/12/12/12), (d) branch length (n=7/12/12/12) and (e) number of branching points (n=7/12/11/12) within the bone marrow area. Data are represented as mean ± s.d., Two-way ANOVA was used for statistical analysis.

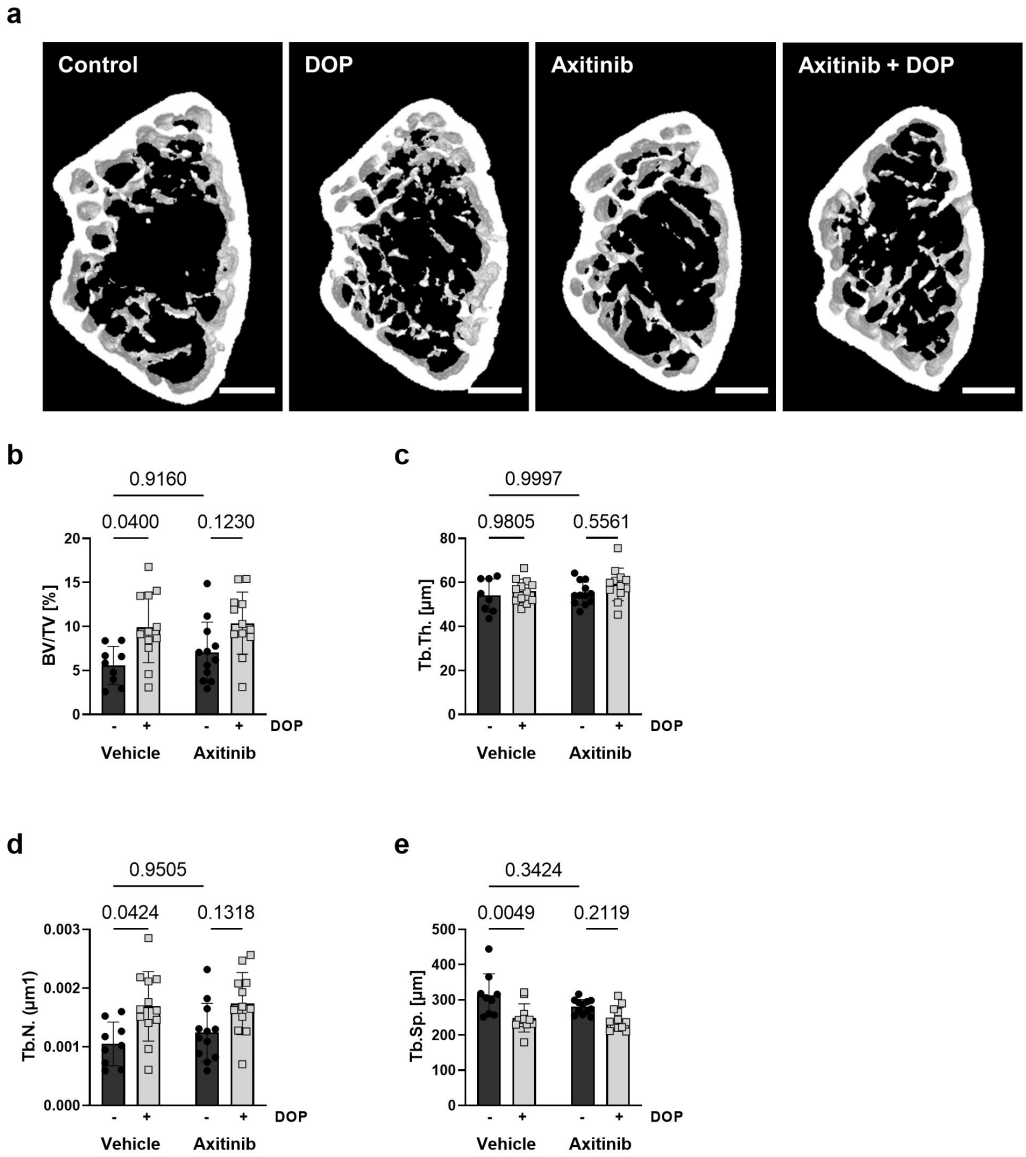

Figure 25: VEGF-receptor blockade prevents the DOP-mediated increase in trabecular bone volume. (a) Representative μCT images of C57BL/6J control animals and animals treated with 3 mg/L DOP for six weeks in addition to 25 mg/kg/d Axitinib or vehicle control administration. Quantification of (b) bone volume/total volume (n= 9/12/10/12), (c) trabecular thickness (8/12/12/12), (d) trabecular number (n=9/12/12/12) and (e) trabecular spacing (n=9/12/11/12). Data are represented as mean ± s.d., Two-way ANOVA was used for statistical analysis.

To further evaluate the involvement of VEGF-receptor signaling in trabecular bone volume formation after DOP treatment, tibiae of the same mice were analyzed using Von Kossa/McNeil´s Tetrachrome staining. Evaluation of BV/TV of the trabecular area revealed a 1.63-fold increase in trabecular bone volume after six weeks of DOP treatment. This was prevented with receptor blockade through Axitinib administration (Figure 26a+b).

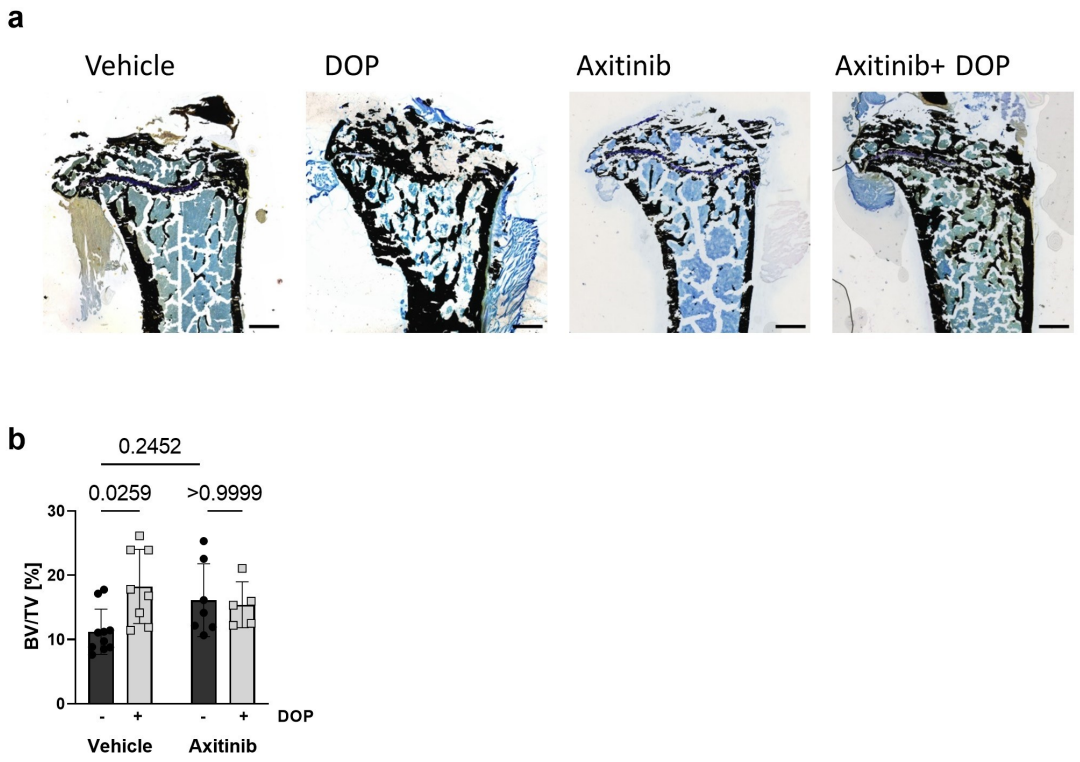

Figure 26: VEGF-receptor blockade prevents the DOP-mediated trabecular bone volume increase in tibiae. (a) Representative images of tibiae of C57BL/6J control animals and after six weeks of 3 mg/L DOP treatment, with additional treatment of 25 mg/kg/d Axitinib or vehicle control stained with Von Kossa/McNeil´s Tretrachrome staining; scale bar=500 μm. (b) Quantification of trabecular bone volume per total tissue volume in these sections (n=10/8/7/5). Data are represented as mean ± s.d., Two-way ANOVA was used for statistical analysis.

The involvement of VEGF-receptor signaling in cortical thickening was further assessed using μCT analysis. Therefore, the cortical thickness of the previously described animals was measured at mid-shaft. An apparent 14% increase in cortical thickness was observed with DOP treatment alone. This effect was again completely inhibited with additional Axitinib treatment (Figure 27a+b). Similar observations were made when evaluating the cortical area per total tissue area in these samples (Figure 27c).

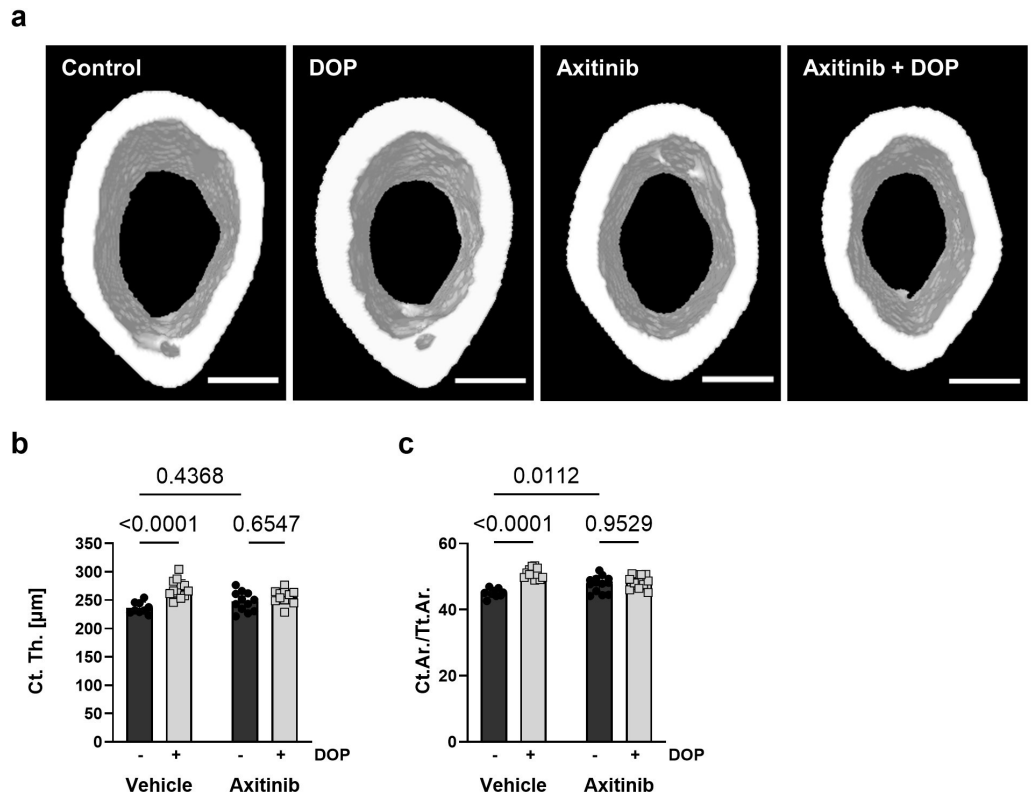

Figure 27: VEGF-receptor blockade prevents DOP-mediated thickening of cortical bone. (a) Representative μCT images of cortical sections at the mid-shaft of femora of C57BL/6J control animals and after six weeks of 3 mg/L DOP treatment in addition to 25 mg/kg/d of Axitinib or vehicle control administration; scale bar= 500 μm. (b) Quantification of cortical thickness (n=9/12/12/12) and (c) cortical area per total tissue area (n=9/12/12/12). Data are represented as mean ± s.d., Two-way ANOVA was used for statistical analysis.

To evaluate the influence of Axitinib treatment on bone strength, femoral bones were tested using a three-point bending test. After DOP treatment alone, the bone displays a 1.27-fold increase in stiffness and a 42% increase in ultimate force needed until bone failure occurs. VEGF-receptor blockade using Axitinib prevented the growth of both parameters (Figure 28a-c). This indicates the necessity of VEGF-receptor signaling in DOP-mediated bone strengthening.

In summary, it was shown that DOP-mediated changes in both the vasculature and the increase in bone density and strength are VEGF-receptor dependent.

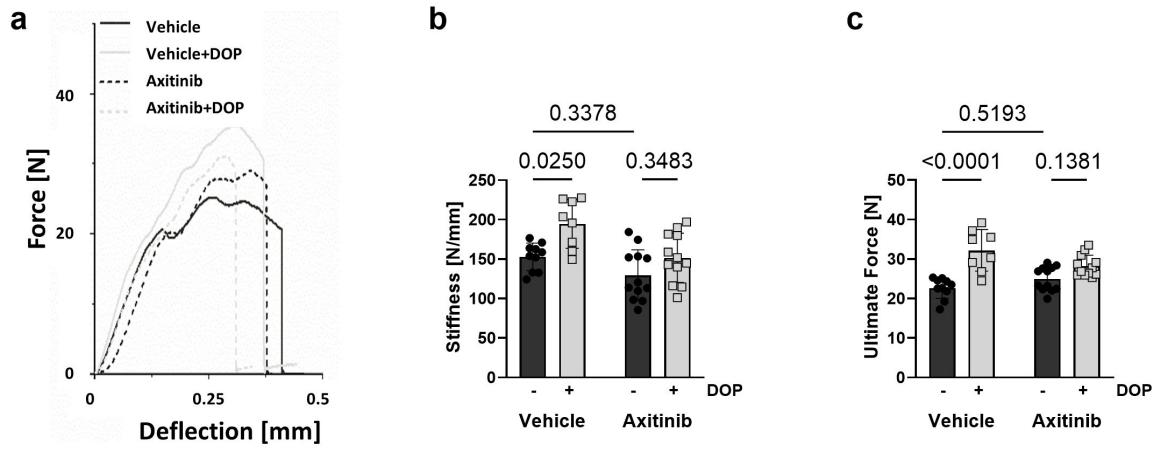

Figure 28: VEGF-Receptor blockade prevents DOP-mediated strengthening of the bone. (a) Representative force/deflection graphs resulting from a three-point bending test of femoral bones from C57BL/6J control animals and after six weeks of 3 mg/L DOP treatment in addition to 25 mg/kg/d Axitinib or vehicle control administration. Quantification of (b) stiffness (n=10/8/12/12) and (c) ultimate force (n=10/8/12/12). Data are represented as mean ± s.d., Two-way ANOVA was used for statistical analysis.

4.7 S1P-Mediated VEGFa Production and Osteoblast Calcification are S1PR3-Dependent

S1P signals through five different receptors,[82] of which S1PR1-3 are expressed in OBs (data not shown). The possible involvement of these receptors in the observed S1P-mediated effects was examined. Therefore, pOBs were treated with S1P in addition to S1P receptor antagonists. S1P treatment combined with the vehicle control showed the expected increase in Vegfa gene expression after six hours of treatment and an increase of VEGFa secretion detected in the cell culture supernatant after 24 hours (Figure 29a+b). Treatment with TY-52156, an S1PR3 antagonist, prevented the observed increase in Vegfa gene expression and protein secretion after S1P treatment (Figure 29a+b), indicating an involvement of this receptor in the underlying signaling cascade.

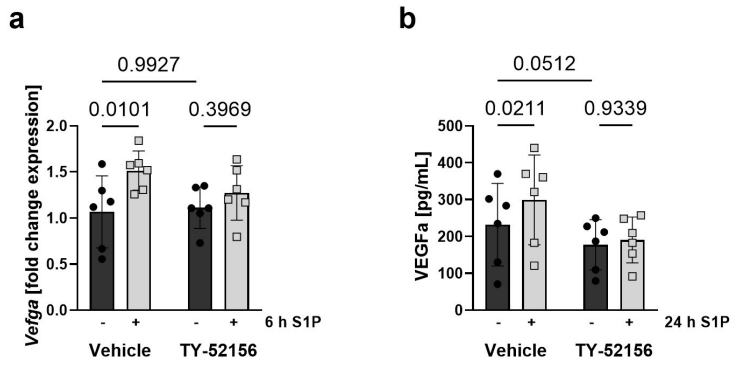

Figure 29: S1PR3 antagonism prevents S1P-mediated increases in VEGFa expression and secretion in pOBs. (a) Fold change *Vegfa* gene expression after six hours of 1 μM S1P or vehicle control treatment in the addition of 10 μM S1PR3 antagonist TY-52156 or vehicle control 30 minutes prior to S1P treatment (n=6/6/6/6). (b) VEGFa levels in the supernatant of equally treated pOBs after 24 hours (n=6/6/6/6) as measured by ELISA. Data are represented as mean ± s.d., Paired Two-way ANOVA was used for statistical analysis.

To further confirm these results, pOBs isolated from *S1PR3*$^{+/+}$ and *S1PR3*$^{-/-}$ mice were treated with 1 μM S1P. A 1.56-fold rise in *Vegfa* gene expression was observed in the wild-type pOBs after 6 hours of S1P treatment (Figure 30 a). There was also a tendency towards elevated Vegfa expression in S1PR3-/- mice (Figure 30a). However, this increase was not represented in VEGFa protein secretion in the supernatant of the knockout pOBs in contrast to a clear 1.4-fold elevation of VEGFa secretion by wild-type pOBs (Figure 30b). These results further confirm the S1PR3-dependent secretion of VEGFa in pOBs after S1P treatment.

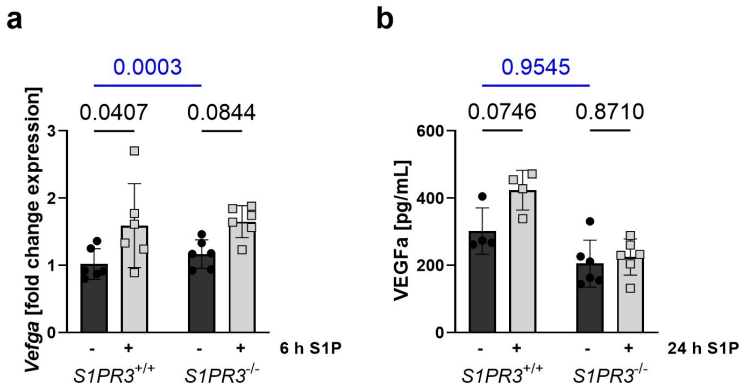

Figure 30: Genetic deletion of *S1PR3* prevents S1P-mediated increases in VEGFa secretion in pOBs. (a) Fold change *Vegfa* gene expression after six hours of 1 μM S1P or vehicle control in pOBs isolated from *S1PR3*$^{+/+}$ and *S1PR3*$^{-/-}$ mice (n=6/6/6/6). (b) VEGFa levels in the supernatant of equally treated pOBs after 24 hours (n=4/4/6/6) as measured by ELISA. Data are represented as mean ± s.d., Paired (black) or unpaired (blue). Two-way ANOVA was used for statistical analysis.

To evaluate whether deletion of *S1PR3* and therefore, reduced VEGFa production plays a role in S1P-mediated calcification of pOBs, wild-type and knockout cells were treated daily with 1 μM S1P for 21 days. Wild-type pOBs show a 27% increase in calcified nodule formation due to S1P treatment, as represented by Alizarin Red staining (Figure 31a+b). This S1P-mediated increase in calcification was prevented by *S1PR3* knockout in these cells (Figure 31a+b).

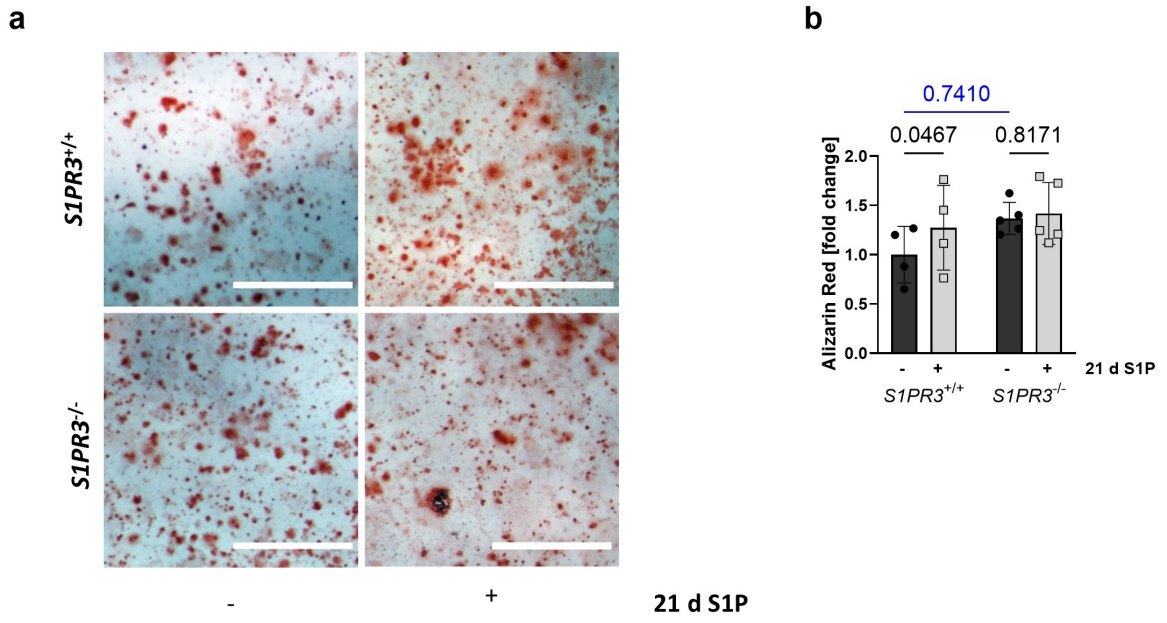

Figure 31: Genetic deletion of *S1PR3* prevents S1P-mediated calcification of pOBs. (a) Representative images of differentiated pOBs isolated from $S1PR3^{+/+}$ and $S1PR3^{-/-}$ mice after 21 days of culture with daily addition of 1 μM S1P or vehicle control. Calcified nodules are stained with Alizarin Red; scale bar=1mm. (b) Quantification of Alizarin Red staining after dissolving the staining in cetylpyrridiumchloride (n=4/4/5/5). Data are represented as mean ± s.d., Paired (black) or unpaired (blue). Two-way ANOVA was used for statistical analysis.

To elucidate the signaling pathways involved in the observed effects in pOBs, gene expression analysis was performed in wild-type and $S1PR3^{-/-}$ pOBs with and without 1 μM S1P treatment. Several target genes were found to be regulated by S1P treatment in wild-type pOBs, including a significant up-regulation of *Osteocalcin* (*Bglp*) and *Osteonectin* (*Sparc*) and an increase in the expression of *Osteopontin* (*Spp1*) and *Periostin* (*Postn*). These effects were absent in $S1PR3^{-/-}$ pOBs (Figure 32). These findings revealed a clear dependency of osteoblastic S1P/S1PR3 signaling on S1P-mediated regulation of osteogenic mechanisms.

Notably, a down-regulation of *Sparc* and *Spp1* was observed in $S1PR3^{-/-}$ pOBs compared to the wild-types (Figure 32). Both factors are known to be involved in regulating OBs and

OCs during bone remodeling.[360–362] In addition, the pro-osteogenic factor *Osterix* (*Sp7*)[363] was found to be upregulated in knockout pOBs compared to wild-type pOBs (Figure 32) . These findings do not only show an essential role of S1PR3 in bone formation but also for the regulation of OB/OC crosstalk.

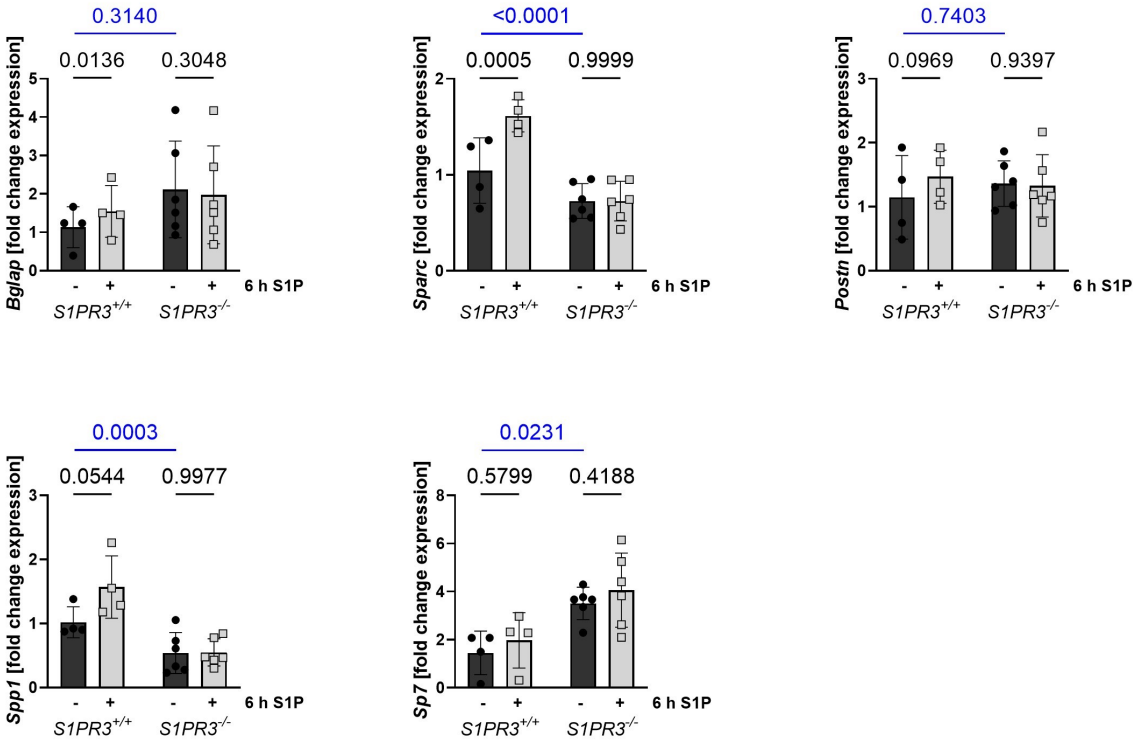

Figure 32: S1P treatment leads to changes in gene expression of several osteogenic markers. Fold change gene expression levels of *Bglap*, *Sparc*, *Postn*, *Spp1* and *Sp7* in S1PR3+/+ and S1PR3-/- osteoblasts with and without 1 μM S1P treatment of 6 hours. Data are presented as mean ± s.d.; a paired two-was ANOVA (black) or unpaired two-way ANOVA (blue) was used for statistical analysis.

These results prove that S1P-mediated expression and secretion of VEGFa through pOBs are S1PR3 dependent. Additionally, the receptor is necessary for S1P-mediated cell calcification, possibly due to increased VEGFa production and OB/OC crosstalk regulation.

4.8 DOP-Mediated Formation of H-Type Vessels and Increases in Trabecular Bone Volume are Mediated Through S1PR3 Signaling *in vivo*

To further evaluate the possible effect of S1PR3 signaling *in vivo*, 20-week-old $S1PR3^{+/+}$ and $S1PR3^{-/-}$ mice were treated with DOP for six weeks. Measurement of plasma VEGFa levels showed a clear increase after six weeks of DOP treatment in wild-type mice. In contrast, no increase in mice lacking S1PR3 was detected (Figure 33). This confirmed the S1PR3-mediated VEGFa production and rise of VEGFa levels in an in vivo model and demonstrated a global increase in circulating VEGFa within the body.

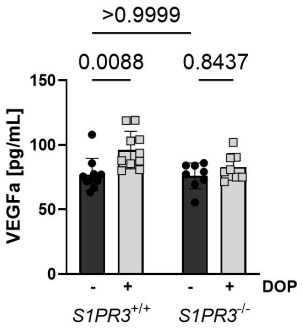

Figure 33: The DOP-mediated elevation of VEGFa plasma levels is S1PR3 dependent. VEGFa plasma levels of $S1PR3^{+/+}$ and $S1PR3^{-/-}$ animals after six weeks of 3 mg/L DOP treatment were measured using ELISA (n=9/10/8/8). Data are represented as mean ± s.d., Two-way ANOVA was used for statistical analysis.

To assess the involvement of S1PR3 in the DOP-mediated densening of the bone vasculature and induction of the phenotypic switch towards H-type vessels, thick Endomucin-stained femoral sections of these mice were evaluated. Wild-type mice showed a clear elevation of Endomucin mean fluorescence intensity as a marker of the phenotypic switch of BMECs towards the pro-osteogenic H-type vessels. This increase was not detected in $S1PR3^{-/-}$ mice (Figure 34a+b). This indicates an S1PR3-dependent switch of the BMECs towards their pro-osteogenic phenotype. An increase in the vascular area within the bone marrow and vascular density was detected in both wild-type and knockout mice after six weeks of DOP treatment (Figure 34c-f). This indicates an involvement of another S1PR, leading to these observed changes.

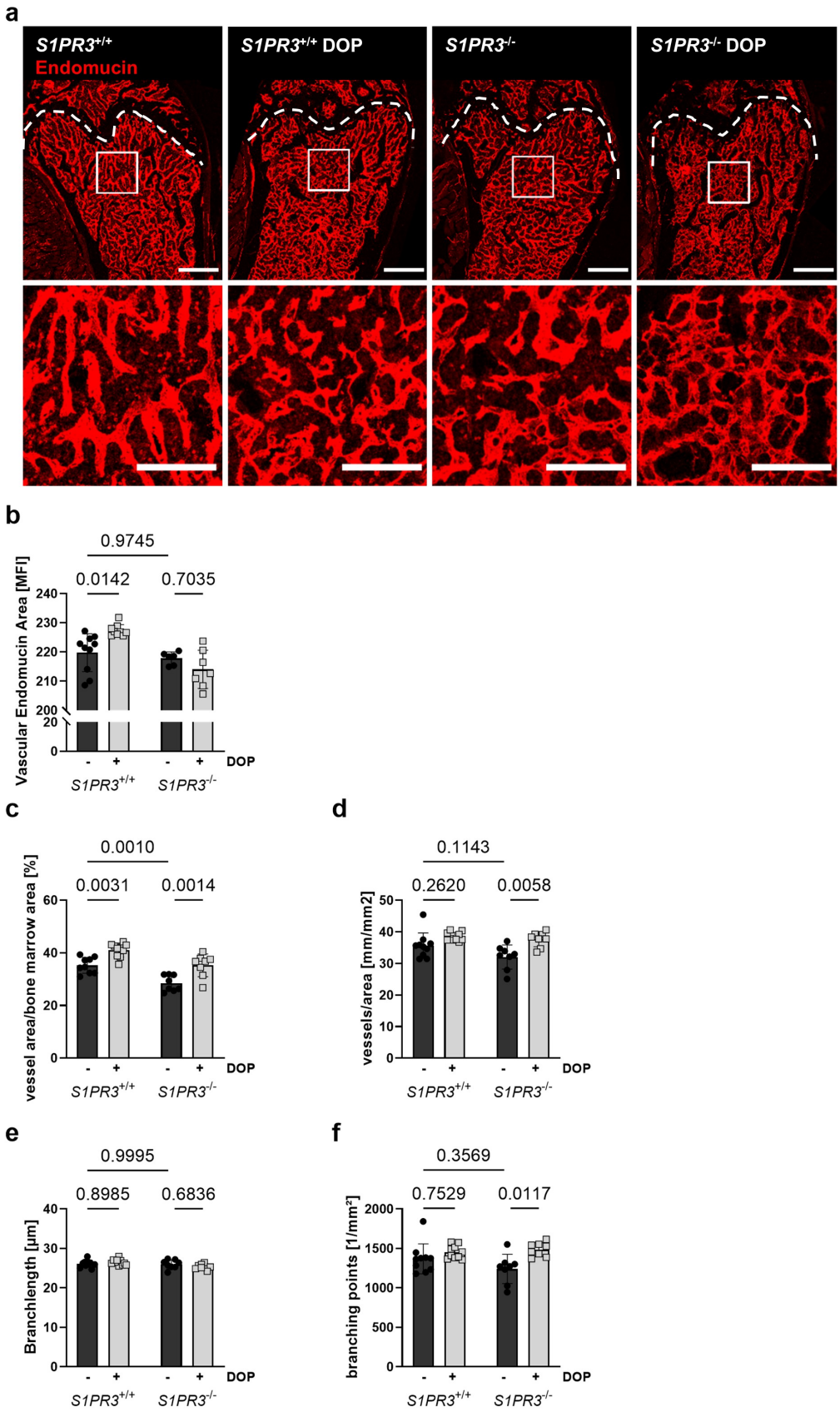

Figure 34: The DOP-mediated phenotypic switch toward H-type vessels is S1PR3 dependent. (a) Representative images of thick Endomucin stained femoral sections of $S1PR3^{+/+}$ control animals and $S1PR3^{-/-}$ knockout animals treated with 3 mg/L DOP for six weeks and their untreated controls; scale bar = 500 μm (top) and 200 μm (bottom).

Figure 34 *(previous page)*: (b) Quantification of mean fluorescence intensities (MFI) of Endomucin staining, (c) vascular area/bone marrow area, (d) vascular density, (e) branch length and (f) number of branching points within the metaphyseal area. Data are represented as mean ± s.d., Two-way ANOVA was used for statistical analysis.

To assess whether the repressed phenotypic switch of the vasculature is enough to prevent an increase in bone volume in *S1PR3*$^{-/-}$ mice, the trabecular area and volume of the distal femur of wild-type and knockout mice were evaluated using μCT analysis after six weeks of DOP treatment. Indeed, the increase in BV/TV, Tb.Th. and Tb.N., and the decrease in Tb.Sp. observed in wild-type mice is prevented through *S1PR3* knockout (Figure 35a-e). This clearly shows an S1P-mediated increase in bone volume due to a phenotypic switch of the bone vasculature towards pro-osteogenic H-type vessels. An increase in BV/TV, Tb.Th. and Tb.N. was observed in *S1PR3*$^{-/-}$ mice compared to *S1PR3*$^{+/+}$ mice (Figure 35a-d), indicating an additional effect of S1PR3 signaling not only on bone regeneration after treatment, but also on a basal level.

To identify the effect of *S1PR3* knockout on cortical thickness and strength of the bone, μCT analysis and 3pbt were used. Analysis of the cortical thickness of femoral bones revealed an increase after DOP treatment in both wild-type and knockout mice (Figure 36a+b). Similar results were observed in the 3-point bending test. Both bones from wild-type and knockout needed higher ultimate force to bend after DOP treatment, and both displayed a slight increase in stiffness (Figure 37a-c).

These results suggest a possible S1P-mediated mechanism of bone strengthening in addition to the S1PR3-mediated effects. The responses in bone depend on the location with clear involvement of S1PR3 in trabecular bone formation and reduced influence in cortical bone formation.

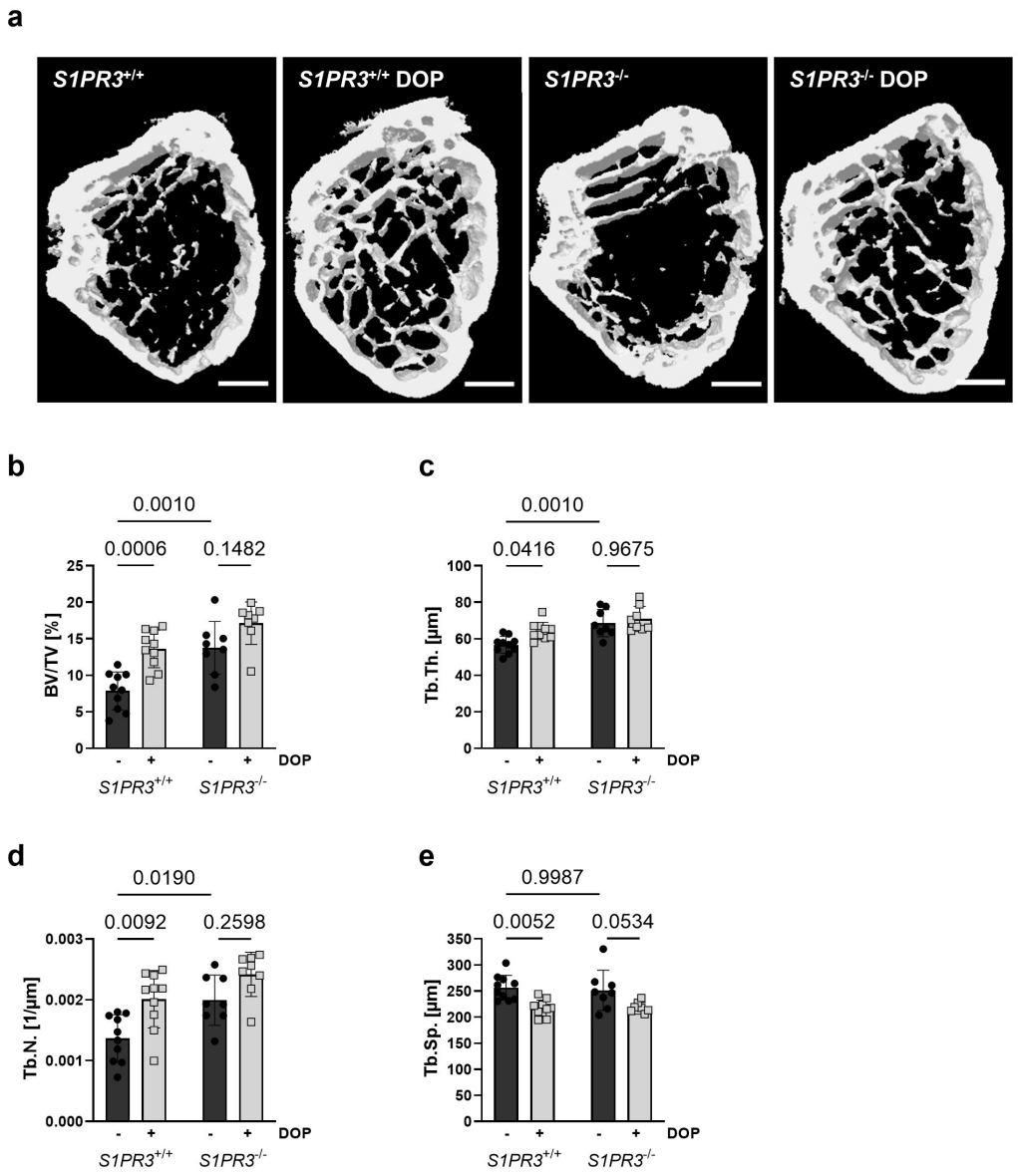

Figure 35: The DOP-mediated increase in trabecular bone volume S1PR3 dependent. Representative μCT images of *S1PR3*$^{+/+}$ control animals and *S1PR3*$^{-/-}$ knockout animals treated with 3 mg/L DOP for six weeks and their untreated controls. Quantification of (b) bone volume/total volume (n=10/10/8/8), (c) trabecular thickness (n=10/10/8/8), (d) trabecular number (n=10/10/8/8) and (e) trabecular spacing (n=10/10/8/8). Data are represented as mean ± s.d., Two-way ANOVA was used for statistical analysis.

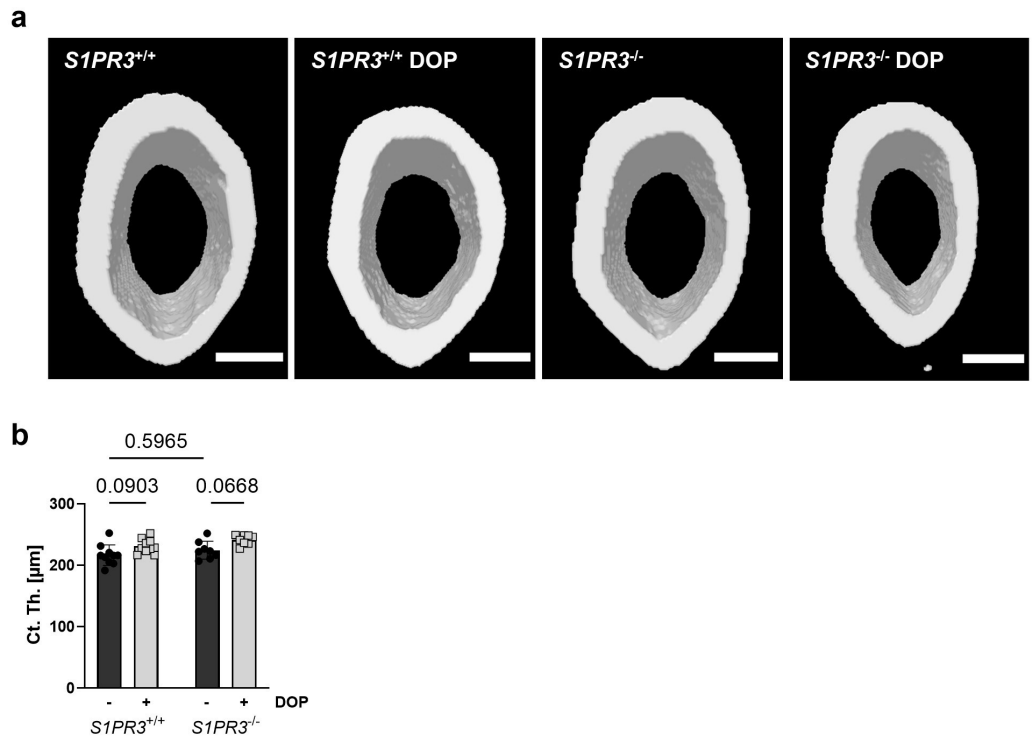

Figure 36: DOP-mediated cortical thickening is S1PR3 independent. (a) Representative images of cortical sections at the mid-shaft of femoral of $S1PR3^{+/+}$ control animals and $S1PR3^{-/-}$ knockout animals treated with 3 mg/L DOP for six weeks and their untreated controls; scale bar= 500 μm. (b) Quantification of cortical thickness (n=10/10/8/8). Data are represented as mean ± s.d., Two-way ANOVA was used for statistical analysis.

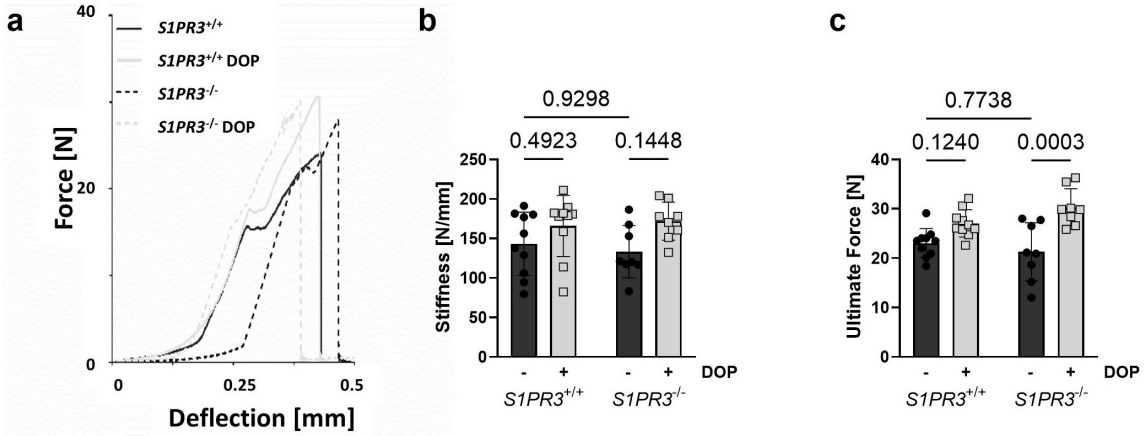

Figure 37: DOP-mediated strengthening of the bone is S1PR3 independent. (a) Representative force/deflection graphs resulting from a three-point bending test of femoral bones from $S1PR3^{+/+}$ control animals and $S1PR3^{-/-}$ knockout animals treated with 3 mg/L DOP for six weeks and their untreated controls. Quantification of (b) stiffness (n=10/10/7/8) and (c) ultimate force (n=10/10/7/8). Data are represented as mean ± s.d., Two-way ANOVA was used for statistical analysis.

Previously, both bone formation and bone resorption markers were shown to be influenced through DOP treatment. These could explain the observations made in cortical and trabecular bone. Therefore, RANKL and OPG plasma values were checked in wild-type and *S1PR3* knockout mice. *S1PR3*$^{+/+}$ mice showed the previously detected decrease in bone resorption as represented through decreased RANKL levels and increased bone formation represented through increased OPG levels after DOP treatment (Figure 38a+b). This led to a reduced RANKL to OPG ratio (Figure 38c), representing the previously observed S1P-mediated pro-osteoanabolic phenotype. In contrast, changes in both RANKL and OPG were not observed after DOP treatment in S1PR3-/- mice (Figure 38a-c).

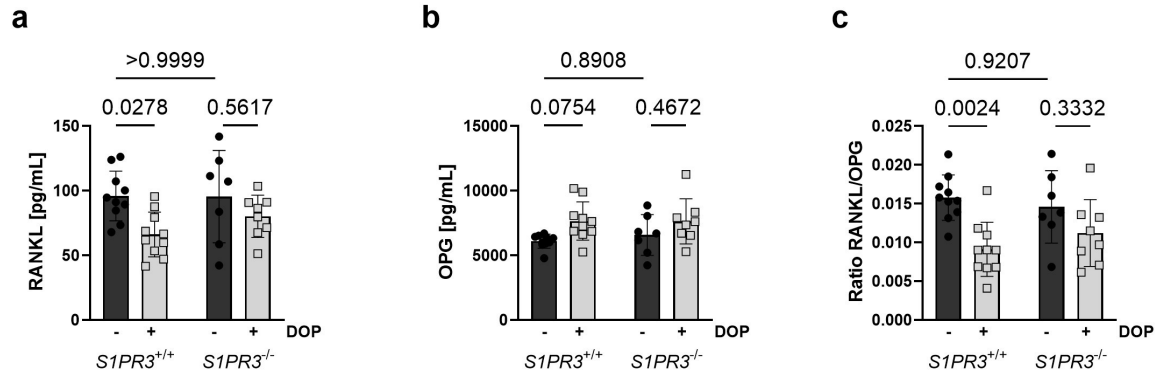

Figure 38: DOP treatment leads to reduced bone resorption and increased bone formation plasma markers, which is prevented in *S1PR3*$^{-/-}$ mice. Quantification of plasma (a) RANKL (n=10/10/7/8) and (b) OPG (n=10/10/7/8) levels in *S1PR3*$^{+/+}$ control animals and *S1PR3*$^{-/-}$ knockout animals treated with 3 mg/L DOP for six weeks and their untreated controls as assessed by ELISA. (c) The resulting RANKL/OPG plasma ratio (n=10/10/7/8). Data are represented as mean ± s.d., Two-way ANOVA was used for statistical analysis.

The observed results demonstrate an S1P/S1PR3-dependent phenotypic switch of the vasculature towards pro-osteogenic H-type vessels, followed by an increase in bone formation and a decrease in bone resorption. This ultimately leads to increased trabecular bone mass. These effects could be explained by an involvement of S1PR3 signaling in OB/OC crosstalk, as evidenced by plasma markers and gene expression data. The S1P-mediated thickening and strengthening of cortical bone is S1PR3 independent.

4.9 S1P Mediates a Vessel-Independent Strengthening of the Bone Through S1PR2

Previously, an influence of S1PR2 on bone density and strength was described. *S1PR2*$^{-/-}$ mice were described to suffer from lower bone density and reduced bone strength.[307] To identify additional influences of S1PR2 in the S1P-mediated bone regeneration, *S1PR2*$^{+/+}$ and *S1PR2*$^{-/-}$ mice were treated with DOP for six weeks. Measurement of VEGFa plasma levels in these mice revealed an increase in both wild-type and knockout animals upon DOP treatment. This indicated an S1PR2-independent rise in VEGFa plasma levels (Figure 39).

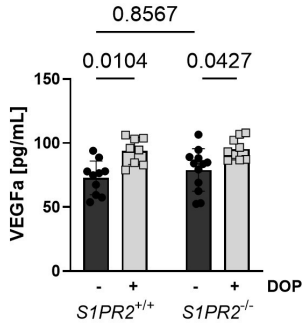

Figure 39: The DOP-mediated increase in VEGFa plasma levels is S1PR2 independent. VEGFa plasma levels of S1PR2+/+ and S1PR2-/- animals after six weeks of 3 mg/L DOP treatment and in untreated control animals were measured using ELISA (n=10/8/12/8). Data are represented as mean ± s.d., Two-way ANOVA was used for statistical analysis.

Analysis of thick Endomucin-stained bone sections revealed an increase in Endomucin MFI in the epiphyseal region of these mice in both wild-type and knockouts (Figure 40a+b). Additionally, an increase in total vessel area was observed upon DOP treatment (Figure 40c). Analysis of vessel density, branch length and number of branches did not show any influence of DOP on both wild-type and knockout mice (Figure 40d-f). These results clearly confirm the S1PR2-independent and S1PR3-dependent phenotypic switch of BMECs after DOP treatment.

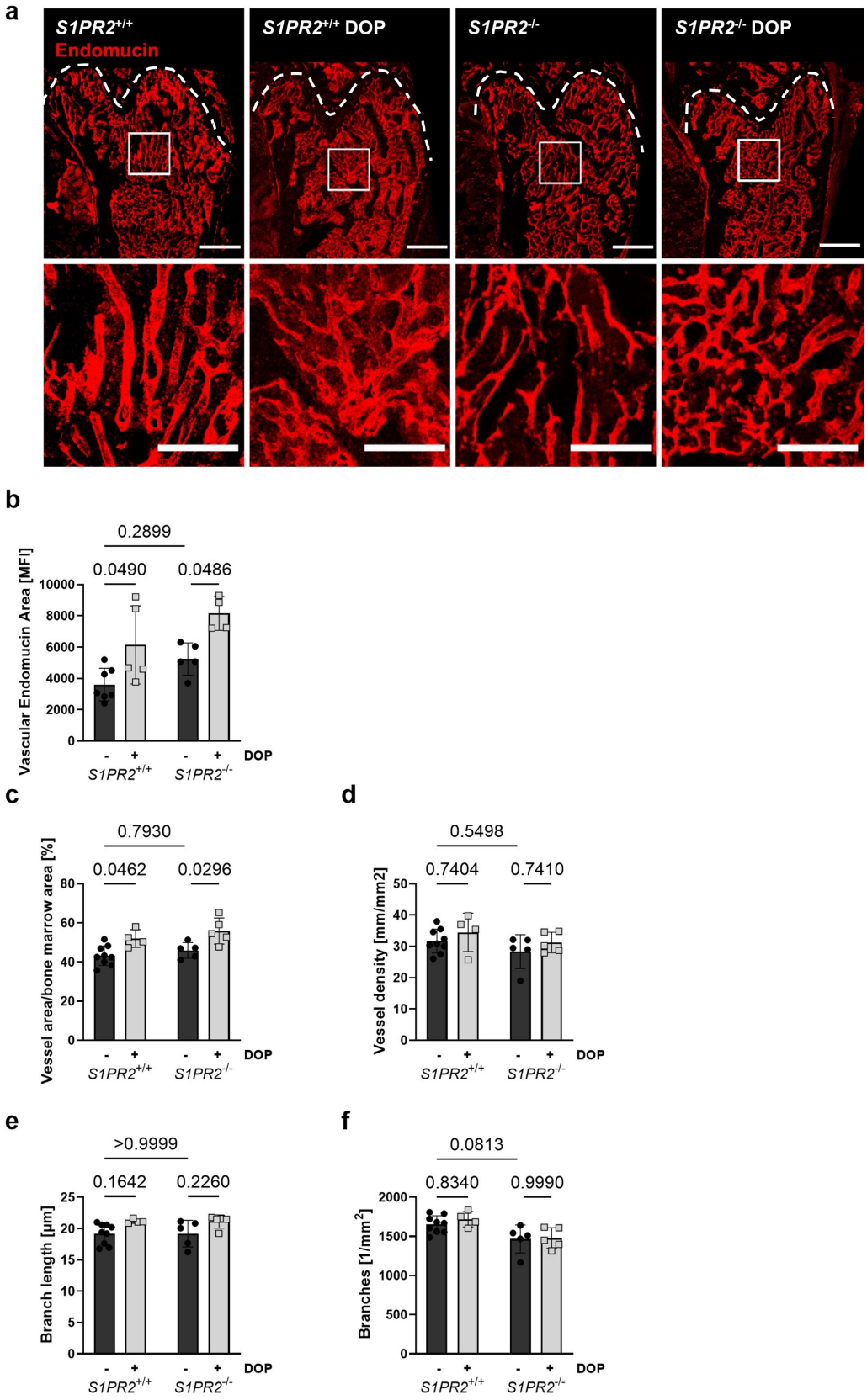

Figure 40: The DOP-mediated increase in vascular Endomucin expression and vascular density and branching is S1PR2 independent. (a) Representative images of thick Endomucin stained femoral sections of *S1PR2*$^{+/+}$ control animals and *S1PR2*$^{-/-}$ knockout animals treated with 3 mg/L DOP for six weeks and their untreated controls; scale bar = 500 μm (top) and 200 μm (bottom).

Figure 40 *(previous page)*: b) Quantification of mean fluorescence intensities (MFI) of Endomucin staining (n=7/5/5/4), (c) vascular area/bone marrow area (n=9/4/5/5), (d) vascular density (n=9/4/5/5), (e) branch length (n=9/4/5/5) and (f) number of branching points (n=9/4/5/5) within bone marrow area. Data are represented as mean ± s.d., Two-way ANOVA was used for statistical analysis.

To evaluate if there is an influence on trabecular bone volume after DOP treatment in *S1PR2*$^{-/-}$ mice, μCT analysis of the distal femoral bones was conducted. As previously described, BV/TV and Tb.Th. reduction was observed in *S1PR2*$^{-/-}$ mice compared to *S1PR2*$^{+/+}$ mice (Figure 41a-e). However, both wild-type and control animals showed increased trabecular bone parameters after DOP treatment (Figure 41 a-e). This means that there is an S1PR2-independent regenerative capacity of S1P within the trabecular bone.

As S1P-mediated thickening of the corticalis and strengthening of the bone was previously observed to be S1PR3 independent, the possible influence of S1PR2 on these parameters was evaluated. Analysis of cortical thickness of femoral bones showed a clear increase in thickness in *S1PR2*$^{+/+}$ animals after DOP treatment. Besides, a decrease in cortical thickness was observed in knockout mice compared to wild-type mice. The DOP-mediated thickening effect was abrogated in *S1PR2*$^{-/-}$ mice (Figure 42a+b).

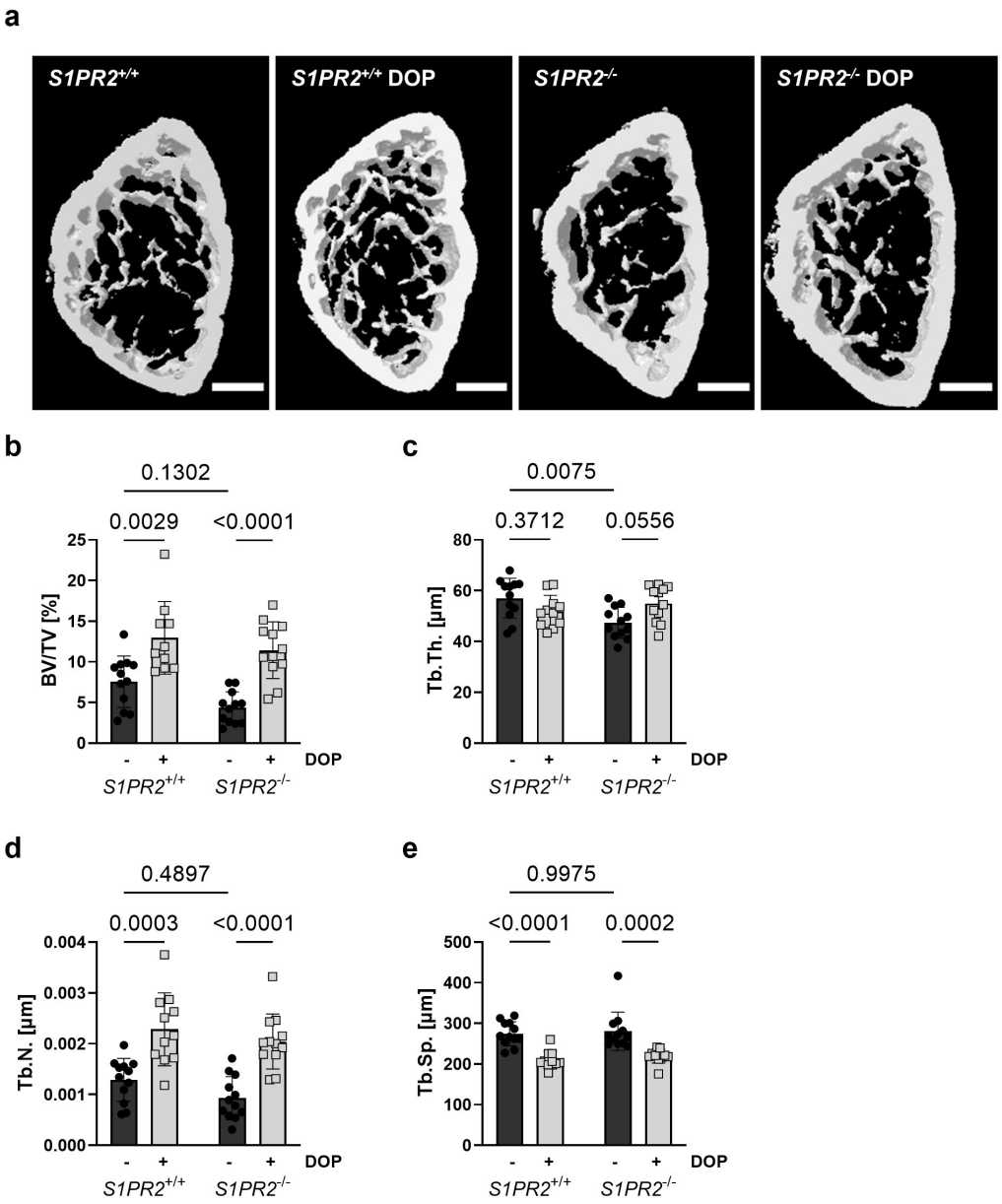

Figure 41: The DOP-mediated increase in trabecular bone volume is S1PR2 independent. (a) Representative µCT images of $S1PR2^{+/+}$ control animals and $S1PR2^{-/-}$ knockout animals treated with 3 mg/L DOP for six weeks and their untreated controls. Quantification of (b) bone volume/total volume (n=12/10/12/12), (c) trabecular thickness (n=12/11/12/12), (d) trabecular number (n=12/11/12/12) and (e) trabecular spacing (n=12/11/12/11). Data are represented as mean ± s.d., Two-way ANOVA was used for statistical analysis.

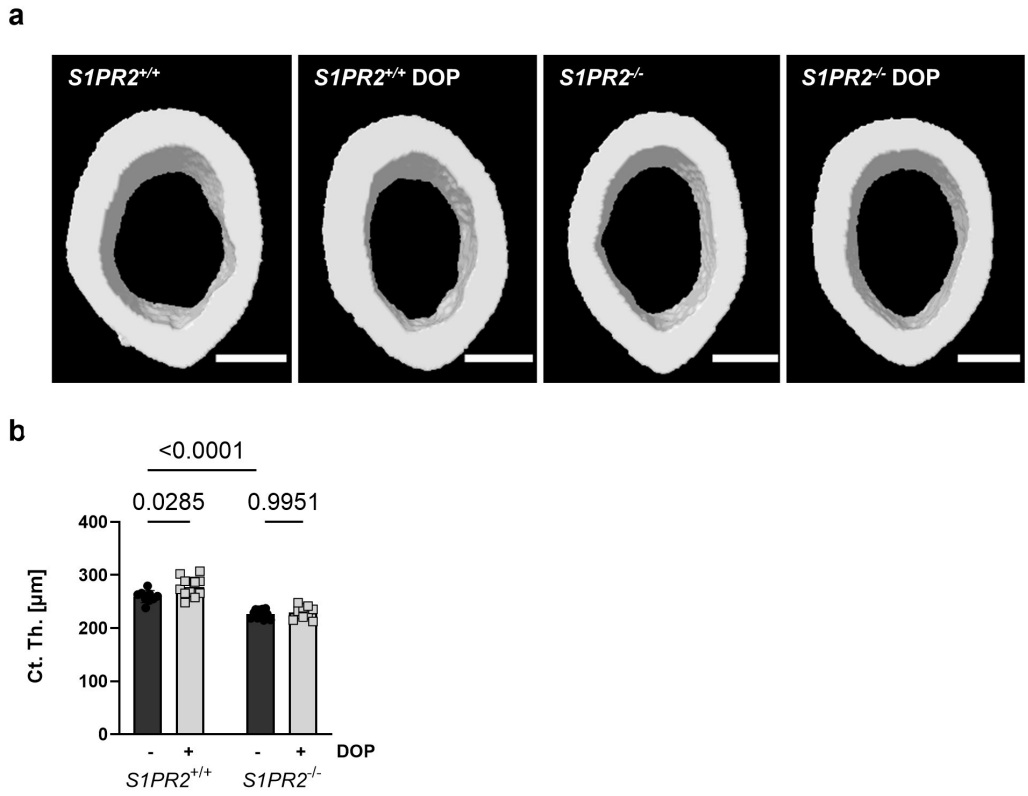

Figure 42: *S1PR2* knockout prevents DOP-mediated thickening of cortical bone.(a) Representative μCT images of cortical sections at the mid-shaft of the femoral of *S1PR2*$^{+/+}$ control animals and *S1PR2*$^{-/-}$ knockout animals treated with 3 mg/L DOP for six weeks and their untreated controls. (b) Quantification of cortical thickness (n=9/11/11/9). Data are represented as mean ± s.d., Two-way ANOVA was used for statistical analysis.

Additionally, strengthening of *S1PR2*$^{+/+}$ bones was observed using a 3-point bending test as represented by increased stiffness and ultimate force needed to reach bone failure (Figure 43a-c). This effect was not observed in *S1PR2*$^{-/-}$ mice (Figure 43a-c).

In summary, these results clearly show that VEGFa production and the phenotypic switch of the bone vasculature towards pro-osteogenic H-type vessels is S1PR2 independent. This is also represented by an S1PR2-independent increase in trabecular bone volume. However, S1P-mediated thickening of the corticalis and increased strength of the bone were shown to be clearly S1PR2 dependent.

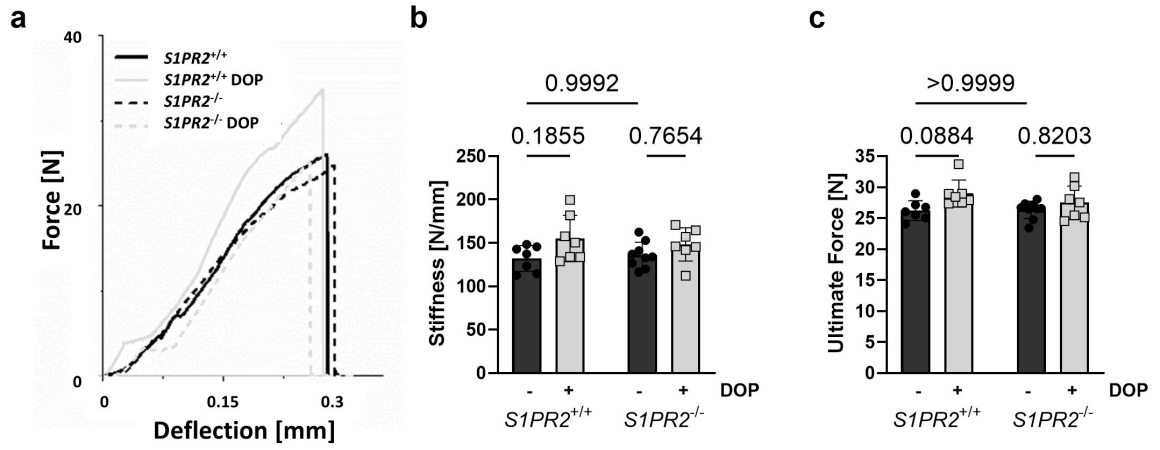

Figure 43: *S1PR2* knockout prevents DOP-mediated strengthening of the cortical bone. (a) Representative force/deflection graphs resulting from a three-point bending test of femoral bones from *S1PR2*$^{+/+}$ control animals and *S1PR2*$^{-/-}$ knockout animals treated with 3 mg/L DOP for six weeks and their untreated controls. Quantification of (b) stiffness (n=7/7/9/7) and (c) ultimate force (n=7/7/9/7). Data are represented as mean ± s.d., Two-way ANOVA was used for statistical analysis.

4.10 DOP Mediates Bone Healing in a Model of Post-Traumatic Osteomyelitis

To determine the effects of S1P lyase inhibition via DOP treatment not only on bone formation in healthy animals, a model of post-traumatic osteomyelitis was used. Post-traumatic osteomyelitis is characterized by infectious conditions within a bone injury.[285,286] Since bone repair and callus formation are closely linked to blood vessel invasion,[364] this model could provide additional insights into vessel-related effects during bone regeneration.

To mimic post-traumatic osteomyelitis, a cortical defect and S. aureus infection were introduced in 12-week-old male C57BL/6J mice. After debridement, the animals were treated with DOP for two weeks. A significant increase in plasma S1P levels was observed compared to control mice (Figure 44a). To assess DOP-mediated healing of the cortical defect, μCT analysis was performed to evaluate the area of the newly formed bone callus surrounding the defect area. Indeed, after two weeks of DOP treatment, a 1.57-fold increase in newly formed callus surrounding the cortical defect was detected in DOP-treated mice compared to untreated controls (Figure 44b+c).

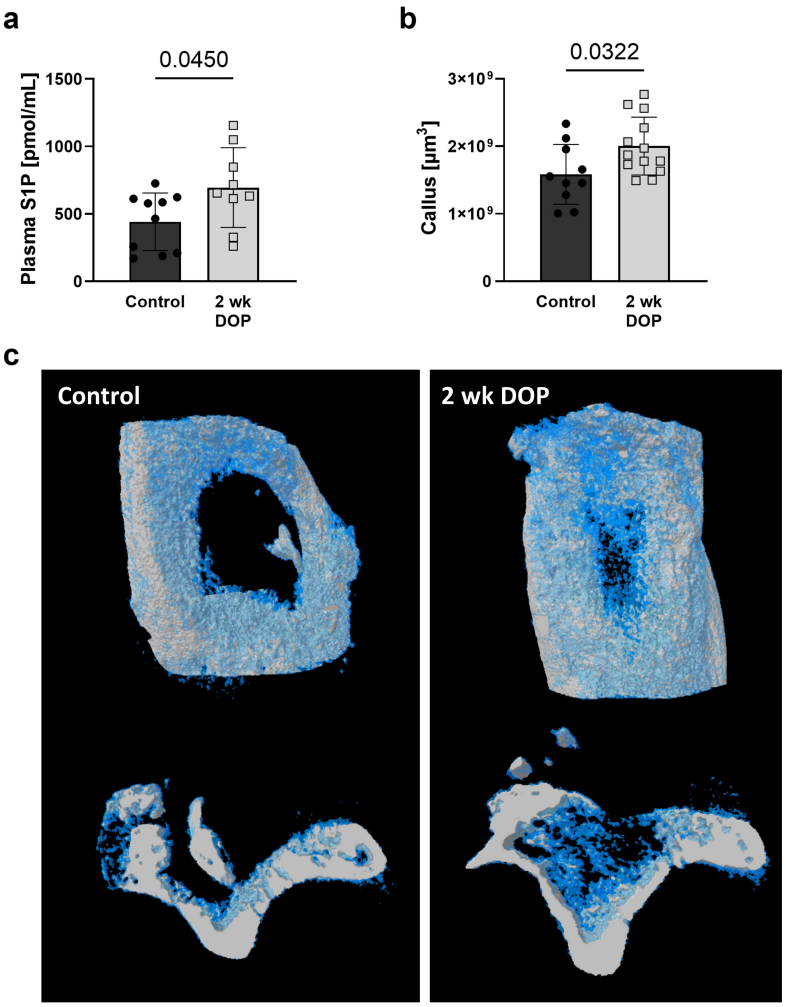

Figure 44: DOP administration leads to an increase in plasma levels of S1P and to the formation of healing callus in a model of post-traumatic osteomyelitis. (a) S1P plasma levels of C57BL/6J mice after two weeks of DOP treatment (180 mg/L) and untreated controls (n=10/9), (b) callus formation in these mice (n=10/9) and (c) representative images showing the defect area (white) and newly formed bone callus (blue). Data are represented as mean ± s.d., Unpaired two-tailed t-test was used for statistical analysis.

To assess the involvement of vascular invasion in the bone healing capacity mediated by S1P lyase inhibition, CD31 staining within the defect area was analyzed. A clear elevation of CD31 staining intensity was observed in DOP-treated animals compared to untreated controls (Figure 45a+b). These results indicate an involvement of the bone marrow microvasculature in the S1P-mediated bone regeneration in a bone defect model.

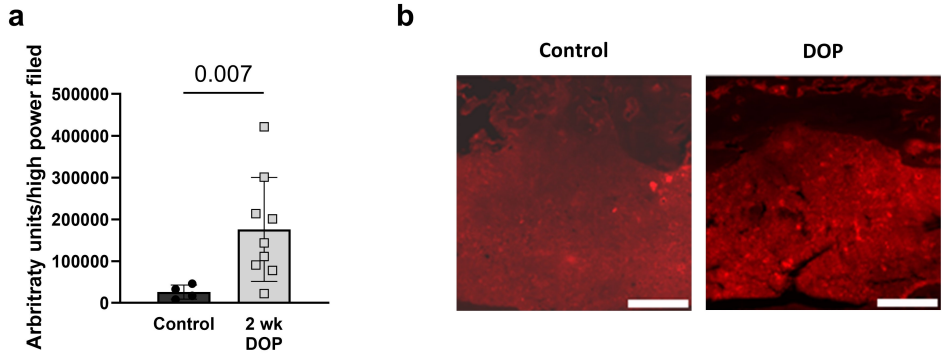

Figure 45: DOP treatment leads to increased CD31 staining in defect sections of a post-traumatic osteomyelitis model. (a) Semi-quantitative analysis of CD31 staining intensities of the post-traumatic osteomyelitis defect area of C57BL/6J control mice and after two weeks of DOP treatment (180 mg/L) (n=4/9), (b) Representative images of CD31 stained sections; scale bar = 200 μm. Data are represented as mean ± s.d., Unpaired two-tailed t-test was used for statistical analysis.

For the investigation of the involvement of S1P receptors in the healing capacity mediated by DOP treatment, an osteomyelitis defect followed by *S. aureus* infection was introduced in *S1PR3*-deficient mice and wild-type controls. After two weeks of DOP treatment, a significant increase in newly formed bone callus was detected in wild-type mice but not in $S1PR3^{-/-}$ mice (Figure 46a+b).

Vascular invasion was assessed by semi-quantitative analysis of CD31 staining within the defect area of these mice. Analysis revealed an increase in vascular invasion as indicated by increased CD31 staining after DOP treatment in $S1PR3^{+/+}$ animals. This effect was prevented through S1PR3 depletion (Figure 47a+b).

These results again confirm the S1PR3-mediated effects of DOP treatment on bone formation and regeneration, also in a model of cortical defect in post-traumatic osteomyelitis. Bone callus formation could be connected to increased endothelial cells within the defect area.

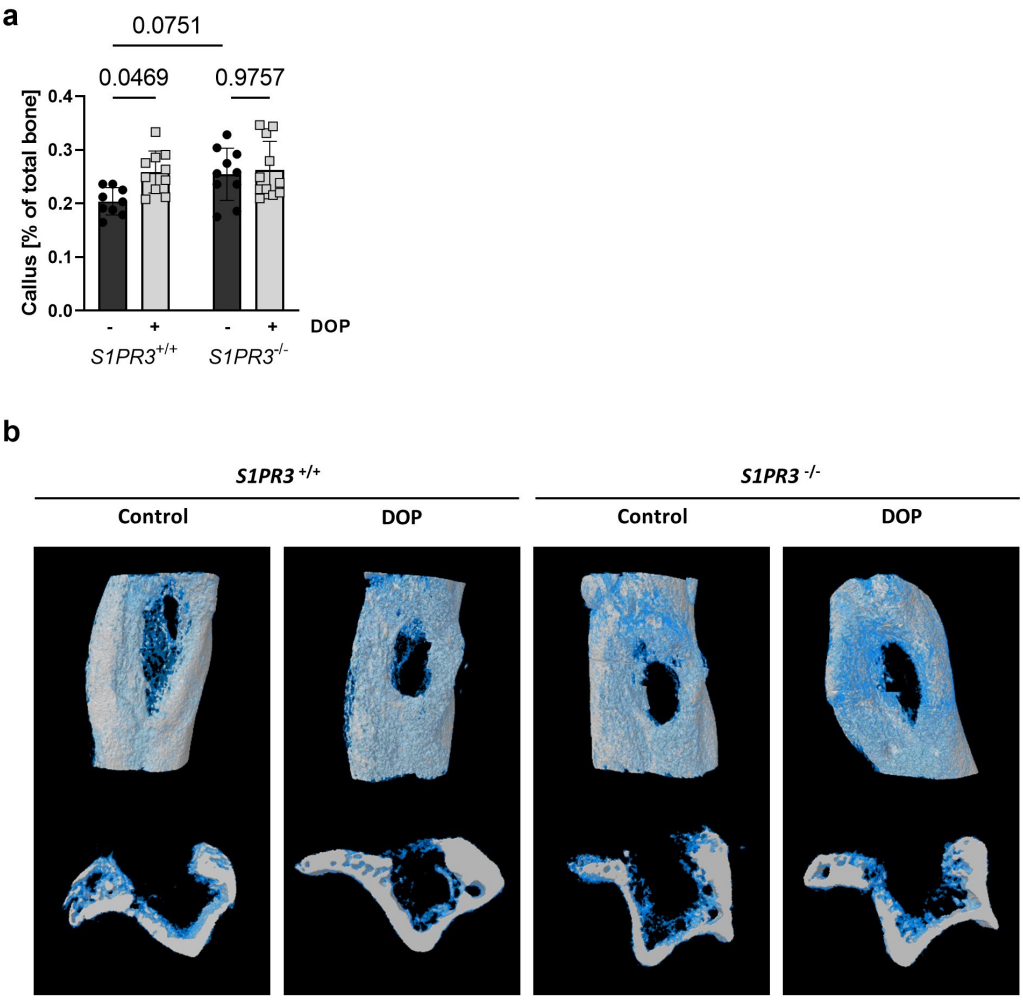

Figure 46: Callus formation during bone healing in a model of post-traumatic osteomyelitis is S1PR3 dependent. (a) Newly formed callus in wild-type and *S1PR3*$^{-/-}$ animals with and without two weeks of DOP treatment (180 mg/L) (n=9/10/10/11) and (b) representative images of the defect area (white) and newly formed callus (blue) of these animals. Data are represented as mean ± s.d., Two-way ANOVA was used for statistical analysis.

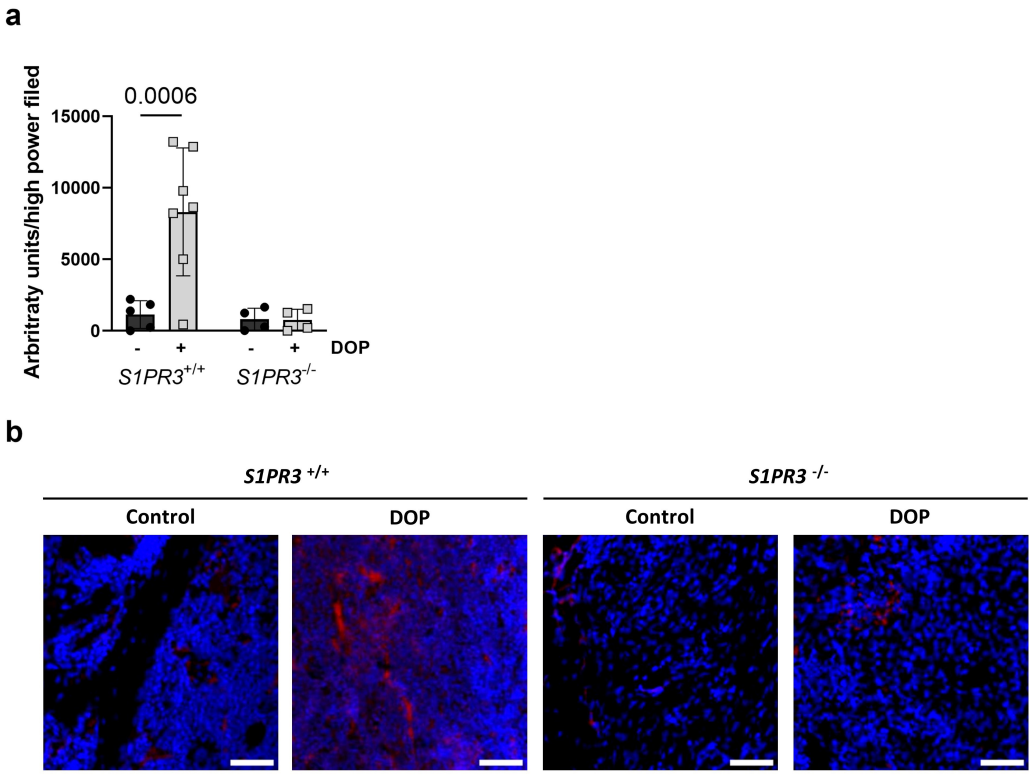

Figure 47: The increase in CD31 staining in the defect area of a post-traumatic osteomyelitis model is S1PR3-dependent. (a) Semi-quantitative analysis of CD31 staining intensities of the post-traumatic osteomyelitis defect area of $S1PR3^{+/+}$ and $S1PR3^{-/-}$ control mice and after two weeks of DOP treatment (180 mg/L) (n=5/7/4/4), (b) Representative images CD31 (red) and DAPI (blue) stained sections; scale bar = 50 μm. Data are represented as mean ± s.d., Two-way ANOVA was used for statistical analysis.

To evaluate the effects observed in the mouse model also in humans, long bone samples taken during surgery from patients with infectious osteomyelitis were cultured in osteogenic medium with and without the addition of DOP for four weeks. Bone volume was measured at the beginning and end of the culture period. Significant increases in bone volume were observed in samples cultured in DOP supplemented medium compared to control samples from the same patients (Figure 48a). Evaluation of CD31 staining in bone sections revealed substantial endothelial staining within DOP-treated samples. However, no CD31 staining could be detected in the section of untreated bone samples (Figure 48b+c).

These results demonstrate the validity and translational potential of S1P-based therapeutic options for human bone pathophysiology.

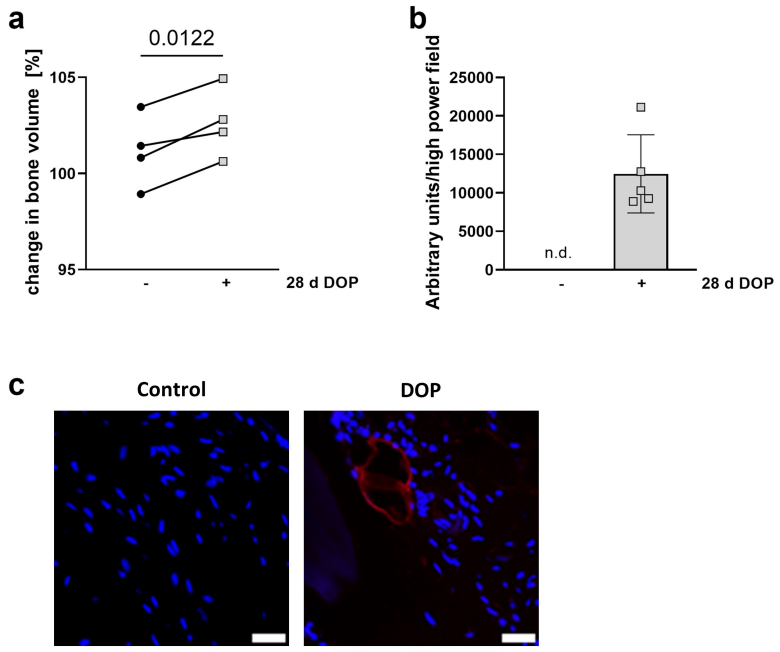

Figure 48: DOP treatment leads to an increased bone volume and vascular CD31 staining in human bone samples after 28 days of culture. (a) Changes in bone volume of untreated human bone samples after 28 days of cultivation and samples from the same patients with the addition of 0.2 mM DOP were assessed by μCT analysis (n=4/4). (b) Semi-quantitative analysis CD31 staining of human bone sections after 28 days of cultivation, (c) representative images showing CD31 (red) and DAPI (blue) staining; scale bar = 100 μm. Data are represented as mean ± s.d., Paired two-tailed t-test was used for statistical analysis, n.d. = not detected.

5 Discussion

S1P is crucial for the development and maintenance of bone, affecting both bone formation and blood vessel growth. Therapeutically targeting the sphingolipid pathway and receptor signaling has been proposed as a potential treatment for osteoporosis.[307,365] However, the exact role of S1P signaling in bone-strengthening therapies remains unclear. Therefore, in this study, the S1P-mediated interaction between the bone marrow microvasculature and osteoblasts was explored to better understand its potential in developing new treatments for bone health.

This work identified four main synergistic mechanisms involving S1PR2 and S1PR3 signaling in bone (Figure 49):

1. S1PR3 signaling in osteoblasts led to enhanced VEGFa secretion, which in turn increased osteoblast mineralization. This effect demonstrated the intrinsic impact of S1P signaling on osteoblasts and their direct bone-forming capacity.

2. Angiogenesis within the bone marrow, accompanied by the formation of pro-osteogenic H-type vessels, was triggered by S1PR3-mediated VEGFa secretion. BMECs then expressed additional pro-osteogenic factors, leading to further stimulation of osteoblast differentiation and bone formation, ultimately resulting in the formation of trabecular bone.

3. The bone-forming capacity of S1P/S1PR3 signaling was confirmed in a model of post-traumatic osteomyelitis. S1PR3 signaling led to the formation of new bone callus and hence, accelerated the healing of bone defects. This S1P-mediated effect was accompanied by increased vascular staining, indicating the involvement of the bone vasculature in this process.

4. S1P directly acted on bone-forming cells through S1PR2 to enhance bone growth.[307] Here, S1PR2 signaling was linked to the thickening of cortical bone and subsequent bone strengthening. Unlike the S1PR3-mediated mechanism, the S1P/S1PR2 axis triggered a VEGFa and vessel-independent mechanism.

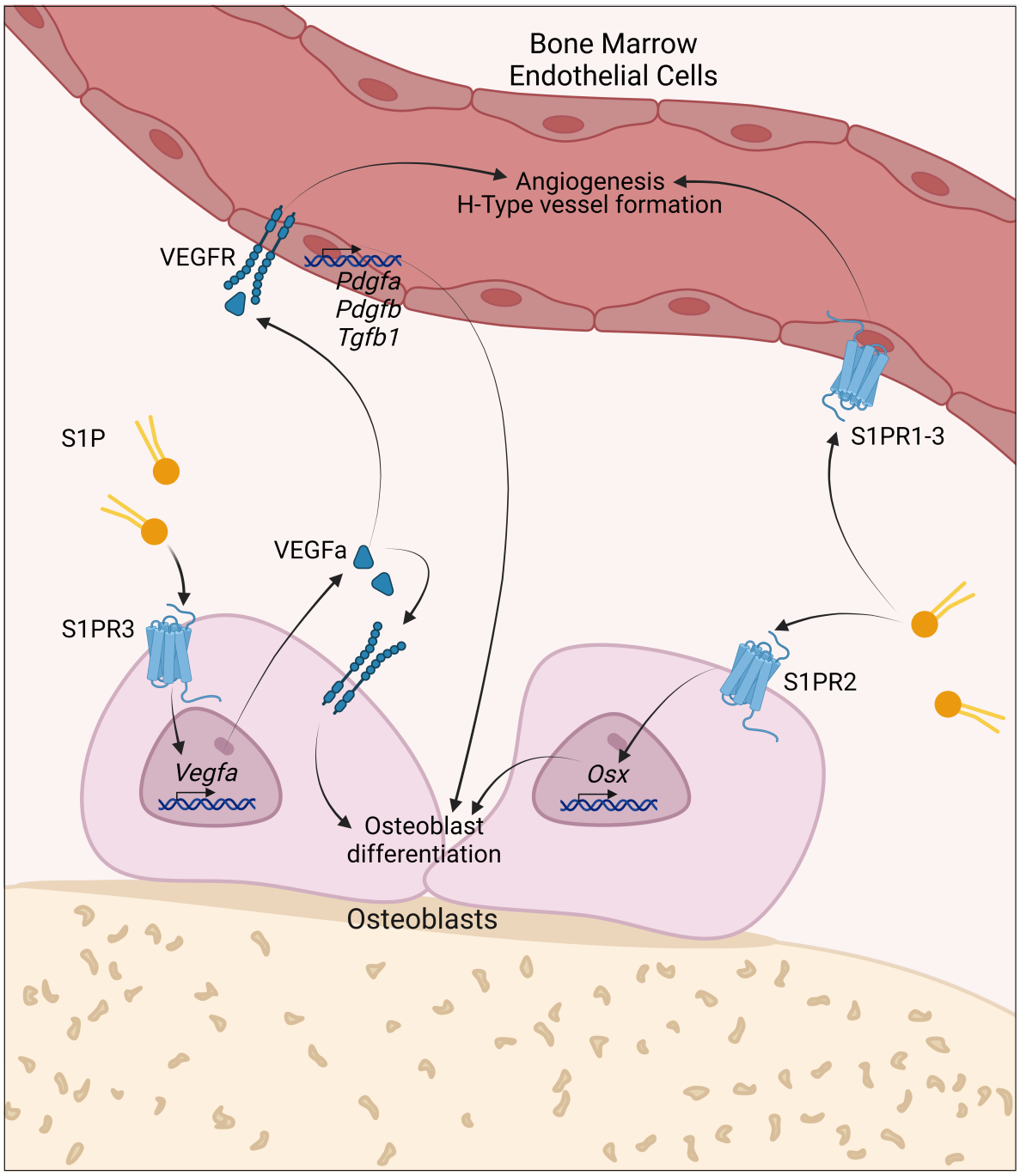

Figure 49: Schematic overview of the S1P-mediated crosstalk between BMECs and pOBs. S1P triggers the production of VEGFa in pOBs via S1PR3, contributing to increased bone mass through autocrine signaling. Simultaneously, it facilitates the formation of H-type vessels and angiogenesis in a paracrine fashion. These vessels play a crucial role in osteoblastogenesis by releasing osteogenic factors such as *Pdgfa*, *Pdgfb* and *Tgfb1*. Additionally, S1P directly influences pOB differentiation through S1PR2 signaling. Created with BioRender.com.

5.1 The Involvement of S1PRs in Bone Homeostasis and Their Potential in Osteoporosis Therapy

5.1.1 S1P Influences OB-Mediated Bone Formation Through Multiple Receptors and Non-Redundant Pathways

This study observed an osteoanabolic effect on trabecular and cortical bone upon S1P lyase inhibition and subsequent S1P level elevation through DOP treatment and genetic deletion of the enzyme. Furthermore, the S1P-mediated impact was confirmed in a model of post-traumatic osteomyelitis, demonstrating the diverse therapeutic potential of S1P in bone biology. Previously, extensive research has examined the involvement of S1PR signaling in healthy bone maintenance and the development of osteoporosis, focusing on S1PR1-3 in OB biology. S1P was found to impact OB differentiation and bone formation directly. S1PR1 was shown to play a direct role in promoting the proliferation of osteoblastic cells with receptor agonism, leading to increased OB proliferation.[306,366] Additionally, S1PR1 signaling was found to reduce OB apoptosis.[367,368] Roelofsen and colleagues further supported the involvement of S1PR2. OB recruitment to bone remodeling sites was reduced after inhibiting S1PR2 signaling via RNA interference and receptor antagonism using JTE-013.[369] Furthermore, *S1PR3* expression increased during OB differentiation, reinforcing its role in this process.[308] An increase in bone volume following S1PR3 agonism was also detected.[309]

The results described here indicate a direct effect of S1P treatment on osteoblastic mineralization in primary osteoblasts. Furthermore, the involvement of S1PR3 in OB differentiation and calcification was confirmed using pOBs isolated from mice lacking this receptor. These pOBs did not exhibit the S1P-mediated calcification observed in wild-type pOBs. *In vivo*, bone formation was shown to be both S1PR2 and S1PR3 dependent, as indicated by reduced effects of DOP treatment in knockout mice. *S1PR3* knockout resulted in the prevention of DOP-mediated increases in trabecular bone volumes. *S1PR2* knockout prevented the DOP-mediated increases in cortical bone thickening and strength. Additionally, bone regeneration after post-traumatic osteomyelitis was identified to be S1PR3 dependent. These results further underline the involvement of S1P signaling in bone formation and regeneration.

5.1.2 Site-Specific Actions of S1PRs in Trabecular and Cortical Bone During Homeostasis, Disease and Therapy

In the present study, S1P receptor-mediated bone formation was shown to be site-specific. While S1PR3 signaling was identified to trigger bone formation in the trabecular bone, S1PR2 signaling mediated cortical thickening. Therefore, this study suggests synergistic effects of S1PR2/S1PR3 signaling on the bone with distinct sites of action. Bone consists of two main structural components: cortical and trabecular structures.[220] Cortical bone comprises the outer layer of bone and is densely packed and organized into concentric lamellar units known as osteons. Within cortical bone, Haversian and Volkmann's channels ensure proper nutrient supply to osteocytes.[370] Due to its relatively small surface area (approximately 20% of the total bone surface), cortical bone undergoes relatively low levels of bone remodeling.[219] In contrast, trabecular bone, mainly found in the interior of long and flat bones, has a highly elastic and less dense structure.[221] With its large surface area (around 80% of the total bone surface), trabecular bone is constantly subjected to bone remodeling.[219]

As the composition of these bone compartments differs, multiple modes of action during bone formation and homeostasis were proposed. Rittweger *et al.* demonstrated differences in cortical and trabecular bone loss during periods of immobilization. Within a 35-day immobilization period, a rapid reduction in trabecular bone volume was observed, followed by a slower but continuous decline in cortical bone volume.[371] Similar observations are associated with the development of osteoporosis. In the early stages of osteoporosis, there is accelerated turnover of trabecular bone due to its larger surface area.[372] As the disease progresses, changes occur in cortical bone as well. Intercortical remodeling and increased osteon and pore size lead to an expansion of cortical surface area. This makes cortical bone more susceptible to bone remodeling and increases the risk of osteoporotic bone loss.[373,374] Ultimately, there is a shift from trabecular to cortical bone loss. As the trabecular bone area diminishes, bone resorption in this compartment decreases. Simultaneously, resorption in the cortical region increases the surface area, further promoting bone resorption.[375] Approximately 70% of bone resorption occurs in cortical bone, which accounts for roughly 80% of total bone mass. In contrast, trabecular bone, constituting about 20% of the total bone mass, contributes to 30% of bone loss during osteoporosis.[221,376]

Differences between cortical and trabecular bone also play a role in bone regeneration. When subjected to loading, there were clear differences in the regenerative capacity of trabecular and cortical bone in mice. Loading resulted in the thickening of cortical bone. The trabecular bone showed a reduced and delayed response to this stimulus.[377] Weatherhold *et al.* confirmed this effect, revealing a significant increase in lamellar bone in the cortical region but no changes in trabecular bone following loading.[378] Given the identified variations in the remodeling capacity of cortical and trabecular bone, Osterhoff *et al.* proposed considering these site-specific effects in the treatment of osteoporosis. The disease stage and the site of ongoing bone resorption are considered.[370] This consideration is particularly important, given the different mechanisms of action of common osteoporosis treatments. Studies assessing the effects of alendronate treatment revealed increased cortical thickness, area and load compared to control groups. Still, no changes were observed in the trabecular region of tibiae.[379,380] Similar findings were reported for ibandronate treatments in post-menopausal women.[381] In contrast, anabolic therapies, such as teriparatide, were found to affect trabecular bone but had no significant impact on cortical bone.[382] The diverse actions of well-known osteoporosis treatments support the importance of considering the disease stage and the site of bone resorption during therapy. Furthermore, treatments targeting both trabecular and cortical bone would be beneficial.

In line with previous research, this study demonstrated an S1P-mediated bone remodeling effect and strengthening in both cortical and trabecular bone. Previously, *S1PR2*-deficient mice were reported to experience cortical bone thinning[307] and the involvement of S1PR2 in cortical regeneration was identified. Similar results were reported in previous studies utilizing S1PR2 agonists.[365] The current study confirms S1PR2-dependent effects on cortical bone remodeling. In S1P lyase-deficient mice, an increase in both cortical and trabecular bone volume was observed. However, cortical bone thickening was independent of S1PR3,[383] which aligns with the observed S1PR3-independent cortical thickening after pharmacologic S1P lyase inhibition in the present study. Nevertheless, the stimulating effect on trabecular bone formation was S1PR3-dependent.

McKenzie *et al.* studied the involvement of VEGFa signaling during the lamellar bone formation of the cortical region of tibial bones. They described a VEGFa-independent strengthening of the corticalis.[384] This effect was confirmed in this study. The S1PR3-mediated effects on bone are VEGFa dependent. However, these effects were only found to be involved in trabecular bone formation and the changes observed in

cortical bone were a result of S1PR2-mediated and VEGFa-independent signaling.

The involvement of S1P signaling in cortical and trabecular remodeling strengthens its possible use as a holistic bone anabolic treatment. It overcomes the often-noted site-specific effects mediated by commonly used osteoporotic treatments.

5.1.3 S1P Signaling is Involved in OB/OC Crosstalk

While this study focused primarily on S1P-mediated signaling in osteoblastic cells, it is worth noting that there is a strong link between S1P signaling and OC regulation. S1PR1 was identified to influence the differentiation and chemoattraction of OC progenitor cells toward the bone surface, with S1PR1 stimulation causing these cells to migrate into the bloodstream.[302] In contrast, OC-specific knockout of *S1PR1* resulted in the accumulation of these cells on the bone surface and decreased bone volume due to increased bone resorption.[302] S1PR2 was identified as a positive regulator of osteoclastic bone resorption, enhancing OC progenitors' chemoattraction toward the bone marrow.[302,303] Moreover, OC-specific suppression of S1PR2 signaling was shown to rescue bone loss in a mouse model of post-menopausal osteoporosis.[305] OC-derived S1P was discovered to stimulate the chemoattraction of mesenchymal stem cells to active bone formation sites through the activation of S1PR1 and S1PR2.[262,385] Elevated levels of S1P were observed to increase alkaline phosphatase activity in OBs, thereby triggering OC activity and mineralization. These effects were inhibited using VPC23019 as an S1PR1/S1PR3 antagonist.[308,311]

This work also provides evidence for crosstalk between OBs and OCs mediated by S1P signaling. An increase in OPG, which is mainly secreted by OBs and is known to regulate the differentiation of both OBs and OCs,[243] was observed following DOP administration. In addition, a decrease in plasma levels of RANKL, which is involved in the maturation of OCs,[241–243] was also observed in DOP-treated mice. The DOP-mediated changes in OPG and RANKL plasma levels were not observed in S1PR3 deficient mice, showing the dependency on S1P/S1PR3 signaling in S1P-mediated regulation of OB/OC crosstalk. The involvement of S1PR3 signaling in these processes could further be confirmed by gene expression analysis in S1P-treated pOBs. This study identified an S1PR3-dependent induction of *Osterix* (*Sp7*) expression. Additionally, *Osteopontin* (*Spp1*) and *Osteonectin* (*Sparc*) expression were reduced after S1P treatment. This suggests inhibition of OB

differentiation via *Osterix*, accompanied by minimized OC motility and attachment to the bone via reduced *Osteopontin* expression.[360,362] As *Osteonectin* is typically located at the site of bone remodeling,[361] the regulation described here further supports S1P's involvement in OC biology. It is worth highlighting that an additional decrease in *Sparc* and *Spp1* expression was observed in *S1PR3* deficient pOBs compared to pOBs isolated from wild-type animals. These factors regulate OBs and OCs during bone remodeling.[360–362] Furthermore, the pro-osteogenic factor *Osterix* (*Sp7*)[363] exhibited an upregulation in *S1PR3* knockout pOBs in contrast to wild-type pOBs. These findings imply that S1PR3 may play a role in the modulation of the crosstalk between OBs and OCs.

When comparing the trabecular bone volumes of *S1PR3* deficient and wild-type mice, an increase in bone mass was detected in the receptor-deficient animals. These results contradict the previously described osteoporotic phenotype observed in *S1PR3*-deficient aged mice.[309] However, age may be an important factor since the mice used in this study were only 20 weeks old. With age, bone remodeling is known to slow down and shift from bone formation towards a more resorptive phenotype. This indicates differences in the regulation of bone homeostasis depending on age.[386] Therefore, differences in the regulation of bone homeostasis between the mice used in this study and the mice used by Keller *et al.* could be involved, potentially explaining the differences observed in *S1PR3*-deficient mice. As *S1PR3*-deficiency led to gene regulation in pOBs, regulation of bone homeostasis via OB/OC crosstalk in these mice is suggested. While the involvement of S1PR3 in osteoclastogenesis is not fully understood, further investigations are needed to unveil its role in these processes. Given the close relationship between OBs and OCs, investigating both cell types is essential for comprehending the mechanisms behind S1P-mediated bone formation.

5.1.4 S1P-Based Approaches May Have the Potential for Osteoanabolic Therapies

The multifaceted influence of S1P signaling in bone metabolism positions it as a promising alternative for treating osteoporosis and triggering bone healing in conditions such as post-traumatic osteomyelitis. In recent years, several studies analyzed S1P-mediated bone regeneration *in vivo*. The S1P analog FTY720 enhanced bone formation by upregulating pro-osteogenic transcription factors, thus preventing ovariectomy-induced osteoporosis.[387]

Simultaneously, it inhibited osteoclastogenesis and OC function.[388] Interestingly, the increase in bone formation seen with FTY720 in wild-type mice was not observed in *S1PR3* knockout mice.[309] This suggests that this receptor is involved during bone regeneration. Notably, S1PR3 activation in OBs induced bone matrix secretion and mineralization *in vitro*.[309] This study confirms the pro-osteogenic effects of S1P elevation *in vivo,* which aligns with previous observations. Similar to the observation of Keller *et al.*,[309] no increase in trabecular bone volume was observed in *S1PR3*-deficient mice after S1P elevation by DOP treatment in the present work. This further confirms the previously proposed involvement of S1PR3 signaling during bone regeneration. Additionally, improved bone healing was observed upon S1PR3 signaling in a model of post-traumatic osteomyelitis.

While S1PR3 signaling mainly led to an increase in trabecular bone, S1PR2 signaling strengthened bone stability and cortical bone thickness, as described in this study. Weske *et al.* described S1PR2 signaling in OBs to promote their differentiation and pro-osteogenic functions. Pharmacological stimulation with the S1PR2 agonist CYM5520 improved osteopenia induced by ovariectomy.[307,365] However, this current study demonstrated that S1P lyase inhibition induced bone growth even in the absence of S1PR2, suggesting the involvement of additional S1PRs. This effect might be attributed to S1PR3 signaling. However, the influence of other S1PRs cannot be neglected. Evaluating DOP-mediated effects in mice lacking both S1PR2 and S1PR3 may help to unravel any residual effects on bone formation. Understanding this specific interaction and its regulation may form the basis for developing novel S1P-based osteoporosis treatment options.

Furthermore, possible off-target effects of DOP treatment should be considered in the model used. While DOP inhibits S1P lyase, it also affects other vitamin B6-dependent enzymes. This suggests that the elevation of S1P levels may not be solely responsible for the observed effects on bone and bone vasculature.[389,390] To validate that the described findings are S1P-mediated, a model with a genetic deletion of S1P lyase was employed. The effects observed in the genetic S1P lyase deletion model were similar to those observed with pharmacological inhibition using DOP. This indicates that the DOP-mediated effects are indeed due to successful S1P lyase inhibition. Additionally, S1P lyase inhibition leads to an accumulation of S1P and affects other sphingolipids upstream of S1P in the sphingolipid pathway. To verify that the observed effects are, in fact, S1P-mediated, S1P receptor knockout animal models were used. The absence of specific effects, such as an increase in cortical or trabecular bone volume in the *S1PR2* and *S1PR3* knockout models,

respectively, suggests that the observed impact through DOP-mediated S1P elevation is due to an increase in S1P levels and subsequent receptor signaling. Additionally, S1P signaling was further elucidated as the underlying mechanism through *in vitro* studies. Stimulation of primary osteoblasts with S1P increased the formation of calcified nodules. These effects were identified to be S1PR3-dependent, further confirming the involvement of S1P. Although experiments with genetic deletion models confirmed S1P signaling as the underlying mechanism, the influence of other vitamin B6-mediated pathways and other sphingolipids cannot be completely ruled out and should be considered. To avoid such off-target effects, employing specific S1PR agonists could be beneficial.

5.2 VEGF is a Potential Therapeutic Option for Bone Regeneration and Repair

S1P has previously been demonstrated to enhance *Vegfa* expression and protein secretion across various cell types, including human umbilical vein endothelial cells (HUVEC), endothelial progenitor cells and the human osteosarcoma cell line MG-63.[391–393] This augmentation of *Vegfa* expression has been implicated in the induction of angiogenesis.[392] In the present study, a connection between angiogenesis and osteogenesis was observed in a VEGFa-dependent manner, linking the osteoanabolic effects of VEGFa to the S1P signaling pathway. Notably, the effects mediated by S1PR3 were shown to be reliant on VEGFa, as evidenced by an increase in VEGFa secretion by pOBs following S1P stimulation. This intrinsic stimulation, in turn, promoted pOB mineralization. VEGFa has previously been recognized for its significant effects on bone development. Inhibiting VEGF signaling during development leads to impaired vascular invasion and diminished chondrocyte recruitment and differentiation. These deficiencies ultimately contribute to decreased trabecular bone formation.[328] Furthermore, the sustained expression of VEGFa appears to be positively correlated with ongoing bone formation, reaching its peak just before the maximum bone formation occurs.[330] Conditional knockout of *Vegfa* in OBs resulted in a reduction in bone mass due to a decrease in osteoprogenitors and impaired mineralization. Consistently blocking VEGFR1 and VEGFR2 has been demonstrated to reduce bone density.[335,336] The data presented here suggest a link between S1P-mediated bone and bone vasculature changes and VEGFR signaling *in vivo*. The administration of

Axitinib, a VEGFR inhibitor, effectively blocked S1P-mediated increases in bone volume and vascular density. This aligns with the previously established role of VEGFa in bone regeneration. These findings provide further confirmation of VEGFa's involvement in S1P-mediated osteogenesis.

As VEGFa is recognized as an osteogenesis inducer, it has been proposed as a potential treatment for bone healing. Administering VEGFa through VEGFa-expressing fibroblasts or a matrix coated with a VEGFa-expressing plasmid at the site of a bone defect has been shown to enhance bone healing significantly. This enhancement is evident in increased ossification and improved vascular invasion at the defect site. This highlights a connection between VEGFa, vascular invasion and bone healing.[341,342] Furthermore, incorporating VEGFa-secreting bone marrow stromal cells into bone grafts increased vascularization and improved bone healing.[394] This study could now link S1PR3 signaling to bone healing after post-traumatic osteomyelitis. As the S1PR3-mediated effect on bone formation is proposed to be VEGFa-dependent, a further possible VEGFa-dependent effect of bone healing could be identified.

While this study focuses primarily on VEGFa-mediated effects in pOBs, it is worth noting that different VEGFa-mediated effects have been described in different osteogenic cells. As shown in the present work, changes in RANKL and OPG plasma levels were found to be S1PR3 dependent. This suggests a possible involvement of VEGFa signaling also in OC regulation. There are conflicting results in the literature regarding the effects of VEGFa on OCs. For instance, *RANK* was shown to be upregulated in OCs upon VEGFa treatment. However, the study did not observe significant effects on osteoclastogenesis.[340] In contrast, Helmrich *et al.* reported an increase in OC recruitment during bone healing after the implantation of osteogenic grafts containing VEGFa-expressing bone marrow stromal cells.[394] Similar observations were described in other studies, where direct treatment of OC cultures affected the survival of OCs, leading to an increased area of bone resorption after VEGFa treatment.[338]

As various cell types play crucial roles in bone formation and homeostasis, it is essential to consider the VEGFa-mediated effects on them. Chondrocytes, for instance, have been identified as expressing VEGFa and these cells also exhibit VEGF receptor expression. However, VEGFa-mediated effects have been primarily observed during development. In VEGFa overexpressing chondrocytes, an autocrine regulation of chondrogenesis was described.[395] The knockout of *Vegfa* in chondrocytes resulted in a delayed invasion of

vessels within the developing bone, leading to a delay in hypertrophic chondrocyte removal and impaired bone development. Additionally, VEGFa has been demonstrated to enhance chondrocyte survival.[329]

Given the diverse cell types influenced by VEGFa expression and signaling within the bone, exploring the VEGFa-mediated effects on these cells during bone regeneration would be interesting. A thorough evaluation of the effects on bone tissue would be necessary to fully understand the S1P/VEGFa-mediated mechanism in the described models.

5.3 The Role of Blood Vessels in Bone Homeostasis and Repair

5.3.1 H-Type Endothelial Cells Enhance Bone Regeneration

This study has identified a novel role of S1P in inducing a phenotypic switch in BMECs, leading to the formation of H-type blood vessels in the bone marrow. The S1P-mediated induction of H-type vessels was found to be S1PR3 dependent, as evidenced by the absence of a phenotypic switch in *S1PR3* knockout mice upon DOP treatment. Furthermore, the lack of an increase in VEGFa plasma levels in S1PR3 knockout animals, unlike the observed rise in wild-type animals, suggests a VEGFa-dependent switch of the endothelial phenotype towards H-type vessels. Recently, a study by Grosso *et al.* identified similar VEGFa-mediated effects in a model of bone regeneration using tissue-engineered bone grafts. They found stimulation of the formation of pro-osteogenic vessels in connection to VEGFa signaling and *Notch1* expression.[396] This further supports the observed results of VEGFa-mediated formation of H-type vessels.

The bone vasculature, specifically the presence of H-type vessels characterized by high *CD31* and *Endomucin* expression, has been directly associated with bone volume. This correlation was also identified in aging mice, where a decline in both the number of H-type ECs and the total number of H-type vessels has been observed.[318] Importantly, this observation has been validated in humans, linking decreased human bone volume to a reduction in H-type vessels.[397] In a mouse model of ovariectomized induced osteoporosis, a reduced number of H-type vessels was observed.[397] Previous studies have already recognized the potential of H-type vessels in initiating bone regeneration. Administering deferoxamine induces the formation of H-type vessels and promotes bone formation in ovariectomized mice.[397] Additionally, the therapeutic potential of H-type blood vessels has

been linked to the S1P signaling pathway. Administration of FTY720, an S1PR modulator, increased H-type blood vessel formation and enhanced bone healing.[398] Since FTY720 is a potent inducer of S1PR1, 3, 4 and 5, the observed induction of H-type vessels observed by Li *et al.* might be attributed to S1PR3 signaling. This is in line with the observations described in the present study. Given the significant correlation between H-type vessels and bone density, the target to generate H-type vessels has emerged as a promising approach for pro-osteogenic therapy. This study observed a phenotypic switch in the vasculature before noticeable changes occurred in the bone, indicating that bone changes depend on H-type vessels. These observations suggest that triggering a phenotypic switch in the bone vasculature towards the H-type could be a potential strategy for bone regenerative therapy.

Moreover, this study identified a VEGFa-dependent increased expression of pro-osteogenic factors (*Pdgfa*, *Pdgfb* and *Tgfb1*) in ECs treated with pOB-pre-conditioned medium after S1P treatment. Several growth factors, including *Pdgfa*, *Pdgfb* and *Tgfb1*, closely associated with the regulation of bone homeostasis, are also expressed in and secreted by specialized H-type BMECs.[318,325,326] These factors are crucial for the pro-osteogenic phenotype of ECs. When their signaling is disrupted, bone volume decreases.[320,326,399] This highlights the induction of pro-osteogenic factors in ECs mediated by paracrine osteoblastic signaling and VEGFa secretion. The observed findings demonstrate that S1P-induced pOB-secreted VEGFa is a paracrine stimulator of pro-osteogenic H-type BMECs in vitro and H-type vessel formation *in vivo*. Vessel-mediated effects on bone regeneration, particularly the close relationship between pOBs and BMECs, were previously described in numerous *in vivo* and *in vitro* studies. Co-culture of HUVEC and osteoblastic cells demonstrated a significant increase in ALP expression and differentiation compared to a monoculture of osteoblastic cells alone.[400] This was accompanied by increased calcium deposition in a co-culture of ECs and mesenchymal stem cells.[401] Pro-angiogenic and pro-osteogenic factors, such as *ANG1*, *BMP2* and *IGF1*, were overexpressed in co-culture conditions, further emphasizing the close association between ECs and OBs.[402] Here, the close connection between pOBs and BMECs was validated in a co-culture setting. Observations revealed that S1P accelerated and amplified vessel- and branch-like structure formation. These *in vitro* results correspond with in vivo experiments, where a DOP-mediated increase in S1P plasma levels led to enhanced vascular branching in the bone marrow vasculature of treated mice compared to untreated controls. These

findings further support the pro-angiogenic potential of S1P within the bone marrow niche.

5.3.2 The Bone Vasculature Supports Bone Regeneration by Supplying Nutrients and Growth Factors

In addition to the observed phenotypic switch of ECs towards the H-type, DOP treatment increased vascular area and density. S1P-mediated vascularization may have an osteogenic effect by increasing blood supply, enhancing the vasculature's pro-osteogenic properties. Blood vessels in the bone ensure the supply of oxygen and nutrients, including a range of vitamins and minerals.[403,404] In addition, OB progenitor cells circulate through the bloodstream to reach sites of active bone formation.[405] Therefore, the pro-osteogenic properties of the vasculature were further enhanced by the increased blood supply, potentially representing an additional osteogenic effect of S1P-mediated vascularization.
DOP treatment not only leads to an increase in vascular density within the bone marrow but also to increased bone marrow S1P concentrations. Discovering the origin of S1P that stimulates OBs and ECs in the bone marrow would be of great interest. While circulating S1P may play a role, local S1P production by OBs and OCs is also a possible contributor. OBs and OCs participate in the OB/OC crosstalk and are known to produce and utilize S1P.[308,310] Furthermore, ECs can function as a local source of S1P. The shear rate in the vasculature is known to stimulate S1P release in ECs from various origins.[52] The high shear rate of blood flow in the long bone vasculature was also identified as a significant physiological stimulus for the generation and maintenance of H-type vessels.[406] Thus, there may be another positive feedback loop in which ECs secrete S1P to initiate signaling in adjacent OBs upon flow-mediated stimulation. In conclusion, valuable insights were provided into the multiple roles of S1P in bone vasculature and its influence on H-type blood vessel formation. This highlights the potential benefits of pro-osteogenic therapies.

5.4 S1P Mediates Angiogenesis in an S1PR2 and S1PR3 Independent Way

It is important to note that angiogenesis is a multifaceted process influenced by various factors. This study observed increased vascular branching and area within the bone

marrow upon S1P lyase inhibition and genetic deletion. However, this increase was still detectable in either *S1PR2*- or *S1PR3*-depleted mice. The independence of S1PR2 and S1PR3 signaling alone in S1P-mediated vascular branching suggests the involvement of other factors in this process. While S1P has been demonstrated to influence blood vessel formation and induce angiogenesis in various tissues, its impact on bone vasculature has not been extensively explored. In other tissues, S1P plays a crucial role in vascular integrity and angiogenesis during development. The regulation of sprouting angiogenesis involves a balance between S1PR1, S1PR2 and S1PR3.[155,156] Additionally, other factors regulated by S1P are known to influence angiogenesis.[91,158] Therefore, signaling mediated by S1PR1, the interplay between S1PRs and other pro-osteogenic factors should be considered to understand the underlying mechanisms.

5.4.1 Various S1P-Receptors are Involved in Angiogenesis

To assess the receptor involvement in S1P-mediated pro-angiogenic processes in the bone vasculature, vascular parameters in the bone marrow were evaluated in *S1PR2* and *S1PR3* knockout mice receiving DOP or in untreated control animals. An increase in vessel density, area and branching was observed in both *S1PR2* and *S1PR3* deficient animals. Both S1PR2 and S1PR3 were identified to have a pro-angiogenic effect influencing tip cell formation and sprouting.[155,156] Deleting only one of these receptors did not result in developing a pathological vascular phenotype during development. However, deletion of both receptors in mice resulted in lethality due to severe hemorrhage formation. These results suggest a synergistic influence of S1PR2 and S1PR3 with compensatory mechanisms during development when one receptor is missing. These effects could explain the increased vascular branching and area upon S1P lyase inhibition in both *S1PR2*- and *S1PR3*-deficient mice described here. Further investigation, including studies in animals lacking both receptors, could clarify the involvement of these compensatory mechanisms.

In contrast to S1PR2 and S1PR3, the role of S1PR1 in angiogenesis, vasculogenesis and vessel maturation has been the subject of much more detailed investigation and characterization. During development, S1PR1 is the dominant receptor regulating vascular maturation and coverage with mural cells.[153,154] After vascular maturity, S1PR1 signaling

contributes to vascular quiescence, diminishing vascular sprouting and branching.[157,158] The loss of S1PR1 results in hyper-sprouting, which contradicts the described findings of activated sprouting during S1P treatment. However, to understand the complex involvement of S1P receptor signaling during bone marrow angiogenesis, it is critical to evaluate bone vasculature in endothelial cell-specific S1PR1 knockout mice[158] after S1P lyase inhibition.

5.4.2 Several S1P-Regulated Growth Factors are Involved in Angiogenesis

As S1P is also known to influence the expression of various other growth factors, it is worth looking at other signaling pathways involved in angiogenesis. Below, several signaling pathways and their connection to S1P are discussed.

Notch Signaling

Previously, a close connection between S1P and components of the Notch signaling pathway was described. Jung *et al.* proposed an epistatic regulation of angiogenesis through S1P and Notch signaling, characterized by parallel mechanisms during vessel formation.[158] Additionally, transactivation of the Notch signaling pathway was identified following S1P stimulation in cancer stem cells, resulting in the regulation of Notch target genes.[407] These interactions suggest a potential involvement of S1P-mediated angiogenesis via the activation of Notch signaling in the here-described experimental setting.

The Notch signaling pathway is known to be involved in several pro- and anti-angiogenic mechanisms. Signaling within the pathway is mediated by binding five ligands, Jagged1+2 and Delta-like ligands (Dll)1,3 and 4, to the four receptors Notch1-4.[408] The ligand binding triggers an intracellular cleavage of the receptor and the notch receptor intracellular domains are translocated to the cell nucleus. This domain exhibits its actions within the nucleus as a transcription factor.[408] The balance between the ligands Jagged1 and Dll4 was shown to play critical roles in the regulation of angiogenesis. During the development phase, Jagged1 was shown to be a pro-angiogenic factor. Additionally, it was described as a regulator of the cell cycle. Upon cellular confluency, a Jagged1-mediated activation of Notch signaling was observed in ECs, leading to cell cycle control and, therefore, a reduction of EC proliferation.[409] This suggests a role of Jagged1 during

vascular maturation. In contrast, Dll4-mediated Notch signaling was shown to inhibit tip cell formation and sprouting during early development[410] and even heterozygous deletion of *Dll4* leads to embryonic lethality.[411] This is further supported by the observation that *Dll4* overexpression reduces endothelial sprouting, migration and proliferation.[411,412] This suggests that Notch signaling is involved in the transition from active angiogenesis to a more mature and quiescent vascular phenotype.[412]

Thus, Notch signaling plays a crucial role in regulating vessel formation and represents a possible mechanism contributing to enhanced angiogenesis within the bone. Although no regulation of *Notch1* expression was detected in BMECs and pOBs after S1P treatment (data not shown), the possible influence of other signaling pathway members cannot be neglected. To fully understand the involvement of the Notch signaling pathway, other members, such as Jagged1 and Dll4, should also be considered.

TGFβ Signaling

The TGFβ signaling pathway plays a pivotal role in both developmental processes and the maintenance of tissue homeostasis. Activation of this pathway involves receptor binding by TGFβ isoforms, BMPs and activins, leading to intracellular signal transduction through the phosphorylation of SMAD proteins.[413] ECs predominantly express two TGFβ receptors, *Activin receptor-like kinase 1* (*ALK1*) and *ALK5*.[414] During the development phase, these receptors regulate the balance between vasculogenesis and angiogenesis, ensuring proper vascular formation. Deactivation of both receptors has been observed to be embryonically lethal.[415,416] ALK1 activation leads to the phosphorylation SMAD1/5, resulting in increased EC proliferation and migration. In contrast, activation of ALK5 leads to decreased proliferation and migration, mediated through SMAD2/3 phosphorylation.[417] Notably, both ALK1 and ALK5 are essential for maintaining vascular development balance.[417,418] BMPs also contribute to EC function by activating SMAD proteins. BMP4 was identified to induce the proliferation and migration of ECs,[419] while BMP9 regulates vascular quiescence by inhibiting vascular sprouting.[420]

Numerous studies have elucidated a close interplay between S1P and TGFβ signaling. Particularly, the transactivation of SMAD proteins through S1P stimulation has been identified across various cell types. Xin *et al.* observed cross-activation of TGFβ signaling via SMAD phosphorylation in renal mesangial cells.[421] Furthermore, BMP-dependent phosphorylation of SMAD in ECs was identified through transactivation via S1P

stimulation.[422] S1P induces the activation of SMAD-mediated signaling and results in the upregulation of several components in the TGFβ signaling pathway in human embryonic stem cells. Enhanced expression of *BMP2*, *BMP6*, *ALK1* and *ALK5*, as well as *SMAD5*, was observed. Additionally, S1P stimulation led to a decrease in *SMAD3* expression.[423] These findings collectively indicate a regulatory role of S1P in modulating TGFβ signaling components across diverse cellular contexts. Considering this interaction when evaluating the S1P-mediated effects on angiogenesis observed in this study is essential.

Here, increased *Tgfb1* expression was observed in BMECs exposed to a pre-conditioned medium of pOBs following S1P stimulation. This additional finding suggests a potential involvement of TGFβ signaling in the observed enhancement of vascular branching and angiogenesis. Further experiments are necessary to identify the specific involvement of TGFβ signaling in these processes. In vivo, measurements of plasma TGFβ levels after pharmacological S1P elevation should be conducted. Additionally, blockade or endothelial-specific deletion of this factor in combination with S1P lyase inhibition in an in vivo model could help elucidate its role in S1P-mediated bone marrow angiogenesis.

FGF Signaling

A wide range of fibroblast growth factor (FGF) family members is expressed in ECs, including *FGFR1-3* and *FGFR5*, along with specific FGFs such as *FGF1*, *FGF2*, *FGF5*, *FGF7*, *FGF8*, *FGF16* and *FGF18*.[424] Notably, FGF signaling has been described as more relevant in vascular regeneration than in developmental vasculogenesis and angiogenesis, as evidenced by normal development in mice lacking *FGF1*, *FGF2*, or a combination of both.[270,425] In contrast, inhibition of FGF signaling during wound healing in adult mice results in impaired vascular regeneration.[426] Furthermore, disruption of FGF receptor signaling leads to VE-cadherin dissociation, disassembling vascular junctions and EC loss. This highlights the crucial role of FGF in regulating vascular integrity during both regeneration and normal homeostasis.[427,428]

FGF family members were found to activate signaling cascades similar to S1P signaling. Specifically, FGF2 and FGF18 activate MAPK and enhance cell migration, proliferation and differentiation.[429,430] FGF signaling activates cell survival through the PI3K and Akt pathways.[430] Similar signal transduction cascades were found to be activated via G_i-associated S1P signaling, which regulates cell cycle control, proliferation and

motility.[86,90,91] Additionally, FGF has been directly linked to S1P-mediated angiogenesis in several studies. As early as 1999, S1P was reported to enhance FGF2-mediated angiogenesis in ECs.[91] During neovascularization, S1P was actively involved in transactivating FGF signaling and the blockade of S1P led to inhibition of FGF-mediated changes during angiogenesis.[431] In the context of vascular regeneration after a stroke, FGF was shown to activate S1P signaling via the activation of S1PR1, resulting in the activation of angiogenesis.[432] These studies collectively indicate a cross-communication between S1P and FGF signaling. This contributes to the regulation of angiogenesis. These close connections may explain the increased vascular area and branching observed following DOP treatment. Measuring FGF expression and protein levels should be considered to elucidate its role during S1P-mediated bone marrow angiogenesis in the model described here.

PDGF Signaling

PDGF signaling is mediated by four distinct PDGF ligands encoded by the *Pdgfa*, *Pdgfb*, *Pdgfc* and *Pdgfd* genes. They operate in various cell types, such as ECs, platelets and vascular smooth muscle cells. Through the dimerization of these ligands into five forms (AA, AB, BB, CC and DD), two receptor tyrosine kinases are activated. The PDGFR-A and PDGFR-B receptors are transmembrane proteins. They contain an extracellular ligand-binding domain and an intracellular tyrosine kinase domain.[433] When they are activated, the phosphorylation of the tyrosine kinases initiates intracellular signaling cascades.[434] PDGF signaling is implicated in numerous cellular and developmental processes, including kidney, neural crest and vascular development.[435–438] Furthermore, the overexpression of *PDGFR-B* has been associated with an increase in PDGF-BB-induced angiogenesis, migration and proliferation.[439]

This study observed an enhanced expression of *Pdgfa* and *Pdgfb* in ECs following treatment with a pre-conditioned medium from S1P-treated pOBs. *Pdgfa* has previously been demonstrated to be upregulated by S1P treatment in ECs, leading to an S1P-mediated and PDGF-dependent enhancement of angiogenesis in endothelial progenitor cells.[440] Additionally, an S1P-mediated transactivation of PDGFRs was demonstrated during vascular injury in vascular smooth muscle cells.[441,442] A close cross-communication between PDGF and S1P was evident in human embryonic kidney cells (HEK293) and mouse embryonic fibroblasts (MEF). On one hand, PDGF was shown to stimulate SK1

expression. They result in increased S1P production and additional PDGF-mediated transactivation of S1PR1. On the other hand, S1P was demonstrated to suppress cellular chemotaxis towards PDGF, thereby regulating cell migration.[443] The connection between PDGF and S1P, coupled with the observed upregulation of *Pdgfa* and *Pdgfb* in ECs in this study, emphasizes the importance of considering this interaction in the context of DOP-mediated angiogenesis.

6 Outlook

This study identified an essential role of S1P signaling in bone regeneration. The involvement of S1PR2 and S1PR3 has been identified. S1PR2 was shown to directly act on bone-forming cells and trigger cortical thickening and strengthening. S1PR3 was identified to act in multiple ways. S1PR3 signaling in osteoblasts led to the secretion of VEGFa, which in turn triggered pOB calcification. Additionally, the secreted VEGFa led to the formation of a pro-osteogenic vessel phenotype. These vessels secreted pro-osteogenic factors, which further contribute to bone formation in trabecular bone. S1PR3-mediated bone regeneration was additionally crucial in bone regeneration after injury.

In particular, the effect on both trabecular and cortical bone formation makes intervention in the S1P signaling pathway a promising therapeutic option. The mechanisms involved in bone degradation[371] and bone regeneration[377] were shown to be different between cortical and trabecular bone. Also, commonly used osteoporosis treatments were shown to exhibit differential effects on trabecular bone and cortical bone, often only influencing one of these sites.[379–382] Interfering with the S1P signaling pathways could help to overcome these site-specific effects of commonly used treatments.

As both S1PR2 and S1PR3 were found to mediate distinct but compensating mechanisms in bone homeostasis, the evaluation of their joint effects on bone regeneration should be examined in mice lacking both receptors. This would also allow the identification of any remaining role of other S1PRs involved in bone regeneration. As S1P signals are based on five distinctive receptors mediating a broad range of mechanisms, other potentially adverse effects mediated through the global elevation of S1P levels should be considered. For example, S1P is known to regulate immune cell egress through S1PR1 signaling. Disruption of the natural S1P gradient by S1P lyase inhibition results in the inhibition of lymphocyte exit and thus, lymphopenia.[112,444] Therefore, S1P might regulate other undesirable effects. Additionally, other sphingolipids are regulated through S1P lyase inhibition. These are known to regulate cellular processes themselves, which might lead to further adverse effects. As the observed mechanisms are mainly S1PR2/S1PR3 dependent, their targeting by specific agonists and antagonists would allow bypassing, e.g., the immunomodulatory effects of S1PR1 engagement. Therefore, using S1PR2 and S1PR3 agonists, such as CYM-5520 and TY-52156, or a combination of both, would be a promising

approach.

A clear effect of S1P on the mineral capacity of pOBs was shown in this study. However, measuring bone resorption markers and analyzing gene expression data in pOBs also indicated an influence of S1P/S1PR3 signaling on OB/OC crosstalk. S1P has previously been described to influence OCs, as evidenced by an increased chemoattraction towards the bone surface upon S1PR1 signaling[302] and suppression of osteoclastogenesis after S1PR2 signaling.[305] To fully understand the processes involved in bone regeneration mediated through S1P signaling, the effect on other cells within the bone needs to be evaluated. In particular, OCs and osteocytes are known to be involved in bone homeostasis in addition to OBs.[244,247] As bone regeneration is a complex process, the S1P-mediated mechanism influencing diverse cell types should also be evaluated *in vivo*. Cell-specific knockout of S1PRs in OBs, OCs and possibly osteocytes could help to understand the complex mechanism underlying S1P-mediated bone regeneration. The complementary effects observed in inhibiting bone resorption and enhancing bone formation further strengthen the value of S1P-based therapy for bone regeneration.

An additional regulatory effect of S1P signaling in BMECs was identified. This led to the formation of H-type vessels via S1PR3 signaling. Additionally, an increase in total vascular area and branching was observed upon S1P treatment. As the vasculature supports the bone with nutrients and oxygen, an additional pro-osteogenic effect is expected through the densening of the vasculature. The involvement of S1P signaling in this process could not be fully elucidated as the deletion of S1PR2 and S1PR3, respectively, still showed an increase in vascular branching and area after elevation of S1P levels. Identifying the underlying mechanism in S1P-mediated angiogenesis could reveal potential additional therapeutic targets. Several growth factors are known to be affected by S1P and influence angiogenesis. To reveal a possible involvement of these factors in S1P-mediated changes in vessel density, it would be interesting to measure the levels of these factors in animals after S1P level elevation. Possible regulated growth factors need to be blocked to identify specific effects. Further understanding these mechanisms could add value to S1P-mediated treatments and pose potential adjuvant therapy options.

References

[1] A. Wille, S. Weske, K. von Wnuck Lipinski, P. Wollnitzke, N. H. Schröder, N. Thomas, M. K. Nowak, J. Deister-Jonas, B. Behr, P. Keul, and B. Levkau, “Sphingosine-1-phosphate promotes osteogenesis by stimulating osteoblast growth and neovascularization in a vascular endothelial growth factor–dependent manner,” *Journal of Bone and Mineral Research*, 2024.

[2] J. M. Wagner, A. Wille, M. Fueth, S. Weske, S. Lotzien, F. Reinkemeier, C. Wallner, A. Sogorski, S. Dittfeld, M. Becerikli, T. A. Schildhauer, M. Lehnhardt, B. Levkau, and B. Behr, “Pharmacological elevation of sphingosine-1-phosphate by s1p lyase inhibition accelerates bone regeneration after post-traumatic osteomyelitis,” *J Cell Mol Med*, vol. 27, no. 23, pp. 3786–3795, 2023.

[3] Y. A. Hannun and L. M. Obeid, “Sphingolipids and their metabolism in physiology and disease,” *Nat Rev Mol Cell Biol*, vol. 19, no. 3, pp. 175–191, 2018.

[4] J. Thudichum, “A treatise on the chemical constitution of the brain: Based throughout upon original researches,” *Glasgow Medical Journal*, vol. 22, no. 5, pp. 363–364, 1884.

[5] A. H. Futerman and Y. A. Hannun, “The complex life of simple sphingolipids,” *EMBO Rep*, vol. 5, no. 8, pp. 777–82, 2004.

[6] A. H. Futerman, *Chapter 9 - Sphingolipids*, pp. 281–316. Elsevier, 2021.

[7] T. Hla and A. J. Dannenberg, “Sphingolipid signaling in metabolic disorders,” *Cell Metab*, vol. 16, no. 4, pp. 420–34, 2012.

[8] N. Bartke and Y. A. Hannun, “Bioactive sphingolipids: metabolism and function,” *J Lipid Res*, 2009.

[9] K. Simons and E. Ikonen, “Functional rafts in cell membranes,” *Nature*, vol. 387, no. 6633, pp. 569–572, 1997.

[10] E. C. Mandon, I. Ehses, J. Rother, G. van Echten, and K. Sandhoff, “Subcellular localization and membrane topology of serine palmitoyltransferase, 3-dehydrosphinganine reductase, and sphinganine n-acyltransferase in mouse liver,” *J Biol Chem*, vol. 267, no. 16, pp. 11144–8, 1992.

[11] W. Stoffel, D. Lekim, and G. Sticht, “Metabolism of sphingosine bases, v. biosynthesis of dihydrosphingosine in vitro,” vol. 349, no. 1, pp. 664–670, 1968.

[12] C. Michel and G. van Echten-Deckert, “Conversion of dihydroceramide to ceramide occurs at the cytosolic face of the endoplasmic reticulum,” *FEBS Lett*, vol. 416, no. 2, pp. 153–5, 1997.

[13] K. Hanada, K. Kumagai, S. Yasuda, Y. Miura, M. Kawano, M. Fukasawa, and M. Nishijima, “Molecular machinery for non-vesicular trafficking of ceramide,” *Nature*, vol. 426, no. 6968, pp. 803–809, 2003.

[14] D. Jeckel, A. Karrenbauer, K. N. Burger, G. van Meer, and F. Wieland, "Glucosylceramide is synthesized at the cytosolic surface of various golgi subfractions," *J Cell Biol*, vol. 117, no. 2, pp. 259–67, 1992.

[15] F. G. Tafesse, P. Ternes, and J. C. Holthuis, "The multigenic sphingomyelin synthase family," *J Biol Chem*, vol. 281, no. 40, pp. 29421–5, 2006.

[16] J. N. Kanfer, O. M. Young, D. Shapiro, and R. O. Brady, "The metabolism of sphingomyelin: I. purification and properties of a sphingolyelin-cleaving enzyme from rat liver tissue," *Journal of Biological Chemistry*, vol. 241, no. 5, pp. 1081–1084, 1966.

[17] Y. Deng, F. E. Rivera-Molina, D. K. Toomre, and C. G. Burd, "Sphingomyelin is sorted at the trans golgi network into a distinct class of secretory vesicle," *Proc Natl Acad Sci U S A*, vol. 113, no. 24, pp. 6677–82, 2016.

[18] L. Riboni, R. Bassi, A. Caminiti, A. Prinetti, P. Viani, and G. Tettamanti, "Metabolic fate of exogenous sphingosine in neuroblastoma neuro2a cells. dose-dependence and biological effects," *Ann N Y Acad Sci*, vol. 845, pp. 46–56, 1998.

[19] C. Mao and L. M. Obeid, "Ceramidases: regulators of cellular responses mediated by ceramide, sphingosine, and sphingosine-1-phosphate," *Biochim Biophys Acta*, vol. 1781, no. 9, pp. 424–34, 2008.

[20] F. Parveen, D. Bender, S. H. Law, V. K. Mishra, C. C. Chen, and L. Y. Ke, "Role of ceramidases in sphingolipid metabolism and human diseases," *Cells*, vol. 8, no. 12, 2019.

[21] S. M. Mandala, R. Thornton, I. Galve-Roperh, S. Poulton, C. Peterson, A. Olivera, J. Bergstrom, M. B. Kurtz, and S. Spiegel, "Molecular cloning and characterization of a lipid phosphohydrolase that degrades sphingosine-1- phosphate and induces cell death," *Proceedings of the National Academy of Sciences*, vol. 97, no. 14, pp. 7859–7864, 2000.

[22] K. Mizugishi, T. Yamashita, A. Olivera, G. F. Miller, S. Spiegel, and R. L. Proia, "Essential role for sphingosine kinases in neural and vascular development," *Molecular and Cellular Biology*, vol. 25, no. 24, pp. 11113–11121, 2005. doi: 10.1128/MCB.25.24.11113-11121.2005.

[23] N. Igarashi, T. Okada, S. Hayashi, T. Fujita, S. Jahangeer, and S. Nakamura, "Sphingosine kinase 2 is a nuclear protein and inhibits dna synthesis," *J Biol Chem*, vol. 278, no. 47, pp. 46832–9, 2003.

[24] K. R. Johnson, K. P. Becker, M. M. Facchinetti, Y. A. Hannun, and L. M. Obeid, "Pkc-dependent activation of sphingosine kinase 1 and translocation to the plasma membrane: Extracellular release of sphingosine-1-phosphate induced by phorbol 12-myristate 13-acetate (pma)," *Journal of Biological Chemistry*, vol. 277, no. 38, pp. 35257–35262, 2002.

[25] G. Ding, H. Sonoda, H. Yu, T. Kajimoto, S. K. Goparaju, S. Jahangeer, T. Okada, and S.-i. Nakamura, "Protein kinase d-mediated phosphorylation and nuclear export of sphingosine kinase 2," *Journal of Biological Chemistry*, vol. 282, no. 37, pp. 27493–27502, 2007.

[26] H. Liu, M. Sugiura, V. E. Nava, L. C. Edsall, K. Kono, S. Poulton, S. Milstien, T. Kohama, and S. Spiegel, “Molecular cloning and functional characterization of a novel mammalian sphingosine kinase type 2 isoform,” *J Biol Chem*, vol. 275, no. 26, pp. 19513–20, 2000.

[27] T. Kohama, A. Olivera, L. Edsall, M. M. Nagiec, R. Dickson, and S. Spiegel, “Molecular cloning and functional characterization of murine sphingosine kinase*,” *Journal of Biological Chemistry*, vol. 273, no. 37, pp. 23722–23728, 1998.

[28] H. Liu, M. Sugiura, V. E. Nava, L. C. Edsall, K. Kono, S. Poulton, S. Milstien, T. Kohama, and S. Spiegel, “Molecular cloning and functional characterization of a novel mammalian sphingosine kinase type 2 isoform *,” *Journal of Biological Chemistry*, vol. 275, no. 26, pp. 19513–19520, 2000.

[29] C. Ogawa, A. Kihara, M. Gokoh, and Y. Igarashi, “Identification and characterization of a novel human sphingosine-1-phosphate phosphohydrolase, hspp2*,” *Journal of Biological Chemistry*, vol. 278, no. 2, pp. 1268–1272, 2003.

[30] H. Le Stunff, I. Galve-Roperh, C. Peterson, S. Milstien, and S. Spiegel, “Sphingosine-1-phosphate phosphohydrolase in regulation of sphingolipid metabolism and apoptosis,” *Journal of Cell Biology*, vol. 158, no. 6, pp. 1039–1049, 2002.

[31] D. N. Brindley and C. Pilquil, “Lipid phosphate phosphatases and signaling,” *J Lipid Res*, 2009.

[32] N. C. Hait, C. A. Oskeritzian, S. W. Paugh, S. Milstien, and S. Spiegel, “Sphingosine kinases, sphingosine 1-phosphate, apoptosis and diseases,” *Biochimica et Biophysica Acta (BBA) - Biomembranes*, vol. 1758, no. 12, pp. 2016–2026, 2006.

[33] T. D. Mullen, Y. A. Hannun, and L. M. Obeid, “Ceramide synthases at the centre of sphingolipid metabolism and biology,” *Biochem J*, vol. 441, no. 3, pp. 789–802, 2012.

[34] N. S. Ferreira, H. Engelsby, D. Neess, S. L. Kelly, G. Volpert, A. H. Merrill, A. H. Futerman, and N. J. Færgeman, “Regulation of very-long acyl chain ceramide synthesis by acyl-coa-binding protein,” *J Biol Chem*, vol. 292, no. 18, pp. 7588–7597, 2017.

[35] M. Serra and J. D. Saba, “Sphingosine 1-phosphate lyase, a key regulator of sphingosine 1-phosphate signaling and function,” *Advances in Enzyme Regulation*, vol. 50, no. 1, pp. 349–362, 2010.

[36] J. Zhou and J. D. Saba, “Identification of the first mammalian sphingosine phosphate lyase gene and its functional expression in yeast,” *Biochem Biophys Res Commun*, vol. 242, no. 3, pp. 502–7, 1998.

[37] J. D. Saba, F. Nara, A. Bielawska, S. Garrett, and Y. A. Hannun, “The bst gene of saccharomyces cerevisiae is the sphingosine-1-phosphate lyase,” *Journal of Biological Chemistry*, vol. 272, no. 42, pp. 26087–26090, 1997.

[38] A. Kumar, H. S. Byun, R. Bittman, and J. D. Saba, “The sphingolipid degradation product trans-2-hexadecenal induces cytoskeletal reorganization and apoptosis in a jnk-dependent manner,” *Cell Signal*, vol. 23, no. 7, pp. 1144–52, 2011.

[39] I. Y. Dobrosotskaya, A. C. Seegmiller, M. S. Brown, J. L. Goldstein, and R. B. Rawson, “Regulation of srebp processing and membrane lipid production by phospholipids in drosophila,” *Science*, vol. 296, no. 5569, pp. 879–883, 2002.

[40] D. Gyamfi, E. Ofori Awuah, and S. Owusu, *Chapter 2 - Lipid Metabolism: An Overview*, pp. 17–32. Academic Press, 2019.

[41] Y. Horibata and Y. Hirabayashi, “Identification and characterization of human ethanolaminephosphotransferase1,” *Journal of Lipid Research*, vol. 48, no. 3, pp. 503–508, 2007.

[42] T. Hla, K. Venkataraman, and J. Michaud, “The vascular s1p gradient-cellular sources and biological significance,” *Biochim Biophys Acta*, vol. 1781, no. 9, pp. 477–82, 2008.

[43] F. Okajima, “Plasma lipoproteins behave as carriers of extracellular sphingosine 1-phosphate: is this an atherogenic mediator or an anti-atherogenic mediator?,” *Biochim Biophys Acta*, vol. 1582, no. 1-3, pp. 132–7, 2002.

[44] S. Massberg, P. Schaerli, I. Knezevic-Maramica, M. Köllnberger, N. Tubo, E. A. Moseman, I. V. Huff, T. Junt, A. J. Wagers, I. B. Mazo, and U. H. von Andrian, “Immunosurveillance by hematopoietic progenitor cells trafficking through blood, lymph, and peripheral tissues,” *Cell*, vol. 131, no. 5, pp. 994–1008, 2007.

[45] P. Hänel, P. Andréani, and M. H. Gräler, “Erythrocytes store and release sphingosine 1-phosphate in blood,” *Faseb j*, vol. 21, no. 4, pp. 1202–9, 2007.

[46] R. Pappu, S. R. Schwab, I. Cornelissen, J. P. Pereira, J. B. Regard, Y. Xu, E. Camerer, Y. W. Zheng, Y. Huang, J. G. Cyster, and S. R. Coughlin, “Promotion of lymphocyte egress into blood and lymph by distinct sources of sphingosine-1-phosphate,” *Science*, vol. 316, no. 5822, pp. 295–8, 2007.

[47] K. Ito, Y. Anada, M. Tani, M. Ikeda, T. Sano, A. Kihara, and Y. Igarashi, “Lack of sphingosine 1-phosphate-degrading enzymes in erythrocytes,” *Biochem Biophys Res Commun*, vol. 357, no. 1, pp. 212–7, 2007.

[48] T. M. Vu, A. N. Ishizu, J. C. Foo, X. R. Toh, F. Zhang, D. M. Whee, F. Torta, A. Cazenave-Gassiot, T. Matsumura, S. Kim, S. E. S. Toh, T. Suda, D. L. Silver, M. R. Wenk, and L. N. Nguyen, “Mfsd2b is essential for the sphingosine-1-phosphate export in erythrocytes and platelets,” *Nature*, vol. 550, no. 7677, pp. 524–528, 2017.

[49] Y. Yatomi, Y. Igarashi, L. Yang, N. Hisano, R. Qi, N. Asazuma, K. Satoh, Y. Ozaki, and S. Kume, “Sphingosine 1-phosphate, a bioactive sphingolipid abundantly stored in platelets, is a normal constituent of human plasma and serum,” *J Biochem*, vol. 121, no. 5, pp. 969–73, 1997.

[50] Y. Yatomi, Y. Ozaki, T. Ohmori, and Y. Igarashi, “Sphingosine 1-phosphate: synthesis and release,” *Prostaglandins Other Lipid Mediat*, vol. 64, no. 1-4, pp. 107–22, 2001.

[51] Y. M. Lee, K. Venkataraman, S. I. Hwang, D. K. Han, and T. Hla, “A novel method to quantify sphingosine 1-phosphate by immobilized metal affinity chromatography (imac),” *Prostaglandins Other Lipid Mediat*, vol. 84, no. 3-4, pp. 154–62, 2007.

[52] K. Venkataraman, Y.-M. Lee, J. Michaud, S. Thangada, Y. Ai, H. L. Bonkovsky, N. S. Parikh, C. Habrukowich, and T. Hla, “Vascular endothelium as a contributor of plasma sphingosine 1-phosphate,” *Circulation Research*, vol. 102, no. 6, pp. 669–676, 2008.

[53] Y. Zhao, S. K. Kalari, P. V. Usatyuk, I. Gorshkova, D. He, T. Watkins, D. N. Brindley, C. Sun, R. Bittman, J. G. N. Garcia, E. V. Berdyshev, and V. Natarajan, “Intracellular generation of sphingosine 1-phosphate in human lung endothelial cells: Role of lipid phosphate phosphatase-1 and sphingosine kinase 1,” *Journal of Biological Chemistry*, vol. 282, no. 19, pp. 14165–14177, 2007.

[54] P. Mitra, C. A. Oskeritzian, S. G. Payne, M. A. Beaven, S. Milstien, and S. Spiegel, “Role of abcc1 in export of sphingosine-1-phosphate from mast cells,” *Proc Natl Acad Sci U S A*, vol. 103, no. 44, pp. 16394–9, 2006.

[55] L. Japtok, K. Schaper, W. Bäumer, H. H. Radeke, S. K. Jeong, and B. Kleuser, “Sphingosine 1-phosphate modulates antigen capture by murine langerhans cells via the s1p2 receptor subtype,” *PLoS One*, vol. 7, no. 11, p. e49427, 2012.

[56] T. A. Cartwright, C. R. Campos, R. E. Cannon, and D. S. Miller, “Mrp1 is essential for sphingolipid signaling to p-glycoprotein in mouse blood-brain and blood-spinal cord barriers,” *J Cereb Blood Flow Metab*, vol. 33, no. 3, pp. 381–8, 2013.

[57] B. Nieuwenhuis, A. Lüth, J. Chun, A. Huwiler, J. Pfeilschifter, M. Schäfer-Korting, and B. Kleuser, “Involvement of the abc-transporter abcc1 and the sphingosine 1-phosphate receptor subtype s1p(3) in the cytoprotection of human fibroblasts by the glucocorticoid dexamethasone,” *J Mol Med (Berl)*, vol. 87, no. 6, pp. 645–57, 2009.

[58] K. Takabe, R. H. Kim, J. C. Allegood, P. Mitra, S. Ramachandran, M. Nagahashi, K. B. Harikumar, N. C. Hait, S. Milstien, and S. Spiegel, “Estradiol induces export of sphingosine 1-phosphate from breast cancer cells via abcc1 and abcg2,” *J Biol Chem*, vol. 285, no. 14, pp. 10477–86, 2010.

[59] N. Kobayashi, N. Kobayashi, A. Yamaguchi, and T. Nishi, “Characterization of the atp-dependent sphingosine 1-phosphate transporter in rat erythrocytes,” *J Biol Chem*, vol. 284, no. 32, pp. 21192–200, 2009.

[60] K. Sato, E. Malchinkhuu, Y. Horiuchi, C. Mogi, H. Tomura, M. Tosaka, Y. Yoshimoto, A. Kuwabara, and F. Okajima, “Critical role of abca1 transporter in sphingosine 1-phosphate release from astrocytes,” *J Neurochem*, vol. 103, no. 6, pp. 2610–9, 2007.

[61] N. Osborne, K. Brand-Arzamendi, E. A. Ober, S. W. Jin, H. Verkade, N. G. Holtzman, D. Yelon, and D. Y. Stainier, "The spinster homolog, two of hearts, is required for sphingosine 1-phosphate signaling in zebrafish," *Curr Biol*, vol. 18, no. 23, pp. 1882–8, 2008.

[62] A. Kawahara, T. Nishi, Y. Hisano, H. Fukui, A. Yamaguchi, and N. Mochizuki, "The sphingolipid transporter spns2 functions in migration of zebrafish myocardial precursors," *Science*, vol. 323, no. 5913, pp. 524–7, 2009.

[63] Y. Hisano, N. Kobayashi, A. Yamaguchi, and T. Nishi, "Mouse spns2 functions as a sphingosine-1-phosphate transporter in vascular endothelial cells," *PLoS One*, vol. 7, no. 6, p. e38941, 2012.

[64] J. Chen, N. Ingham, J. Kelly, S. Jadeja, D. Goulding, J. Pass, V. B. Mahajan, S. H. Tsang, A. Nijnik, I. J. Jackson, J. K. White, A. Forge, D. Jagger, and K. P. Steel, "Spinster homolog 2 (spns2) deficiency causes early onset progressive hearing loss," *PLoS Genet*, vol. 10, no. 10, p. e1004688, 2014.

[65] Y. Duan, N. C. P. Leong, J. Zhao, Y. Zhang, D. T. Nguyen, H. T. T. Ha, N. Wang, R. Xia, Z. Xu, Z. Ma, Y. Qian, H. Yin, X. Zhu, A. Zhang, C. Guo, Y. Xia, L. N. Nguyen, and Y. He, "Structural basis of sphingosine-1-phosphate transport via human spns2," *Cell Res*, vol. 34, no. 2, pp. 177–180, 2024.

[66] H. Chen, S. Ahmed, H. Zhao, N. Elghobashi-Meinhardt, Y. Dai, J. H. Kim, J. G. McDonald, X. Li, and C. H. Lee, "Structural and functional insights into spns2-mediated transport of sphingosine-1-phosphate," *Cell*, vol. 186, no. 12, pp. 2644–2655.e16, 2023.

[67] T. Q. Nguyen, T. M. Vu, F. Tukijan, S. Muralidharan, J. C. Foo, J. F. Li Chin, Z. Hasan, F. Torta, and L. N. Nguyen, "Erythrocytes efficiently utilize exogenous sphingosines for s1p synthesis and export via mfsd2b," *J Biol Chem*, vol. 296, p. 100201, 2021.

[68] N. Kobayashi, S. Kawasaki-Nishi, M. Otsuka, Y. Hisano, A. Yamaguchi, and T. Nishi, "Mfsd2b is a sphingosine 1-phosphate transporter in erythroid cells," *Sci Rep*, vol. 8, no. 1, p. 4969, 2018.

[69] T. N. U. Le, T. Q. Nguyen, P. Kalailingam, Y. T. K. Nguyen, V. K. Sukumar, C. K. H. Tan, F. Tukijan, L. Couty, Z. Hasan, I. Del Gaudio, M. R. Wenk, A. Cazenave-Gassiot, E. Camerer, and L. N. Nguyen, "Mfsd2b and spns2 are essential for maintenance of blood vessels during development and in anaphylactic shock," *Cell Rep*, vol. 40, no. 7, p. 111208, 2022.

[70] M. Chandrakanthan, T. Q. Nguyen, Z. Hasan, S. Muralidharan, T. M. Vu, A. W. L. Li, U. T. N. Le, H. Thi Thuy Ha, S. H. Baik, S. H. Tan, J. C. Foo, M. R. Wenk, A. Cazenave-Gassiot, F. Torta, W. Y. Ong, M. Y. Y. Chan, and L. N. Nguyen, "Deletion of mfsd2b impairs thrombotic functions of platelets," *Nat Commun*, vol. 12, no. 1, p. 2286, 2021.

[71] U. Peest, S. C. Sensken, P. Andréani, P. Hänel, P. P. Van Veldhoven, and M. H. Gräler, "S1p-lyase independent clearance of extracellular sphingosine 1-phosphate after dephosphorylation and cellular uptake," *J Cell Biochem*, vol. 104, no. 3, pp. 756–72, 2008.

[72] K. R. Feingold, *Introduction to Lipids and Lipoproteins*. South Dartmouth (MA): MDText.com, Inc. Copyright 2000-2024, MDText.com, Inc., 2000.

[73] P. M. Christensen, M. H. Bosteen, S. Hajny, L. B. Nielsen, and C. Christoffersen, "Apolipoprotein m mediates sphingosine-1-phosphate efflux from erythrocytes," *Scientific Reports*, vol. 7, no. 1, p. 14983, 2017.

[74] S. M. Hammad, M. M. Al Gadban, A. J. Semler, and R. L. Klein, "Sphingosine 1-phosphate distribution in human plasma: associations with lipid profiles," *J Lipids*, vol. 2012, p. 180705, 2012.

[75] C. Christoffersen, H. Obinata, S. B. Kumaraswamy, S. Galvani, J. Ahnström, M. Sevvana, C. Egerer-Sieber, Y. A. Muller, T. Hla, L. B. Nielsen, and B. Dahlbäck, "Endothelium-protective sphingosine-1-phosphate provided by hdl-associated apolipoprotein m," *Proc Natl Acad Sci U S A*, vol. 108, no. 23, pp. 9613–8, 2011.

[76] C. Christoffersen, L. B. Nielsen, O. Axler, A. Andersson, A. H. Johnsen, and B. Dahlbaäck, "Isolation and characterization of human apolipoprotein m-containing lipoproteins," *Journal of Lipid Research*, vol. 47, no. 8, pp. 1833–1843, 2006.

[77] G. Zhang, L. Yang, G. S. Kim, K. Ryan, S. Lu, R. K. O'Donnell, K. Spokes, N. Shapiro, W. C. Aird, M. J. Kluk, K. Yano, and T. Sanchez, "Critical role of sphingosine-1-phosphate receptor 2 (s1pr2) in acute vascular inflammation," *Blood*, vol. 122, no. 3, pp. 443–55, 2013.

[78] M. Ruiz, C. Frej, A. Holmér, L. J. Guo, S. Tran, and B. Dahlbäck, "High-density lipoprotein–associated apolipoprotein m limits endothelial inflammation by delivering sphingosine-1-phosphate to the sphingosine-1-phosphate receptor 1," *Arteriosclerosis, Thrombosis, and Vascular Biology*, vol. 37, no. 1, pp. 118–129, 2017.

[79] K. M. Argraves and W. S. Argraves, "Hdl serves as a s1p signaling platform mediating a multitude of cardiovascular effects," *J Lipid Res*, vol. 48, no. 11, pp. 2325–33, 2007.

[80] C. Christoffersen, "Apolipoprotein m-a marker or an active player in type ii diabetes?," *Front Endocrinol (Lausanne)*, vol. 12, p. 665393, 2021.

[81] S. Galvani, M. Sanson, V. A. Blaho, S. L. Swendeman, H. Obinata, H. Conger, B. Dahlbäck, M. Kono, R. L. Proia, J. D. Smith, and T. Hla, "Hdl-bound sphingosine 1-phosphate acts as a biased agonist for the endothelial cell receptor s1p1 to limit vascular inflammation," *Science Signaling*, vol. 8, no. 389, pp. ra79–ra79, 2015.

[82] T. Hla, "Sphingosine 1-phosphate receptors," *Prostaglandins & Other Lipid Mediators*, vol. 64, no. 1, pp. 135–142, 2001.

[83] S. S. Karnik and H. G. Khorana, "Assembly of functional rhodopsin requires a disulfide bond between cysteine residues 110 and 187," *Journal of Biological Chemistry*, vol. 265, no. 29, pp. 17520–17524, 1990.

[84] D. M. Perez and S. S. Karnik, “Multiple signaling states of g-protein-coupled receptors,” *Pharmacological Reviews*, vol. 57, no. 2, pp. 147–161, 2005.

[85] W. M. Oldham and H. E. Hamm, “Heterotrimeric g protein activation by g-protein-coupled receptors,” *Nature Reviews Molecular Cell Biology*, vol. 9, no. 1, pp. 60–71, 2008.

[86] M. J. Lee, M. Evans, and T. Hla, “The inducible g protein-coupled receptor edg-1 signals via the g(i)/mitogen-activated protein kinase pathway,” *J Biol Chem*, vol. 271, no. 19, pp. 11272–9, 1996.

[87] R. T. Windh, M. J. Lee, T. Hla, S. An, A. J. Barr, and D. R. Manning, “Differential coupling of the sphingosine 1-phosphate receptors edg-1, edg-3, and h218/edg-5 to the g(i), g(q), and g(12) families of heterotrimeric g proteins,” *J Biol Chem*, vol. 274, no. 39, pp. 27351–8, 1999.

[88] J. R. Van Brocklyn, M. H. Graäler, G. Bernhardt, J. P. Hobson, M. Lipp, and S. Spiegel, “Sphingosine-1-phosphate is a ligand for the g protein-coupled receptor edg-6,” *Blood*, vol. 95, no. 8, pp. 2624–2629, 2000.

[89] M. H. Gräler, R. Grosse, A. Kusch, E. Kremmer, T. Gudermann, and M. Lipp, “The sphingosine 1-phosphate receptor s1p4 regulates cell shape and motility via coupling to gi and g12/13,” *J Cell Biochem*, vol. 89, no. 3, pp. 507–19, 2003.

[90] I. Ishii, N. Fukushima, X. Ye, , and J. Chun, “Lysophospholipid receptors: Signaling and biology,” *Annual Review of Biochemistry*, vol. 73, no. 1, pp. 321–354, 2004.

[91] M.-J. Lee, S. Thangada, K. P. Claffey, N. Ancellin, C. H. Liu, M. Kluk, M. Volpi, R. I. Sha’afi, and T. Hla, “Vascular endothelial cell adherens junction assembly and morphogenesis induced by sphingosine-1-phosphate,” *Cell*, vol. 99, no. 3, pp. 301–312, 1999.

[92] A. Roggeri, M. Schepers, A. Tiane, B. Rombaut, L. van Veggel, N. Hellings, J. Prickaerts, A. Pittaluga, and T. Vanmierlo, “Sphingosine-1-phosphate receptor modulators and oligodendroglial cells: Beyond immunomodulation,” *International Journal of Molecular Sciences*, vol. 21, no. 20, p. 7537, 2020.

[93] Y. Yamazaki, J. Kon, K. Sato, H. Tomura, M. Sato, T. Yoneya, H. Okazaki, F. Okajima, and H. Ohta, “Edg-6 as a putative sphingosine 1-phosphate receptor coupling to ca(2+) signaling pathway,” *Biochem Biophys Res Commun*, vol. 268, no. 2, pp. 583–9, 2000.

[94] C. Jaillard, S. Harrison, B. Stankoff, M. S. Aigrot, A. R. Calver, G. Duddy, F. S. Walsh, M. N. Pangalos, N. Arimura, K. Kaibuchi, B. Zalc, and C. Lubetzki, “Edg8/s1p5: an oligodendroglial receptor with dual function on process retraction and cell survival,” *J Neurosci*, vol. 25, no. 6, pp. 1459–69, 2005.

[95] T. Kozasa, X. Jiang, M. J. Hart, P. M. Sternweis, W. D. Singer, A. G. Gilman, G. Bollag, and P. C. Sternweis, “p115 rhogef, a gtpase activating protein for galpha12 and galpha13,” *Science*, vol. 280, no. 5372, pp. 2109–11, 1998.

[96] S. E. Alvarez, K. B. Harikumar, N. C. Hait, J. Allegood, G. M. Strub, E. Y. Kim, M. Maceyka, H. Jiang, C. Luo, T. Kordula, S. Milstien, and S. Spiegel, "Sphingosine-1-phosphate is a missing cofactor for the e3 ubiquitin ligase traf2," *Nature*, vol. 465, no. 7301, pp. 1084–8, 2010.

[97] K. Park, H. Ikushiro, H. S. Seo, K. O. Shin, Y. I. Kim, J. Y. Kim, Y. M. Lee, T. Yano, W. M. Holleran, P. Elias, and Y. Uchida, "Er stress stimulates production of the key antimicrobial peptide, cathelicidin, by forming a previously unidentified intracellular s1p signaling complex," *Proc Natl Acad Sci U S A*, vol. 113, no. 10, pp. E1334–42, 2016.

[98] T. Kajimoto, A. D. Caliman, I. S. Tobias, T. Okada, C. A. Pilo, A. N. Van, J. Andrew McCammon, S. I. Nakamura, and A. C. Newton, "Activation of atypical protein kinase c by sphingosine 1-phosphate revealed by an apkc-specific activity reporter," *Sci Signal*, vol. 12, no. 562, 2019.

[99] K. A. Parham, J. R. Zebol, K. L. Tooley, W. Y. Sun, L. M. Moldenhauer, M. P. Cockshell, B. L. Gliddon, P. A. Moretti, G. Tigyi, S. M. Pitson, and C. S. Bonder, "Sphingosine 1-phosphate is a ligand for peroxisome proliferator-activated receptor-γ that regulates neoangiogenesis," *Faseb j*, vol. 29, no. 9, pp. 3638–53, 2015.

[100] G. H. Seol, M. Y. Kim, G. H. Liang, J. A. Kim, Y. J. Kim, S. Oh, and S. H. Suh, "Sphingosine-1-phosphate-induced intracellular ca2+ mobilization in human endothelial cells," *Endothelium*, vol. 12, no. 5-6, pp. 263–9, 2005.

[101] D. Meyer zu Heringdorf, K. Liliom, M. Schaefer, K. Danneberg, J. H. Jaggar, G. Tigyi, and K. H. Jakobs, "Photolysis of intracellular caged sphingosine-1-phosphate causes ca2+ mobilization independently of g-protein-coupled receptors," *FEBS Letters*, vol. 554, no. 3, pp. 443–449, 2003.

[102] W. Haotian, L. Bingqian, L. Canjun, Z. Wenping, Q. Lili, and C. Chunlei, "Sphingosine-1-phosphate induces ca2+ mobilization via trpc6 channels in sh-sy5y cells and hippocampal neurons," *JUSTC*, vol. 52, no. 9, pp. 2–1–2–10, 2022.

[103] S.-Z. Xu, K. Muraki, F. Zeng, J. Li, P. Sukumar, S. Shah, A. M. Dedman, P. K. Flemming, D. McHugh, J. Naylor, A. Cheong, A. N. Bateson, C. M. Munsch, K. E. Porter, and D. J. Beech, "A sphingosine-1–phosphate-activated calcium channel controlling vascular smooth muscle cell motility," *Circulation Research*, vol. 98, no. 11, pp. 1381–1389, 2006.

[104] N. C. Hait, J. Allegood, M. Maceyka, G. M. Strub, K. B. Harikumar, S. K. Singh, C. Luo, R. Marmorstein, T. Kordula, S. Milstien, and S. Spiegel, "Regulation of histone acetylation in the nucleus by sphingosine-1-phosphate," *Science*, vol. 325, no. 5945, pp. 1254–7, 2009.

[105] K. Ihlefeld, R. F. Claas, A. Koch, J. M. Pfeilschifter, and D. Meyer Zu Heringdorf, "Evidence for a link between histone deacetylation and ca^{2}+ homoeostasis in sphingosine-1-phosphate lyase-deficient fibroblasts," *Biochem J*, vol. 447, no. 3, pp. 457–64, 2012.

[106] L. Gong, Y. Shen, S. Wang, X. Wang, H. Ji, X. Wu, L. Hu, and L. Zhu, "Nuclear sphk2/s1p induces oxidative stress and nlrp3 inflammasome activation via promoting p53 acetylation in lipopolysaccharide-induced acute lung injury," *Cell Death Discovery*, vol. 9, no. 1, p. 12, 2023.

[107] X. Ji, Z. Chen, Q. Wang, B. Li, Y. Wei, Y. Li, J. Lin, W. Cheng, Y. Guo, S. Wu, L. Mao, Y. Xiang, T. Lan, S. Gu, M. Wei, J. Z. Zhang, L. Jiang, J. Wang, J. Xu, and N. Cao, "Sphingolipid metabolism controls mammalian heart regeneration," *Cell Metabolism*, vol. 36, no. 4, pp. 839–856.e8, 2024.

[108] N. C. Hait, L. E. Wise, J. C. Allegood, M. O'Brien, D. Avni, T. M. Reeves, P. E. Knapp, J. Lu, C. Luo, M. F. Miles, S. Milstien, A. H. Lichtman, and S. Spiegel, "Active, phosphorylated fingolimod inhibits histone deacetylases and facilitates fear extinction memory," *Nat Neurosci*, vol. 17, no. 7, pp. 971–80, 2014.

[109] S. Panneer Selvam, R. M. De Palma, J. J. Oaks, N. Oleinik, Y. K. Peterson, R. V. Stahelin, E. Skordalakes, S. Ponnusamy, E. Garrett-Mayer, C. D. Smith, and B. Ogretmen, "Binding of the sphingolipid s1p to htert stabilizes telomerase at the nuclear periphery by allosterically mimicking protein phosphorylation," *Sci Signal*, vol. 8, no. 381, p. ra58, 2015.

[110] G. M. Strub, M. Paillard, J. Liang, L. Gomez, J. C. Allegood, N. C. Hait, M. Maceyka, M. M. Price, Q. Chen, D. C. Simpson, T. Kordula, S. Milstien, E. J. Lesnefsky, and S. Spiegel, "Sphingosine-1-phosphate produced by sphingosine kinase 2 in mitochondria interacts with prohibitin 2 to regulate complex iv assembly and respiration," *Faseb j*, vol. 25, no. 2, pp. 600–12, 2011.

[111] L. Gomez, M. Paillard, M. Price, Q. Chen, G. Teixeira, S. Spiegel, and E. J. Lesnefsky, "A novel role for mitochondrial sphingosine-1-phosphate produced by sphingosine kinase-2 in ptp-mediated cell survival during cardioprotection," *Basic Res Cardiol*, vol. 106, no. 6, pp. 1341–53, 2011.

[112] S. R. Schwab, J. P. Pereira, M. Matloubian, Y. Xu, Y. Huang, and J. G. Cyster, "Lymphocyte sequestration through s1p lyase inhibition and disruption of s1p gradients," *Science*, vol. 309, no. 5741, pp. 1735–9, 2005.

[113] C. N. Jenne, A. Enders, R. Rivera, S. R. Watson, A. J. Bankovich, J. P. Pereira, Y. Xu, C. M. Roots, J. N. Beilke, A. Banerjee, S. L. Reiner, S. A. Miller, A. S. Weinmann, C. C. Goodnow, L. L. Lanier, J. G. Cyster, and J. Chun, "T-bet-dependent s1p5 expression in nk cells promotes egress from lymph nodes and bone marrow," *J Exp Med*, vol. 206, no. 11, pp. 2469–81, 2009.

[114] J. Milara, M. Mata, M. D. Mauricio, E. Donet, E. J. Morcillo, and J. Cortijo, "Sphingosine-1-phosphate increases human alveolar epithelial il-8 secretion, proliferation and neutrophil chemotaxis," *Eur J Pharmacol*, vol. 609, no. 1-3, pp. 132–9, 2009.

[115] P. K. Coyle, M. S. Freedman, B. A. Cohen, B. A. C. Cree, and C. E. Markowitz, "Sphingosine 1-phosphate receptor modulators in multiple sclerosis treatment: A practical review," *Ann Clin Transl Neurol*, vol. 11, no. 4, pp. 842–855, 2024.

[116] J. A. Cohen, F. Barkhof, G. Comi, H. P. Hartung, B. O. Khatri, X. Montalban, J. Pelletier, R. Capra, P. Gallo, G. Izquierdo, K. Tiel-Wilck, A. de Vera, J. Jin, T. Stites, S. Wu, S. Aradhye, and L. Kappos, "Oral fingolimod or intramuscular interferon for relapsing multiple sclerosis," *N Engl J Med*, vol. 362, no. 5, pp. 402–15, 2010.

[117] L. Kappos, J. Antel, G. Comi, X. Montalban, P. O'Connor, C. H. Polman, T. Haas, A. A. Korn, G. Karlsson, and E. W. Radue, "Oral fingolimod (fty720) for relapsing multiple sclerosis," *N Engl J Med*, vol. 355, no. 11, pp. 1124–40, 2006.

[118] L. Kappos, E. W. Radue, P. O'Connor, C. Polman, R. Hohlfeld, P. Calabresi, K. Selmaj, C. Agoropoulou, M. Leyk, L. Zhang-Auberson, and P. Burtin, "A placebo-controlled trial of oral fingolimod in relapsing multiple sclerosis," *N Engl J Med*, vol. 362, no. 5, pp. 387–401, 2010.

[119] L. Kappos, A. Bar-Or, B. A. C. Cree, R. J. Fox, G. Giovannoni, R. Gold, P. Vermersch, D. L. Arnold, S. Arnould, T. Scherz, C. Wolf, E. Wallström, F. Dahlke, A. Achiron, L. Achtnichts, K. Agan, G. Akman-Demir, A. B. Allen, J. P. Antel, A. R. Antiguedad, M. Apperson, A. M. Applebee, G. I. Ayuso, M. Baba, O. Bajenaru, R. Balasa, B. P. Balci, M. Barnett, A. Bass, V. U. Becker, M. Bejinariu, F. T. Bergh, A. Bergmann, E. Bernitsas, A. Berthele, V. Bhan, F. Bischof, R. J. Bjork, G. Blevins, M. Boehringer, T. Boerner, R. Bonek, J. D. Bowen, A. Bowling, A. N. Boyko, C. Boz, V. Bracknies, S. Braune, V. Brescia Morra, B. Brochet, W. Brola, P. K. Brownstone, M. Brozman, D. Brunet, I. Buraga, M. Burnett, M. Buttmann, H. Butzkueven, J. Cahill, J. C. Calkwood, W. Camu, M. Cascione, G. Castelnovo, D. Centonze, J. Cerqueira, A. Chan, A. Cimprichova, S. Cohan, G. Comi, J. Conway, J. A. Cooper, J. Corboy, J. Correale, B. Costell, D. A. Cottrell, P. K. Coyle, M. Craner, L. Cui, L. Cunha, A. Czlonkowska, A. M. da Silva, J. de Sa, J. de Seze, M. Debouverie, J. Debruyne, D. Decoo, G. Defer, T. Derfuss, N. H. Deri, B. Dihenia, P. Dioszeghy, V. Donath, B. Dubois, M. Duddy, P. Duquette, G. Edan, H. Efendi, S. Elias, P. J. Emrich, B. C. Estruch, *et al.*, "Siponimod versus placebo in secondary progressive multiple sclerosis (expand): a double-blind, randomised, phase 3 study," *The Lancet*, vol. 391, no. 10127, pp. 1263–1273, 2018.

[120] J. A. Cohen, G. Comi, K. W. Selmaj, A. Bar-Or, D. L. Arnold, L. Steinman, H.-P. Hartung, X. Montalban, E. Kubala Havrdová, B. A. C. Cree, J. K. Sheffield, N. Minton, K. Raghupathi, V. Huang, and L. Kappos, "Safety and efficacy of ozanimod versus interferon beta-1a in relapsing multiple sclerosis (radiance): a multicentre, randomised, 24-month, phase 3 trial," *The Lancet Neurology*, vol. 18, no. 11, pp. 1021–1033, 2019.

[121] G. Comi, L. Kappos, K. W. Selmaj, A. Bar-Or, D. L. Arnold, L. Steinman, H.-P. Hartung, X. Montalban, E. Kubala Havrdová, B. A. C. Cree, J. K. Sheffield, N. Minton, K. Raghupathi, N. Ding, and J. A. Cohen, "Safety and efficacy of ozanimod versus interferon beta-1a in relapsing multiple sclerosis (sunbeam): a multicentre, randomised, minimum 12-month, phase 3 trial," *The Lancet Neurology*, vol. 18, no. 11, pp. 1009–1020, 2019.

[122] L. Kappos, R. J. Fox, M. Burcklen, M. S. Freedman, E. K. Havrdová, B. Hennessy, R. Hohlfeld, F. Lublin, X. Montalban, C. Pozzilli, T. Scherz, D. D'Ambrosio, P. Linscheid, A. Vaclavkova, M. Pirozek-Lawniczek, H. Kracker, and T. Sprenger, "Ponesimod compared with teriflunomide in patients with relapsing multiple sclerosis in the active-comparator phase 3 optimum study: A randomized clinical trial," *JAMA Neurology*, vol. 78, no. 5, pp. 558–567, 2021.

[123] I. Karaca, I. Y. Tamboli, K. Glebov, J. Richter, L. H. Fell, M. O. Grimm, V. J. Haupenthal, T. Hartmann, M. H. Gräler, G. van Echten-Deckert, and J. Walter, "Deficiency of

sphingosine-1-phosphate lyase impairs lysosomal metabolism of the amyloid precursor protein," *J Biol Chem*, vol. 289, no. 24, pp. 16761–72, 2014.

[124] N. Takasugi, T. Sasaki, K. Suzuki, S. Osawa, H. Isshiki, Y. Hori, N. Shimada, T. Higo, S. Yokoshima, T. Fukuyama, V. M. Lee, J. Q. Trojanowski, T. Tomita, and T. Iwatsubo, "Bace1 activity is modulated by cell-associated sphingosine-1-phosphate," *J Neurosci*, vol. 31, no. 18, pp. 6850–7, 2011.

[125] P. Keul, S. Lucke, K. von Wnuck Lipinski, C. Bode, M. Gräler, G. Heusch, and B. Levkau, "Sphingosine-1-phosphate receptor 3 promotes recruitment of monocyte/macrophages in inflammation and atherosclerosis," *Circ Res*, vol. 108, no. 3, pp. 314–23, 2011.

[126] P. Keul, M. Tölle, S. Lucke, K. von Wnuck Lipinski, G. Heusch, M. Schuchardt, M. van der Giet, and B. Levkau, "The sphingosine-1-phosphate analogue fty720 reduces atherosclerosis in apolipoprotein e-deficient mice," *Arterioscler Thromb Vasc Biol*, vol. 27, no. 3, pp. 607–13, 2007.

[127] J. R. Nofer, M. Bot, M. Brodde, P. J. Taylor, P. Salm, V. Brinkmann, T. van Berkel, G. Assmann, and E. A. Biessen, "Fty720, a synthetic sphingosine 1 phosphate analogue, inhibits development of atherosclerosis in low-density lipoprotein receptor-deficient mice," *Circulation*, vol. 115, no. 4, pp. 501–8, 2007.

[128] K. Sattler, I. Lehmann, M. Gräler, M. Bröcker-Preuss, R. Erbel, G. Heusch, and B. Levkau, "Hdl-bound sphingosine 1-phosphate (s1p) predicts the severity of coronary artery atherosclerosis," *Cellular Physiology and Biochemistry*, vol. 34, no. 1, pp. 172–184, 2014.

[129] K. M. Argraves, A. A. Sethi, P. J. Gazzolo, B. A. Wilkerson, A. T. Remaley, A. Tybjaerg-Hansen, B. G. Nordestgaard, S. D. Yeatts, K. S. Nicholas, J. L. Barth, and W. S. Argraves, "S1p, dihydro-s1p and c24:1-ceramide levels in the hdl-containing fraction of serum inversely correlate with occurrence of ischemic heart disease," *Lipids Health Dis*, vol. 10, p. 70, 2011.

[130] A. Polzin, K. Piayda, P. Keul, L. Dannenberg, A. Mohring, M. Gräler, T. Zeus, M. Kelm, and B. Levkau, "Plasma sphingosine-1-phosphate concentrations are associated with systolic heart failure in patients with ischemic heart disease," *J Mol Cell Cardiol*, vol. 110, pp. 35–37, 2017.

[131] M. Knapp, M. Baranowski, D. Czarnowski, A. Lisowska, P. Zabielski, J. Górski, and W. Musiał, "Plasma sphingosine-1-phosphate concentration is reduced in patients with myocardial infarction," *Med Sci Monit*, vol. 15, no. 9, pp. Cr490–3, 2009.

[132] M. Knapp, A. Lisowska, P. Zabielski, W. Musiał, and M. Baranowski, "Sustained decrease in plasma sphingosine-1-phosphate concentration and its accumulation in blood cells in acute myocardial infarction," *Prostaglandins Other Lipid Mediat*, vol. 106, pp. 53–61, 2013.

[133] D. Atkinson, J. Nikodinovic Glumac, B. Asselbergh, B. Ermanoska, D. Blocquel, R. Steiner, A. Estrada-Cuzcano, K. Peeters, T. Ooms, E. De Vriendt, X. L. Yang, T. Hornemann, V. Milic Rasic, and A. Jordanova, "Sphingosine 1-phosphate lyase deficiency causes charcot-marie-tooth neuropathy," *Neurology*, vol. 88, no. 6, pp. 533–542, 2017.

[134] D. Bamborschke, M. Pergande, K. Becker, F. Koerber, J. Dötsch, A. Vierzig, L. T. Weber, and S. Cirak, "A novel mutation in sphingosine-1-phosphate lyase causing congenital brain malformation," *Brain Dev*, vol. 40, no. 6, pp. 480–483, 2018.

[135] A. R. Janecke, R. Xu, E. Steichen-Gersdorf, S. Waldegger, A. Entenmann, T. Giner, I. Krainer, L. A. Huber, M. W. Hess, Y. Frishberg, H. Barash, S. Tzur, N. Schreyer-Shafir, R. Sukenik-Halevy, T. Zehavi, A. Raas-Rothschild, C. Mao, and T. Müller, "Deficiency of the sphingosine-1-phosphate lyase sgpl1 is associated with congenital nephrotic syndrome and congenital adrenal calcifications," *Hum Mutat*, vol. 38, no. 4, pp. 365–372, 2017.

[136] N. D. Linhares, R. R. Arantes, S. A. Araujo, and S. D. J. Pena, "Nephrotic syndrome and adrenal insufficiency caused by a variant in sgpl1," *Clin Kidney J*, vol. 11, no. 4, pp. 462–467, 2018.

[137] N. O'Brien, S. T. Jones, D. G. Williams, H. B. Cunningham, K. Moreno, B. Visentin, A. Gentile, J. Vekich, W. Shestowsky, M. Hiraiwa, R. Matteo, A. Cavalli, D. Grotjahn, M. Grant, G. Hansen, M. A. Campbell, and R. Sabbadini, "Production and characterization of monoclonal anti-sphingosine-1-phosphate antibodies," *J Lipid Res*, vol. 50, no. 11, pp. 2245–57, 2009.

[138] P. Zhao, G. B. Tassew, J. Y. Lee, B. Oskouian, D. P. Muñoz, J. B. Hodgin, G. L. Watson, F. Tang, J. Y. Wang, J. Luo, Y. Yang, S. King, R. M. Krauss, N. Keller, and J. D. Saba, "Efficacy of aav9-mediated sgpl1 gene transfer in a mouse model of s1p lyase insufficiency syndrome," *JCI Insight*, vol. 6, no. 8, 2021.

[139] H. Naito, T. Iba, and N. Takakura, "Mechanisms of new blood-vessel formation and proliferative heterogeneity of endothelial cells," *Int Immunol*, vol. 32, no. 5, pp. 295–305, 2020.

[140] P. Carmeliet, "Angiogenesis in health and disease," *Nat Med*, vol. 9, no. 6, pp. 653–60, 2003.

[141] S. Rafii, J. M. Butler, and B.-S. Ding, "Angiocrine functions of organ-specific endothelial cells," *Nature*, vol. 529, no. 7586, pp. 316–325, 2016.

[142] W. C. Aird, "Phenotypic heterogeneity of the endothelium: I. structure, function, and mechanisms," *Circ Res*, vol. 100, no. 2, pp. 158–73, 2007.

[143] A. Caprioli, K. Minko, C. Drevon, A. Eichmann, F. Dieterlen-Lièvre, and T. Jaffredo, "Hemangioblast commitment in the avian allantois: cellular and molecular aspects," *Dev Biol*, vol. 238, no. 1, pp. 64–78, 2001.

[144] L. Pardanaud and F. Dieterlen-Liévre, "Emergence of endothelial and hemopoietic cells in the avian embryo," *Anatomy and Embryology*, vol. 187, no. 2, pp. 107–114, 1993.

[145] S. Patel-Hett and P. A. D'Amore, "Signal transduction in vasculogenesis and developmental angiogenesis," *Int J Dev Biol*, vol. 55, no. 4-5, pp. 353–63, 2011.

[146] G. Eelen, L. Treps, X. Li, and P. Carmeliet, "Basic and therapeutic aspects of angiogenesis updated," *Circulation Research*, vol. 127, no. 2, pp. 310–329, 2020.

[147] W. Risau and V. Lemmon, “Changes in the vascular extracellular matrix during embryonic vasculogenesis and angiogenesis,” *Dev Biol*, vol. 125, no. 2, pp. 441–50, 1988.

[148] S. Isogai, N. D. Lawson, S. Torrealday, M. Horiguchi, and B. M. Weinstein, “Angiogenic network formation in the developing vertebrate trunk,” *Development*, vol. 130, no. 21, pp. 5281–5290, 2003.

[149] M. Hellström, L.-K. Phng, J. J. Hofmann, E. Wallgard, L. Coultas, P. Lindblom, J. Alva, A.-K. Nilsson, L. Karlsson, N. Gaiano, K. Yoon, J. Rossant, M. L. Iruela-Arispe, M. Kalén, H. Gerhardt, and C. Betsholtz, “Dll4 signalling through notch1 regulates formation of tip cells during angiogenesis,” *Nature*, vol. 445, no. 7129, pp. 776–780, 2007.

[150] V. Gebala, R. Collins, I. Geudens, L.-K. Phng, and H. Gerhardt, “Blood flow drives lumen formation by inverse membrane blebbing during angiogenesis in vivo,” *Nature Cell Biology*, vol. 18, no. 4, pp. 443–450, 2016.

[151] R. del Toro, C. Prahst, T. Mathivet, G. Siegfried, J. S. Kaminker, B. Larrivee, C. Breant, A. Duarte, N. Takakura, A. Fukamizu, J. Penninger, and A. Eichmann, “Identification and functional analysis of endothelial tip cell–enriched genes,” *Blood*, vol. 116, no. 19, pp. 4025–4033, 2010.

[152] T. Hla and T. Maciag, “An abundant transcript induced in differentiating human endothelial cells encodes a polypeptide with structural similarities to g-protein-coupled receptors,” *Journal of Biological Chemistry*, vol. 265, no. 16, pp. 9308–9313, 1990.

[153] M. L. Allende, T. Yamashita, and R. L. Proia, “G-protein-coupled receptor s1p1 acts within endothelial cells to regulate vascular maturation,” *Blood*, vol. 102, no. 10, pp. 3665–7, 2003.

[154] M. Kono, Y. Mi, Y. Liu, T. Sasaki, M. L. Allende, Y. P. Wu, T. Yamashita, and R. L. Proia, “The sphingosine-1-phosphate receptors s1p1, s1p2, and s1p3 function coordinately during embryonic angiogenesis,” *J Biol Chem*, vol. 279, no. 28, pp. 29367–73, 2004.

[155] S. Del Galdo, C. Vettel, D. M. Heringdorf, and T. Wieland, “The activation of rhoc in vascular endothelial cells is required for the s1p receptor type 2-induced inhibition of angiogenesis,” *Cell Signal*, vol. 25, no. 12, pp. 2478–84, 2013.

[156] J. G. Garcia, F. Liu, A. D. Verin, A. Birukova, M. A. Dechert, W. T. Gerthoffer, J. R. Bamberg, and D. English, “Sphingosine 1-phosphate promotes endothelial cell barrier integrity by edg-dependent cytoskeletal rearrangement,” *J Clin Invest*, vol. 108, no. 5, pp. 689–701, 2001.

[157] K. Gaengel, C. Niaudet, K. Hagikura, B. Laviña, L. Muhl, J. J. Hofmann, L. Ebarasi, S. Nyström, S. Rymo, L. L. Chen, M. F. Pang, Y. Jin, E. Raschperger, P. Roswall, D. Schulte, R. Benedito, J. Larsson, M. Hellström, J. Fuxe, P. Uhlén, R. Adams, L. Jakobsson, A. Majumdar, D. Vestweber, A. Uv, and C. Betsholtz, “The sphingosine-1-phosphate receptor s1pr1 restricts sprouting angiogenesis by regulating the interplay between ve-cadherin and vegfr2,” *Dev Cell*, vol. 23, no. 3, pp. 587–99, 2012.

[158] B. Jung, H. Obinata, S. Galvani, K. Mendelson, B.-s. Ding, A. Skoura, B. Kinzel, V. Brinkmann, S. Rafii, T. Evans, and T. Hla, "Flow-regulated endothelial s1p receptor-1 signaling sustains vascular development," *Developmental cell*, vol. 23, no. 3, pp. 600–610, 2012.

[159] A. Ben Shoham, G. Malkinson, S. Krief, Y. Shwartz, Y. Ely, N. Ferrara, K. Yaniv, and E. Zelzer, "S1p1 inhibits sprouting angiogenesis during vascular development," *Development*, vol. 139, no. 20, pp. 3859–69, 2012.

[160] Y. Liu, R. Wada, T. Yamashita, Y. Mi, C.-X. Deng, J. P. Hobson, H. M. Rosenfeldt, V. E. Nava, S.-S. Chae, M.-J. Lee, C. H. Liu, T. Hla, S. Spiegel, and R. L. Proia, "Edg-1, the g protein–coupled receptor for sphingosine-1-phosphate, is essential for vascular maturation," *The Journal of Clinical Investigation*, vol. 106, no. 8, pp. 951–961, 2000.

[161] L. Wang, R. Bittman, J. G. Garcia, and S. M. Dudek, "Junctional complex and focal adhesion rearrangement mediates pulmonary endothelial barrier enhancement by fty720 s-phosphonate," *Microvasc Res*, vol. 99, pp. 102–9, 2015.

[162] V. Krump-Konvalinkova, S. Yasuda, T. Rubic, N. Makarova, J. Mages, W. Erl, C. Vosseler, C. J. Kirkpatrick, G. Tigyi, and W. Siess, "Stable knock-down of the sphingosine 1-phosphate receptor s1p1 influences multiple functions of human endothelial cells," *Arterioscler Thromb Vasc Biol*, vol. 25, no. 3, pp. 546–52, 2005.

[163] T. Sanchez, A. Skoura, M. T. Wu, B. Casserly, E. O. Harrington, and T. Hla, "Induction of vascular permeability by the sphingosine-1-phosphate receptor–2 (s1p2r) and its downstream effectors rock and pten," *Arteriosclerosis, Thrombosis, and Vascular Biology*, vol. 27, no. 6, pp. 1312–1318, 2007.

[164] J. F. Lee, Q. Zeng, H. Ozaki, L. Wang, A. R. Hand, T. Hla, E. Wang, and M. J. Lee, "Dual roles of tight junction-associated protein, zonula occludens-1, in sphingosine 1-phosphate-mediated endothelial chemotaxis and barrier integrity," *J Biol Chem*, vol. 281, no. 39, pp. 29190–200, 2006.

[165] I. Singer, M. Tian, L. A. Wickham, J. Lin, S. S. Matheravidathu, M. J. Forrest, S. Mandala, and E. J. Quackenbush, "Sphingosine-1-phosphate agonists increase macrophage homing, lymphocyte contacts, and endothelial junctional complex formation in murine lymph nodes," *J Immunol*, vol. 175, no. 11, pp. 7151–61, 2005.

[166] J. H. Paik, A. Skoura, S. S. Chae, A. E. Cowan, D. K. Han, R. L. Proia, and T. Hla, "Sphingosine 1-phosphate receptor regulation of n-cadherin mediates vascular stabilization," *Genes Dev*, vol. 18, no. 19, pp. 2392–403, 2004.

[167] B. A. Wilkerson and K. M. Argraves, "The role of sphingosine-1-phosphate in endothelial barrier function," *Biochim Biophys Acta*, vol. 1841, no. 10, pp. 1403–1412, 2014.

[168] J. Jeya Paul, C. Weigel, T. Müller, R. Heller, S. Spiegel, and M. H. Gräler, "Inflammatory conditions disrupt constitutive endothelial cell barrier stabilization by alleviating autonomous secretion of sphingosine 1-phosphate," *Cells*, vol. 9, no. 4, p. 928, 2020.

[169] E. Camerer, J. B. Regard, I. Cornelissen, Y. Srinivasan, D. N. Duong, D. Palmer, T. H. Pham, J. S. Wong, R. Pappu, and S. R. Coughlin, "Sphingosine-1-phosphate in the plasma compartment regulates basal and inflammation-induced vascular leak in mice," *The Journal of Clinical Investigation*, vol. 119, no. 7, pp. 1871–1879, 2009.

[170] A. Nitzsche, M. Poittevin, A. Benarab, P. Bonnin, G. Faraco, H. Uchida, J. Favre, L. Garcia-Bonilla, M. C. Garcia, P.-L. Léger, P. Thérond, T. Mathivet, G. Autret, V. Baudrie, L. Couty, M. Kono, A. Chevallier, H. Niazi, P.-L. Tharaux, J. Chun, S. R. Schwab, A. Eichmann, B. Tavitian, R. L. Proia, C. Charriaut-Marlangue, T. Sanchez, N. Kubis, D. Henrion, C. Iadecola, T. Hla, and E. Camerer, "Endothelial s1p1 signaling counteracts infarct expansion in ischemic stroke," *Circulation Research*, vol. 128, no. 3, pp. 363–382, 2021.

[171] M. Nagahashi, S. Ramachandran, E. Y. Kim, J. C. Allegood, O. M. Rashid, A. Yamada, R. Zhao, S. Milstien, H. Zhou, S. Spiegel, and K. Takabe, "Sphingosine-1-phosphate produced by sphingosine kinase 1 promotes breast cancer progression by stimulating angiogenesis and lymphangiogenesis," *Cancer Res*, vol. 72, no. 3, pp. 726–35, 2012.

[172] V. A. Balaji Ragunathrao, M. Anwar, M. Z. Akhter, A. Chavez, Y. Mao, V. Natarajan, S. Lakshmikanthan, M. Chrzanowska-Wodnicka, A. Z. Dudek, L. Claesson-Welsh, J. K. Kitajewski, K. K. Wary, A. B. Malik, and D. Mehta, "Sphingosine-1-phosphate receptor 1 activity promotes tumor growth by amplifying vegf-vegfr2 angiogenic signaling," *Cell Rep*, vol. 29, no. 11, pp. 3472–3487.e4, 2019.

[173] S. S. Chae, J. H. Paik, H. Furneaux, and T. Hla, "Requirement for sphingosine 1-phosphate receptor-1 in tumor angiogenesis demonstrated by in vivo rna interference," *J Clin Invest*, vol. 114, no. 8, pp. 1082–9, 2004.

[174] L. Lupino, T. Perry, S. Margielewska, R. Hollows, M. Ibrahim, M. Care, J. Allegood, R. Tooze, R. Sabbadini, G. Reynolds, R. Bicknell, Z. Rudzki, Y. Lin Hock, U. Zanetto, W. Wei, W. Simmons, S. Spiegel, C. B. J. Woodman, M. Rowe, K. Vrzalikova, and P. G. Murray, "Sphingosine-1-phosphate signalling drives an angiogenic transcriptional programme in diffuse large b cell lymphoma," *Leukemia*, vol. 33, no. 12, pp. 2884–2897, 2019.

[175] W. Du, N. Takuwa, K. Yoshioka, Y. Okamoto, K. Gonda, K. Sugihara, A. Fukamizu, M. Asano, and Y. Takuwa, "S1p2, the g protein–coupled receptor for sphingosine-1-phosphate, negatively regulates tumor angiogenesis and tumor growth in vivo in mice," *Cancer Research*, vol. 70, no. 2, pp. 772–781, 2010.

[176] A. Cantalupo, A. Gargiulo, E. Dautaj, C. Liu, Y. Zhang, T. Hla, and A. Di Lorenzo, "S1pr1 (sphingosine-1-phosphate receptor 1) signaling regulates blood flow and pressure," *Hypertension*, vol. 70, no. 2, pp. 426–434, 2017.

[177] J. Igarashi and T. Michel, "Sphingosine-1-phosphate and modulation of vascular tone," *Cardiovascular Research*, vol. 82, no. 2, pp. 212–220, 2009.

[178] J. R. Nofer, M. van der Giet, M. Tölle, I. Wolinska, K. von Wnuck Lipinski, H. A. Baba, U. J. Tietge, A. Gödecke, I. Ishii, B. Kleuser, M. Schäfers, M. Fobker, W. Zidek, G. Assmann, J. Chun, and B. Levkau, "Hdl induces no-dependent vasorelaxation via the lysophospholipid receptor s1p3," *J Clin Invest*, vol. 113, no. 4, pp. 569–81, 2004.

[179] S. Salomone, E. M. Potts, S. Tyndall, P. C. Ip, J. Chun, V. Brinkmann, and C. Waeber, "Analysis of sphingosine 1-phosphate receptors involved in constriction of isolated cerebral arteries with receptor null mice and pharmacological tools," *Br J Pharmacol*, vol. 153, no. 1, pp. 140–7, 2008.

[180] B. F. Peter, D. Lidington, A. Harada, H. J. Bolz, L. Vogel, S. Heximer, S. Spiegel, U. Pohl, and S. S. Bolz, "Role of sphingosine-1-phosphate phosphohydrolase 1 in the regulation of resistance artery tone," *Circ Res*, vol. 103, no. 3, pp. 315–24, 2008.

[181] N. Ferrara, H.-P. Gerber, and J. Lecouter, "The biology of vegf and its receptors," *Nature Medicine*, vol. 9, no. 6, pp. 669–676, 2003.

[182] J. E. Park, G. A. Keller, and N. Ferrara, "The vascular endothelial growth factor (vegf) isoforms: differential deposition into the subepithelial extracellular matrix and bioactivity of extracellular matrix-bound vegf," *Mol Biol Cell*, vol. 4, no. 12, pp. 1317–26, 1993.

[183] E. Tischer, R. Mitchell, T. Hartman, M. Silva, D. Gospodarowicz, J. C. Fiddes, and J. A. Abraham, "The human gene for vascular endothelial growth factor. multiple protein forms are encoded through alternative exon splicing," *J Biol Chem*, vol. 266, no. 18, pp. 11947–54, 1991.

[184] R. S. Apte, D. S. Chen, and N. Ferrara, "Vegf in signaling and disease: Beyond discovery and development," *Cell*, vol. 176, no. 6, pp. 1248–1264, 2019.

[185] P. Carmeliet, V. Ferreira, G. Breier, S. Pollefeyt, L. Kieckens, M. Gertsenstein, M. Fahrig, A. Vandenhoeck, K. Harpal, C. Eberhardt, C. Declercq, J. Pawling, L. Moons, D. Collen, W. Risau, and A. Nagy, "Abnormal blood vessel development and lethality in embryos lacking a single vegf allele," *Nature*, vol. 380, no. 6573, pp. 435–9, 1996.

[186] N. Ferrara, K. Carver-Moore, H. Chen, M. Dowd, L. Lu, K. S. O'Shea, L. Powell-Braxton, K. J. Hillan, and M. W. Moore, "Heterozygous embryonic lethality induced by targeted inactivation of the vegf gene," *Nature*, vol. 380, no. 6573, pp. 439–42, 1996.

[187] G. H. Fong, L. Zhang, D. M. Bryce, and J. Peng, "Increased hemangioblast commitment, not vascular disorganization, is the primary defect in flt-1 knock-out mice," *Development*, vol. 126, no. 13, pp. 3015–25, 1999.

[188] Y. Sakurai, K. Ohgimoto, Y. Kataoka, N. Yoshida, and M. Shibuya, "Essential role of flk-1 (vegf receptor 2) tyrosine residue 1173 in vasculogenesis in mice," *Proceedings of the National Academy of Sciences*, vol. 102, no. 4, pp. 1076–1081, 2005.

[189] F. Shalaby, J. Rossant, T. P. Yamaguchi, M. Gertsenstein, X. F. Wu, M. L. Breitman, and A. C. Schuh, "Failure of blood-island formation and vasculogenesis in flk-1-deficient mice," *Nature*, vol. 376, no. 6535, pp. 62–6, 1995.

[190] H. Gerhardt, M. Golding, M. Fruttiger, C. Ruhrberg, A. Lundkvist, A. Abramsson, M. Jeltsch, C. Mitchell, K. Alitalo, D. Shima, and C. Betsholtz, "Vegf guides angiogenic sprouting utilizing endothelial tip cell filopodia," *J Cell Biol*, vol. 161, no. 6, pp. 1163–77, 2003.

[191] C. Ruhrberg, H. Gerhardt, M. Golding, R. Watson, S. Ioannidou, H. Fujisawa, C. Betsholtz, and D. T. Shima, "Spatially restricted patterning cues provided by heparin-binding vegf-a control blood vessel branching morphogenesis," *Genes Dev*, vol. 16, no. 20, pp. 2684–98, 2002.

[192] C. de Vries, J. A. Escobedo, H. Ueno, K. Houck, N. Ferrara, and L. T. Williams, "The fms-like tyrosine kinase, a receptor for vascular endothelial growth factor," *Science*, vol. 255, no. 5047, pp. 989–991, 1992.

[193] S. Hiratsuka, O. Minowa, J. Kuno, T. Noda, and M. Shibuya, "Flt-1 lacking the tyrosine kinase domain is sufficient for normal development and angiogenesis in mice," *Proceedings of the National Academy of Sciences*, vol. 95, no. 16, pp. 9349–9354, 1998.

[194] J. B. Kearney, C. A. Ambler, K. A. Monaco, N. Johnson, R. G. Rapoport, and V. L. Bautch, "Vascular endothelial growth factor receptor flt-1 negatively regulates developmental blood vessel formation by modulating endothelial cell division," *Blood*, vol. 99, no. 7, pp. 2397–407, 2002.

[195] J. B. Kearney, N. C. Kappas, C. Ellerstrom, F. W. DiPaola, and V. L. Bautch, "The vegf receptor flt-1 (vegfr-1) is a positive modulator of vascular sprout formation and branching morphogenesis," *Blood*, vol. 103, no. 12, pp. 4527–4535, 2004.

[196] L. Jakobsson, C. A. Franco, K. Bentley, R. T. Collins, B. Ponsioen, I. M. Aspalter, I. Rosewell, M. Busse, G. Thurston, A. Medvinsky, S. Schulte-Merker, and H. Gerhardt, "Endothelial cells dynamically compete for the tip cell position during angiogenic sprouting," *Nature Cell Biology*, vol. 12, no. 10, pp. 943–953, 2010.

[197] P. Lee, K. Goishi, A. J. Davidson, R. Mannix, L. Zon, and M. Klagsbrun, "Neuropilin-1 is required for vascular development and is a mediator of vegf-dependent angiogenesis in zebrafish," *Proc Natl Acad Sci U S A*, vol. 99, no. 16, pp. 10470–5, 2002.

[198] S. Soker, S. Takashima, H. Q. Miao, G. Neufeld, and M. Klagsbrun, "Neuropilin-1 is expressed by endothelial and tumor cells as an isoform-specific receptor for vascular endothelial growth factor," *Cell*, vol. 92, no. 6, pp. 735–45, 1998.

[199] L. E. Benjamin, D. Golijanin, A. Itin, D. Pode, and E. Keshet, "Selective ablation of immature blood vessels in established human tumors follows vascular endothelial growth factor withdrawal," *J Clin Invest*, vol. 103, no. 2, pp. 159–65, 1999.

[200] H. P. Gerber, K. J. Hillan, A. M. Ryan, J. Kowalski, G. A. Keller, L. Rangell, B. D. Wright, F. Radtke, M. Aguet, and N. Ferrara, "Vegf is required for growth and survival in neonatal mice," *Development*, vol. 126, no. 6, pp. 1149–59, 1999.

[201] I. Kim, S. O. Moon, S. H. Kim, H. J. Kim, Y. S. Koh, and G. Y. Koh, "Vascular endothelial growth factor expression of intercellular adhesion molecule 1 (icam-1), vascular cell adhesion molecule

1 (vcam-1), and e-selectin through nuclear factor-kappa b activation in endothelial cells," *J Biol Chem*, vol. 276, no. 10, pp. 7614–20, 2001.

[202] K. Shukla, H. Sonowal, A. Saxena, and K. V. Ramana, "Didymin by suppressing nf-κb activation prevents vegf-induced angiogenesis in vitro and in vivo," *Vascular Pharmacology*, vol. 115, pp. 18–25, 2019.

[203] X. Li, N. Padhan, E. O. Sjöström, F. P. Roche, C. Testini, N. Honkura, M. Sainz-Jaspeado, E. Gordon, K. Bentley, A. Philippides, V. Tolmachev, E. Dejana, R. V. Stan, D. Vestweber, K. Ballmer-Hofer, C. Betsholtz, K. Pietras, L. Jansson, and L. Claesson-Welsh, "Vegfr2 py949 signalling regulates adherens junction integrity and metastatic spread," *Nat Commun*, vol. 7, p. 11017, 2016.

[204] S. Weis, J. Cui, L. Barnes, and D. Cheresh, "Endothelial barrier disruption by vegf-mediated src activity potentiates tumor cell extravasation and metastasis," *J Cell Biol*, vol. 167, no. 2, pp. 223–9, 2004.

[205] B. Barleon, S. Sozzani, D. Zhou, H. A. Weich, A. Mantovani, and D. Marmé, "Migration of human monocytes in response to vascular endothelial growth factor (vegf) is mediated via the vegf receptor flt-1," *Blood*, vol. 87, no. 8, pp. 3336–43, 1996.

[206] M. Clauss, H. Weich, G. Breier, U. Knies, W. Röckl, J. Waltenberger, and W. Risau, "The vascular endothelial growth factor receptor flt-1 mediates biological activities. implications for a functional role of placenta growth factor in monocyte activation and chemotaxis," *J Biol Chem*, vol. 271, no. 30, pp. 17629–34, 1996.

[207] J. E. Bluff, M. W. J. Ferguson, S. O'Kane, and G. Ireland, "Bone marrow derived endothelial progenitor cells do not contribute significantly to new vessels during incisional wound healing," *Experimental Hematology*, vol. 35, no. 3, pp. 500–506, 2007.

[208] N. J. Brown, E. A. E. Smyth, S. S. Cross, and M. W. R. Reed, "Angiogenesis induction and regression in human surgical wounds," *Wound Repair and Regeneration*, vol. 10, no. 4, pp. 245–251, 2002.

[209] S. Banai, M. T. Jaklitsch, M. Shou, D. F. Lazarous, M. Scheinowitz, S. Biro, S. E. Epstein, and E. F. Unger, "Angiogenic-induced enhancement of collateral blood flow to ischemic myocardium by vascular endothelial growth factor in dogs," *Circulation*, vol. 89, no. 5, pp. 2183–9, 1994.

[210] P. Carmeliet, "Vegf as a key mediator of angiogenesis in cancer," *Oncology*, vol. 69 Suppl 3, pp. 4–10, 2005.

[211] R. S. Warren, H. Yuan, M. R. Matli, N. A. Gillett, and N. Ferrara, "Regulation by vascular endothelial growth factor of human colon cancer tumorigenesis in a mouse model of experimental liver metastasis," *J Clin Invest*, vol. 95, no. 4, pp. 1789–97, 1995.

[212] N. Ohga, S. Ishikawa, N. Maishi, K. Akiyama, Y. Hida, T. Kawamoto, Y. Sadamoto, T. Osawa, K. Yamamoto, M. Kondoh, H. Ohmura, N. Shinohara, K. Nonomura, M. Shindoh, and K. Hida,

"Heterogeneity of tumor endothelial cells: comparison between tumor endothelial cells isolated from high- and low-metastatic tumors," *Am J Pathol*, vol. 180, no. 3, pp. 1294–1307, 2012.

[213] L. Meng, Z. Fuhao, Z. Xiaoming, Z. Yuxiu, D. Zhaojun, L. Bingcheng, X. Meiling, and S. Shuyan, "Survivin is critically involved in vegfr2 signaling-mediated esophageal cancer cell survival," *Biomedicine & Pharmacotherapy*, vol. 107, pp. 139–145, 2018.

[214] P. Borgström, K. J. Hillan, P. Sriramarao, and N. Ferrara, "Complete inhibition of angiogenesis and growth of microtumors by anti-vascular endothelial growth factor neutralizing antibody: novel concepts of angiostatic therapy from intravital videomicroscopy," *Cancer Res*, vol. 56, no. 17, pp. 4032–9, 1996.

[215] F. F. Kabbinavar, J. Hambleton, R. D. Mass, H. I. Hurwitz, E. Bergsland, and S. Sarkar, "Combined analysis of efficacy: the addition of bevacizumab to fluorouracil/leucovorin improves survival for patients with metastatic colorectal cancer," *J Clin Oncol*, vol. 23, no. 16, pp. 3706–12, 2005.

[216] K. J. Kim, B. Li, J. Winer, M. Armanini, N. Gillett, H. S. Phillips, and N. Ferrara, "Inhibition of vascular endothelial growth factor-induced angiogenesis suppresses tumour growth in vivo," *Nature*, vol. 362, no. 6423, pp. 841–4, 1993.

[217] C. B. Prasad, D. Singh, L. K. Pandey, S. Pradhan, S. Singh, and G. Narayan, "Vegfa/vegfr2 autocrine and paracrine signaling promotes cervical carcinogenesis via β-catenin and snail," *The International Journal of Biochemistry & Cell Biology*, vol. 142, p. 106122, 2022.

[218] B. Clarke, "Normal bone anatomy and physiology," *Clin J Am Soc Nephrol*, vol. 3 Suppl 3, no. Suppl 3, pp. S131–9, 2008.

[219] D. J. Hadjidakis and I. I. Androulakis, "Bone remodeling," *Annals of the New York Academy of Sciences*, vol. 1092, no. 1, pp. 385–396, 2006.

[220] C.-P. Adler, *Normal Anatomy and Histology*, pp. 13–29. Berlin, Heidelberg: Springer Berlin Heidelberg, 2000.

[221] E. F. Eriksen, D. W. Axelrod, and F. Melsen, *Bone histomorphometry*. New York (N.Y.) : Raven, 1994.

[222] E. Bonucci, "Bone mineralization," *Front Biosci (Landmark Ed)*, vol. 17, no. 1, pp. 100–28, 2012.

[223] A. D. Berendsen and B. R. Olsen, "Bone development," *Bone*, vol. 80, pp. 14–18, 2015.

[224] C. Maes, T. Kobayashi, M. K. Selig, S. Torrekens, S. I. Roth, S. Mackem, G. Carmeliet, and H. M. Kronenberg, "Osteoblast precursors, but not mature osteoblasts, move into developing and fractured bones along with invading blood vessels," *Dev Cell*, vol. 19, no. 2, pp. 329–44, 2010.

[225] H. M. Kronenberg, "Developmental regulation of the growth plate," *Nature*, vol. 423, no. 6937, pp. 332–6, 2003.

[226] S. Mundlos and B. Zabel, "Developmental expression of human cartilage matrix protein," *Developmental Dynamics*, vol. 199, no. 3, pp. 241–252, 1994.

[227] P. Ducy, R. Zhang, V. Geoffroy, A. L. Ridall, and G. Karsenty, “Osf2/cbfa1: a transcriptional activator of osteoblast differentiation,” *Cell*, vol. 89, no. 5, pp. 747–54, 1997.

[228] T. Komori, H. Yagi, S. Nomura, A. Yamaguchi, K. Sasaki, K. Deguchi, Y. Shimizu, R. T. Bronson, Y. H. Gao, M. Inada, M. Sato, R. Okamoto, Y. Kitamura, S. Yoshiki, and T. Kishimoto, “Targeted disruption of cbfa1 results in a complete lack of bone formation owing to maturational arrest of osteoblasts,” *Cell*, vol. 89, no. 5, pp. 755–64, 1997.

[229] K. Nakashima, X. Zhou, G. Kunkel, Z. Zhang, J. M. Deng, R. R. Behringer, and B. de Crombrugghe, “The novel zinc finger-containing transcription factor osterix is required for osteoblast differentiation and bone formation,” *Cell*, vol. 108, no. 1, pp. 17–29, 2002.

[230] D. A. Glass, P. Bialek, J. D. Ahn, M. Starbuck, M. S. Patel, H. Clevers, M. M. Taketo, F. Long, A. P. McMahon, R. A. Lang, and G. Karsenty, “Canonical wnt signaling in differentiated osteoblasts controls osteoclast differentiation,” *Dev Cell*, vol. 8, no. 5, pp. 751–64, 2005.

[231] H. Hu, M. J. Hilton, X. Tu, K. Yu, D. M. Ornitz, and F. Long, “Sequential roles of hedgehog and wnt signaling in osteoblast development,” *Development*, vol. 132, no. 1, pp. 49–60, 2005.

[232] J. Delgado-Calle and T. Bellido, “The osteocyte as a signaling cell,” *Physiol Rev*, vol. 102, no. 1, pp. 379–410, 2022.

[233] K. Irie, S. Ejiri, Y. Sakakura, T. Shibui, and T. Yajima, “Matrix mineralization as a trigger for osteocyte maturation,” *Journal of Histochemistry & Cytochemistry*, vol. 56, no. 6, pp. 561–567, 2008.

[234] M. Hirao, J. Hashimoto, N. Yamasaki, W. Ando, H. Tsuboi, A. Myoui, and H. Yoshikawa, “Oxygen tension is an important mediator of the transformation of osteoblasts to osteocytes,” *Journal of Bone and Mineral Metabolism*, vol. 25, no. 5, pp. 266–276, 2007.

[235] M. A. Karsdal, T. A. Andersen, L. Bonewald, and C. Christiansen, “Matrix metalloproteinases (mmps) safeguard osteoblasts from apoptosis during transdifferentiation into osteocytes: Mt1-mmp maintains osteocyte viability,” *DNA Cell Biol*, vol. 23, no. 3, pp. 155–65, 2004.

[236] N. Udagawa, N. Takahashi, T. Akatsu, H. Tanaka, T. Sasaki, T. Nishihara, T. Koga, T. J. Martin, and T. Suda, “Origin of osteoclasts: mature monocytes and macrophages are capable of differentiating into osteoclasts under a suitable microenvironment prepared by bone marrow-derived stromal cells,” *Proceedings of the National Academy of Sciences*, vol. 87, no. 18, pp. 7260–7264, 1990.

[237] H. Yoshida, S. Hayashi, T. Kunisada, M. Ogawa, S. Nishikawa, H. Okamura, T. Sudo, L. D. Shultz, and S. Nishikawa, “The murine mutation osteopetrosis is in the coding region of the macrophage colony stimulating factor gene,” *Nature*, vol. 345, no. 6274, pp. 442–4, 1990.

[238] T. Miyamoto, O. Ohneda, F. Arai, K. Iwamoto, S. Okada, K. Takagi, D. M. Anderson, and T. Suda, “Bifurcation of osteoclasts and dendritic cells from common progenitors,” *Blood*, vol. 98, no. 8, pp. 2544–2554, 2001.

[239] M. M. Tondravi, S. R. McKercher, K. Anderson, J. M. Erdmann, M. Quiroz, R. Maki, and S. L. Teitelbaum, "Osteopetrosis in mice lacking haematopoietic transcription factor pu.1," *Nature*, vol. 386, no. 6620, pp. 81–84, 1997.

[240] O. H. Kwon, C.-K. Lee, Y. I. Lee, S.-G. Paik, and H.-J. Lee, "The hematopoietic transcription factor pu.1 regulates rank gene expression in myeloid progenitors," *Biochemical and Biophysical Research Communications*, vol. 335, no. 2, pp. 437–446, 2005.

[241] G. Franzoso, L. Carlson, L. Xing, L. Poljak, E. W. Shores, K. D. Brown, A. Leonardi, T. Tran, B. F. Boyce, and U. Siebenlist, "Requirement for nf-kappab in osteoclast and b-cell development," *Genes Dev*, vol. 11, no. 24, pp. 3482–96, 1997.

[242] A.-S. Hobolt-Pedersen, J.-M. Delaissé, and K. Søe, "Osteoclast fusion is based on heterogeneity between fusion partners," *Calcified Tissue International*, vol. 95, no. 1, pp. 73–82, 2014.

[243] D. L. Lacey, E. Timms, H. L. Tan, M. J. Kelley, C. R. Dunstan, T. Burgess, R. Elliott, A. Colombero, G. Elliott, S. Scully, H. Hsu, J. Sullivan, N. Hawkins, E. Davy, C. Capparelli, A. Eli, Y. X. Qian, S. Kaufman, I. Sarosi, V. Shalhoub, G. Senaldi, J. Guo, J. Delaney, and W. J. Boyle, "Osteoprotegerin ligand is a cytokine that regulates osteoclast differentiation and activation," *Cell*, vol. 93, no. 2, pp. 165–176, 1998.

[244] M. Capulli, R. Paone, and N. Rucci, "Osteoblast and osteocyte: Games without frontiers," *Archives of Biochemistry and Biophysics*, vol. 561, pp. 3–12, 2014.

[245] H. C. Anderson, "Matrix vesicles and calcification," *Current Rheumatology Reports*, vol. 5, no. 3, pp. 222–226, 2003.

[246] P. J. Bekker and C. V. Gay, "Biochemical characterization of an electrogenic vacuolar proton pump in purified chicken osteoclast plasma membrane vesicles," *Journal of Bone and Mineral Research*, vol. 5, no. 6, pp. 569–579, 1990.

[247] K. Frost, A. J. Naylor, and H. M. McGettrick, "The ying and yang of sphingosine-1-phosphate signalling within the bone," *Int J Mol Sci*, vol. 24, no. 8, 2023.

[248] A. V. Rousselle and D. Heymann, "Osteoclastic acidification pathways during bone resorption," *Bone*, vol. 30, no. 4, pp. 533–540, 2002.

[249] M. Cecchini, W. Hofstetter, J. Halasy, A. Wetterwald, and R. Felix, "Role of csf-1 in bone and bone marrow development," *Molecular Reproduction and Development*, vol. 46, no. 1, pp. 75–84, 1997.

[250] K. Fuller, J. M. Owens, C. J. Jagger, A. Wilson, R. Moss, and T. J. Chambers, "Macrophage colony-stimulating factor stimulates survival and chemotactic behavior in isolated osteoclasts," *Journal of Experimental Medicine*, vol. 178, no. 5, pp. 1733–1744, 1993.

[251] S. Tanaka, N. Takahashi, N. Udagawa, T. Tamura, T. Akatsu, E. R. Stanley, T. Kurokawa, and T. Suda, "Macrophage colony-stimulating factor is indispensable for both proliferation and

differentiation of osteoclast progenitors," *The Journal of Clinical Investigation*, vol. 91, no. 1, pp. 257–263, 1993.

[252] Y.-Y. Kong, H. Yoshida, I. Sarosi, H.-L. Tan, E. Timms, C. Capparelli, S. Morony, A. J. Oliveira-dos Santos, G. Van, A. Itie, W. Khoo, A. Wakeham, C. R. Dunstan, D. L. Lacey, T. W. Mak, W. J. Boyle, and J. M. Penninger, "Opgl is a key regulator of osteoclastogenesis, lymphocyte development and lymph-node organogenesis," *Nature*, vol. 397, no. 6717, pp. 315–323, 1999.

[253] W. S. Simonet, D. L. Lacey, C. R. Dunstan, M. Kelley, M. S. Chang, R. Lüthy, H. Q. Nguyen, S. Wooden, L. Bennett, T. Boone, G. Shimamoto, M. DeRose, R. Elliott, A. Colombero, H. L. Tan, G. Trail, J. Sullivan, E. Davy, N. Bucay, L. Renshaw-Gegg, T. M. Hughes, D. Hill, W. Pattison, P. Campbell, S. Sander, G. Van, J. Tarpley, P. Derby, R. Lee, and W. J. Boyle, "Osteoprotegerin: A novel secreted protein involved in the regulation of bone density," *Cell*, vol. 89, no. 2, pp. 309–319, 1997.

[254] H. Yasuda, N. Shima, N. Nakagawa, K. Yamaguchi, M. Kinosaki, S.-i. Mochizuki, A. Tomoyasu, K. Yano, M. Goto, A. Murakami, E. Tsuda, T. Morinaga, K. Higashio, N. Udagawa, N. Takahashi, and T. Suda, "Osteoclast differentiation factor is a ligand for osteoprotegerin/osteoclastogenesis-inhibitory factor and is identical to trance/rankl," *Proceedings of the National Academy of Sciences*, vol. 95, no. 7, pp. 3597–3602, 1998.

[255] Y. Hakeda, Y. Kobayashi, K. Yamaguchi, H. Yasuda, E. Tsuda, K. Higashio, T. Miyata, and M. Kumegawa, "Osteoclastogenesis inhibitory factor (ocif) directly inhibits bone-resorbing activity of isolated mature osteoclasts," *Biochem Biophys Res Commun*, vol. 251, no. 3, pp. 796–801, 1998.

[256] K. M. Cawley, N. C. Bustamante-Gomez, A. G. Guha, R. S. MacLeod, J. Xiong, I. Gubrij, Y. Liu, R. Mulkey, M. Palmieri, J. D. Thostenson, J. J. Goellner, and C. A. O'Brien, "Local production of osteoprotegerin by osteoblasts suppresses bone resorption," *Cell Reports*, vol. 32, no. 10, p. 108052, 2020.

[257] M. Tsukasaki, T. Asano, R. Muro, N. C.-N. Huynh, N. Komatsu, K. Okamoto, K. Nakano, T. Okamura, T. Nitta, and H. Takayanagi, "Opg production matters where it happened," *Cell Reports*, vol. 32, no. 10, p. 108124, 2020.

[258] T. Nakashima, M. Hayashi, T. Fukunaga, K. Kurata, M. Oh-hora, J. Q. Feng, L. F. Bonewald, T. Kodama, A. Wutz, E. F. Wagner, J. M. Penninger, and H. Takayanagi, "Evidence for osteocyte regulation of bone homeostasis through rankl expression," *Nature Medicine*, vol. 17, no. 10, pp. 1231–1234, 2011.

[259] J. Xiong, M. Piemontese, M. Onal, J. Campbell, J. J. Goellner, V. Dusevich, L. Bonewald, S. C. Manolagas, and C. A. O'Brien, "Osteocytes, not osteoblasts or lining cells, are the main source of the rankl required for osteoclast formation in remodeling bone," *PLOS ONE*, vol. 10, no. 9, p. e0138189, 2015.

[260] R. L. v. Bezooijen, P. t. Dijke, S. E. Papapoulos, and C. W. G.M. Löwik, “Sost/sclerostin, an osteocyte-derived negative regulator of bone formation,” *Cytokine & Growth Factor Reviews*, vol. 16, no. 3, pp. 319–327, 2005.

[261] K. E. S. Poole, R. L. Van Bezooijen, N. Loveridge, H. Hamersma, S. E. Papapoulos, C. W. Löwik, and J. Reeve, “Sclerostin is a delayed secreted product of osteocytes that inhibits bone formation,” *The FASEB Journal*, vol. 19, no. 13, pp. 1842–1844, 2005.

[262] L. Pederson, M. Ruan, J. J. Westendorf, S. Khosla, and M. J. Oursler, “Regulation of bone formation by osteoclasts involves wnt/bmp signaling and the chemokine sphingosine-1-phosphate,” *Proceedings of the National Academy of Sciences*, vol. 105, no. 52, pp. 20764–20769, 2008.

[263] E. C. Walker, N. E. McGregor, I. J. Poulton, S. Pompolo, E. H. Allan, J. M. Quinn, M. T. Gillespie, T. J. Martin, and N. A. Sims, “Cardiotrophin-1 is an osteoclast-derived stimulus of bone formation required for normal bone remodeling,” *Journal of Bone and Mineral Research*, vol. 23, no. 12, pp. 2025–2032, 2008.

[264] “Consensus development conference: Diagnosis, prophylaxis, and treatment of osteoporosis,” *The American Journal of Medicine*, vol. 94, no. 6, pp. 646–650, 1993.

[265] J. A. Kanis, C. Cooper, R. Rizzoli, and J. Y. Reginster, “European guidance for the diagnosis and management of osteoporosis in postmenopausal women,” *Osteoporos Int*, vol. 30, no. 1, pp. 3–44, 2019.

[266] J. Fuchs, C. Scheidt-Nave, and R. Kuhnert, “12-month prevalence of osteoporosis in germany,” 2017.

[267] N. Sarafrazi, E. A. Wambogo, and J. A. Shepherd, “Osteoporosis or low bone mass in older adults : United states, 2017–2018,” 2021.

[268] D. M. Black, A. V. Schwartz, K. E. Ensrud, J. A. Cauley, S. Levis, S. A. Quandt, S. Satterfield, R. B. Wallace, D. C. Bauer, L. Palermo, L. E. Wehren, A. Lombardi, A. C. Santora, S. R. Cummings, and f. t. FLEX Research Group, “Effects of continuing or stopping alendronate after 5 years of treatmentthe fracture intervention trial long-term extension (flex): A randomized trial,” *JAMA*, vol. 296, no. 24, pp. 2927–2938, 2006.

[269] P. D. Delmas, C. L. Benhamou, Z. Man, W. Tlustochowicz, E. Matzkin, R. Eusebio, J. Zanchetta, W. P. Olszynski, R. R. Recker, and M. R. McClung, “Monthly dosing of 75 mg risedronate on 2 consecutive days a month: efficacy and safety results,” *Osteoporos Int*, vol. 19, no. 7, pp. 1039–45, 2008.

[270] P. D. Miller, M. R. McClung, L. Macovei, J. A. Stakkestad, M. Luckey, B. Bonvoisin, J. Y. Reginster, R. R. Recker, C. Hughes, E. M. Lewiecki, D. Felsenberg, P. D. Delmas, D. L. Kendler, M. A. Bolognese, N. Mairon, and C. Cooper, “Monthly oral ibandronate therapy in postmenopausal osteoporosis: 1-year results from the mobile study,” *J Bone Miner Res*, vol. 20, no. 8, pp. 1315–22, 2005.

[271] I. R. Reid, A. M. Horne, B. Mihov, A. Stewart, E. Garratt, S. Wong, K. R. Wiessing, M. J. Bolland, S. Bastin, and G. D. Gamble, "Fracture prevention with zoledronate in older women with osteopenia," *New England Journal of Medicine*, vol. 379, no. 25, pp. 2407–2416, 2018.

[272] I. R. Reid, P. D. Miller, J. P. Brown, D. L. Kendler, A. Fahrleitner-Pammer, I. Valter, K. Maasalu, M. A. Bolognese, G. Woodson, H. Bone, B. Ding, R. B. Wagman, J. San Martin, M. S. Ominsky, and D. W. Dempster, "Effects of denosumab on bone histomorphometry: the freedom and stand studies," *J Bone Miner Res*, vol. 25, no. 10, pp. 2256–65, 2010.

[273] H. G. Bone, R. B. Wagman, M. L. Brandi, J. P. Brown, R. Chapurlat, S. R. Cummings, E. Czerwiński, A. Fahrleitner-Pammer, D. L. Kendler, K. Lippuner, J. Y. Reginster, C. Roux, J. Malouf, M. N. Bradley, N. S. Daizadeh, A. Wang, P. Dakin, N. Pannacciulli, D. W. Dempster, and S. Papapoulos, "10 years of denosumab treatment in postmenopausal women with osteoporosis: results from the phase 3 randomised freedom trial and open-label extension," *Lancet Diabetes Endocrinol*, vol. 5, no. 7, pp. 513–523, 2017.

[274] H. G. Bone, M. A. Bolognese, C. K. Yuen, D. L. Kendler, P. D. Miller, Y. C. Yang, L. Grazette, J. San Martin, and J. C. Gallagher, "Effects of denosumab treatment and discontinuation on bone mineral density and bone turnover markers in postmenopausal women with low bone mass," *J Clin Endocrinol Metab*, vol. 96, no. 4, pp. 972–80, 2011.

[275] B. Ettinger, D. M. Black, B. H. Mitlak, R. K. Knickerbocker, T. Nickelsen, H. K. Genant, C. Christiansen, P. D. Delmas, J. R. Zanchetta, J. Stakkestad, C. C. Glüer, K. Krueger, F. J. Cohen, S. Eckert, K. E. Ensrud, L. V. Avioli, P. Lips, and S. R. Cummings, "Reduction of vertebral fracture risk in postmenopausal women with osteoporosis treated with raloxifene: results from a 3-year randomized clinical trial. multiple outcomes of raloxifene evaluation (more) investigators," *Jama*, vol. 282, no. 7, pp. 637–45, 1999.

[276] S. R. Cummings, B. Ettinger, P. D. Delmas, P. Kenemans, V. Stathopoulos, P. Verweij, M. Mol-Arts, L. Kloosterboer, L. Mosca, C. Christiansen, J. Bilezikian, E. M. Kerzberg, S. Johnson, J. Zanchetta, D. E. Grobbee, W. Seifert, and R. Eastell, "The effects of tibolone in older postmenopausal women," *N Engl J Med*, vol. 359, no. 7, pp. 697–708, 2008.

[277] R. M. Neer, C. D. Arnaud, J. R. Zanchetta, R. Prince, G. A. Gaich, J. Y. Reginster, A. B. Hodsman, E. F. Eriksen, S. Ish-Shalom, H. K. Genant, O. Wang, and B. H. Mitlak, "Effect of parathyroid hormone (1-34) on fractures and bone mineral density in postmenopausal women with osteoporosis," *N Engl J Med*, vol. 344, no. 19, pp. 1434–41, 2001.

[278] K. G. Saag, E. Shane, S. Boonen, F. Marín, D. W. Donley, K. A. Taylor, G. P. Dalsky, and R. Marcus, "Teriparatide or alendronate in glucocorticoid-induced osteoporosis," *N Engl J Med*, vol. 357, no. 20, pp. 2028–39, 2007.

[279] R. Eastell, T. Nickelsen, F. Marin, C. Barker, P. Hadji, J. Farrerons, M. Audran, S. Boonen, K. Brixen, J. M. Gomes, B. Obermayer-Pietsch, A. Avramidis, G. Sigurdsson, and C. C. Glüer, "Sequential treatment of severe postmenopausal osteoporosis after teriparatide: final results of

the randomized, controlled european study of forsteo (eurofors)," *J Bone Miner Res*, vol. 24, no. 4, pp. 726–36, 2009.

[280] P. D. Miller, G. Hattersley, B. J. Riis, G. C. Williams, E. Lau, L. A. Russo, P. Alexandersen, C. A. Zerbini, M. Y. Hu, A. G. Harris, L. A. Fitzpatrick, F. Cosman, and C. Christiansen, "Effect of abaloparatide vs placebo on new vertebral fractures in postmenopausal women with osteoporosis: A randomized clinical trial," *Jama*, vol. 316, no. 7, pp. 722–33, 2016.

[281] M. R. McClung, A. Grauer, S. Boonen, M. A. Bolognese, J. P. Brown, A. Diez-Perez, B. L. Langdahl, J. Y. Reginster, J. R. Zanchetta, S. M. Wasserman, L. Katz, J. Maddox, Y. C. Yang, C. Libanati, and H. G. Bone, "Romosozumab in postmenopausal women with low bone mineral density," *N Engl J Med*, vol. 370, no. 5, pp. 412–20, 2014.

[282] P. Chavassieux, R. Chapurlat, N. Portero-Muzy, J. P. Roux, P. Garcia, J. P. Brown, C. Libanati, R. W. Boyce, A. Wang, and A. Grauer, "Bone-forming and antiresorptive effects of romosozumab in postmenopausal women with osteoporosis: Bone histomorphometry and microcomputed tomography analysis after 2 and 12 months of treatment," *J Bone Miner Res*, vol. 34, no. 9, pp. 1597–1608, 2019.

[283] A. Papaioannou, C. C. Kennedy, L. Dolovich, E. Lau, and J. D. Adachi, "Patient adherence to osteoporosis medications: problems, consequences and management strategies," *Drugs Aging*, vol. 24, no. 1, pp. 37–55, 2007.

[284] G. Russow, D. Jahn, J. Appelt, S. Märdian, S. Tsitsilonis, and J. Keller, "Anabolic therapies in osteoporosis and bone regeneration," *Int J Mol Sci*, vol. 20, no. 1, 2018.

[285] H. M. Kremers, M. E. Nwojo, J. E. Ransom, C. M. Wood-Wentz, L. J. I. Melton, and P. M. I. Huddleston, "Trends in the epidemiology of osteomyelitis: A population-based study, 1969 to 2009," *JBJS*, vol. 97, no. 10, pp. 837–845, 2015.

[286] E. A. Masters, B. F. Ricciardi, K. L. d. M. Bentley, T. F. Moriarty, E. M. Schwarz, and G. Muthukrishnan, "Skeletal infections: microbial pathogenesis, immunity and clinical management," *Nature Reviews Microbiology*, vol. 20, no. 7, pp. 385–400, 2022.

[287] M. Dudareva, A. J. Hotchen, J. Ferguson, S. Hodgson, M. Scarborough, B. L. Atkins, and M. A. McNally, "The microbiology of chronic osteomyelitis: Changes over ten years," *Journal of Infection*, vol. 79, no. 3, pp. 189–198, 2019.

[288] A. M. Edwards, J. R. Potts, E. Josefsson, and R. C. Massey, "Staphylococcus aureus host cell invasion and virulence in sepsis is facilitated by the multiple repeats within fnbpa," *PLOS Pathogens*, vol. 6, no. 6, p. e1000964, 2010.

[289] C. Garzoni and W. L. Kelley, "Return of the trojan horse: intracellular phenotype switching and immune evasion by staphylococcus aureus," *EMBO Molecular Medicine*, vol. 3, no. 3, pp. 115–117, 2011.

[290] S. Ahmed, S. Meghji, R. J. Williams, B. Henderson, J. H. Brock, and S. P. Nair, “Staphylococcus aureus fibronectin binding proteins are essential for internalization by osteoblasts but do not account for differences in intracellular levels of bacteria,” *Infection and Immunity*, vol. 69, no. 5, pp. 2872–2877, 2001.

[291] J. K. Ellington, M. Harris, L. Webb, B. Smith, T. Smith, K. Tan, and M. Hudson, “Intracellularstaphylococcus aureus,” *The Journal of Bone & Joint Surgery British Volume*, vol. 85-B, no. 6, pp. 918–921, 2003.

[292] D. Yang, A. R. Wijenayaka, L. B. Solomon, S. M. Pederson, D. M. Findlay, S. P. Kidd, and G. J. Atkins, “Novel insights into staphylococcus aureus deep bone infections: the involvement of osteocytes,” *mBio*, vol. 9, no. 2, pp. 10.1128/mbio.00415–18, 2018.

[293] J. Krauss, P. Roper, A. Ballard, C. Shih, J. Fitzpatrick, J. Cassat, P. Ng, N. Pavlos, and D. Veis, “Staphylococcus aureus infects osteoclasts and replicates intracellularly. mbio 10: e02447-19,” 2019.

[294] K. L. de Mesy Bentley, R. Trombetta, K. Nishitani, S. N. Bello-Irizarry, M. Ninomiya, L. Zhang, H. L. Chung, J. L. McGrath, J. L. Daiss, H. A. Awad, S. L. Kates, and E. M. Schwarz, “Evidence of staphylococcus aureus deformation, proliferation, and migration in canaliculi of live cortical bone in murine models of osteomyelitis,” *Journal of Bone and Mineral Research*, vol. 32, no. 5, pp. 985–990, 2017.

[295] K. L. de Mesy Bentley, A. MacDonald, E. M. Schwarz, and I. Oh, “Chronic osteomyelitis with staphylococcus aureus deformation in submicron canaliculi of osteocytes: A case report,” *JBJS Case Connector*, vol. 8, no. 1, p. e8, 2018.

[296] J. L. Harmer, J. Pickard, and S. J. Stinchcombe, “The role of diagnostic imaging in the evaluation of suspected osteomyelitis in the foot: a critical review,” *Foot (Edinb)*, vol. 21, no. 3, pp. 149–53, 2011.

[297] M. Arias, S. Hassan-Reshat, and W. Newsholme, “Retrospective analysis of diabetic foot osteomyelitis management and outcome at a tertiary care hospital in the uk,” *PLOS ONE*, vol. 14, no. 5, p. e0216701, 2019.

[298] M. F. Zhu, K. Kim, A. Cavadino, B. Coleman, J. T. Munro, and S. W. Young, “Success rates of debridement, antibiotics, and implant retention in 230 infected total knee arthroplasties: Implications for classification of periprosthetic joint infection,” *The Journal of Arthroplasty*, vol. 36, no. 1, pp. 305–310.e1, 2021.

[299] M. J. Bosse, H. E. Gruber, and W. K. Ramp, “Internalization of bacteria by osteoblasts in a patient with recurrent, long-term osteomyelitis: A case report,” *JBJS*, vol. 87, no. 6, pp. 1343–1347, 2005.

[300] J. M. Wagner, H. Zöllner, C. Wallner, B. Ismer, J. Schira, S. Abraham, K. Harati, M. Lehnhardt, and B. Behr, “Surgical debridement is superior to sole antibiotic therapy in a novel murine posttraumatic osteomyelitis model,” *PLOS ONE*, vol. 11, no. 2, p. e0149389, 2016.

[301] J. M. Wagner, H. Jaurich, C. Wallner, S. Abraham, M. Becerikli, M. Dadras, K. Harati, V. Duhan, V. Khairnar, M. Lehnhardt, and B. Behr, "Diminished bone regeneration after debridement of posttraumatic osteomyelitis is accompanied by altered cytokine levels, elevated b cell activity, and increased osteoclast activity," *J Orthop Res*, vol. 35, no. 11, pp. 2425–2434, 2017.

[302] M. Ishii, J. G. Egen, F. Klauschen, M. Meier-Schellersheim, Y. Saeki, J. Vacher, R. L. Proia, and R. N. Germain, "Sphingosine-1-phosphate mobilizes osteoclast precursors and regulates bone homeostasis," *Nature*, vol. 458, no. 7237, pp. 524–8, 2009.

[303] M. Ishii, J. Kikuta, Y. Shimazu, M. Meier-Schellersheim, and R. N. Germain, "Chemorepulsion by blood s1p regulates osteoclast precursor mobilization and bone remodeling in vivo," *J Exp Med*, vol. 207, no. 13, pp. 2793–8, 2010.

[304] E. Matsuzaki, S. Hiratsuka, T. Hamachi, F. Takahashi-Yanaga, Y. Hashimoto, K. Higashi, M. Kobayashi, T. Hirofuji, M. Hirata, and K. Maeda, "Sphingosine-1-phosphate promotes the nuclear translocation of β-catenin and thereby induces osteoprotegerin gene expression in osteoblast-like cell lines," *Bone*, vol. 55, no. 2, pp. 315–24, 2013.

[305] J. Kikuta, S. Kawamura, F. Okiji, M. Shirazaki, S. Sakai, H. Saito, and M. Ishii, "Sphingosine-1-phosphate-mediated osteoclast precursor monocyte migration is a critical point of control in antibone-resorptive action of active vitamin d," *Proc Natl Acad Sci U S A*, vol. 110, no. 17, pp. 7009–13, 2013.

[306] D. Tantikanlayaporn, I. L. Tourkova, Q. Larrouture, J. Luo, P. Piyachaturawat, M. R. Witt, H. C. Blair, and L. J. Robinson, "Sphingosine-1-phosphate modulates the effect of estrogen in human osteoblasts," *JBMR Plus*, vol. 2, no. 4, pp. 217–226, 2018.

[307] S. Weske, M. Vaidya, A. Reese, K. von Wnuck Lipinski, P. Keul, J. K. Bayer, J. W. Fischer, U. Flögel, J. Nelsen, M. Epple, M. Scatena, E. Schwedhelm, M. Dörr, H. Völzke, E. Moritz, A. Hannemann, B. H. Rauch, M. H. Gräler, G. Heusch, and B. Levkau, "Targeting sphingosine-1-phosphate lyase as an anabolic therapy for bone loss," *Nature Medicine*, vol. 24, no. 5, pp. 667–678, 2018.

[308] L. Brizuela, C. Martin, P. Jeannot, I. Ader, C. Gstalder, G. Andrieu, M. Bocquet, J. M. Laffosse, A. Gomez-Brouchet, B. Malavaud, R. A. Sabbadini, and O. Cuvillier, "Osteoblast-derived sphingosine 1-phosphate to induce proliferation and confer resistance to therapeutics to bone metastasis-derived prostate cancer cells," *Mol Oncol*, vol. 8, no. 7, pp. 1181–95, 2014.

[309] J. Keller, P. Catala-Lehnen, A. K. Huebner, A. Jeschke, T. Heckt, A. Lueth, M. Krause, T. Koehne, J. Albers, J. Schulze, S. Schilling, M. Haberland, H. Denninger, M. Neven, I. Hermans-Borgmeyer, T. Streichert, S. Breer, F. Barvencik, B. Levkau, B. Rathkolb, E. Wolf, J. Calzada-Wack, F. Neff, V. Gailus-Durner, H. Fuchs, M. H. de Angelis, S. Klutmann, E. Tsourdi, L. C. Hofbauer, B. Kleuser, J. Chun, T. Schinke, and M. Amling, "Calcitonin controls bone formation by inhibiting the release of sphingosine 1-phosphate from osteoclasts," *Nat Commun*, vol. 5, p. 5215, 2014.

[310] J. Ryu, H. J. Kim, E. J. Chang, H. Huang, Y. Banno, and H. H. Kim, “Sphingosine 1-phosphate as a regulator of osteoclast differentiation and osteoclast-osteoblast coupling,” *Embo j*, vol. 25, no. 24, pp. 5840–51, 2006.

[311] S. Lotinun, R. Kiviranta, T. Matsubara, J. A. Alzate, L. Neff, A. Lüth, I. Koskivirta, B. Kleuser, J. Vacher, E. Vuorio, W. C. Horne, and R. Baron, “Osteoclast-specific cathepsin k deletion stimulates s1p-dependent bone formation,” *J Clin Invest*, vol. 123, no. 2, pp. 666–81, 2013.

[312] S. J. Bae, S. H. Lee, S. H. Ahn, H. M. Kim, B. J. Kim, and J. M. Koh, “The circulating sphingosine-1-phosphate level predicts incident fracture in postmenopausal women: a 3.5-year follow-up observation study,” *Osteoporos Int*, vol. 27, no. 8, pp. 2533–41, 2016.

[313] B. J. Kim, J. M. Koh, S. Y. Lee, Y. S. Lee, S. H. Lee, K. H. Lim, E. H. Cho, S. W. Kim, T. H. Kim, S. Y. Kim, and G. S. Kim, “Plasma sphingosine 1-phosphate levels and the risk of vertebral fracture in postmenopausal women,” *J Clin Endocrinol Metab*, vol. 97, no. 10, pp. 3807–14, 2012.

[314] S. H. Lee, J. Y. Lee, K. H. Lim, Y. S. Lee, S. H. Kim, S. Choi, S. H. Cho, J. S. Kim, and J. M. Koh, “Associations of circulating levels of sphingosine 1-phosphate with the trabecular bone score and bone mineral density in postmenopausal women,” *J Clin Densitom*, vol. 24, no. 3, pp. 414–421, 2021.

[315] S. H. Lee, S. Y. Lee, Y. S. Lee, B. J. Kim, K. H. Lim, E. H. Cho, S. W. Kim, J. M. Koh, and G. S. Kim, “Higher circulating sphingosine 1-phosphate levels are associated with lower bone mineral density and higher bone resorption marker in humans,” *J Clin Endocrinol Metab*, vol. 97, no. 8, pp. E1421–8, 2012.

[316] B. J. Kim, K. O. Shin, H. Kim, S. H. Ahn, S. H. Lee, C. H. Seo, S. E. Byun, J. S. Chang, J. M. Koh, and Y. M. Lee, “The effect of sphingosine-1-phosphate on bone metabolism in humans depends on its plasma/bone marrow gradient,” *J Endocrinol Invest*, vol. 39, no. 3, pp. 297–303, 2016.

[317] J. Trueta and J. D. Morgan, “The vascular contribution to osteogenesis. i. studies by the injection method,” *J Bone Joint Surg Br*, vol. 42-b, pp. 97–109, 1960.

[318] A. P. Kusumbe, S. K. Ramasamy, and R. H. Adams, “Coupling of angiogenesis and osteogenesis by a specific vessel subtype in bone,” *Nature*, vol. 507, no. 7492, pp. 323–328, 2014.

[319] S. K. Ramasamy, A. P. Kusumbe, L. Wang, and R. H. Adams, “Endothelial notch activity promotes angiogenesis and osteogenesis in bone,” *Nature*, vol. 507, no. 7492, pp. 376–380, 2014.

[320] U. H. Langen, M. E. Pitulescu, J. M. Kim, R. Enriquez-Gasca, K. K. Sivaraj, A. P. Kusumbe, A. Singh, J. Di Russo, M. G. Bixel, B. Zhou, L. Sorokin, J. M. Vaquerizas, and R. H. Adams, “Cell-matrix signals specify bone endothelial cells during developmental osteogenesis,” *Nat Cell Biol*, vol. 19, no. 3, pp. 189–201, 2017.

[321] H. Xie, Z. Cui, L. Wang, Z. Xia, Y. Hu, L. Xian, C. Li, L. Xie, J. Crane, M. Wan, G. Zhen, Q. Bian, B. Yu, W. Chang, T. Qiu, M. Pickarski, L. T. Duong, J. J. Windle, X. Luo, E. Liao, and X. Cao, “Pdgf-bb secreted by preosteoclasts induces angiogenesis during coupling with osteogenesis,” *Nat Med*, vol. 20, no. 11, pp. 1270–8, 2014.

[322] K. Hu and B. R. Olsen, “The roles of vascular endothelial growth factor in bone repair and regeneration,” *Bone*, vol. 91, pp. 30–8, 2016.

[323] B. Huang, W. Wang, Q. Li, Z. Wang, B. Yan, Z. Zhang, L. Wang, M. Huang, C. Jia, J. Lu, S. Liu, H. Chen, M. Li, D. Cai, Y. Jiang, D. Jin, and X. Bai, “Osteoblasts secrete cxcl9 to regulate angiogenesis in bone,” *Nat Commun*, vol. 7, p. 13885, 2016.

[324] R. Xu, A. Yallowitz, A. Qin, Z. Wu, D. Y. Shin, J.-M. Kim, S. Debnath, G. Ji, M. P. Bostrom, X. Yang, C. Zhang, H. Dong, P. Kermani, S. Lalani, N. Li, Y. Liu, M. G. Poulos, A. Wach, Y. Zhang, K. Inoue, A. Di Lorenzo, B. Zhao, J. M. Butler, J.-H. Shim, L. H. Glimcher, and M. B. Greenblatt, “Targeting skeletal endothelium to ameliorate bone loss,” *Nature Medicine*, vol. 24, no. 6, pp. 823–833, 2018.

[325] M. E. Pitulescu, I. Schmidt, B. D. Giaimo, T. Antoine, F. Berkenfeld, F. Ferrante, H. Park, M. Ehling, D. Biljes, S. F. Rocha, U. H. Langen, M. Stehling, T. Nagasawa, N. Ferrara, T. Borggrefe, and R. H. Adams, “Dll4 and notch signalling couples sprouting angiogenesis and artery formation,” *Nat Cell Biol*, vol. 19, no. 8, pp. 915–927, 2017.

[326] C. Xu, V. V. Dinh, K. Kruse, H. W. Jeong, E. C. Watson, S. Adams, F. Berkenfeld, M. Stehling, S. J. Rasouli, R. Fan, R. Chen, I. Bedzhov, Q. Chen, K. Kato, M. E. Pitulescu, and R. H. Adams, “Induction of osteogenesis by bone-targeted notch activation,” *Elife*, vol. 11, 2022.

[327] E. Zelzer, W. McLean, Y. S. Ng, N. Fukai, A. M. Reginato, S. Lovejoy, P. A. D’Amore, and B. R. Olsen, “Skeletal defects in vegf(120/120) mice reveal multiple roles for vegf in skeletogenesis,” *Development*, vol. 129, no. 8, pp. 1893–904, 2002.

[328] H. P. Gerber, T. H. Vu, A. M. Ryan, J. Kowalski, Z. Werb, and N. Ferrara, “Vegf couples hypertrophic cartilage remodeling, ossification and angiogenesis during endochondral bone formation,” *Nat Med*, vol. 5, no. 6, pp. 623–8, 1999.

[329] E. Zelzer, R. Mamluk, N. Ferrara, R. S. Johnson, E. Schipani, and B. R. Olsen, “Vegfa is necessary for chondrocyte survival during bone development,” *Development*, vol. 131, no. 9, pp. 2161–71, 2004.

[330] A. B. Rabie, L. Shum, and A. Chayanupatkul, “Vegf and bone formation in the glenoid fossa during forward mandibular positioning,” *Am J Orthod Dentofacial Orthop*, vol. 122, no. 2, pp. 202–9, 2002.

[331] J. Fiedler, F. Leucht, J. Waltenberger, C. Dehio, and R. E. Brenner, “Vegf-a and plgf-1 stimulate chemotactic migration of human mesenchymal progenitor cells,” *Biochem Biophys Res Commun*, vol. 334, no. 2, pp. 561–8, 2005.

[332] U. Mayr-Wohlfart, J. Waltenberger, H. Hausser, S. Kessler, K. P. Günther, C. Dehio, W. Puhl, and R. E. Brenner, “Vascular endothelial growth factor stimulates chemotactic migration of primary human osteoblasts,” *Bone*, vol. 30, no. 3, pp. 472–7, 2002.

[333] M. M. Deckers, M. Karperien, C. van der Bent, T. Yamashita, S. E. Papapoulos, and C. W. Löwik, "Expression of vascular endothelial growth factors and their receptors during osteoblast differentiation," *Endocrinology*, vol. 141, no. 5, pp. 1667–74, 2000.

[334] Y. S. Hah, J. S. Jun, S. G. Lee, B. W. Park, D. R. Kim, U. K. Kim, J. R. Kim, and J. H. Byun, "Vascular endothelial growth factor stimulates osteoblastic differentiation of cultured human periosteal-derived cells expressing vascular endothelial growth factor receptors," *Mol Biol Rep*, vol. 38, no. 2, pp. 1443–50, 2011.

[335] K. Hu and B. R. Olsen, "Osteoblast-derived vegf regulates osteoblast differentiation and bone formation during bone repair," *J Clin Invest*, vol. 126, no. 2, pp. 509–26, 2016.

[336] Y. Liu, A. D. Berendsen, S. Jia, S. Lotinun, R. Baron, N. Ferrara, and B. R. Olsen, "Intracellular vegf regulates the balance between osteoblast and adipocyte differentiation," *J Clin Invest*, vol. 122, no. 9, pp. 3101–13, 2012.

[337] X. Duan, S. R. Bradbury, B. R. Olsen, and A. D. Berendsen, "Vegf stimulates intramembranous bone formation during craniofacial skeletal development," *Matrix Biol*, vol. 52-54, pp. 127–140, 2016.

[338] M. Nakagawa, T. Kaneda, T. Arakawa, S. Morita, T. Sato, T. Yomada, K. Hanada, M. Kumegawa, and Y. Hakeda, "Vascular endothelial growth factor (vegf) directly enhances osteoclastic bone resorption and survival of mature osteoclasts," *FEBS Lett*, vol. 473, no. 2, pp. 161–4, 2000.

[339] J. K. Min, Y. M. Kim, Y. M. Kim, E. C. Kim, Y. S. Gho, I. J. Kang, S. Y. Lee, Y. Y. Kong, and Y. G. Kwon, "Vascular endothelial growth factor up-regulates expression of receptor activator of nf-kappa b (rank) in endothelial cells. concomitant increase of angiogenic responses to rank ligand," *J Biol Chem*, vol. 278, no. 41, pp. 39548–57, 2003.

[340] S. Yao, D. Liu, F. Pan, and G. E. Wise, "Effect of vascular endothelial growth factor on rank gene expression in osteoclast precursors and on osteoclastogenesis," *Arch Oral Biol*, vol. 51, no. 7, pp. 596–602, 2006.

[341] F. Geiger, H. Bertram, I. Berger, H. Lorenz, O. Wall, C. Eckhardt, H. G. Simank, and W. Richter, "Vascular endothelial growth factor gene-activated matrix (vegf165-gam) enhances osteogenesis and angiogenesis in large segmental bone defects," *J Bone Miner Res*, vol. 20, no. 11, pp. 2028–35, 2005.

[342] R. Li, D. J. Stewart, H. P. von Schroeder, E. S. Mackinnon, and E. H. Schemitsch, "Effect of cell-based vegf gene therapy on healing of a segmental bone defect," *J Orthop Res*, vol. 27, no. 1, pp. 8–14, 2009.

[343] J. Street, M. Bao, L. deGuzman, S. Bunting, F. V. Peale, N. Ferrara, H. Steinmetz, J. Hoeffel, J. L. Cleland, A. Daugherty, N. van Bruggen, H. P. Redmond, R. A. D. Carano, and E. H. Filvaroff, "Vascular endothelial growth factor stimulates bone repair by promoting angiogenesis and bone turnover," *Proceedings of the National Academy of Sciences*, vol. 99, no. 15, pp. 9656–9661, 2002.

[344] Q. Zhao, X. Shen, W. Zhang, G. Zhu, J. Qi, and L. Deng, “Mice with increased angiogenesis and osteogenesis due to conditional activation of hif pathway in osteoblasts are protected from ovariectomy induced bone loss,” *Bone*, vol. 50, no. 3, pp. 763–770, 2012.

[345] Z. Yao, M. H. Lafage-Proust, J. Plouët, S. Bloomfield, C. Alexandre, and L. Vico, “Increase of both angiogenesis and bone mass in response to exercise depends on vegf,” *J Bone Miner Res*, vol. 19, no. 9, pp. 1471–80, 2004.

[346] H. Cebi, E. Akşahin, H. Y. Yüksel, L. Celebi, C. N. Aktekin, O. Hapa, H. H. Muratli, and A. Biçimoğlu, “Plasma vascular endothelial growth factor levels are similar in subjects with and without osteoporosis,” *Eklem Hastalik Cerrahisi*, vol. 21, no. 2, pp. 91–7, 2010.

[347] N. Costa, S. Paramanathan, D. Mac Donald, A. S. Wierzbicki, and G. Hampson, “Factors regulating circulating vascular endothelial growth factor (vegf): association with bone mineral density (bmd) in post-menopausal osteoporosis,” *Cytokine*, vol. 46, no. 3, pp. 376–81, 2009.

[348] K. Senel, T. Baykal, B. Seferoglu, E. U. Altas, F. Baygutalp, M. Ugur, and A. Kiziltunc, “Circulating vascular endothelial growth factor concentrations in patients with postmenopausal osteoporosis,” *Arch Med Sci*, vol. 9, no. 4, pp. 709–12, 2013.

[349] M. E. Nasser, H. F. Khaled, E. A. Kaddah, A. M. Elbadrawy, S. M. Mahdi, and M. A. Sharobeem, “Role of vascular endothelial growth factor expression in pathogenesis of postmenopausal osteoporosis,” *Egyptian Rheumatology and Rehabilitation*, vol. 40, no. 4, pp. 211–223, 2013.

[350] J. Schindelin, I. Arganda-Carreras, E. Frise, V. Kaynig, M. Longair, T. Pietzsch, S. Preibisch, C. Rueden, S. Saalfeld, B. Schmid, J. Y. Tinevez, D. J. White, V. Hartenstein, K. Eliceiri, P. Tomancak, and A. Cardona, “Fiji: an open-source platform for biological-image analysis,” *Nat Methods*, vol. 9, no. 7, pp. 676–82, 2012.

[351] A. Billich, T. Baumruker, C. Beerli, M. Bigaud, C. Bruns, T. Calzascia, A. Isken, B. Kinzel, E. Loetscher, B. Metzler, M. Mueller, B. Nuesslein-Hildesheim, and B. Kleylein-Sohn, “Partial deficiency of sphingosine-1-phosphate lyase confers protection in experimental autoimmune encephalomyelitis,” *PLOS ONE*, vol. 8, no. 3, p. e59630, 2013.

[352] I. Ishii, X. Ye, B. Friedman, S. Kawamura, J. J. Contos, M. A. Kingsbury, A. H. Yang, G. Zhang, J. H. Brown, and J. Chun, “Marked perinatal lethality and cellular signaling deficits in mice null for the two sphingosine 1-phosphate (s1p) receptors, s1p(2)/lp(b2)/edg-5 and s1p(3)/lp(b3)/edg-3,” *J Biol Chem*, vol. 277, no. 28, pp. 25152–9, 2002.

[353] H. Declercq, N. Van den Vreken, E. De Maeyer, R. Verbeeck, E. Schacht, L. De Ridder, and M. Cornelissen, “Isolation, proliferation and differentiation of osteoblastic cells to study cell/biomaterial interactions: comparison of different isolation techniques and source,” *Biomaterials*, vol. 25, no. 5, pp. 757–768, 2004.

[354] K. J. Livak and T. D. Schmittgen, “Analysis of relative gene expression data using real-time quantitative pcr and the $2^{-\Delta\Delta CT}$ method,” *Methods*, vol. 25, no. 4, pp. 402–408, 2001.

[355] T. D. Schmittgen and K. J. Livak, “Analyzing real-time pcr data by the comparative ct method,” *Nature Protocols*, vol. 3, no. 6, pp. 1101–1108, 2008.

[356] M. L. Bouxsein, S. K. Boyd, B. A. Christiansen, R. E. Guldberg, K. J. Jepsen, and R. Müller, “Guidelines for assessment of bone microstructure in rodents using micro-computed tomography,” *J Bone Miner Res*, vol. 25, no. 7, pp. 1468–86, 2010.

[357] T. Kawamoto and K. Kawamoto, “Preparation of thin frozen sections from nonfixed and undecalcified hard tissues using kawamoto’s film method (2020),” *Methods Mol Biol*, vol. 2230, pp. 259–281, 2021.

[358] B. Behr, P. Leucht, M. T. Longaker, and N. Quarto, “Fgf-9 is required for angiogenesis and osteogenesis in long bone repair,” *Proc Natl Acad Sci U S A*, vol. 107, no. 26, pp. 11853–8, 2010.

[359] L. Lu, D. Saha, R. L. Martuza, S. D. Rabkin, and H. Wakimoto, “Single agent efficacy of the vegfr kinase inhibitor axitinib in preclinical models of glioblastoma,” *J Neurooncol*, vol. 121, no. 1, pp. 91–100, 2015.

[360] M. A. Chellaiah and K. A. Hruska, “The integrin alpha(v)beta(3) and cd44 regulate the actions of osteopontin on osteoclast motility,” *Calcif Tissue Int*, vol. 72, no. 3, pp. 197–205, 2003.

[361] A. M. Delany, M. Amling, M. Priemel, C. Howe, R. Baron, and E. Canalis, “Osteopenia and decreased bone formation in osteonectin-deficient mice,” *J Clin Invest*, vol. 105, no. 7, pp. 915–23, 2000.

[362] J. Sodek, J. Chen, T. Nagata, S. Kasuhai, R. Todescan JR., I. W. S. Li, and R. H. Kim, “Regulation of osteopontin expression in osteoblasts,” *Annals of the New York Academy of Sciences*, vol. 760, no. 1, pp. 223–241, 1995.

[363] X. Zhou, Z. Zhang, J. Q. Feng, V. M. Dusevich, K. Sinha, H. Zhang, B. G. Darnay, and B. de Crombrugghe, “Multiple functions of osterix are required for bone growth and homeostasis in postnatal mice,” *Proceedings of the National Academy of Sciences*, vol. 107, no. 29, pp. 12919–12924, 2010.

[364] S. K. Ramasamy, A. P. Kusumbe, T. Itkin, S. Gur-Cohen, T. Lapidot, and R. H. Adams, “Regulation of hematopoiesis and osteogenesis by blood vessel-derived signals,” *Annu Rev Cell Dev Biol*, vol. 32, pp. 649–675, 2016.

[365] S. Weske, M. Vaidya, K. von Wnuck Lipinski, P. Keul, K. Manthe, C. Burkhart, G. Haberhauer, G. Heusch, and B. Levkau, “Agonist-induced activation of the s1p receptor 2 constitutes a novel osteoanabolic therapy for the treatment of osteoporosis in mice,” *Bone*, vol. 125, pp. 1–7, 2019.

[366] R. Dziak, B. M. Yang, B. W. Leung, S. Li, N. Marzec, J. Margarone, and L. Bobek, “Effects of sphingosine-1-phosphate and lysophosphatidic acid on human osteoblastic cells,” *Prostaglandins Leukot Essent Fatty Acids*, vol. 68, no. 3, pp. 239–49, 2003.

[367] A. Grey, X. Xu, B. Hill, M. Watson, K. Callon, I. R. Reid, and J. Cornish, “Osteoblastic cells express phospholipid receptors and phosphatases and proliferate in response to sphingosine-1-phosphate,” *Calcif Tissue Int*, vol. 74, no. 6, pp. 542–50, 2004.

[368] A. Grey, Q. Chen, K. Callon, X. Xu, I. R. Reid, and J. Cornish, “The phospholipids sphingosine-1-phosphate and lysophosphatidic acid prevent apoptosis in osteoblastic cells via a signaling pathway involving gi proteins and phosphatidylinositol-3 kinase,” *Endocrinology*, vol. 143, no. 12, pp. 4755–4763, 2002.

[369] T. Roelofsen, R. Akkers, W. Beumer, M. Apotheker, I. Steeghs, J. van de Ven, C. Gelderblom, A. Garritsen, and K. Dechering, “Sphingosine-1-phosphate acts as a developmental stage specific inhibitor of platelet-derived growth factor-induced chemotaxis of osteoblasts,” *J Cell Biochem*, vol. 105, no. 4, pp. 1128–38, 2008.

[370] G. Osterhoff, E. F. Morgan, S. J. Shefelbine, L. Karim, L. M. McNamara, and P. Augat, “Bone mechanical properties and changes with osteoporosis,” *Injury*, 2016.

[371] J. Rittweger, B. Simunic, G. Bilancio, N. G. De Santo, M. Cirillo, G. Biolo, R. Pisot, O. Eiken, I. B. Mekjavic, and M. Narici, “Bone loss in the lower leg during 35 days of bed rest is predominantly from the cortical compartment,” *Bone*, vol. 44, no. 4, pp. 612–8, 2009.

[372] R. J. Tower, G. M. Campbell, M. Müller, C. C. Glüer, and S. Tiwari, “Utilizing time-lapse micro-ct-correlated bisphosphonate binding kinetics and soft tissue-derived input functions to differentiate site-specific changes in bone metabolism in vivo,” *Bone*, vol. 74, pp. 171–81, 2015.

[373] X. Tong, I. S. Burton, H. Isaksson, J. S. Jurvelin, and H. Kröger, “Cortical bone histomorphometry in male femoral neck: the investigation of age-association and regional differences,” *Calcif Tissue Int*, vol. 96, no. 4, pp. 295–306, 2015.

[374] R. M. D. Zebaze, A. Ghasem-Zadeh, A. Bohte, S. Iuliano-Burns, M. Mirams, R. I. Price, E. J. Mackie, and E. Seeman, “Intracortical remodelling and porosity in the distal radius and post-mortem femurs of women: a cross-sectional study,” *The Lancet*, vol. 375, no. 9727, pp. 1729–1736, 2010.

[375] A. Bjørnerem, A. Ghasem-Zadeh, M. Bui, X. Wang, C. Rantzau, T. V. Nguyen, J. L. Hopper, R. Zebaze, and E. Seeman, “Remodeling markers are associated with larger intracortical surface area but smaller trabecular surface area: a twin study,” *Bone*, vol. 49, no. 6, pp. 1125–30, 2011.

[376] E. Seeman, “Age- and menopause-related bone loss compromise cortical and trabecular microstructure,” *J Gerontol A Biol Sci Med Sci*, vol. 68, no. 10, pp. 1218–25, 2013.

[377] B. M. Willie, A. I. Birkhold, H. Razi, T. Thiele, M. Aido, B. Kruck, A. Schill, S. Checa, R. P. Main, and G. N. Duda, “Diminished response to in vivo mechanical loading in trabecular and not cortical bone in adulthood of female c57bl/6 mice coincides with a reduction in deformation to load,” *Bone*, vol. 55, no. 2, pp. 335–46, 2013.

[378] A. M. Weatherholt, R. K. Fuchs, and S. J. Warden, “Cortical and trabecular bone adaptation to incremental load magnitudes using the mouse tibial axial compression loading model,” *Bone*, vol. 52, no. 1, pp. 372–9, 2013.

[379] A. J. Burghardt, G. J. Kazakia, M. Sode, A. E. de Papp, T. M. Link, and S. Majumdar, “A longitudinal hr-pqct study of alendronate treatment in postmenopausal women with low bone density: Relations among density, cortical and trabecular microarchitecture, biomechanics, and bone turnover,” *J Bone Miner Res*, vol. 25, no. 12, pp. 2558–71, 2010.

[380] E. Seeman, P. D. Delmas, D. A. Hanley, D. Sellmeyer, A. M. Cheung, E. Shane, A. Kearns, T. Thomas, S. K. Boyd, S. Boutroy, C. Bogado, S. Majumdar, M. Fan, C. Libanati, and J. Zanchetta, “Microarchitectural deterioration of cortical and trabecular bone: differing effects of denosumab and alendronate,” *J Bone Miner Res*, vol. 25, no. 8, pp. 1886–94, 2010.

[381] S. Hansen, E. M. Hauge, J. E. Beck Jensen, and K. Brixen, “Differing effects of pth 1-34, pth 1-84, and zoledronic acid on bone microarchitecture and estimated strength in postmenopausal women with osteoporosis: an 18-month open-labeled observational study using hr-pqct,” *J Bone Miner Res*, vol. 28, no. 4, pp. 736–45, 2013.

[382] H. M. Macdonald, K. K. Nishiyama, D. A. Hanley, and S. K. Boyd, “Changes in trabecular and cortical bone microarchitecture at peripheral sites associated with 18 months of teriparatide therapy in postmenopausal women with osteoporosis,” *Osteoporos Int*, vol. 22, no. 1, pp. 357–62, 2011.

[383] T. Heckt, L. J. Brylka, M. Neven, M. Amling, and T. Schinke, “Deficiency of sphingosine-1-phosphate receptor 3 does not affect the skeletal phenotype of mice lacking sphingosine-1-phosphate lyase,” *PLOS ONE*, vol. 14, no. 7, p. e0219734, 2019.

[384] J. A. McKenzie, I. M. Galbreath, A. F. Coello, K. R. Hixon, and M. J. Silva, “Vegfa from osteoblasts is not required for lamellar bone formation following tibial loading,” *Bone*, vol. 163, p. 116502, 2022.

[385] P. Quint, M. Ruan, L. Pederson, M. Kassem, J. J. Westendorf, S. Khosla, and M. J. Oursler, “Sphingosine 1-phosphate (s1p) receptors 1 and 2 coordinately induce mesenchymal cell migration through s1p activation of complementary kinase pathways,” *J Biol Chem*, vol. 288, no. 8, pp. 5398–406, 2013.

[386] A. Chandra and J. Rajawat, “Skeletal aging and osteoporosis: Mechanisms and therapeutics,” *Int J Mol Sci*, vol. 22, no. 7, 2021.

[387] C. Huang, R. Ling, F. J. Li, E. C. Li, Q. K. Huang, B. G. Liu, Y. Ding, and S. W. You, “Fty720 enhances osteogenic differentiation of bone marrow mesenchymal stem cells in ovariectomized rats,” *Mol Med Rep*, vol. 14, no. 1, pp. 927–35, 2016.

[388] C. Chen, S. Zong, Z. Wang, R. Yang, Y. Guo, Y. Wang, X. Chen, Y. Li, and S. Wang, “Fty720 attenuates lps-induced inflammatory bone loss by inhibiting osteoclastogenesis via the nf-κb and hdac4/atf pathways,” *J Immunol Res*, vol. 2023, p. 8571649, 2023.

[389] J. Babor, A. Tramonti, C. Nardella, A. Deutschbauer, R. Contestabile, and V. de Crecy-Lagard, "4´-deoxypyridoxine disrupts vitamin b6 homeostasis in escherichia coli k12 through combined inhibition of cumulative b6 uptake and plp-dependent enzyme activity," *Microbiology*, vol. 169, no. 4, 2023.

[390] T. A. Scott and R. C. Hockney, "Synthesis of vitamin b6 by a mutant of escherichia coli k12 and the action of 4´-deoxypyridoxine," *Microbiology*, vol. 110, no. 2, pp. 285–289, 1979.

[391] K. Heo, K. A. Park, Y. H. Kim, S. H. Kim, Y. S. Oh, I. H. Kim, S. H. Ryu, and P. G. Suh, "Sphingosine 1-phosphate induces vascular endothelial growth factor expression in endothelial cells," *BMB Rep*, vol. 42, no. 10, pp. 685–90, 2009.

[392] C. C. Huang, T. T. Tseng, S. C. Liu, Y. Y. Lin, Y. Y. Law, S. L. Hu, S. W. Wang, C. H. Tsai, and C. H. Tang, "S1p increases vegf production in osteoblasts and facilitates endothelial progenitor cell angiogenesis by inhibiting mir-16-5p expression via the c-src/fak signaling pathway in rheumatoid arthritis," *Cells*, vol. 10, no. 8, 2021.

[393] H. Wang, K. Y. Cai, W. Li, and H. Huang, "Sphingosine-1-phosphate induces the migration and angiogenesis of epcs through the akt signaling pathway via sphingosine-1-phosphate receptor 3/platelet-derived growth factor receptor-β," *Cell Mol Biol Lett*, vol. 20, no. 4, pp. 597–611, 2015.

[394] U. Helmrich, N. Di Maggio, S. Güven, E. Groppa, L. Melly, R. D. Largo, M. Heberer, I. Martin, A. Scherberich, and A. Banfi, "Osteogenic graft vascularization and bone resorption by vegf-expressing human mesenchymal progenitors," *Biomaterials*, vol. 34, no. 21, pp. 5025–35, 2013.

[395] G. Bluteau, M. Julien, D. Magne, F. Mallein-Gerin, P. Weiss, G. Daculsi, and J. Guicheux, "Vegf and vegf receptors are differentially expressed in chondrocytes," *Bone*, vol. 40, no. 3, pp. 568–76, 2007.

[396] A. Grosso, A. Lunger, M. G. Burger, P. S. Briquez, F. Mai, J. A. Hubbell, D. J. Schaefer, A. Banfi, and N. Di Maggio, "Vegf dose controls the coupling of angiogenesis and osteogenesis in engineered bone," *NPJ Regen Med*, vol. 8, no. 1, p. 15, 2023.

[397] L. Wang, F. Zhou, P. Zhang, H. Wang, Z. Qu, P. Jia, Z. Yao, G. Shen, G. Li, G. Zhao, J. Li, Y. Mao, Z. Xie, W. Xu, Y. Xu, and Y. Xu, "Human type h vessels are a sensitive biomarker of bone mass," *Cell Death & Disease*, vol. 8, no. 5, pp. e2760–e2760, 2017.

[398] S. Li, C. Song, S. Yang, W. Yu, W. Zhang, G. Zhang, Z. Xi, and E. Lu, "Supercritical co(2) foamed composite scaffolds incorporating bioactive lipids promote vascularized bone regeneration via hif-1α upregulation and enhanced type h vessel formation," *Acta Biomater*, vol. 94, pp. 253–267, 2019.

[399] A. P. Kusumbe and R. H. Adams, "Osteoclast progenitors promote bone vascularization and osteogenesis," *Nat Med*, vol. 20, no. 11, pp. 1238–40, 2014.

[400] K. Inomata and M. Honda, “Co-culture of osteoblasts and endothelial cells on a microfiber scaffold to construct bone-like tissue with vascular networks,” *Materials (Basel)*, vol. 12, no. 18, 2019.

[401] C. Xu, H. Liu, Y. He, Y. Li, and X. He, “Endothelial progenitor cells promote osteogenic differentiation in co-cultured with mesenchymal stem cells via the mapk-dependent pathway,” *Stem Cell Research & Therapy*, vol. 11, no. 1, p. 537, 2020.

[402] D. P. Herzog, E. Dohle, I. Bischoff, and C. J. Kirkpatrick, “Cell communication in a coculture system consisting of outgrowth endothelial cells and primary osteoblasts,” *Biomed Res Int*, vol. 2014, p. 320123, 2014.

[403] M. Marenzana and T. R. Arnett, “The key role of the blood supply to bone,” *Bone Res*, vol. 1, no. 3, pp. 203–15, 2013.

[404] M. K. Pugsley and R. Tabrizchi, “The vascular system: An overview of structure and function,” *Journal of Pharmacological and Toxicological Methods*, vol. 44, no. 2, pp. 333–340, 2000.

[405] G. Z. Eghbali-Fatourechi, J. Lamsam, D. Fraser, D. Nagel, B. L. Riggs, and S. Khosla, “Circulating osteoblast-lineage cells in humans,” *N Engl J Med*, vol. 352, no. 19, pp. 1959–66, 2005.

[406] S. K. Ramasamy, A. P. Kusumbe, M. Schiller, D. Zeuschner, M. G. Bixel, C. Milia, J. Gamrekelashvili, A. Limbourg, A. Medvinsky, M. M. Santoro, F. P. Limbourg, and R. H. Adams, “Blood flow controls bone vascular function and osteogenesis,” *Nature Communications*, vol. 7, no. 1, p. 13601, 2016.

[407] N. Hirata, S. Yamada, T. Shoda, M. Kurihara, Y. Sekino, and Y. Kanda, “Sphingosine-1-phosphate promotes expansion of cancer stem cells via s1pr3 by a ligand-independent notch activation,” *Nature Communications*, vol. 5, no. 1, p. 4806, 2014.

[408] A. Akil, A. K. Gutiérrez-García, R. Guenter, J. B. Rose, A. W. Beck, H. Chen, and B. Ren, “Notch signaling in vascular endothelial cells, angiogenesis, and tumor progression: An update and prospective,” *Frontiers in Cell and Developmental Biology*, vol. 9, 2021.

[409] M. Noseda, L. Chang, G. McLean, J. E. Grim, B. E. Clurman, L. L. Smith, and A. Karsan, “Notch activation induces endothelial cell cycle arrest and participates in contact inhibition: role of p21cip1 repression,” *Mol Cell Biol*, vol. 24, no. 20, pp. 8813–22, 2004.

[410] R. Benedito, C. Roca, I. Sörensen, S. Adams, A. Gossler, M. Fruttiger, and R. H. Adams, “The notch ligands dll4 and jagged1 have opposing effects on angiogenesis,” *Cell*, vol. 137, no. 6, pp. 1124–35, 2009.

[411] A. Trindade, S. R. Kumar, J. S. Scehnet, L. Lopes-da Costa, J. Becker, W. Jiang, R. Liu, P. S. Gill, and A. Duarte, “Overexpression of delta-like 4 induces arterialization and attenuates vessel formation in developing mouse embryos,” *Blood*, vol. 112, no. 5, pp. 1720–9, 2008.

[412] L. S. Harrington, R. C. A. Sainson, C. K. Williams, J. M. Taylor, W. Shi, J.-L. Li, and A. L. Harris, "Regulation of multiple angiogenic pathways by dll4 and notch in human umbilical vein endothelial cells," *Microvascular Research*, vol. 75, no. 2, pp. 144–154, 2008.

[413] M.-J. Goumans, Z. Liu, and P. ten Dijke, "Tgf-β signaling in vascular biology and dysfunction," *Cell Research*, vol. 19, no. 1, pp. 116–127, 2009.

[414] M. J. Goumans, G. Valdimarsdottir, S. Itoh, A. Rosendahl, P. Sideras, and P. ten Dijke, "Balancing the activation state of the endothelium via two distinct tgf-beta type i receptors," *Embo j*, vol. 21, no. 7, pp. 1743–53, 2002.

[415] S. P. Oh, T. Seki, K. A. Goss, T. Imamura, Y. Yi, P. K. Donahoe, L. Li, K. Miyazono, P. ten Dijke, S. Kim, and E. Li, "Activin receptor-like kinase 1 modulates transforming growth factor-beta 1 signaling in the regulation of angiogenesis," *Proc Natl Acad Sci U S A*, vol. 97, no. 6, pp. 2626–31, 2000.

[416] M. Oshima, H. Oshima, and M. M. Taketo, "Tgf-beta receptor type ii deficiency results in defects of yolk sac hematopoiesis and vasculogenesis," *Dev Biol*, vol. 179, no. 1, pp. 297–302, 1996.

[417] M. J. Goumans, G. Valdimarsdottir, S. Itoh, F. Lebrin, J. Larsson, C. Mummery, S. Karlsson, and P. ten Dijke, "Activin receptor-like kinase (alk)1 is an antagonistic mediator of lateral tgfbeta/alk5 signaling," *Mol Cell*, vol. 12, no. 4, pp. 817–28, 2003.

[418] C. Mallet, D. Vittet, J. J. Feige, and S. Bailly, "Tgfbeta1 induces vasculogenesis and inhibits angiogenic sprouting in an embryonic stem cell differentiation model: respective contribution of alk1 and alk5," *Stem Cells*, vol. 24, no. 11, pp. 2420–7, 2006.

[419] Y. Suzuki, K. Montagne, A. Nishihara, T. Watabe, and K. Miyazono, "Bmps promote proliferation and migration of endothelial cells via stimulation of vegf-a/vegfr2 and angiopoietin-1/tie2 signalling," *J Biochem*, vol. 143, no. 2, pp. 199–206, 2008.

[420] L. David, C. Mallet, M. Keramidas, N. Lamandé, J. M. Gasc, S. Dupuis-Girod, H. Plauchu, J. J. Feige, and S. Bailly, "Bone morphogenetic protein-9 is a circulating vascular quiescence factor," *Circ Res*, vol. 102, no. 8, pp. 914–22, 2008.

[421] C. Xin, S. Ren, B. Kleuser, S. Shabahang, W. Eberhardt, H. Radeke, M. Schäfer-Korting, J. Pfeilschifter, and A. Huwiler, "Sphingosine 1-phosphate cross-activates the smad signaling cascade and mimics transforming growth factor-β-induced cell responses," *Journal of Biological Chemistry*, vol. 279, no. 34, pp. 35255–35262, 2004.

[422] B. Wang, N. Dong, D. Wu, Y. Fang, J. Chen, Y. Lin, S. Bellusci, J. S. Zhang, K. Dai, and C. Chen, "Sphingosine 1-phosphate receptor 1 governs endothelial barrier function and angiogenesis by upregulating endoglin signaling," *Ann Transl Med*, vol. 10, no. 3, p. 136, 2022.

[423] K. Avery, S. Avery, J. Shepherd, P. R. Heath, and H. Moore, "Sphingosine-1-phosphate mediates transcriptional regulation of key targets associated with survival, proliferation, and pluripotency in human embryonic stem cells," *Stem Cells Dev*, vol. 17, no. 6, pp. 1195–205, 2008.

[424] M. Antoine, W. Wirz, C. G. Tag, M. Mavituna, N. Emans, T. Korff, V. Stoldt, A. M. Gressner, and P. Kiefer, "Expression pattern of fibroblast growth factors (fgfs), their receptors and antagonists in primary endothelial cells and vascular smooth muscle cells," *Growth Factors*, vol. 23, no. 2, pp. 87–95, 2005.

[425] M. Zhou, R. L. Sutliff, R. J. Paul, J. N. Lorenz, J. B. Hoying, C. C. Haudenschild, M. Yin, J. D. Coffin, L. Kong, E. G. Kranias, W. Luo, G. P. Boivin, J. J. Duffy, S. A. Pawlowski, and T. Doetschman, "Fibroblast growth factor 2 control of vascular tone," *Nat Med*, vol. 4, no. 2, pp. 201–7, 1998.

[426] S. S. Oladipupo, C. Smith, A. Santeford, C. Park, A. Sene, L. A. Wiley, P. Osei-Owusu, J. Hsu, N. Zapata, F. Liu, R. Nakamura, K. J. Lavine, K. J. Blumer, K. Choi, R. S. Apte, and D. M. Ornitz, "Endothelial cell fgf signaling is required for injury response but not for vascular homeostasis," *Proc Natl Acad Sci U S A*, vol. 111, no. 37, pp. 13379–84, 2014.

[427] K. Hatanaka, A. A. Lanahan, M. Murakami, and M. Simons, "Fibroblast growth factor signaling potentiates ve-cadherin stability at adherens junctions by regulating shp2," *PLoS One*, vol. 7, no. 5, p. e37600, 2012.

[428] M. Murakami, L. T. Nguyen, Z. W. Zhuang, K. L. Moodie, P. Carmeliet, R. V. Stan, and M. Simons, "The fgf system has a key role in regulating vascular integrity," *J Clin Invest*, vol. 118, no. 10, pp. 3355–66, 2008.

[429] M. Antoine, W. Wirz, C. G. Tag, A. M. Gressner, M. Wycislo, R. Müller, and P. Kiefer, "Fibroblast growth factor 16 and 18 are expressed in human cardiovascular tissues and induce on endothelial cells migration but not proliferation," *Biochem Biophys Res Commun*, vol. 346, no. 1, pp. 224–33, 2006.

[430] S. H. Ong, Y. R. Hadari, N. Gotoh, G. R. Guy, J. Schlessinger, and I. Lax, "Stimulation of phosphatidylinositol 3-kinase by fibroblast growth factor receptors is mediated by coordinated recruitment of multiple docking proteins," *Proc Natl Acad Sci U S A*, vol. 98, no. 11, pp. 6074–9, 2001.

[431] B. Visentin, J. A. Vekich, B. J. Sibbald, A. L. Cavalli, K. M. Moreno, R. G. Matteo, W. A. Garland, Y. Lu, S. Yu, H. S. Hall, V. Kundra, G. B. Mills, and R. A. Sabbadini, "Validation of an anti-sphingosine-1-phosphate antibody as a potential therapeutic in reducing growth, invasion, and angiogenesis in multiple tumor lineages," *Cancer Cell*, vol. 9, no. 3, pp. 225–38, 2006.

[432] Y. Zou, J. Hu, W. Huang, S. Ye, F. Han, J. Du, M. Shao, R. Guo, J. Lin, Y. Zhao, Y. Xiong, and X. Wang, "Non-mitogenic fibroblast growth factor 1 enhanced angiogenesis following ischemic stroke by regulating the sphingosine-1-phosphate 1 pathway," *Frontiers in Pharmacology*, vol. 11, 2020.

[433] P. Pandey, F. Khan, T. K. Upadhyay, M. Seungjoon, M. N. Park, and B. Kim, "New insights about the pdgf/pdgfr signaling pathway as a promising target to develop cancer therapeutic strategies," *Biomedicine & Pharmacotherapy*, vol. 161, p. 114491, 2023.

[434] A. Kazlauskas, "Pdgfs and their receptors," *Gene*, vol. 614, pp. 1–7, 2017.

[435] H. Ding, X. Wu, H. Boström, I. Kim, N. Wong, B. Tsoi, M. O'Rourke, G. Y. Koh, P. Soriano, C. Betsholtz, T. C. Hart, M. L. Marazita, L. L. Field, P. P. L. Tam, and A. Nagy, "A specific requirement for pdgf-c in palate formation and pdgfr-α signaling," *Nature Genetics*, vol. 36, no. 10, pp. 1111–1116, 2004.

[436] P. Levéen, M. Pekny, S. Gebre-Medhin, B. Swolin, E. Larsson, and C. Betsholtz, "Mice deficient for pdgf b show renal, cardiovascular, and hematological abnormalities," *Genes & Development*, vol. 8, no. 16, pp. 1875–1887, 1994.

[437] P. Soriano, "Abnormal kidney development and hematological disorders in pdgf beta-receptor mutant mice," *Genes & Development*, vol. 8, no. 16, pp. 1888–1896, 1994.

[438] P. Soriano, "The pdgfα receptor is required for neural crest cell development and for normal patterning of the somites," *Development*, vol. 124, no. 14, pp. 2691–2700, 1997.

[439] H. Wang, Y. Yin, W. Li, X. Zhao, Y. Yu, J. Zhu, Z. Qin, Q. Wang, K. Wang, W. Lu, J. Liu, and L. Huang, "Over-expression of pdgfr-β promotes pdgf-induced proliferation, migration, and angiogenesis of epcs through pi3k/akt signaling pathway," *PLOS ONE*, vol. 7, no. 2, p. e30503, 2012.

[440] C. Q. Wang, C. Y. Lin, Y. L. Huang, S. W. Wang, Y. Wang, B. F. Huang, Y. W. Lai, S. L. Weng, Y. C. Fong, C. H. Tang, and Z. Lv, "Sphingosine-1-phosphate promotes pdgf-dependent endothelial progenitor cell angiogenesis in human chondrosarcoma cells," *Aging (Albany NY)*, vol. 11, no. 23, pp. 11040–11053, 2019.

[441] G. Boguslawski, J. R. Grogg, Z. Welch, S. Ciechanowicz, D. Sliva, A. T. Kovala, P. McGlynn, D. N. Brindley, R. A. Rhoades, and D. English, "Migration of vascular smooth muscle cells induced by sphingosine 1-phosphate and related lipids: Potential role in the angiogenic response," *Experimental Cell Research*, vol. 274, no. 2, pp. 264–274, 2002.

[442] T. Tanimoto, A. O. Lungu, and B. C. Berk, "Sphingosine 1-phosphate transactivates the platelet-derived growth factor β receptor and epidermal growth factor receptor in vascular smooth muscle cells," *Circulation Research*, vol. 94, no. 8, pp. 1050–1058, 2004.

[443] J. P. Hobson, H. M. Rosenfeldt, L. S. Barak, A. Olivera, S. Poulton, M. G. Caron, S. Milstien, and S. Spiegel, "Role of the sphingosine-1-phosphate receptor edg-1 in pdgf-induced cell motility," *Science*, vol. 291, no. 5509, pp. 1800–3, 2001.

[444] H. Rosen, G. Sanna, and C. Alfonso, "Egress: a receptor-regulated step in lymphocyte trafficking," *Immunol Rev*, vol. 195, pp. 160–77, 2003.

Contributions

Annalena Wille planned, designed, performed, analyzed and interpreted the majority of the experiments under the supervision and guidance of Prof. Dr. Bodo Levkau.

Aspects of the research benefited from the expertise and collaboration of other researchers, as listed below:

Post-Traumatic Osteomyelitis

- Conceptualization: The experiments investigating bone regeneration in the post-traumatic osteomyelitis model were conceptualized by Prof. Dr. Björn Behr and Dr. Maximilian Wagner from the Department of Plastic Surgery at BG University Hospital Bergmannsheil Bochum, Germany.
- Surgical Procedures: Conducted by Dr. Maximilian Wagner in collaboration with Annalena Wille.
- Bone Sample Collection and Analysis: Collected and analyzed using µCT by Annalena Wille.
- Interpretation of Results: Conducted by Annalena Wille and Dr. Maximilian Wagner.
- Staining and Analysis of Bone Samples: Performed at the Department of Plastic Surgery, BG University Hospital Bergmannsheil Bochum, Germany.

LC-MS/MS Measurements

- Animal Experiments: Planned and conducted by Annalena Wille.
- Sample Preparation: Conducted by Annalena Wille.
- Sample Measurement and Analysis: Conducted by Philipp Wollnitzke.
- Interpretation of Results: Conducted by Annalena Wille.

Supplementary

Source Codes

The following source codes were used for automated image analysis using ImageJ.

Analysis of vessel-length and branching:

```
run("Z Project...", "projection=[Max Intensity]");
run("Subtract Background...", "rolling=50");
setAutoThreshold("Default dark");
//run("Threshold...");
setOption("BlackBackground", true);
run("Convert to Mask");
//run("Close-");
roiManager("Select", 0);
run("Clear Outside");
//setThreshold(255, 255);
run("Convert to Mask");
run("Options...", "iterations=4 count=1 black do=Nothing");
run("Tubeness", "sigma=6 use");
setAutoThreshold("Default dark");
//run("Threshold...");
setAutoThreshold("Li dark");
run("Convert to Mask");
//run("Close-");
run("Skeletonize");
run("Analyze Skeleton (2D/3D)", "prune=none show");
```

Analysis of vascular Emdomucin MFI:

```
run("Z Project...", "projection=[Max Intensity]");
run("Select None");
run("Duplicate...", " ");
setThreshold(0, 65535);
//run("Threshold...");
roiManager("Select", 0);
run("Convert to Mask");
roiManager("Select", 0);
run("Clear Outside");
//setTool("freehand");
```

Bone area was selected by hand

```
run("Clear Outside");
run("Select None");
run("Invert");
run("Create Selection");
roiManager("Add");
close();
roiManager("Select", 1);
setAutoThreshold("Default dark");
run("Measure");
```

Publication and Licensing Rights

49 Spadina Ave. Suite 200
Toronto ON M5V 2J1 Canada
www.biorender.com

Confirmation of Publication and Licensing Rights

June 4th, 2024
Science Suite Inc.

Subscription:	*Student Plan*
Agreement number:	*YO26WGPKPS*
Journal name:	*Dissertation*

To whom this may concern,

This document is to confirm that Annalena Wille has been granted a license to use the BioRender content, including icons, templates and other original artwork, appearing in the attached completed graphic pursuant to BioRender's Academic License Terms. This license permits BioRender content to be sublicensed for use in journal publications.

All rights and ownership of BioRender content are reserved by BioRender. All completed graphics must be accompanied by the following citation: "Created with BioRender.com".

BioRender content included in the completed graphic is not licensed for any commercial uses beyond publication in a journal. For any commercial use of this figure, users may, if allowed, recreate it in BioRender under an Industry BioRender Plan.

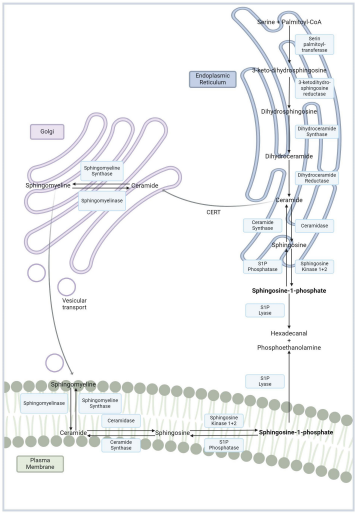

For any questions regarding this document, or other questions about publishing with BioRender refer to our BioRender Publication Guide, or contact BioRender Support at support@biorender.com.

49 Spadina Ave. Suite 200
Toronto ON M5V 2J1 Canada
www.biorender.com

Confirmation of Publication and Licensing Rights

June 4th, 2024
Science Suite Inc.

Subscription:	*Student Plan*
Agreement number:	*EA26WGOSIU*
Journal name:	*Dissertation*

To whom this may concern,

This document is to confirm that Annalena Wille has been granted a license to use the BioRender content, including icons, templates and other original artwork, appearing in the attached completed graphic pursuant to BioRender's Academic License Terms. This license permits BioRender content to be sublicensed for use in journal publications.

All rights and ownership of BioRender content are reserved by BioRender. All completed graphics must be accompanied by the following citation: "Created with BioRender.com".

BioRender content included in the completed graphic is not licensed for any commercial uses beyond publication in a journal. For any commercial use of this figure, users may, if allowed, recreate it in BioRender under an Industry BioRender Plan.

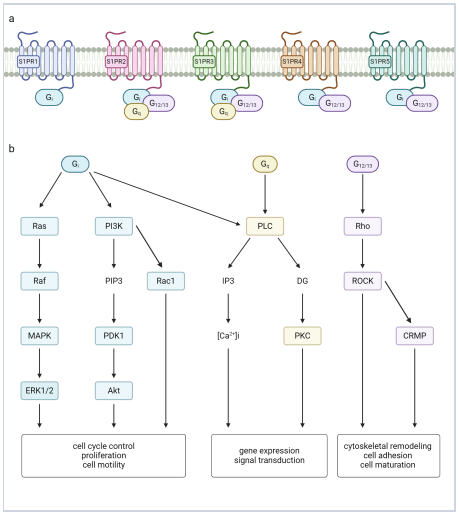

For any questions regarding this document, or other questions about publishing with BioRender refer to our BioRender Publication Guide, or contact BioRender Support at support@biorender.com.

49 Spadina Ave. Suite 200
Toronto ON M5V 2J1 Canada
www.biorender.com

Confirmation of Publication and Licensing Rights

June 4th, 2024
Science Suite Inc.

Subscription:	*Student Plan*
Agreement number:	*VR26WGOXSI*
Journal name:	*Dissertation*

To whom this may concern,

This document is to confirm that Annalena Wille has been granted a license to use the BioRender content, including icons, templates and other original artwork, appearing in the attached completed graphic pursuant to BioRender's Academic License Terms. This license permits BioRender content to be sublicensed for use in journal publications.

All rights and ownership of BioRender content are reserved by BioRender. All completed graphics must be accompanied by the following citation: "Created with BioRender.com".

BioRender content included in the completed graphic is not licensed for any commercial uses beyond publication in a journal. For any commercial use of this figure, users may, if allowed, recreate it in BioRender under an Industry BioRender Plan.

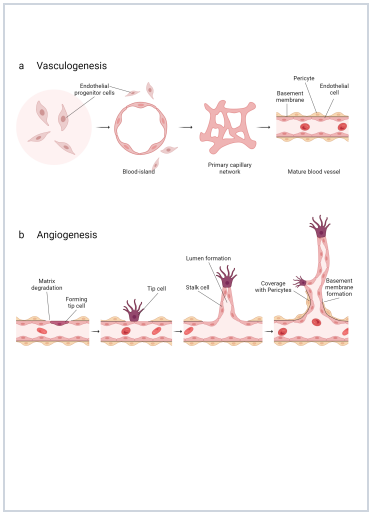

For any questions regarding this document, or other questions about publishing with BioRender refer to our BioRender Publication Guide, or contact BioRender Support at support@biorender.com.

49 Spadina Ave. Suite 200
Toronto ON M5V 2J1 Canada
www.biorender.com

Confirmation of Publication and Licensing Rights

June 4th, 2024
Science Suite Inc.

Subscription:	*Student Plan*
Agreement number:	*JR26WGP7XS*
Journal name:	*Dissertation*

To whom this may concern,

This document is to confirm that Annalena Wille has been granted a license to use the BioRender content, including icons, templates and other original artwork, appearing in the attached completed graphic pursuant to BioRender's Academic License Terms. This license permits BioRender content to be sublicensed for use in journal publications.

All rights and ownership of BioRender content are reserved by BioRender. All completed graphics must be accompanied by the following citation: "Created with BioRender.com".

BioRender content included in the completed graphic is not licensed for any commercial uses beyond publication in a journal. For any commercial use of this figure, users may, if allowed, recreate it in BioRender under an Industry BioRender Plan.

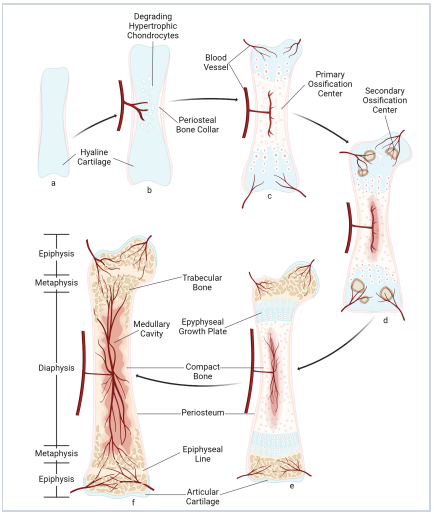

For any questions regarding this document, or other questions about publishing with BioRender refer to our BioRender Publication Guide, or contact BioRender Support at support@biorender.com.

49 Spadina Ave. Suite 200
Toronto ON M5V 2J1 Canada
www.biorender.com

Confirmation of Publication and Licensing Rights

June 4th, 2024
Science Suite Inc.

Subscription:	*Student Plan*
Agreement number:	*YY26WGPG12*
Journal name:	*Dissertation*

To whom this may concern,

This document is to confirm that Annalena Wille has been granted a license to use the BioRender content, including icons, templates and other original artwork, appearing in the attached completed graphic pursuant to BioRender's Academic License Terms. This license permits BioRender content to be sublicensed for use in journal publications.

All rights and ownership of BioRender content are reserved by BioRender. All completed graphics must be accompanied by the following citation: "Created with BioRender.com".

BioRender content included in the completed graphic is not licensed for any commercial uses beyond publication in a journal. For any commercial use of this figure, users may, if allowed, recreate it in BioRender under an Industry BioRender Plan.

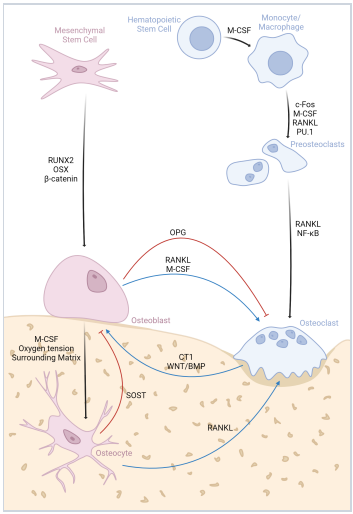

For any questions regarding this document, or other questions about publishing with BioRender refer to our BioRender Publication Guide, or contact BioRender Support at support@biorender.com.

49 Spadina Ave. Suite 200
Toronto ON M5V 2J1 Canada
www.biorender.com

Confirmation of Publication and Licensing Rights

June 4th, 2024
Science Suite Inc.

Subscription:	*Student Plan*
Agreement number:	*MY26WGP3EQ*
Journal name:	*Dissertation*

To whom this may concern,

This document is to confirm that Annalena Wille has been granted a license to use the BioRender content, including icons, templates and other original artwork, appearing in the attached completed graphic pursuant to BioRender's Academic License Terms. This license permits BioRender content to be sublicensed for use in journal publications.

All rights and ownership of BioRender content are reserved by BioRender. All completed graphics must be accompanied by the following citation: "Created with BioRender.com".

BioRender content included in the completed graphic is not licensed for any commercial uses beyond publication in a journal. For any commercial use of this figure, users may, if allowed, recreate it in BioRender under an Industry BioRender Plan.

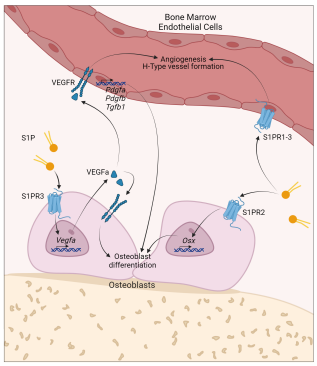

For any questions regarding this document, or other questions about publishing with BioRender refer to our BioRender Publication Guide, or contact BioRender Support at support@biorender.com.

Affidavit

I declare under oath that I have produced my thesis independently and without any undue assistance by third parties under consideration of the ‘Principles for the Safeguarding of Good Scientific Practice at Heinrich Heine University Düsseldorf’. The dissertation has not been submitted to any other institution or in comparable form. Furthermore, I have not made any unsuccessful attempts at obtaining a doctorate to date.

_____

Annalena Wille, Düsseldorf, June 2024